


**THE** SEPTEMBER 1978  
VOL. 57, NO. 7, PART 1 OF 2



**BELL SYSTEM**  
**TECHNICAL JOURNAL**

ISSN0005-8580

**SG UNDERSEA CABLE SYSTEM**

R. D. Ehrbar, A. E. Ford, and G. Gerbier	Introduction and Development Plan	2313
S. T. Brewer, R. L. Easton, H. Soulier, and S. A. Taylor	Requirements and Performance	2319
C. D. Anderson, W. E. Hower, J. J. Kassig, V. M. Krygowski, R. L. Lynch, G. A. Reinold, and P. A. Yeisley	Repeater and Equalizer Design and Manufacture	2355
W. M. Fox, W. H. Yocom, P. R. Munk, and E. F. Sartori	Semiconductor Devices and Passive Components	2405
G. E. Morse, S. Ayers, R. F. Gleason, and J. R. Stauffer	Cable and Coupling Design	2435
M. Brouant, C. Chalhoub, P. Delage, D. N. Harper, H. Soulier, and R. L. Lynch	Terminal Transmission Equipment	2471
E. T. Calkin, I. Golioto, W. J. Schatz, R. E. Schroeder, and D. S. Shull	Undersea System Power	2497
J. E. H. Cosier, A. P. Davies, S. W. Dawson, Jr. R. F. Gleason, F. E. Kirkland, and T. A. McKenzie	Installation and Maintenance of the Undersea System	2523
D. N. Harper, B. O. Larson, and M. Laurette	Commissioning: Final System Alignment and Evaluation	2547
	Contributors to This Issue	2565

# THE BELL SYSTEM TECHNICAL JOURNAL

## ADVISORY BOARD

D. E. PROCKNOW, *President, Western Electric Company, Incorporated*

W. O. BAKER, *President, Bell Telephone Laboratories, Incorporated*

C. L. BROWN, *President, American Telephone and Telegraph Company*

## EDITORIAL COMMITTEE

D. GILLETTE, *Chairman*

W. S. BOYLE

I. DORROS

A. G. CHYNOWETH

H. B. HEILIG

S. J. BARBERA

C. B. SHARP

T. H. CROWLEY

B. E. STRASSER

W. A. DEPP

I. WELBER

## EDITORIAL STAFF

G. E. SCHINDLER, JR., *Editor*

J. B. FRY, *Associate Editor*

H. M. PURVIANCE, *Art Editor*

B. G. GRUBER, *Circulation*

R. D. EHRBAR and S. T. BREWER, *Coordinating Editors  
of SG Undersea Cable System*

**THE BELL SYSTEM TECHNICAL JOURNAL** is published monthly, except for the May-June and July-August combined issues, by the American Telephone and Telegraph Company, J. D. deButts, Chairman and Chief Executive Officer; C. L. Brown, President; W. G. Burns, Vice President and Treasurer; F. A. Hutson, Jr., Secretary. Editorial enquiries should be addressed to the Editor, The Bell System Technical Journal, Bell Laboratories, 600 Mountain Ave., Murray Hill, N.J. 07974. Checks for subscriptions should be made payable to The Bell System Technical Journal and should be addressed to Bell Laboratories, Circulation Group, Whippany Road, Whippany, N.J. 07981. Subscriptions \$20.00 per year; single copies \$2.00 each. Foreign postage \$1.00 per year; 15 cents per copy. Printed in U.S.A. Second-class postage paid at New Providence, New Jersey 07974 and additional mailing offices.

© 1978 American Telephone and Telegraph Company

Single copies of material from this issue of the Bell System Technical Journal may be reproduced for personal, noncommercial use. Permission to make multiple copies must be obtained from the editor.

# THE BELL SYSTEM TECHNICAL JOURNAL

DEVOTED TO THE SCIENTIFIC AND ENGINEERING  
ASPECTS OF ELECTRICAL COMMUNICATION

---

Volume 57

September 1978

Number 7, Part 1

---

*Copyright © 1978 American Telephone and Telegraph Company, Printed in U.S.A.*

## ***SG Undersea Cable System:***

### **Introduction and Development Plan**

By R. D. EHRBAR, A. E. FORD, and G. GERBIER

(Manuscript received June 30, 1977)

*This paper describes the background of the three-nation SG development and the structure of the organization, and comments on the success with which the mission was carried out.*

#### **I. INTRODUCTION**

Communications traffic across the North Atlantic has increased around 20 percent per annum for some years, carried partly by cable and partly by satellite. This growth continued beyond 1970, following the start of service on the then-newest undersea cable facility, an SF system called TAT-5, in March of that year.<sup>1</sup> There was no reason to think that the growth rate would fall significantly in the next decade. Satellites were carrying a significant part of the North Atlantic traffic, and it was generally recognized that both cable and satellite technologies should be carried forward to their maximum potential. This provided the impetus for pursuing the new cable technology designated SG.

In this paper, we do not discuss the merits of the different transmission technologies or predict future deployment. Instead, we devote our attention to the development of the SG undersea cable system, which as

TAT-6 (3400 nmi long) was turned up for initial service on July 27, 1976 between the United States and France.

## II. NEW DEVELOPMENT PLANS

An exploratory program was under way at Bell Laboratories, even before the completion of TAT-5, to determine practical objectives for the next undersea system that would logically follow SF and would continue the reduction in cost per channel mile. In the United Kingdom, production of a system with a top frequency of 14 MHz was also under way. This system, developed for short distance cables, was capable of providing a nominal voice capacity of 1840 two-way channels spaced at 3 kHz. Ongoing development to extend the system to intercontinental distances was well advanced.

A tentative plan for deployment of cables in the North Atlantic had been formulated in negotiations among the many parties sharing responsibility for these communications. One plan called for another SF system between the U.S. and France in 1973, and then a new large capacity system (perhaps as many as 4000 channels) from the U.S. to the U.K. at a later date. To further this plan, two projects were set in motion in 1970: (i) Application was made to the American Federal Communications Commission (FCC) in August for permission to lay an SF system from the United States to France and (ii) plans were formulated within the Bell System for the development of a new, higher capacity system to be called SG.

The FCC ruled against the SF system in mid-1971 as not being in the public interest and recommended that the development of the proposed SG system be expedited so as to be ready for service as rapidly as possible. This put considerable pressure on completing the SG development so that manufacture could be started at an early date, since there was likely to be a cable circuit deficit across the Atlantic between 1973 and the earliest time considered practical for completion of a transatlantic SG (about 1976).

The pressure to provide another transatlantic system at an earlier date was reduced significantly by a decision of the British Post Office (BPO) and the Canadian Overseas Telecommunications Corporation (now Teleglobe, Canada) to install CANTAT-2, producing 1840 3-kHz message channels between Widemouth, Cornwall and Halifax, Nova Scotia.<sup>2</sup> This link was brought into service in 1974.

## III. SHARED DEVELOPMENT PLAN

The idea of a shared development approach to the new SG system had been considered in the early planning stage, and the first joint meeting of AT&T, Bell Laboratories, and the BPO was held in June 1970 in London. In view of the development work already being undertaken by



both the BPO and Bell Labs, partnership in the development of the SG system seemed natural. The division of the development work was changed several times. Only two decisions made at the early meetings remained constant: (i) Bell System responsibility for repeater development and (ii) BPO responsibility for a new 1.7-in. cable development. Originally, it was intended that the BPO would be responsible for the development of the terminal transmission equipment, but in a three-party agreement, the French Ministry for Postes and Telecommunications (FPTT) accepted responsibility for this work. This was a logical step since, by 1971, it had been internationally agreed that the new, high-capacity system TAT-6 would be installed between Green Hill, Rhode Island and St. Hilaire de Riez, France.

#### **IV. DIVISION OF RESPONSIBILITY**

While the division of responsibility could not be completely specified, an attempt was made to define it in some detail. Some responsibilities were common to all, while others were assigned to individual groups.

##### **4.1 Common responsibilities**

These can be summarized as follows: Development of overall system design parameters and specification, system planning principles and engineering, specification of test equipment and procedures for installation, commissioning, and maintenance of the system.

##### **4.2 Individual responsibilities**

AT&T (Bell Laboratories) was given the development responsibility for the following portions of the system: repeaters and devices for repeaters, repeater factory test sets, laying test sets, couplings and junction boxes, ocean-block equalizers, supervisory tone and repeater monitoring test set, shipboard and shore high-voltage power-feeding equipment, and order wire equipments for cable laying and burying.

BPO was given the development responsibility for cable, jointing methods, cable handling procedures, cable fault location test sets, cable factory test sets, and other associated test equipment.

The FPTT was given the development responsibility for the terminal transmission equipment (multiplex and wide-band line) between the supergroup distribution point and the transmission equipment side of the power separating filter, the order wire and associated terminal signaling equipment, and maintenance test sets.

##### **4.3 Formal agreement**

Arrangements were formalized in a document titled "Agreement for Shared Development of a High Capacity Submarine Cable System"

signed on May 2, 1973 although, by mutual agreement, work had started in 1971. The document contained descriptions of the various responsibilities, a method for distribution of development costs, means for handling technical information and inventions, and a list of tentative objectives for system characteristics.

## **V. PROJECT ORGANIZATION**

An undersea cable system is a complex transmission system design consisting of many parts and processes, as is shown in the companion articles in this issue. Each part must have individual objectives, and the complete system must function to produce an end result that is both economical and reliable.

For these reasons, a relatively complex organization was required to guide and monitor the joint development work by technical representatives of the three countries working together for a common goal. Overall guidance was provided by a Development Steering Committee (DSC) consisting of two members each from the BPO, FPTT, and AT&T-BTL. The detailed work was carried out by seven working parties, each having from 8 to 10 members.

A second agreement titled "TAT-6 (SG) Cable Construction and Maintenance Agreement" was a vital part of the project. This agreement assumed the use of the SG system for TAT-6 and defined ownership interest, assignment of channels, responsibility for procurement, installation, etc. of this first SG link to be installed. It was signed by the appropriate telecommunications agency in 16 European countries plus AT&T, ITT Worldcom, RCA Globcom, and Western Union International. From this agreement, the TAT-6 General Committee was formed. A subcommittee, responsible for procurement and installation, was the main point of contact with the SG Development Steering Committee.

## **VI. METHOD OF OPERATION**

Meetings of the development working parties were scheduled as required, and the location of the meetings was rotated among the three countries. Prior to each meeting of the Development Steering Committee, reports of the working parties were circulated for review. The report of each DSC meeting consisted of general discussion and agreements and the following specific sections for control of the project:

- (i) Review of memoranda from the TAT-6 subcommittee B and memoranda to that subcommittee covering outstanding points.
- (ii) Review of working party chairmen's reports and instructions to working parties.
- (iii) Report to administrations.
- (iv) Review and allocation of development costs.

## VII. RESULTS

While the joint development seemed to be overly complex at times and introduced the added expense of traveling, it was a successful endeavor. The interchange of technical information contributed to the development of the SG system and was valuable to each organization for its future work.

The technical results of the development program are discussed in the succeeding papers. The decision to install a 3400-nmi transatlantic system as the first project was rather daring. Laying cable in the North Atlantic early in the year proved to be a hazardous adventure, as the weather refused to be cooperative and accounted for considerable delay and apprehension. Many last-minute decisions were required, but nevertheless, except for the fact that the system objective for intermodulation noise was not fully met, the project was successfully accomplished.

The causes of the intermodulation noise have since been established and development work actively pursued to eliminate these problems, both in future SG systems and by the use of special equipment at one terminal of TAT-6. Bell Laboratories intends to continue to improve the cost effectiveness of the system, and it is hoped that future cable system requirements can take advantage of the facility successfully developed as a result of this unique international cooperation.

## REFERENCES

1. "SF Submarine Cable System," *B.S.T.J.* 49, No. 5 (May-June 1970), pp. 601-889.
2. "CANTAT-2 Submarine Cable System," *Post Off. Elec. Eng. J.*, 67, Part 3 (October 1974).



## ***SG Undersea Cable System:***

# **Requirements and Performance**

By S. T. BREWER, R. L. EASTON, H. SOULIER,  
and S. A. TAYLOR

(Manuscript received September 8, 1977)

*This paper reviews the major parameters of the SG Undersea Cable System. SG transmission goals and signal statistics were established, which led to a specific system and equalization design. As the SG design evolved, information on cable aging led to the introduction of four shore-controlled equalizers in the SG transatlantic link (TAT-6). Performance delivered by the TAT-6 link has been generally satisfactory, though some excess noise was encountered in the top third of the high band. Equalization results permit the link to handle 4200 two-way voice channels, 200 more than the objective.*

## **I. INTRODUCTION AND BACKGROUND\***

### **1.1 Traffic growth and forecast**

Since 1956, when voice communication across the Atlantic by undersea cable began, growth in traffic has continued at a rapid rate.<sup>1,2,4,5</sup> The two upper curves of Fig. 1 indicate the growth of (i) total U.S. overseas phone messages and (ii) transatlantic phone messages. Data plotted here include traffic by satellite and radio, as well as by cable. Between 1960 and 1976, annual overseas phone messages have increased from 3.7 to 87.7 million. This represents an exponential growth of 22 percent per year. Transatlantic phone messages to Europe have increased from 1.0 million in 1960 to 29.7 million in 1976. Thus, Atlantic basin growth rate is 24 percent per year. Projecting 1976 traffic at growth rates experienced to date yields an expected 520 million total overseas phone messages in

---

\* This paper broadly covers all aspects of the SG system. For greater detail on any particular facet of the system, the reader is referred to the appropriate subsequent article in this issue of the B.S.T.J.

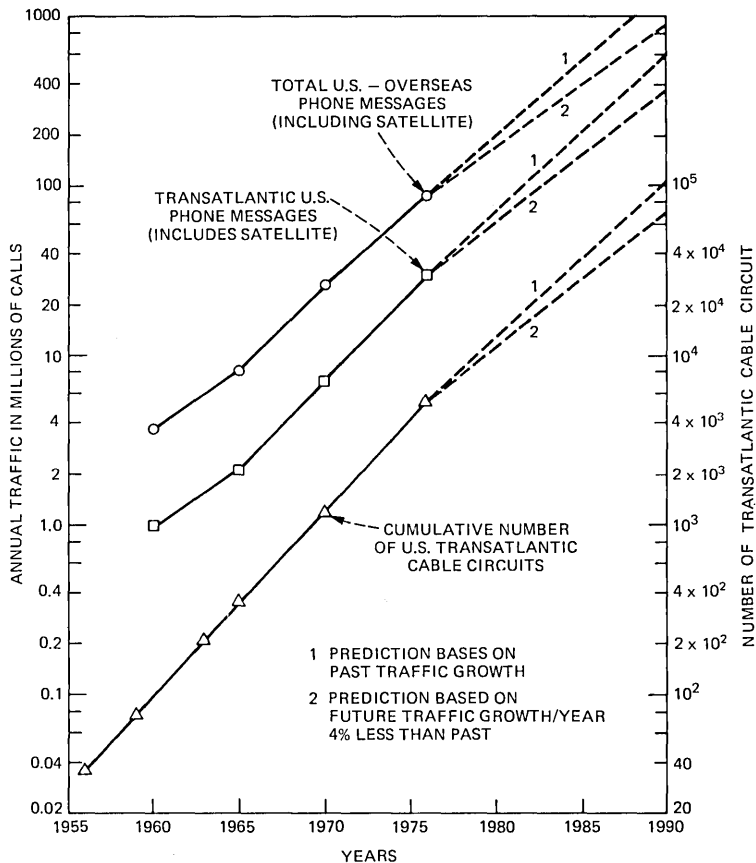


Fig. 1—U.S. overseas and transatlantic growth.

1985, of which 203 million would be transatlantic. These projections are plotted as the upper dashed curves of Fig. 1. If we assume that future growth rates will be 4 percent less than past ones, we get the lower dashed curves of Fig. 1. This more conservative forecast anticipates 385 million total overseas phone messages by 1985, of which 151 million would be transatlantic. The lower cost to the customer that can be expected to result from further economies of advanced technology, plus the convenience of direct subscriber dialing of overseas calls, will be powerful forces to continued rapid traffic growth.

### 1.2 Transatlantic cable circuit growth

The bottom curve of Fig. 1 shows the transatlantic undersea cable circuits installed to meet traffic needs. Beyond 1976, the circuit projection is at two rates, the past transatlantic traffic-growth rate of 24

Table I — U.S. transatlantic cable circuits

Actual Year	Cumulative Circuits*	Added Circuits	New System
1956	36	36	TAT-1
1959	72	36	TAT-2
1963	212	140	TAT-3
1965	352	140	TAT-4
1970	1172	820	TAT-5
1976	5372	4200	TAT-6

Forecast Year	24%/yr Growth	20%/yr Growth	Additional Cable Circuits Needed Beyond TAT-6	
			24%/yr	20%/yr
1980	12,700	11,140.	7330.	5770.
1985	37,200	27,720.	31,900.	22,300.
1990	109,200	68,970.	103,800.	63,600.

\* Figures are for physical circuits, and do not include a limited number of TASI-derived circuits on installed systems.

percent per year, plus the more conservative rate of 20 percent per year.

Table I shows this growth in tabular form. The lower part of the table indicates the cumulative number of circuits we expect to need up through 1990. If the 24 percent growth rate is sustained, by 1980 another 7330 cable circuits will be needed beyond TAT-6, and by 1985 some 31,900 added cable circuits will be needed.\* If we experience the more modest 20 percent per year growth, we will need 5770 additional cable circuits by 1980 and 22,300 new cable circuits by 1985.

With such exponential growth, it is interesting to consider the possible effect speech concentrators such as TASI (Time Assignment Speech Interpolation) could have on future demand. Moderate application of TASI could defer the forecasted circuit needs by one year. Fairly extensive application of TASI could yield a 2-year postponement. After the transient resulting from the introduction of TASI, circuit needs would be expected to grow at the same rate as before.

## II. PLANNING THE SG SYSTEM

### 2.1 Repeater performance

Table II shows key repeater parameters of the SF and SG systems.† Although the SG repeater has five times the top frequency of the earlier SF repeater, it actually has slightly better performance. Better noise figure, linearity, and output power capability result from (i) use of silicon

\* Future cable circuit needs shown in Table I assume that both cables and satellites will share future growth and that this sharing will continue on the basis of the present cable-satellite facility ratio.

† The appendix following this paper defines various terms and symbols which are used.

Table II — SF and SG repeater parameters

	SF	SG
Nominal top frequency	6.0 MHz	29.5 MHz
At repeater top frequency:		
Insertion gain	40.1 dB	41.0 dB
Noise figure	7.6 dB	3.5 dB
Maximum output power, rms single sine wave	20.0 dBm	23.0 dBm
Loss, amplitude output-to-cable	0.3 dB	1.2 dB
Modulation coefficients*		
$M_{2E}$	-65 dB	-70 dB
$M_{3E}$	-95 dB	-113 dB
Nominal impedance	59.4 ohms	50 ohms
Type transistor	Ge mesa	Si planar
Supervisory tone power at repeater output		
Low band	-60 dBm	-50 dBm
High band	-50 dBm	-40 dBm
DC current	136 mA	657 mA
DC potential drop	13.1 V	12 V

\* Referenced at power amplifier output.

planar transistors rather than the earlier germanium mesa transistors, (ii) use of active rather than passive terminations at the amplifier's input and output ports, and (iii) more compact physical structure.

## 2.2 Channel capacity

The rapid growth in traffic and the state of electronic technology were major factors determining the channel capacity of the SG system. As the start of development, our target was 3500 channels; this goal was later shifted to 4000 channels. The actual U.S.-to-France SG installation satisfactorily equalizes 4200 channels.

## 2.3 Cable diameter

A separate article describes in detail the SG cable design.<sup>6</sup> Early in the development, studies considered the economics of various possible systems as a function of cable diameter. A larger diameter cable, while more expensive and more demanding of ship capacity, has less loss and therefore saves repeaters and equalizers. Thus, as systems increase in capacity and therefore top frequency, larger cables become more desirable. Our studies showed that cable of 1.7-in. dielectric diameter would yield near-minimum system cost. This size cable also offered the possibility of lower dc resistance, which would reduce terminal voltage.

## 2.4 Repeater configuration

Figure 2 shows the two repeater configurations considered for SG. Separate high-band and low-band amplifiers avoid the nonlinear sing problem<sup>3</sup> and make design somewhat easier. This configuration also prevents second-order distortion from falling in the high band. On the other hand, the single-amplifier configuration improves reliability by



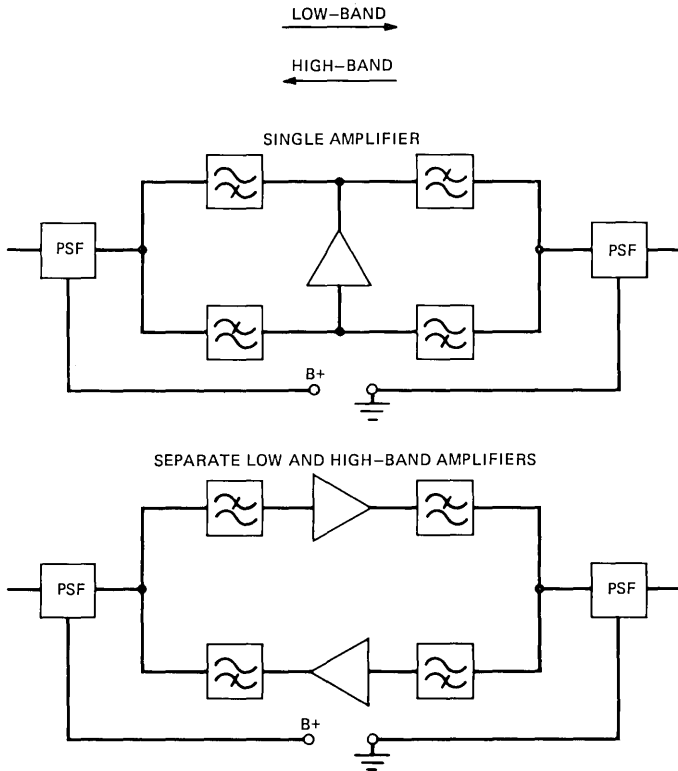


Fig. 2—Possible SG repeater configurations.

reducing the total number of components and devices. Exploratory studies indicated that the noise sing and the other design problems could be solved. These studies led to the choice of the single amplifier repeater configuration.

A side benefit of the single amplifier configuration is the use of intermodulation products from the repeaters to perform fault location and supervision, including detection of a badly modulating repeater. This supervision is done by a frequency-sweeping repeater monitoring set. In addition to the repeater monitoring set, the SG system includes a supervisory oscillator in each repeater, similar to the SF system arrangement.<sup>7</sup> Successive repeaters alternately have low-band and high-band quartz crystal supervisory oscillators by which each repeater may be identified. Since these supervisory oscillators inject known amounts of power, the individual supervisory powers received in the terminal also indicate transmission levels within the system.

### III. GENERAL DESCRIPTION

SG is an equivalent four-wire coaxial cable system, with a nominal capacity of 4000 two-way, 3-kHz-spaced channels, and a maximum length capability of 4000 nautical miles (nmi). The TAT-6 physical layout is shown in Fig. 3.

SG frequency allocations are specified in Fig. 4. The nominal low and high bands shown correspond to adequate bandwidth for the 4000 channels and allow for supervisory tone bands, 8-kHz guard bands between supergroups, and three order-wire channels. In the development, transmission was extended as far beyond all band edges as possible without added complexity in the repeaters and without impairing transmission within the nominal band. Practically, this meant that attention had to be paid to transmission in the extended bands of 0.5 to 13.9 MHz and 16.1 to 29.5 MHz. The bandwidths actually achieved on TAT-6 (corresponding to about 4200 two-way channels) are also indicated on Fig. 4.

A noise objective of 1 picowatt per kilometer\* applied to the average noise in the 4000 channels that form the basic system, with none of these channels to exceed 2 pW/km.

The ocean-block equalizers (OBES) equalize the gain deviations present at the time of installation due to the difference between actual repeater gain and cable section loss. The equalizers obtain the gain needed for equalization by shortening to one mile the total cable length between the two repeaters adjoining an equalizer. This makes 80 percent of the gain of a repeater available for equalization. Additional equalization gain is provided in the low band by designing excess gain relative to cable loss into each repeater (low-band gain boost).

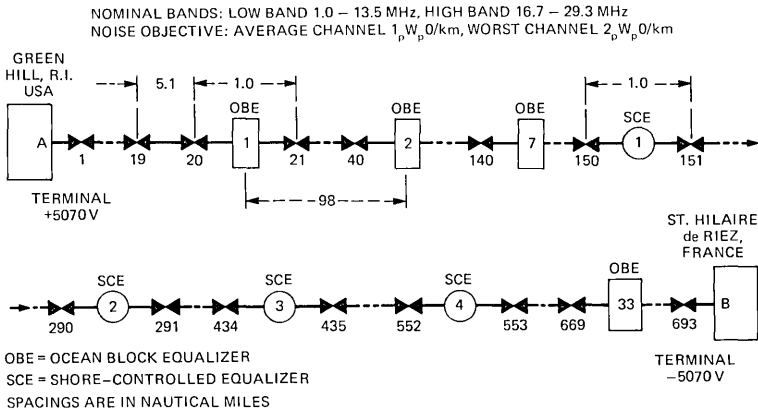


Fig. 3—TAT-6 SG link.

\* The 1 pW0p/km channel noise objective corresponds to 38.5 dBBrnc0 for TAT-6. Our "ideal" performance target was 36.5 dBBrnc0. Thus, 2 dB of noise performance was allowed for the effects of misalignment, etc.

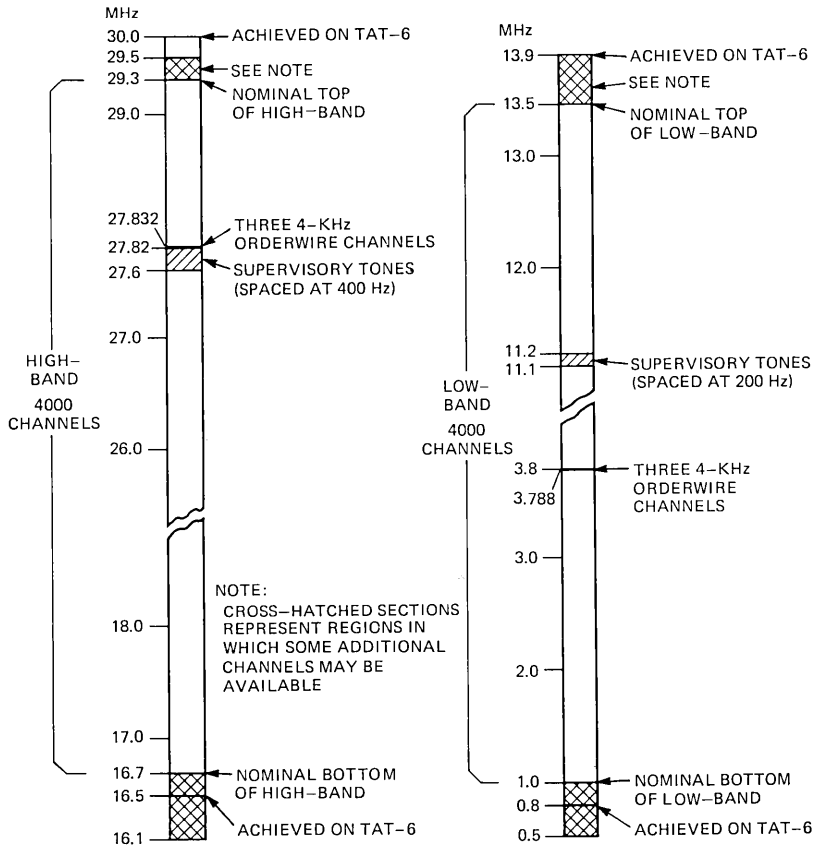


Fig. 4—SG frequency allocation.

Fairly late in the development, problems encountered during the manufacture of cable led to the discovery of phenomena that could cause the attenuation of installed cable to change with time (cable aging). Since the magnitude, frequency characteristic, and even the direction of such cable aging was uncertain, some means of adjusting the equalization along the length of the system subsequent to installation appeared to be required. On a crash basis a shore-controlled equalizer (SCE) was developed. Four such units were included in the TAT-6 link, dividing the system into five approximately equal-length "sectors." The SCEs obtain gain for equalization in the same way as the OBEs, as described above.

### 3.1 Transmission objectives and computed performance

The average power per channel,  $P_c$ , assumed in the SG system design is  $-13$  dBm0. This is a conservative value for present signals and mixtures of voice and data. The  $-13$  dBm0 figure would allow use of speech concentrators on about one-half the channels used to carry voice.

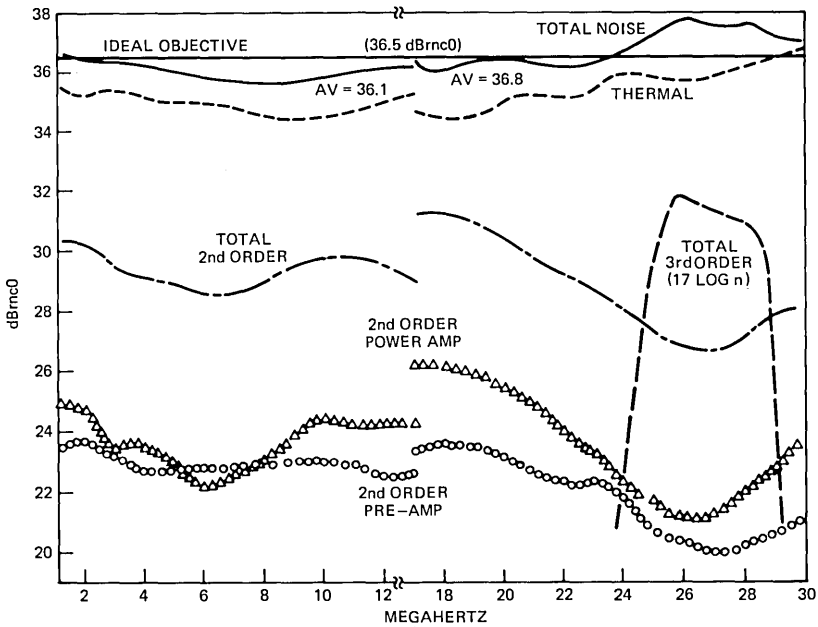


Fig. 5—SG system calculated noise performance (no misalignment, 3500 nmi, 700 repeaters, dBm0/channel = -13, overload margin = 6.2 dB).

Actually, initial conservatism and a continuing decrease in average talker and data volumes will make the -13 dBm0 average channel power adequate in the future even if there should be an increase in power on all voice channels due to the general use of speech concentrators.

A broadband load of 4000 two-way channels carrying the -13 dBm0 load per one-way channel has an average power,  $P_{av}$  of 26 dBm0 and a peak value of 39 dBm0.\*

The anticipated repeater performance is discussed further in a subsequent section. From this performance, the assumed load, and the number of repeaters necessary to span the Atlantic (about 700), it is possible to compute the expected system noise performance for any assumed transmission levels across the two transmission bands. The goal is to arrive at optimum signal level vs. frequency shaping that corresponds to the minimum flat noise for a particular link. Final shaping is determined by experimentally shaping signals and evaluating the results by system noise power ratio tests.

Figure 5 is the computed noise performance of an ideal system (with only the intentional gain boost appearing as misalignment), corresponding to the transmission levels shown in Fig. 6. The objective for

\* Average load =  $-13 + 10 \log_{10} (2 \times 4000) = +26$  dBm0. The signal has peaks extending 13 dB higher than this 0.001 percent of the time. This peak-to-average ratio is the multi-channel peak factor,  $k_m$ .

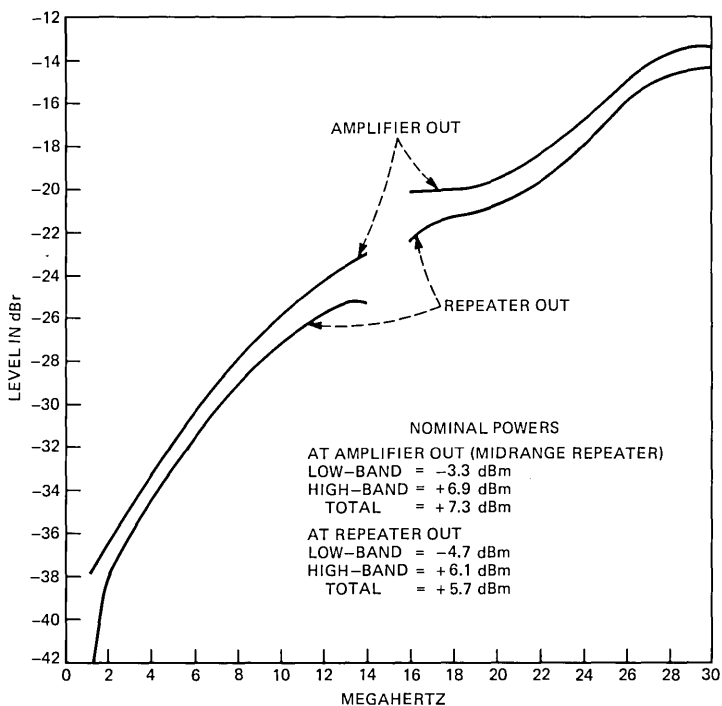


Fig. 6—Nominal transmission levels.

a 3400-nmi transatlantic length on this basis is 36.5 dB<sub>rnc0</sub>, to allow the 2-dB performance margin mentioned earlier. The results of Fig. 5 show that the estimated noise performance is approximately the desired 36.5 dB<sub>rnc0</sub>.

As stated in Fig. 5, the overload margin to take care of the highest level repeater is about 6 dB.\* A *total* flat misalignment of 12 dB would use up about 1.3 dB of the performance margin. This misalignment is the maximum that can be equalized *equally* at the transmitting and receiving terminals. To avoid overloading any repeaters, additional misalignment would have to be equalized entirely in the transmitting terminal if the misalignment is gain, or entirely in the receiving terminal if the misalignment is loss.† Such nonsymmetric equalization results in considerably greater misalignment penalty than does symmetric equalization.

### 3.2 Equalization plan

The first level of equalization in the SG Undersea Cable System is to

\* That is, the zero-misalignment repeater operates at an average signal power output which is 6 dB below the repeater's capability.

† Ripples across the transmission load that average out (i.e., leave the broadband load unchanged) can always be symmetrically equalized.

match the gain of the repeater to the computed loss of 5.1-nmi of cable under the nominal condition of 2.5°C and 2.5 kilofathoms (kF).

The next level of equalization is provided only in shallow-water repeaters that are subject to seasonal temperature variations. These repeaters have a temperature-sensitive gain characteristic that will compensate for loss changes in the cable resulting from ambient temperature variations.

After a route for a particular installation has been selected, cable sections are ordered from the factories by 29-MHz attenuation, not by length. The idea is to obtain a top-frequency cable section attenuation at sea bottom which corresponds to the mean top-frequency repeater gain. The ordered loss which a particular section is to measure in the factory (at 10°C, 0 fathoms) is computed so that the attenuation of this section will match repeater gain at the depth and temperature corresponding to its position in the system. This procedure thus tends to correct for manufacturing deviations and differences between actual sea-bottom conditions and the nominal conditions (2.5°C, 2.5 kF) assumed in the repeater gain objective.\* The accuracy with which this correction can be done depends, of course, on factory measurement accuracy and the accuracy with which temperature coefficients, pressure coefficients, handling or laying effects, and actual seabottom temperatures and depths are known. The coefficients used to predict the seabottom loss are refined, and the accuracy with which the loss is matched to repeater gain can be expected to improve as experience is gained from actual SG installations.

### **3.2.1 Ocean-block equalizer**

In the SG system, a group of 30 repeaters is followed by an ocean-block equalizer (OBE).† Each OBE is adjusted just before being laid and is designed to compensate most of the transmission deviations that have accumulated up to this point in the installation. The OBE contains directional filters that permit the independent equalization of the two transmission bands. The equalization is effected by fixed (mop-up) networks and switchable networks. In addition, each band has a build-out network. The build-out networks are designed so that the total OBE loss is at its nominal value when the switchable shapes are at mid-range.

---

\* Superposed on the procedure described is a small cyclical length perturbation to reduce the systematic addition of interaction ripple due to finite repeater return losses.

† Because of uncertainties associated with first-time installation, the TAT-6 link has an OBE following every 20 repeaters.

This arrangement allows an OBE to provide either system gain or loss around a nominal setting.\*

**3.2.1.1 Mop-up networks.** The mop-up networks are bridged-T designs whose purpose is to equalize deviations known at the time the equalizer is manufactured.† The mop-ups are built from a stockpile of pre-aged components on standardized circuit boards, with maximum utilization of special-purpose computer programs. The aim is to minimize the time required to incorporate new knowledge about cable or repeaters into the OBE characteristics.

It is possible, for example, to incorporate knowledge acquired in the first lay (shipload) of a system in the equalizers being manufactured for the third lay. In fact, if there is sufficient reason, an equalizer can, on an expedited basis, have special mop-ups inserted and be ready for use in the next lay. It should be made clear that different equalizers can contain different mop-up networks. Up to seven mop-up networks may be used in each band. The excess gain available for mop-up networks is 9.5 dB in the low band and 12.5 dB in the high band.

**3.2.1.2 Switchable networks.** The shapes available in the switched networks are shown in Fig. 7; they are relatively smooth and are related to attenuation versus frequency characteristics associated with the undersea cable. (Figure 7 shows the equalization shapes. The actual bump and  $\sqrt{f} - f$  networks have some added  $\sqrt{f}$  for physical realizability.) The functional forms are listed in a companion article.<sup>8</sup> Each of seven switchable networks in each band can be independently switched either in or out of the transmission path through the equalizer ( $2^7 = 128$  combinations are available in each band). The best combination in a particular equalizer is selected on shipboard just prior to overboarding that equalizer. The choice is based on minimizing the misalignment indicated by transmission measurements made during laying. The measured transmission path extends from the shore terminal through the equalizer whose setting is to be determined.

The available amount of shape having a square-root-of-frequency characteristic ( $\pm 7.5 \sqrt{f/30}$ ) is somewhat larger than the misalignment allowed in the misalignment allocation discussed later. However, the large noise penalty which results if equalization range is exceeded dictates a comfortable margin.

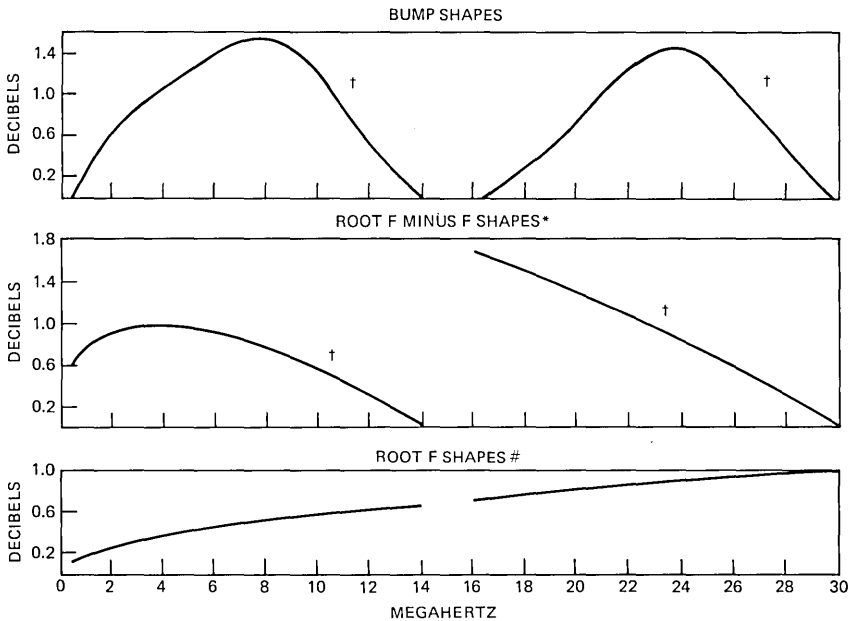
### **3.2.2 Shore-controlled equalizer**

As mentioned previously, four shore-controlled equalizers (SCE), di-

---

\* The source of any gain, of course, is an adjoining repeater. In effect, the switchable networks may be set so that the total OBE loss is less than the loss of the 4.1 nmi of cable which are omitted from the section containing an OBE.

† Known deviations whose shape is well matched by the broad switchable network shapes can be equalized by switchable network settings during laying. In using the switchable networks to aid in the mop-up function, one must leave enough range to handle deviations between predicted and actual sea-bottom cable transmission.



\*ADDITIONAL NETWORKS ARE PROVIDED, WITH 2 TIMES THE LOSSES INDICATED

# ADDITIONAL NETWORKS ARE PROVIDED, WITH 2 TIMES, 4 TIMES, AND 8 TIMES THE LOSSES INDICATED

† THE CURVES SHOWN ARE THE DESIRED FUNCTIONAL SHAPES. ACTUAL SHAPES PROVIDED HAVE SMALL AMOUNTS OF  $\sqrt{f/30}$  ADDED TO MAKE THEM PHYSICALLY REALIZABLE.

Fig. 7—OBE switchable shapes.

viding the system into five sectors, were included in the TAT-6 link to compensate cable aging. These equalizers contain directional filters, build-out networks, and switchable networks, but do not incorporate the mop-up function. The switchable shapes are the same as those used in the OBE but with about twice the decibel range. The larger range is possible because no gain is allocated to the mop-ups.

The ranges provided by the SCEs in TAT-6 are adequate to handle up to about 75 dB of top-frequency aging in either direction (i.e., gain or loss) and are consistent with the nonlinear sing margins discussed later in this paper. This amount of aging exceeds our forecasts based on modeling of aging to date. System aging is discussed further in Section IX.

The adjustment of SCEs is controlled from the low-band transmit terminal by a pair of control frequencies unique to each equalizer. A first control frequency is used to select the network to be switched in or out, and the second activates the switching. Second harmonics of the transmitted tones are returned to the terminal. By tuning the frequencies of the control tones to maximize the amplitudes of the returned second harmonics, it is possible to center the control frequencies in the pass-



bands of the SCE's crystal filters. Also, level changes of the returned second harmonic are produced by padding switched in by contacts on a deck of the network-select switch. These level changes indicate which SCE network is being addressed.

By the time deep-sea laying commenced on TAT-6, indications were fairly clear that, at least initially, aging would be in the direction of increasing loss. Thus, the OBES were adjusted to be a little deficient in loss initially, and each SCE was adjusted to compensate this intentional misalignment, which amounted to 2 dB excess gain per sector at the top frequency.

### ***3.2.3 Terminal equalization and protection***

The final level of equalization is provided in the shore terminals. A combination of smooth adjustable shapes, custom-designed residual equalizers, and regulation in the receiving multiplex holds transmission levels within acceptable limits.

At the output of the transmitting wideband line, a special circuit switches in extra loss if an excessive broadband signal is sensed. This is done to provide adequate protection against an accidental gross overload which might be capable of inducing gain changes in the undersea repeaters.

### ***3.2.4 Misalignment allocation***

In the design of a system, it is necessary to set misalignment objectives consistent with performance objectives and equalization ranges. These misalignment allocations then determine the permissible tolerances for the various contributors to misalignments. Table III shows the SG misalignment objectives, and Table IV shows the unit accuracies required to meet these misalignment objectives.

The initial uniform misalignment is in the form of sharp ripples, whose shapes preclude their equalization by the simple mop-up networks of the OBE. Sharp ripples have little effect on multichannel load and therefore can be equalized equally at the two shore terminals without cutting into the overload margin. Those ripples which are so sharp that they cannot be equalized in the broadband portion of the shore terminals may be eliminated by supergroup equalizers in the receive terminal. In the latter case, positively misaligned channels would be quieter than most, while negatively misaligned channels would be noisier than most.

### ***3.2.5 Noise penalties due to misalignment***

In estimating a noise penalty associated with the allocations of Table III, it is assumed that repeaters are fairly uniformly spread across the 5-dB level range of item I. A few repeaters that fall outside this limit on

Table III — Top-frequency\* misalignment objectives for 4000-nmi link

I. Initial within-block misalignment (not including effect of OBE)		
A. Maximum difference between highest- and lowest-level repeater in block		5 dB
B. Maximum difference between extreme-level repeaters of this block and extreme-level repeaters in rest of system		5 dB
C. Allocation of above		
1. Repeaters—total in any block		±1 dB/block
a. Systematic (within each block)		±0.02 dB/repeater
b. Random (within each block)		±0.07 dB/repeater
2. Cable		
a. Same in every block (e.g., error in coefficient)		+2.5 dB/block or -2.5 dB/block ±1.5 dB
b. Different in every block (error in sea-bottom temperature or pressure and manufacturing variations)		
II. Uniform misalignment along length of system		
A. Initial <sup>†</sup> (±0.2 dB/block for a maximum-length system with 30-repeater blocks)		±5 dB/system
B. Aging		±5 dB/sector <sup>‡</sup>

\* Allowance at lower frequencies obtained by multiplying top-frequency values by the smaller of 1.5 or  $\sqrt{30/f}$  and does not include intentional low-band boost.

<sup>†</sup> Assumed to be ripply and thus to have negligible effect on overload margin.

<sup>‡</sup> The stated range is consistent with the system noise objective. A total equalization range consistent with up to 75 dB of system aging is provided in the SCEs.

Table IV — Accuracy objectives to meet misalignment objectives for a 4000-nmi SG link with 30-repeater ocean blocks

	dB per unit	Percent
I. Repeater		
A. Average deviation from objective within a block (known and equalizable in OBE)*	±0.02/repeater	±0.05
B. Random (within each block) deviation <sup>†</sup>	±0.07/repeater	±0.15
C. Unequalizable (from Table III, item II A, ±5/800 repeaters = ±0.006 dB/repeater) (Cause: error in knowledge of gain characteristic, especially any component too sharp to be equalized by the OBE's mop-up networks)	±0.006/repeater	±0.015
II. Cable loss deviations		
A. Average sea-bottom loss deviations (causes are errors in the average: temperature coefficient, pressure coefficient, and laying effect) Limits on total error*	±0.08/section	±0.2
B. Random variations (block to block) (causes are: manufacturing variations, errors in seabottom temperature and pressure, and measuring error) Limits on total error*	±0.05/section	±0.1

\* Increased by a factor of 1.5 if block length = 20 repeaters.

<sup>†</sup> Increased by a factor of 1.2 if block length = 20 repeaters.

the low-level side do not have much effect on system noise performance. On the other hand, a few high-level repeaters, appreciably higher than most repeaters, cut into overload margin, and may cost almost decibel for decibel in performance. This must be kept in mind in equalizing the system as it is laid. In other words, if a high-level repeater occurs early in the installation, subsequent equalization should bring repeaters as close as possible to this level. As the installation approaches completion and a level range has been established by the repeaters already laid,

special care should be taken in equalization so that the levels of subsequently laid repeaters do not exceed the maximum of the established range. With these qualifications, a broadband misalignment of 10 dB would increase the ideal noise of Fig. 5 by only 1.25 dB. The ripply uniform misalignment, insofar as it is equalizable in the terminal, could bring the penalty up to 2 dB. The unequalizable portion might degrade a few channels by about 3 dB, improving others by about the same amount.

### **3.2.6 Nonlinear sing margin**

In addition to its effect on noise performance, misalignment is of interest in connection with nonlinear sing margin.

Nonlinear sing is a phenomenon which is possible in equivalent-four-wire systems using a single amplifier for both directions of transmission. Under conditions of gross overload (usually in the presence of large misalignments), these systems can lock themselves up in a so-called noise sing.<sup>3</sup> Under this situation, the nonlinearities result in so much cumulative energy shift from the low to the high band that the energy shifted to the high band can overload that band. The overloaded high band can, in turn, via the common amplifier, produce enough energy shift back to the low band to sustain the whole process.

Detailed computer studies were made using empirical data on repeater behavior under overload for a variety of conditions. It was found that the system would remain stable for superposed misalignments up to 15 to 20 dB.

## **IV. CABLE**

The bulk of any SG system is made up of 1.7-in. core diameter armorless deep-sea cable. The portions on continental shelves are largely composed of single armored cable. The portion from the terminal to the shore as well as the first mile or so out from the shore is shielded and uses a smaller diameter dielectric. The shielding is protection against radio interference in the portions of the system that are exposed to radio fields.

Out to depths of 640 m (350 fathoms), in addition to using armored cable, the cable and repeaters of TAT-6 are buried approximately 0.6 m (24 in.) beneath the ocean floor. These measures should provide excellent protection against cable breaks due to trawlers and dredges.

The attenuation of the 1.7-in. cable at seabottom conditions (2.5 kilofathoms and 2.5°C) is given approximately by  $(\alpha = 1.383 \sqrt{f} + 0.0178f \text{ dB/nmi})$ , where  $f$  is in MHz. The square-root term is due to resistive losses in the copper, whereas the linear term is caused by dissipation in the polyethylene. At the top frequency of 30 MHz, total loss is about 8.1 dB/nmi. Of this loss, 0.53 dB, or 6.6 percent, is due to dissipation in the polyethylene.

## V. REPEATER CHARACTERISTICS

### 5.1 Supervisory arrangements and insertion gain

The SG repeater consists of a two-stage preamplifier, a three-stage power amplifier, an output band-limiting filter and shaping network, directional filters, power-separation filters, and a supervisory oscillator. Each supervisory oscillator has its unique frequency, which may be used to identify its associated repeater, and to pinpoint undersea system problems. Normally, repeaters with low-band oscillators alternate with repeaters having high-band oscillators.

The gain objective for the SG repeater is the sum of the loss of 5.1 nmi of cable at 2.5 kilofathoms and 2.5°C and the low-band gain boost. The gain shape is shown in Fig. 8.

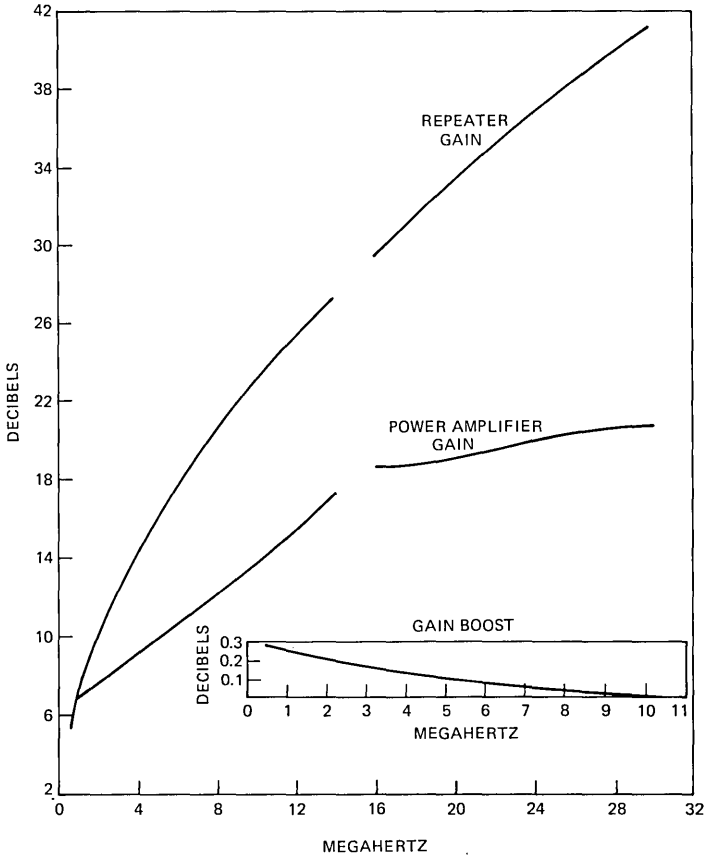


Fig. 8—Repeater and power amplifier gain.

## 5.2 Noise and modulation performance

Figures 9 through 15 show the values of the various parameters\* which, along with repeater gain, determine the noise performance of the system. As was indicated in Fig. 5, the pre-amplifier and power amplifier contribute about equally to the second-order intermodulation noise. The total for the repeater is the voltage sum of the noise produced by the pre-amplifier and power amplifier. The power amplifier is the dominant contributor of third-order noise. The computed contribution of the pre-amplifier raises the total amplifier noise by less than  $\frac{1}{2}$  dB, even when the two sources are added on a voltage basis.

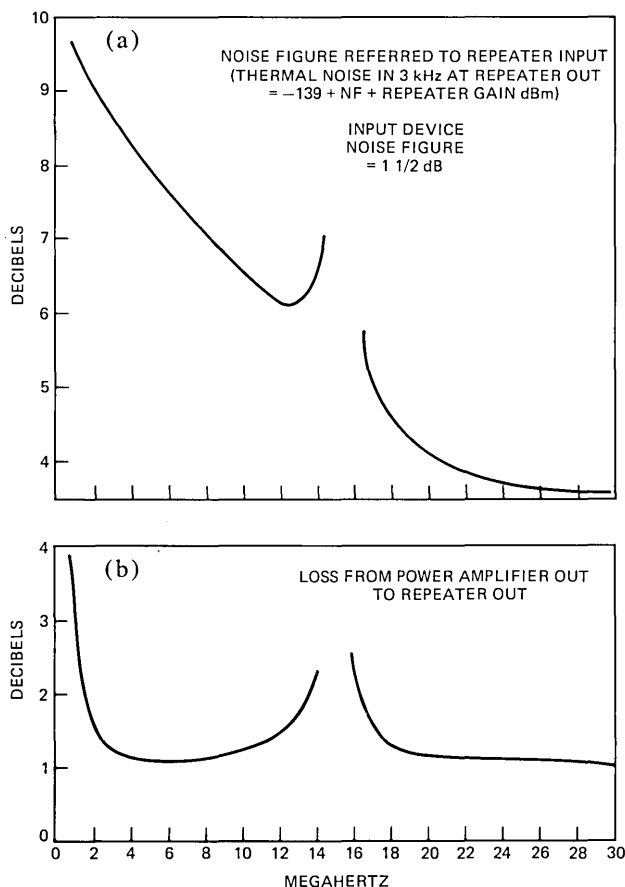


Fig. 9—(a) Repeater noise figure. (b) Output loss.

\* These data are the ones determined prior to the installation of TAT-6 and used for the noise computation results of Fig. 5. As discussed later in this paper, the  $M_{3E}$  values shown were better than actual repeater performance over the upper portion of the high band.

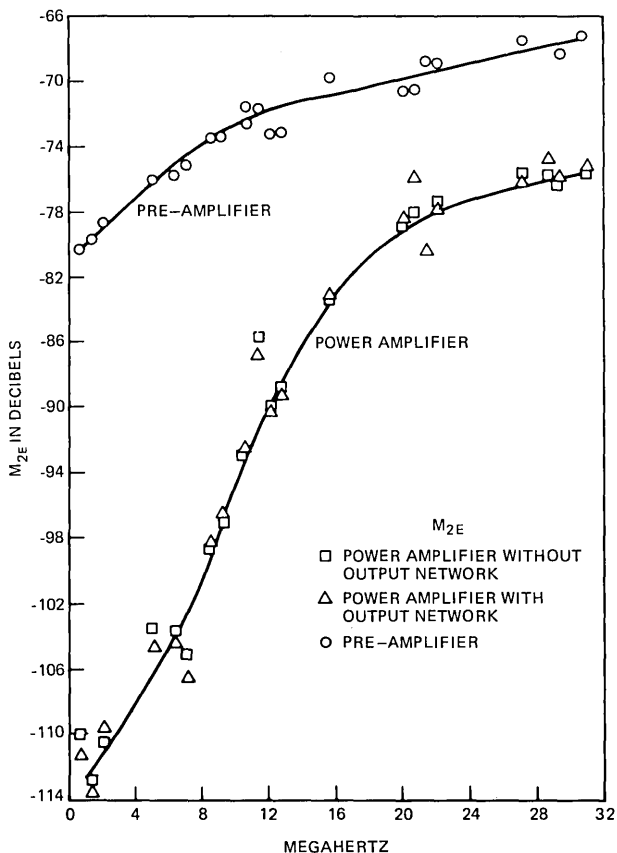


Fig. 10— $M_{2E}$  repeater modulation coefficients (referred to POWER AMP OUT and to PRE-AMP OUT, respectively).

### 5.3 Load-carrying capacity

Figure 13 shows the behavior of  $M_{2E}$  and  $M_{3E}$  coefficients as a function of peak repeater output power. Four frequencies are used in the test to give a reasonable peak factor, even though only two or three of the four sine waves are involved in the measured product.

If the repeater behaved according to the classical Taylor series model, the curves displayed on Fig. 13 would be horizontal lines, i.e., intermodulation coefficients would be constant. Actually, the coefficients deviate from this ideal picture as the load is increased, eventually going off in the unfavorable (upward) direction. One can define the load capability in terms of a departure of the coefficients by a few decibels from their low-level values. One can conclude from Fig. 13 that the peak power capability of the SG repeater is approximately 26 dBm.

To obtain the results shown in Fig. 14, the circuit is loaded with frequency-shaped thermal noise except for a slot at 27 MHz. In this slot,

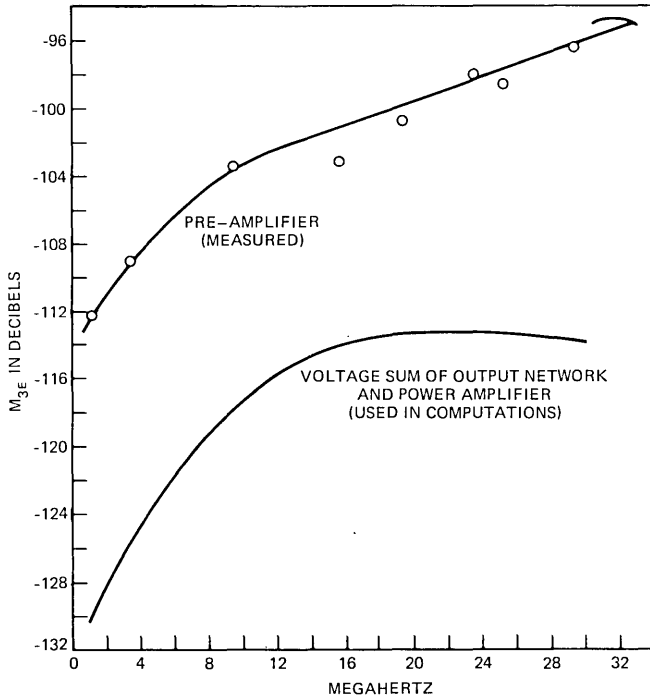


Fig. 11— $M_{3E}$  repeater modulation coefficients (referred to POWER AMP OUT and to PRE-AMP OUT, respectively).

the intermodulation noise of a single repeater is fed into a 1.74-kHz bandwidth detector and then into a multi-channel amplitude analyzer.

The resulting amplitude distributions are plotted for a number of repeater output powers in Fig. 14. As the curve shows, at +14 dBm, very slight departures from a Gaussian distribution are noted. By the time the test signal has been raised to +15 and +16 dBm, gross departure from a Gaussian distribution is observed. Although the results are not plotted in Fig. 14, for test signals of +13 dBm and lower, the amplitude distribution of intermodulation noise is indistinguishable from a Gaussian distribution.

The test results shown on Fig. 14 prove to be a very sensitive means of determining the repeater's load capacity. Note that a random noise test signal of +13 dBm corresponds to a peak power of +26 dBm or an rms sine wave power of +23 dBm. Thus, the load capability determined from Fig. 14 agrees with that determined from Fig. 13 and the value used in the system layout shown in Table II.

Finally, Fig. 15 presents the limits on gross overload; exceeding these would risk inducing repeater gain change. These last limiting powers, which exceed considerably the load capacities defined by Figs. 13 and

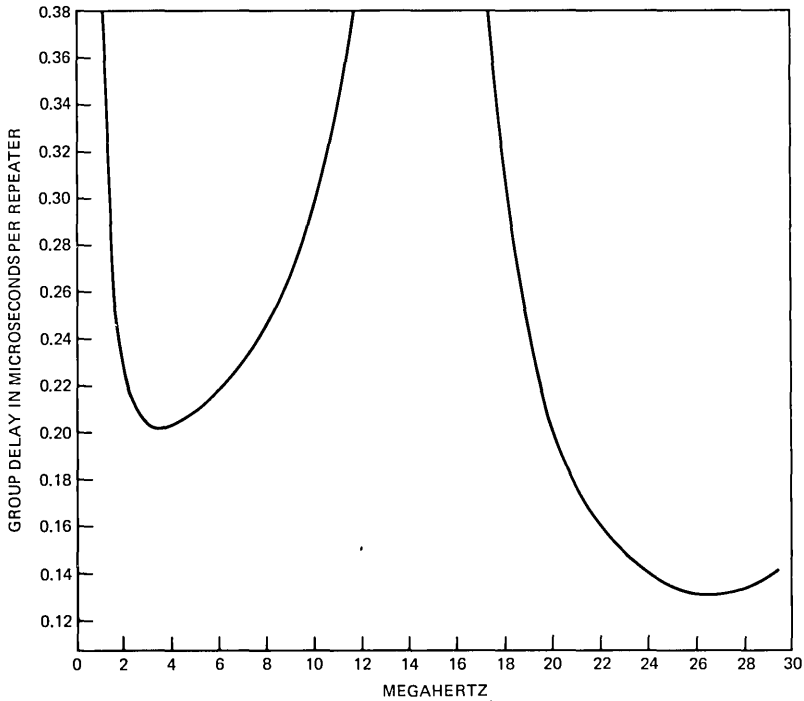


Fig. 12—Repeater group delay.

14, form the basis for adjusting the SG terminal's undersea system protection circuit, which was referred to in Section 3.2.3 and is covered in greater detail in Section VII.

## VI. RELIABILITY OBJECTIVES

Newer generations of undersea cable systems pose ever more challenging problems. Between one generation and the next, the number of repeaters for a given length approximately doubles. At the same time, the complexity of each repeater increases. Despite these trends, the newer generation goal is to achieve approximately the same system reliability as that of earlier systems.

In the SG development, reliability was enhanced by a number of measures. Throughout development, mechanical design proceeded hand-in-hand with electrical design. (This was necessary for both performance and reliability reasons.) Highest quality raw materials were used. Inspection extended all the way from raw materials to the finished product. The 30-MHz top frequency required components and devices which were close to the state of the art. Each such new item was accompanied by its own carefully thought-out reliability testing and inspection program tailored to the new art.



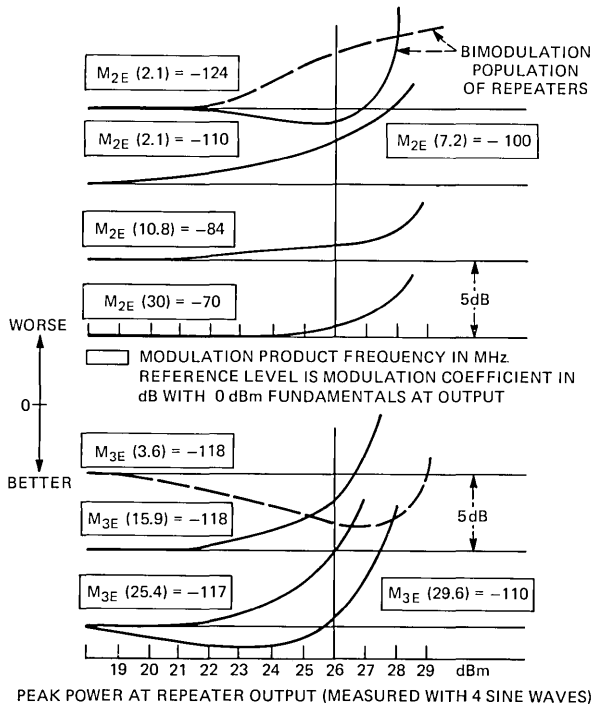


Fig. 13—Repeater excess modulation vs load power.

Early in the project, studies allocated reliability targets to various devices and components. Table V compares the device and component objectives of the SG system with reliability achieved in earlier generations of undersea cable systems. Note that the design objectives of the SG system correspond approximately to those which have been achieved in field experience on the earlier systems.

Achievement of the SG reliability targets would result in a repeater electronics reliability of 21 FITS. On the basis of experience, one might expect an approximately equal number of failures associated with other portions of the undersea link. If this proved to be the case for SG, the TAT-6 link would experience a mean system rate of 0.26 failures per year.

At the time of writing, TAT-6 has functioned reliably with no interruption since it went into service in July 1976.

## VII. SHORE TERMINALS

Functionally, the shore terminal consists of: (i) terminal transmission

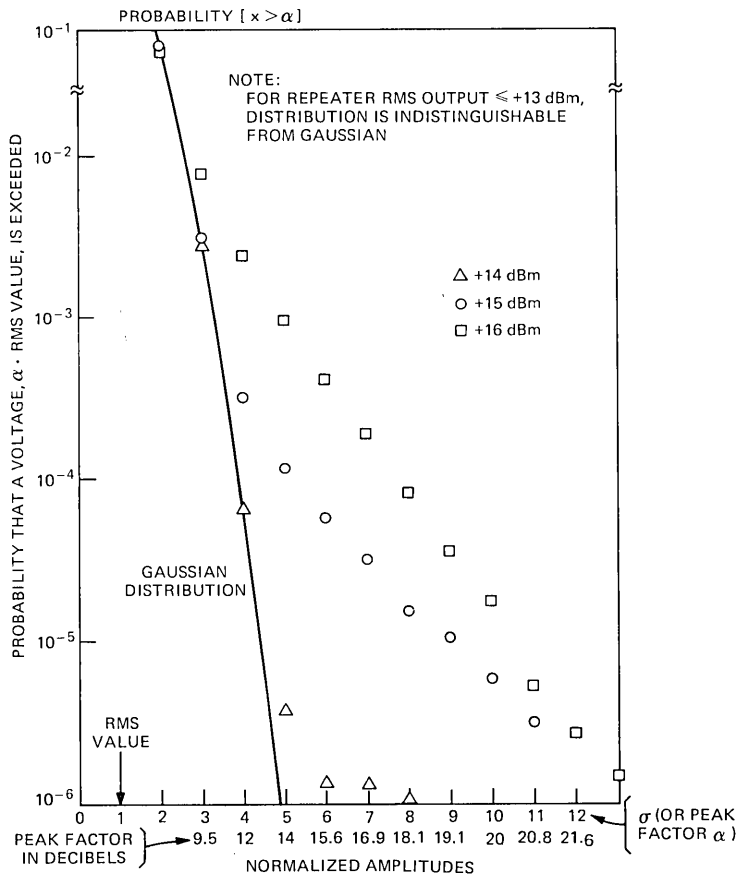


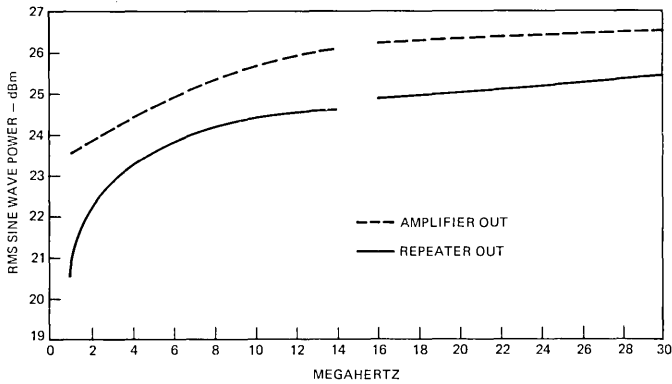
Fig. 14—Normalized amplitude distribution of 27-MHz intermodulation noise of a single repeater as a load-capacity defining phenomenon.

equipment made up of the multiplex, wideband line, and pilot monitoring equipment, (ii) power feed equipment for the undersea repeaters, and (iii) fault location measuring equipment.

From a transmission point of view, the SG system is defined from transmit supergroup input to receive supergroup output. The multiplex (and its associated carrier supply) consists of supergroup and hypergroup\* frequency translation. Terminal wideband lines provide equalization capability to optimize noise performance and provide end-to-end flat transmission.

Signal limiting is provided at the input of each transmitting super-

\* In SG, the hypergroup consists of an assemblage of 10 supergroups. Hypergroup 1, an exception, contains 14 supergroups.



NOTES:

1. RMS BROADBAND POWER OF A MULTI-CHANNEL SIGNAL AT AMPLIFIER OUT SHOULD BE LIMITED TO +18 dBm.
2. EXCEEDING LEVELS SHOW IN GRAPHS CAN RESULT IN REPEATER GAIN CHANGE

Fig. 15—Maximum permissible single sine-wave power.

Table V — Reliability of active and passive components

Component Type	Component Reliabilities in FITS*	
	SG Design Objectives	Field Experience†
Active device (transistor or electron tube)	1.0	0.9
Diodes	0.5	0.0
Passive components	0.05	0.06

\* FITS are defined as the number of failures in 10<sup>9</sup> component hours.

† Basis is failures observed on the earlier generations of U.S. systems designated SB, SD, and SF.

group. In addition, a protection arrangement in the transmit wideband line introduces added loss if necessary to avoid gain change in undersea repeaters due to gross broadband or single-frequency overload. (Figure 15, referred to earlier, shows these repeater limits.) This protection is adequate, even in the presence of positive misalignment.

The power feed equipment provides a current-regulated source of 657 ± 0.3 mA to power the undersea repeaters. It is capable of providing up to 7500 volts and shuts down in the presence of voltages and currents capable of damaging the system.

Fault location equipment consists of general purpose dc and low-frequency test sets, and a repeater monitoring set. The repeater monitoring set is capable of measuring: (i) repeater supervisory tones and (ii) "echoes" produced by high-level test signals acting on repeater nonlinearities.

## VIII. ACHIEVED PERFORMANCE

### 8.1 Transmission equalization

Initial misalignments encountered during installation of TAT-6 were generally within the allocations of the system plan. Figure 16 shows the within-block misalignment (i.e., net gain or loss from the first repeater to the last repeater in an ocean block, ignoring the intentional low-band gain boost) averaged over all the blocks. Comparison of the two curves of Fig. 16 shows the effect of OBES in reducing misalignment. The broad component of pre-OBE misalignment was less than  $\pm 2$  dB in most blocks and was about  $\pm 4$  dB in the worst block. The ripply structure was somewhat larger than expected and hard to predict since it was mostly a result of reflection at the repeater termination. It is a function of the exact length of the pigtail (flexible coaxial lead) between repeater and cable termination and is different for a pigtail surrounded by water as compared to one in air. The actual pigtail length depends on the relative orientation of repeater and termination aboard ship at the time of splicing. The ripple is very small per termination (and therefore hard to measure) but becomes important when many terminations occur in series (1400 in a system).

The solid curve of Fig. 17 shows the transmission of the undersea system from first to last repeater. The dashed curve in the figure shows transmission from a flat level point in one terminal to that in the other. Comparison of the two curves shows the effect of the terminal broadband equalization. Beyond this, there is still equalization at the receive supergroup level, where required, to flatten out the transmission.

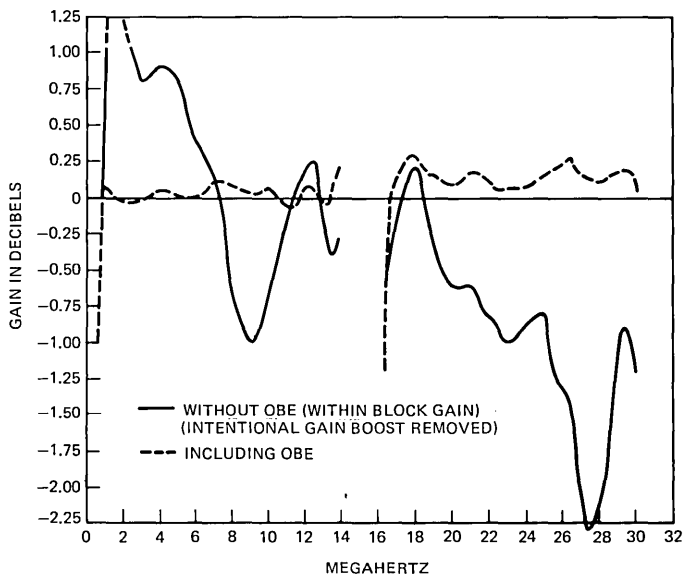


Fig. 16—Average misalignment/block.

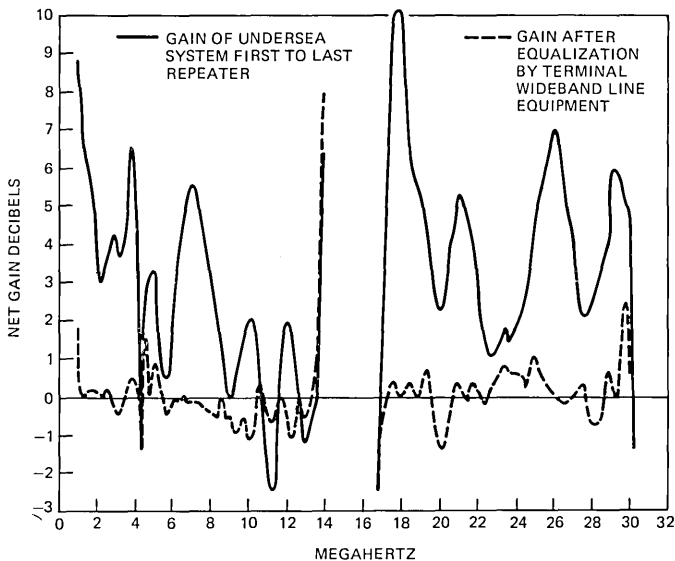


Fig. 17—Gain of TAT-6 before and after equalization by terminal wideband line equipment.

Figure 18 shows some level diagrams along the length of the system at some sample frequencies to illustrate SG equalization as a function of length. Most of the diagrams show behavior at ripple maxima and minima, with only the cases at 10.5 and 22 MHz representing behavior near zero crossings. The sawtooth pattern at 2 MHz is due to the gain boost. The data in these figures are obtained from laying measurements.

## 8.2 Noise performance

Noise performance of a new system is measured and optimized during commissioning<sup>9</sup> by means of noise loading tests. Commissioning refers to the large number of tests and adjustments required to carry a system from the time of the final splice to the time of initial commercial service. In these tests, the multichannel load is simulated by a noise “signal,” and the system noise is measured in selected frequency slots, which can be cleared of signal by inserting band-stop filters in the transmitting terminal. The stop filters are sufficiently narrow to have negligible effect on the total load. A signal-to-noise ratio is determined by the ratio of the received power in the selected slot without and with the insertion of the corresponding band-stop filter (this ratio is referred to as the noise power ratio, or NPR). Transmitting levels are adjusted to give the best achievable signal-to-noise ratios.

Initial noise loading tests on TAT-6 were made with the noise power

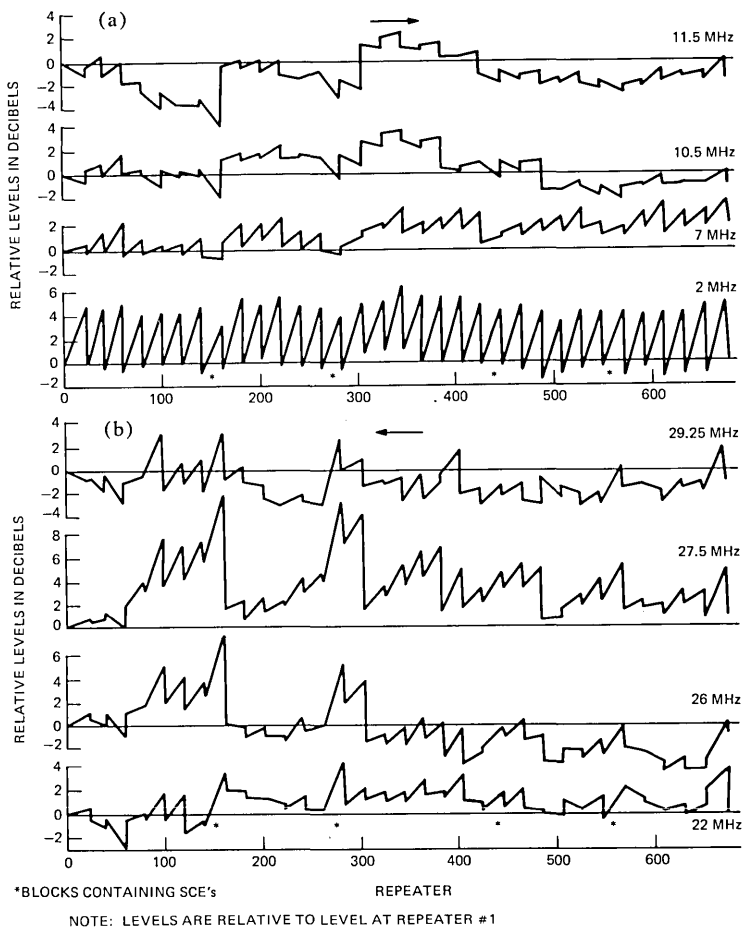


Fig. 18—Levels along length of TAT-6 at selected frequencies. (a) Low band. (b) High band.

density shaped vs frequency in such a way as to realize near-optimum noise performance if the repeater behaved in the expected manner. Actually, in these tests, the low band and the lower two-thirds of the high band came out largely as expected. However, the top one-third of the high band was noisier than anticipated. After considerable time was spent verifying that this was due neither to a measuring problem nor to a few repeaters suffering from some kind of a fault condition, it became apparent that this was an intrinsic property of the system.

Figure 19 shows the noise performance achieved after level re-optimization, as compared to that originally expected. Figure 20 shows optimized levels corresponding to this result, also compared to those expected. The results of Fig. 19 were obtained by measuring thermal noise

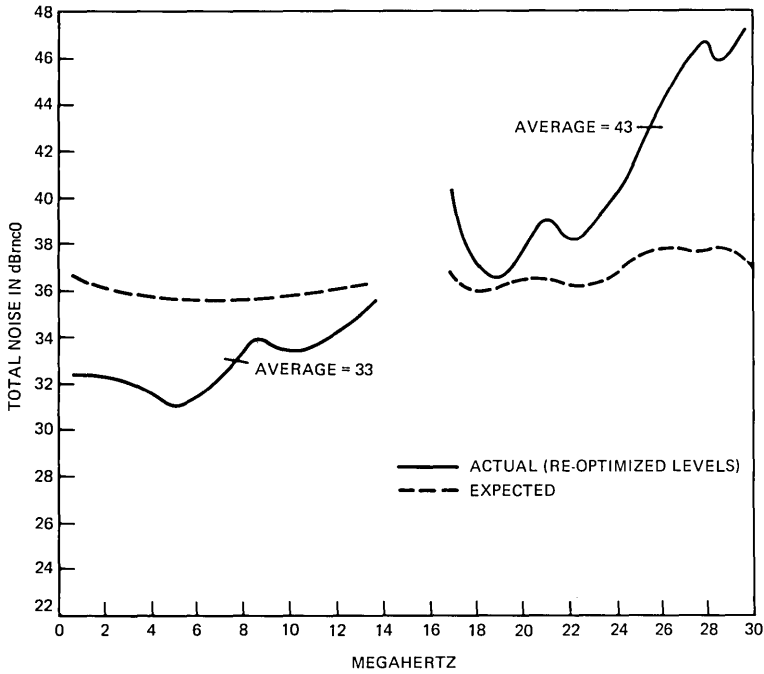


Fig. 19—System noise performance.

and calculating the increase due to modulation noise. The modulation noise for this calculation was obtained from noise loading measurements, interpolating between measured points where necessary. System noise performance shown on Fig. 19 was better than anticipated at lower frequencies. This was because optimized levels at the higher frequencies were lower than expected, thus reducing the *A-B* intermodulation products falling in the low band.

### 8.2.1 Nature of excess noise

The portion of the frequency spectrum in which the excess noise occurred suggested that the source of excess noise was third (or higher)-order intermodulation. This was confirmed by loading the high band only. Since this band is less than one octave wide, no second-order intermodulation can contribute to noise within it.

The NPR curves of Fig. 21 show that, whereas one would expect the curve at higher loads to have a slope of  $-2$ ,\* the system shows a much

\* Third-order products or noise are expected to increase 3 dB for each 1-dB increase in signal. Thus, the signal-to-third-order noise ratio should decrease 2 dB per 1 dB increase in signal.

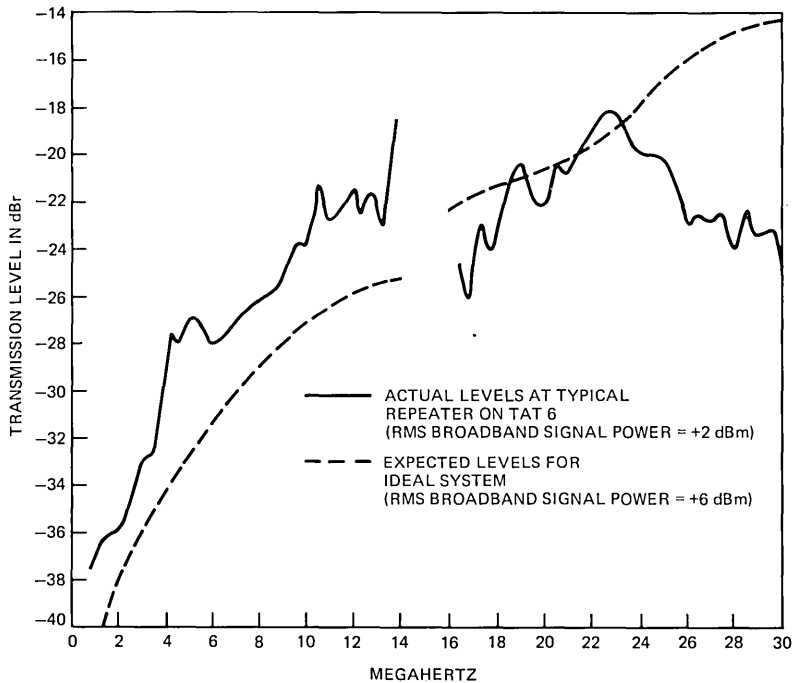


Fig. 20—Transmission levels at repeater out.

shallower slope. This is clearly indicative of anomalous behavior and provides the beginning of an explanation of why this behavior had not been clear from measurements on single repeaters or from testing an assembly of ten repeaters during SG development. The dashed curves show what was expected from the assumed constant values of  $M_{3E}$ , but using the “actual” levels of Fig. 20.

Third-order intermodulation noise is only of system significance compared to second order and thermal noise because, in the absence of delay distortion, it adds on a voltage (systematic) basis while the other two noises add on a power (rms) basis. Thus, by normal measuring techniques, the only way to see third-order intermodulation noise produced by noise loading of one or a few repeaters is to load with a power much higher than normal for a system, and extrapolate down to the operating point, assuming the classic 2-for-1 slope. The results of Fig. 21 show that a much shallower slope prevails, so that such an extrapolation would be much too optimistic.

The usual way to compute intermodulation performance is to measure intermodulation products produced by two or three discrete fundamental frequencies. Techniques then exist to estimate performance with a real load from the modulation ( $M$ ) coefficients determined from the discrete tone measurements.<sup>10</sup> However, these techniques assume that



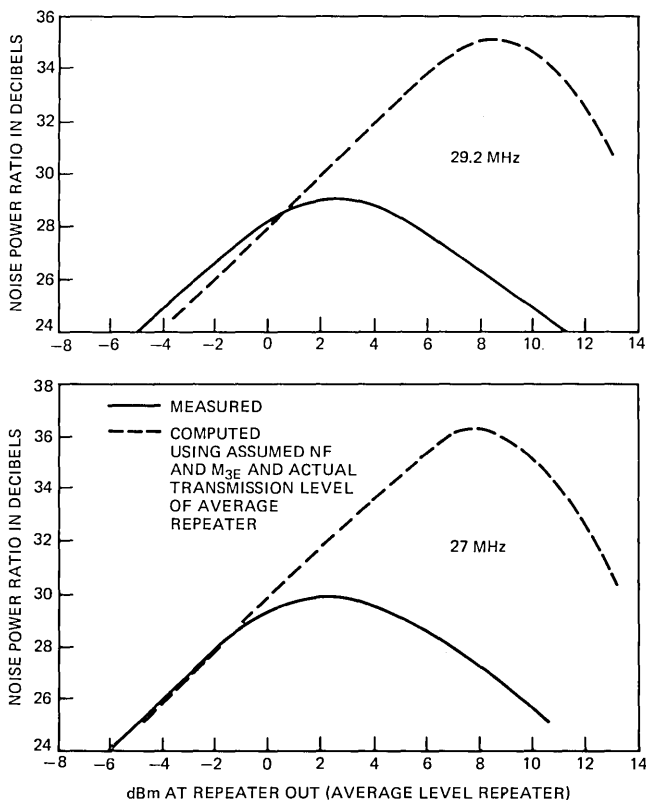


Fig. 21—NPR (signal-to-noise ratios) on system—highband only loaded.

the discrete tone intermodulation is a function only of product frequency and not of the frequencies of the fundamentals. This assumption had been substantially true in earlier systems.

In the development and manufacture of SG, a set of fundamental frequencies believed to be typical had been selected to measure intermodulation. The behavior of products generated by these fundamentals was normal, and the values obtained were those shown in Fig. 11. These results led to computed noise performance consistent with the objective, as shown in Fig. 5.

After the discovery of the third-order intermodulation problem, extensive additional measurements were made. It was found that fundamentals existed which produced products of a much higher level than those produced by the standard fundamentals used during development and manufacture. Furthermore, these products did not vary 3 dB for each decibel of change in the power of fundamental power (i.e.,  $M$  coefficients were not fixed, but were a function of power). Finally, whereas third-order modulation from the standard fundamentals was

slightly better at sea-bottom temperature as compared to room temperature, these new fundamentals generated much more intermodulation at the cooler sea-bottom temperature than at room temperature.

What made the problem much worse was that many of these "bad" fundamentals were in the portion of the spectrum where there was almost no delay distortion (see Fig. 12). This meant that the intermodulation products of highest amplitude were the very ones that added in-phase from repeater to repeater. Figure 22 shows some  $M_{3E}$  coefficients determined from discrete tone measurements on the system using fundamentals very close to the product frequencies. These can be compared to the "nominal"  $-113$  dB  $M_{3E}$  and to the  $M_{3E}$  coefficients of Fig. 11. The values in Fig. 11 which were measured with "standard" fundamentals had been thought to be the correct ones.

Figure 23 shows the dependence of  $M_{3E}$  on source frequencies. These modulation coefficients were measured on a single repeater at sea-bottom temperature at a particular power level and for a particular product frequency. Instead of the usual situation in which one might expect at most a few decibel variation over the whole range of possible source frequencies (up to the overload power), these "isomods" show gross changes as a function of fundamental frequencies.

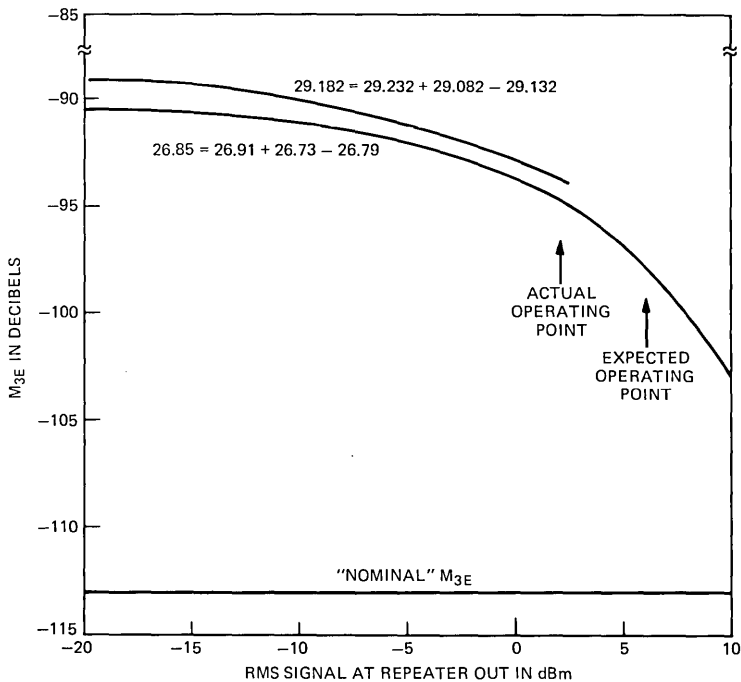


Fig. 22— $M_{3E}$  determined from system measurements using fundamentals close to product frequencies.

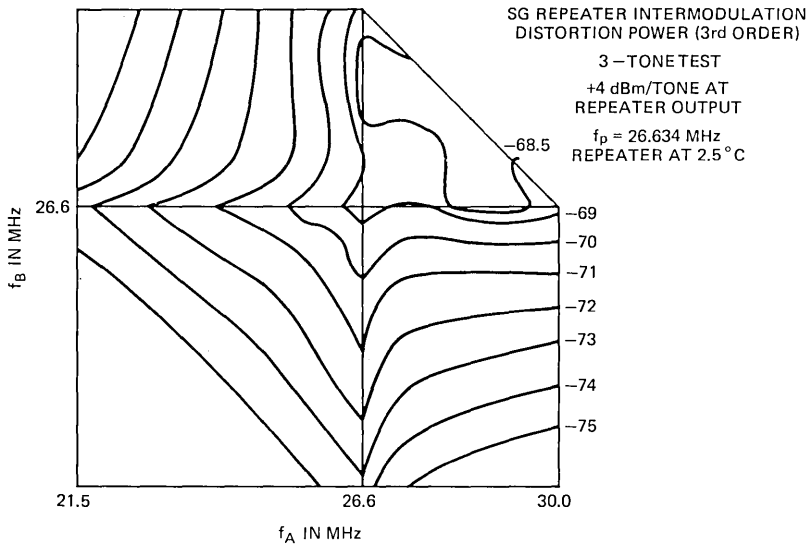


Fig. 23—Three-tone ( $A + B + C$ ) isomod contours for SG repeater with surge protection diodes (sea-bottom temperature).

Thus, the much-worse-than-anticipated values of  $M_{3E}$  at the anticipated operating level were the source of the problem. It was then further aggravated by the shallow slope; that is, signal-to-noise ratio improved at a much more gradual rate than 2 for 1 as levels were reduced to diminish the third-order noise. This behavior forced us to reduce levels even more, degrading the signal-to-thermal noise ratio in the process.

In the top third of the high band, the achieved noise performance is poorer than the worst-channel objective by as much as 5 dB, and the average noise in the high band exceeds the average-channel noise objective by about 4.5 dB. These levels of noise do not render circuits unusable, but do represent an undesirable service degradation.

### 8.2.2 TAT-6 modulation improvement

Our program of modulation improvement involves placing equipment at the Green Hill, Rhode Island terminal to cancel third-order distortion in the upper portion of the high band. Transmission and delay equalizers will duplicate the electrical conditions at the middle of each ocean block of the undersea system. Then at each such virtual ocean-block point, a distortion generator will introduce distortion to balance out third-order distortion of the corresponding ocean block of the undersea link.

Field trials at Green Hill with a single distortion generator have achieved significant noise cancellation. These were feasibility trials performed by noise-loading a single supergroup at a time in the part of the high band where delay is relatively flat. Indications are a 12- to 15-dB reduction in third-order intermodulation can be realized, which will allow the TAT-6 link to meet its original performance objectives.

The Green Hill installation will include duplicate distortion canceling chains. Normal terminal monitoring and automatic switching arrangements will assure service continuity.

### **8.2.3 Intermodulation improvement of future SG links**

Studies of the third-order modulation concluded that the reverse-biased output protector diodes were a major source of anomalous distortion. These diodes protect the power amplifier output stage against surge damage.

Independent of the modulation problem, Bell Laboratories had examined a double-epitaxial transistor design. The deeper second epitaxial layer makes these transistors highly resistant to second-breakdown damage. Using double-epitaxial transistors in the output stage eliminates entirely the need for the reverse-biased diodes. Laboratory tests indicate that the new combination is actually more rugged than the earlier arrangement.

Studies of intermodulation further indicated that interface states at the boundary between silicon and silicon-oxide layers of the transistor were a second source of the anomalous third-order distortion. This boundary, or interface, is produced by the transistor's silicon oxide (plus silicon nitride) passivation. Experiments suggested that shifting the crystalline orientation of the transistor starting material from  $\langle 111 \rangle$  to  $\langle 100 \rangle$  would greatly reduce the number of interface states, and hence the amount of anomalous distortion. Future SG links will have improved performance based on such a change in the output stage of the power amplifier. The first two stages of the power amplifier will retain transistors with the  $\langle 111 \rangle$  orientation, since experiments established that a *small* amount of anomalous distortion will cancel some of the normal distortion, leading to an amplifier which is more linear than one using  $\langle 100 \rangle$  transistors in every stage.

## **IX. SYSTEM AGING**

In its two years of service (since commissioning), the system has aged in the direction of increased loss by about 25 dB at 30 MHz with a shape that is approximately linear with frequency. The incorporation of shore-controlled equalizers is thus seen to have been well worth while. Work is currently going on to identify the physical mechanisms responsible for the transmission change. Until a particular physical mechanism or mechanisms are proven to be the cause, predictions of aging over the life of the system must be made with caution. On a pure curve-fitting basis, log or exponential functions of time appear to fit the observed data. These functions would predict end-of-life top frequency aging as large as 50 dB or as low as 30 dB.

Suppose end-of-life total aging proves to be 35 dB. This is 7 dB per

SCE sector. Since the TAT-6 link was pre-equalized by 2 dB per sector, as described in Section 3.2.2, we would be left with a net loss per sector of 5 dB, which is within the system misalignment allocations.

## **X. EQUALIZATION AND PERFORMANCE**

The initial equalization results achieved on TAT-6 are satisfactory and in keeping with misalignment allocations. Equalization knowledge gained in laying TAT-6 will allow the use of 30-repeater ocean blocks in future systems, still keeping misalignments within the desired range.

Regarding reliability, definitive statements require further operational experience. However, the TAT-6 link has been operating continuously since commissioning in July 1976. We fully expect that the superior job of burying the shore ends with Sea Plow IV, plus the great care in each step of design and of manufacture, will result in meeting our reliability targets.

Although less than six months elapsed between the start of design and initial shipment of shore-controlled equalizers, the four SCEs in the TAT-6 link are performing satisfactorily. These have been reset once since commissioning, to compensate cable aging.

It now appears that there will be enough range in the SCEs to compensate aging throughout TAT-6's lifetime. By keeping misalignment within bounds, and thus minimizing the noise penalty associated with cable aging, the SCEs are contributing importantly to the performance of TAT-6.

## **APPENDIX**

### ***Glossary***

#### ***A.1 Terms for system description***

**REPEATER SECTION** A length of cable with its associated repeater. Nominal deep-sea repeater sections for SG are 5.1 nmi long.

**OCEAN-BLOCK EQUALIZER (OBE)** Passive unit designed to reduce the residual gain or loss at the time the system is laid, which results from discrepancies between the gain of repeaters and the loss of the associated cable sections.

**OCEAN BLOCK** A number of repeater sections and their associated OBE. For TAT-6, ocean blocks were 20 repeater sections (98 nmi) long. Future SG links will have 30-repeater (149-nmi) ocean blocks.

**SHORE-CONTROLLED EQUALIZER (SCE)** Undersea unit placed following a number of ocean blocks. The basic purpose of the SCE is to compensate long-term changes in transmission occurring after installation, such as those due to cable aging.

**SECTOR, OR SCE SECTOR** An SCE and its associated ocean blocks. In TAT-6 there are seven ocean blocks per SCE; hence, sectors are about 680 nmi long.

## A.2 Terms for signal description

**ZERO LEVEL POINT (0 dBr)** Used to provide a reference for expressing transmission level.

**TRANSMISSION LEVEL** The net gain or loss in decibels from a reference point (the zero level point) to the point in question. For net gains, the transmission level is positive; for net losses, it is negative. Transmission level may be expressed as  $\pm X$  dBr.

**CHANNEL LOAD,  $P_c$**  The average signal power in a one-way voice channel. This power is expressed in dBm0, decibels relative to one milliwatt at the zero-level point. The SG average channel load was taken as  $-13$  dBm0.

**BROADBAND LOAD,  $P_{av}$**  The total average power in a wide-band signal. Where this signal is composed of  $N$  two-way voice channels combined with equal weighting,  $P_{av} = P_c + 10 \log_{10} 2N$  dBm0.

**MULTI-CHANNEL PEAK FACTOR,  $k_m$**  The ratio, expressed in dB, between the 0.001 percent peak power and the average power of the multi-channel signal. When the number of channels is very large, the signal's  $k_m$  approaches that of Gaussian noise. Thus, for SG the multi-channel peak factor = 13 dB.

**PEAK FACTOR,  $\alpha$**  The ratio of peak voltage to rms voltage. A peak factor of 5 would indicate voltage five times larger than the rms voltage. To express the peak factor as a power ratio in decibels, we take  $20 \log \alpha$ .

## A.3 Channel noise terms

**CHANNEL NOISE** The background interfering power in the bandwidth of a single channel.

**WEIGHTING** The function vs frequency which allows for the fact that different frequencies interfere with voice communication to different degrees.

**PSOPHOMETRIC WEIGHTING, ( $p$ )** A noise weighting curve adopted as international standard by the CCITT.

**C-MESSAGE WEIGHTING, ( $c$ )** Noise weighting currently in use in the Bell System domestic plant.

**REFERENCE NOISE,  $m$**  One picowatt, or  $-90$  dBm before applying any weighting.

## A.4 Equalization terms

**EQUALIZATION** The process of adjusting system elements (typically equalizers) so that transmission is kept within prescribed limits at all frequencies and points in the system.

**MISALIGNMENT (dB)** The extent to which equalization departs from the ideal. Positive misalignment represents gain, while negative

represents loss. Misalignment can be absolute (departure from a nominal level), or relative (departure of level from levels at other units along the system). In laying an undersea system, one is concerned with relative misalignment, since all undersea levels may be shifted up or down by terminal adjustments after the system is laid.

**UNIFORM MISALIGNMENT** Misalignment which increases at a constant rate going along the system.

### **A.5 Cable terms**

**NAUTICAL MILE (nmi)** When used for cable, refers to a cable nautical mile, 1855.3 meters, or 6087 feet.

**DISSIPATION FACTOR,  $\tan \delta$**  The tangent of the polyethylene dielectric loss angle. For high quality dielectrics,  $\tan \delta \approx \delta$ , and the dissipation factor is given in microradians at a particular frequency.

**TEMPERATURE COEFFICIENT,  $\Delta\alpha_t$**  The change in loss of cable with change in temperature. Usually given in percent per degree Celsius at specified frequency and reference temperature and pressure.

**PRESSURE COEFFICIENT,  $\Delta\alpha_p$**  The change in loss of cable with change in pressure. Usually given in percent change per kilofathom at specified frequency and reference temperature and pressure.

### **A.6 Repeater terms**

**NOISE FIGURE, NF\*** The number of decibels by which the output thermal noise power of a repeater, when referred to the input by the repeater's available power gain, exceeds the ideal value given by  $kTB$  ( $k$  = Boltzman's constant =  $1.3806 \times 10^{-23}$  joules/degree Kelvin,  $T$  = temperature in degrees Kelvin, and  $B$  = bandwidth in hertz). At room temperature of  $17^\circ\text{C}$ , or  $290^\circ\text{K}$ , this limiting or ideal value of noise is given by  $P = (-174 + 10 \log B)$  dBm.

**MODULATION COEFFICIENT,  $M_{2E}$**  An equivalent second harmonic coefficient which, acting in a repeater whose nonlinearity can be modeled by a Taylor series, would give the observed  $A-B$  products. If  $M_{\alpha-\beta}$  is the  $A-B$  coefficient,  $M_{2E} = M_{\alpha-\beta} - 6$  dB. For an  $M_{2E}$  of  $-70$  dB, application of  $\alpha$  and  $\beta$  frequencies, each with a power of  $0$  dBm at the point at which the modulation coefficient is defined, would result in a power at frequency  $(\alpha - \beta)$  given by:  $P_{\alpha-\beta} = -70 + 6 = -64$  dBm.

**MODULATION COEFFICIENT,  $M_{3E}$**  An equivalent third-harmonic coefficient which, acting in a repeater whose nonlinearity can be modeled by a Taylor series, would give the observed  $A + B - C$  product. If  $M_{\alpha+\beta-\gamma}$  is the  $A + B - C$  coefficient,  $M_{3E} = M_{\alpha+\beta-\gamma} - 15.6$  dB. For an  $M_{3E}$  of  $-113$  dB, application of  $\alpha$ ,  $\beta$ , and  $\gamma$  frequencies, each with power of  $0$  dBm at the point at which the modulation coefficient is defined, would result in an  $\alpha + \beta - \gamma$  power given by  $P_{\alpha+\beta-\gamma} = -113 + 15.6 = -97.4$  dBm.

\* Reference 10 discusses noise figures in detail.

MAXIMUM SINE WAVE OUTPUT POWER,  $P_R$  The maximum power the repeater can handle before some specified impairment or distortion occurs.

## REFERENCES

1. Special Transatlantic Cable issue, B.S.T.J., 36, No. 1 (January 1957), pp. 1-326.
2. Special SD Submarine Cable System issue, B.S.T.J., 43, No 4, Part 1 (July 1964), pp. 1155-1467.
3. C. D. Anderson "Overload Stability Problem in Submarine Cable Systems," B.S.T.J., 48, No. 6 (July-August 1969), pp. 1853-1864.
4. "SF Submarine Cable System," B.S.T.J., 49, No. 5 (May-June 1970), pp. 601-798.
5. R. L. Easton, "Undersea Cable Systems—A Survey," IEEE Communications Society, 13, No. 5 (September 1975).
6. G. E. Morse, S. Ayers, R. F. Gleason, and J. R. Stauffer, "SG Undersea Cable System: Cable and Coupling Design," B.S.T.J., this issue, pp. 2435-2469.
7. R. G. Buus, J. J. Kassig, and P. A. Yeisley, "Repeater and Equalizer Design," B.S.T.J., 49, No. 5 (May-June 1970), pp. 631-651.
8. C. D. Anderson, W. E. Hower, J. J. Kassig, V. M. Krygowski, R. L. Lynch, G. A. Reinold, and P. A. Yeisley, "SG Undersea Cable System: Repeater and Equalizer Design and Manufacture," B.S.T.J., this issue, pp. 2355-2402.
9. D. N. Harper, B. O. Larson, and M. Laurette, "SG Undersea Cable System: Commissioning: Final System Alignment and Evaluation," B.S.T.J., this issue, pp. 2547-2564.
10. Members of Technical Staff, *Transmission Systems for Communication*, 4th ed., Murray Hill, N.J.: Bell Laboratories, 1970.



## **SG Undersea Cable System:**

# **Repeater and Equalizer Design and Manufacture**

By C. D. ANDERSON, W. E. HOWER, J. J. KASSIG, V. M.  
KRYGOWSKI, R. L. LYNCH, G. A. REINOLD, and P. A. YEISLEY

(Manuscript received May 30, 1978)

*Linearity and reproducibility of undersea electronics play key roles in determining the achievable performance of an undersea cable system. This paper describes the characteristics of undersea electronics and the measures taken in design and manufacture to achieve the desired performance and reliability, giving special emphasis to new features and applications. It describes in detail the performance achieved in the recently completed SG system linking the U.S. and France.*

## **I. INTRODUCTION**

Exploratory work on undersea amplifiers and devices in the late 1960s produced models of repeaters with the performance required for a 3500-channel, 4000-nmi system with a top frequency of 27.5 MHz. The specific development of the 30-MHz, 4000-channel, SG system was started early in 1971. The first SG installation, TAT-6, which connects Green Hill, R.I., with St. Hilaire, France, was completed in July 1976, yielding 4200 channels.

The fivefold increase in bandwidth of SG over SF<sup>1</sup> was made technically possible by advances in the design of reliable, ultralinear, silicon microwave transistors.<sup>6</sup> Manufacturing the necessary numbers of undersea bodies economically and on schedule required substantial innovations in the basic mechanical construction and assembly techniques of the electronic units.

## II. GENERAL OBJECTIVES

### 2.1 Noise and load

The SG system was designed to meet the international objectives of 1 pWp0/km (38.6 dBm0 for 3500 nmi), average, with a signal load of -13 dBm0 per 3-kHz spaced channel. The "worst channel" could be 2 pWp0/km. Once the noise, load, channel capacity, and cable diameter are specified, and the achievable amplifier noise figure and modulation coefficients are known, the repeater gain (and spacing) can be determined from the following approximate relationship:

$$s/n = -1.8 - \frac{1}{3} \left[ M_{A+B-C} + 10 \log(\overline{n}_p) + 20 \log(n) \right] \quad (1)$$
$$- \frac{2}{3} \left[ 10 \log(KTB) + N_F + G_R + 10 \log(n) \right],$$

where

- $s/n$  = signal-to-noise ratio in decibels,
- $M_{A+B-C}$  = repeater third-order modulation coefficient for 3-tone products of the  $A + B - C$  type (-95.0 dBm),
- $n$  = number of repeaters in the system (690),
- $\overline{n}_p$  = equivalent number of third-order intermodulation products which add in phase from repeater to repeater (376,000),
- $KTB$  = thermal noise = -139 dBm at 300°K in 3 kHz,
- $N_F$  = repeater noise figure (3.5 dB),
- $G_R$  = repeater insertion gain (41.0 dB).

The numbers in parentheses indicate the approximate 29.5-MHz values. The channel noise and load objectives (38.6 dBm0 and -13 dBm0, respectively) translate to a system  $s/n$  ratio of 36.4 dB. Equation (1) evaluated at 29.5 MHz yields an  $s/n$  ratio of 36.4 dB. More detailed analysis showed that proper signal level shaping would significantly reduce the noise at lower frequencies. It thus appeared that we could meet the noise objectives.

### 2.2 Transmission

Because optimum repeater noise performance can be obtained only over a narrow range of signal power, it is necessary to accurately match the repeater gain to the cable section loss. The errors between the two are compensated for in the ocean-block equalizers (OBES) which follow every 20 or 30 repeaters. The allocation of repeater, equalizer, and cable loss deviations are detailed in another article.<sup>2</sup> For a 20-repeater block (TAT-6), the top frequency loss deviation allowances are  $\pm 0.03$ -dB systematic and  $\pm 0.1$  dB random for repeaters and  $\pm 0.1$  dB total for OBES.

The deviation allocations are increased at lower frequencies up to a maximum of  $1\frac{1}{2}$  times the top-frequency value, in proportion to  $30/f$ , where  $f$  is in MHz.

Available gain for the equalizers is obtained by reducing the length of cable by 4.1 nmi, that is, from 5.1 nmi for repeater sections to 1.0 nmi for equalizer sections. Additional low-frequency gain range is derived from a repeater gain boost of the form:

$$\begin{aligned} \text{repeater gain boost (dB)} &= 0.00218(11.5-f)^2 & f \leq 11.5 & \quad (2) \\ &= 0 & f > 11.5, & \end{aligned}$$

where  $f$  is in MHz.

Cable loss variations due to the seasonal temperature changes on the continental shelves are equalized by temperature-controlled repeaters. The gain of these repeaters is controlled by an ambient-temperature-sensing thermistor in the amplifier feedback circuit. The objective was to equalize at least  $\frac{2}{3}$  of the shallow-water loss variation, leaving only a smooth residual which could be readily equalized in the terminals.

To meet noise objectives over the 20-year minimum life of the system requires means of equalizing any reasonably likely transmission change which occurs during that period. Shore-controlled equalizers (SCEs) were introduced when cable "aging" (change in attenuation with time) was predicted to be of serious consequence.<sup>3</sup> Each SCE has a controllable loss range of  $\pm 16$  dB at 30 MHz with 2-dB step sizes.

### 2.3 Mechanical

To ensure that the repeaters and equalizers survive the shocks associated with laying and recovery, they are designed to withstand:

- (i) A 60-g shock peak for 60-ms duration between half-amplitude points along each of the three principal axes.
- (ii) A vibration limit of 1.27-cm sinusoidal peak-to-peak displacement from 5 to 11 Hz.
- (iii) A sinusoidal vibration at 3-g maximum from 11 to 500 Hz.

The underwater electronics are designed to operate over a temperature range of  $0^\circ$  to  $30^\circ\text{C}$  ( $32^\circ$  to  $86^\circ\text{F}$ ). The allowable storage temperature range is:  $-18^\circ$  to  $57^\circ\text{C}$  ( $0^\circ$  to  $135^\circ\text{F}$ ).

The maximum permissible leak rate of a sealed pressure housing under helium pressure test is  $1 \times 10^{-7}$  standard cc/s at 844 kg/cm<sup>2</sup> (12,000 psi). This is the pressure at a depth of 8050 m (26,000 ft). Individual components such as seals are allowed a maximum leak rate of  $5 \times 10^{-8}$  standard cc/s.

Table I — New materials, processes, and techniques

Materials	
Aluminum	AA 356.0 and AA-6061
Bronze	CA-725
Thermoplastic	Glass-reinforced polybutylene terephthalate (PBT)
Stainless steel	Types 305, 310, and 384

Processes	Techniques
Back extrusion	Printed-wiring boards
Electron beam welding	Vacuum drying
Low-pressure permanent-mold castings	

### III. MECHANICAL DESIGN

#### 3.1 *New techniques*

The physical design of the SG underwater hardware (Fig. 1) embodies some principles proven in the past and some which are new to undersea use. Those materials, processes, and techniques newly exploited in undersea cable use are listed in Table I.

#### 3.2 *Pressure hull*

The cylindrical copper beryllium housing is back-extruded rather than forward-extruded. This change has led to a housing which costs about the same as those used for the earlier SD and SF systems in current dollars. The back-extruded housing more than satisfies the corrosion resistance, grain size, porosity, and strength requirements.

The tungsten inert gas (TIG) method of welding the cover to the housing has been replaced by electron beam (eB) welding. A high-intensity (about 1.4 MW/cm<sup>2</sup>) stream of electrons is focused to a controlled beam size upon the weld seam in a vacuum. The kinetic energy of the beam is converted into heat upon impact with the copper beryllium, causing it to melt, vaporize, and then condense on the cooled material surrounding the melt trough. The weld progresses continuously as the cover and housing rotate under the beam.

The weld depth and melt zone geometry have been optimized for minimum stress by rigidly controlling the beam current, diameter, accelerating voltage, focal distance, work distance, and welding speed. Weld depths are typically 3.8 mm. In the rare case of a process or apparatus failure during assembly, the eB process permits up to two repair welds. Such a failure with the TIG process required a machining operation which destroyed either housing or cover.

#### 3.3 *Electronics unit*

The most significant departure from previous practice was the elimination of hermetic sealing of the electronics block of the repeater and equalizer units. Analyses had shown that by taking advantage of the

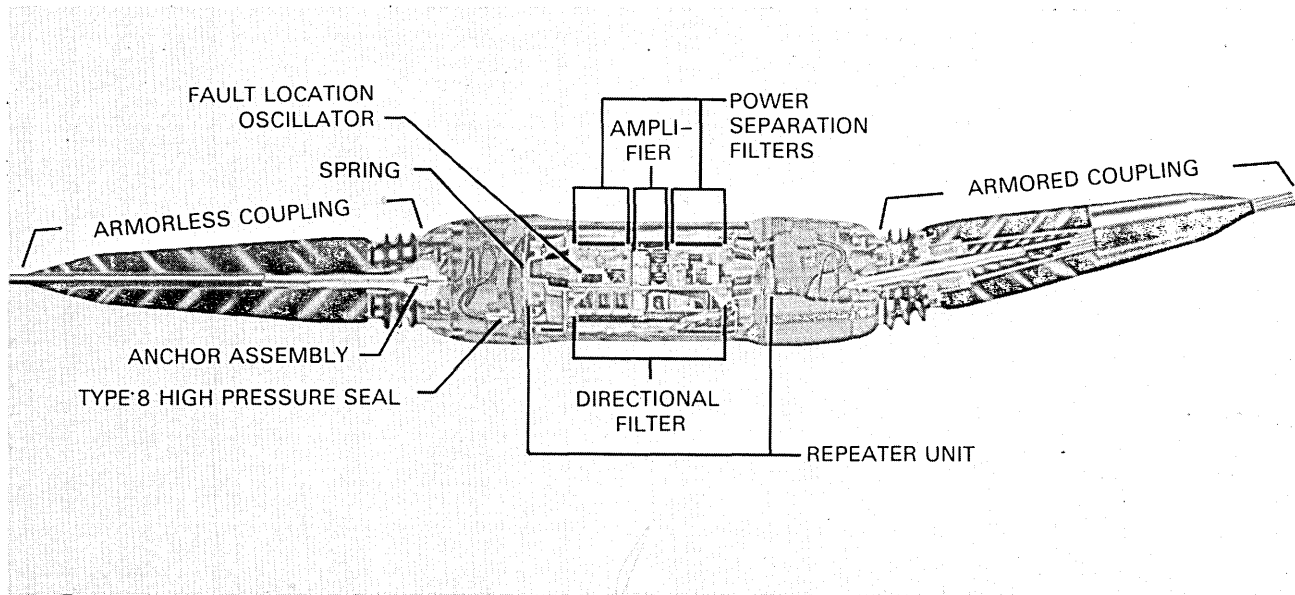


Fig. 1—SG repeater.

water absorption properties of the plastic materials within the electronics unit, the inner assembly (Fig. 2) can be left open inside the pressure housing without danger of moisture condensation. This greatly simplified the design of the inner unit. It allowed the cylinder to be extruded, which simplified the epoxy coating procedure and subsequent assembly with the main frame. The main frame and associated structures were cast by the low-pressure permanent-mold process (LPPM).

The frequency range of the SG system necessitated close coordination of the electrical and physical designs of the electronics units to achieve the needed performance and to minimize unit-to-unit variations. In the repeater, assembly procedures allowed adjustment of over 30 inductors. Five of these adjustments are made after final assembly of all the networks.

Each individual circuit was mounted on its own aluminum frame as a separate module (Fig. 3). Functional partitioning allowed networks to be assembled, tested, adjusted, and "locked" individually. Each module was mounted on a main frame which in turn was slid into the epoxy-coated aluminum cylinder. The main frame was then locked to the cylinder and the ends covered with plastic end caps.

The modular type construction using cast frames provided low thermal impedance (about  $1^{\circ}\text{C}/\text{W}$ ) between the transistor mounting studs and the housing. This type of construction also minimizes corona due to the high voltages (up to 7 kV) by maintaining isolation, proper spacing, and smooth surfaces.

Glass epoxy double- and single-sided circuit boards, 1.588 mm (0.0625 in.) and 2.381 mm (0.0935 in.) thick, supplied the structural rigidity needed for mounting components and highly repeatable circuit paths to minimize variations in electrical characteristics. Path widths were set at 2.54 mm (0.100 in.) with a minimum spacing of 1.27 mm (0.050 in.). Dielectric constant, insulation resistance, peel strength, plating thickness, and breakdown voltage were required to meet stringent limits to insure high reliability.

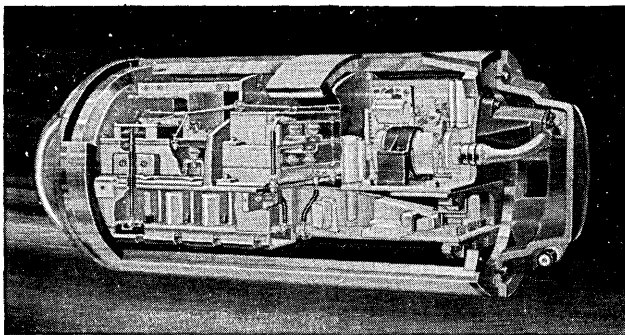


Fig. 2—Electronics unit, inner assembly.

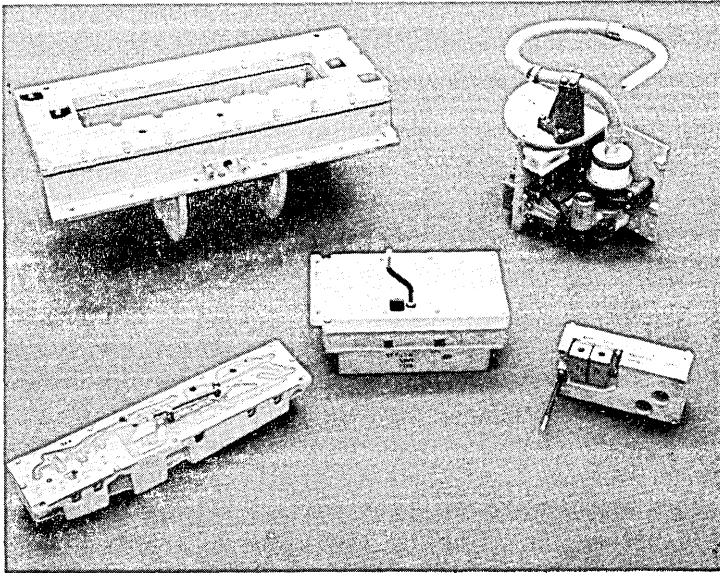


Fig. 3—Circuit modules. Top left, directional filter (DF); top right, ground separation filter (GSF); bottom left, output network; center, amplifier; bottom right, oscillator.

Because of the high potential of the electronic units, it was desirable to make the end caps from insulating material. A glass-filled polybutylene terephthalate (PBT) was selected because of its excellent mechanical and electrical properties. In addition, its low shrink factor and good flow characteristics make it a good material for injection molding. PBT has a melting temperature greater than  $216^{\circ}\text{C}$  ( $420^{\circ}\text{F}$ ) and therefore allows for soldering on or near its surface. The material has also been used for electrical standoffs and insulating covers.

Although the decision to use a nonhermetically sealed electronics unit permitted the exploitation of new materials and processes, it required a new vacuum drying procedure which considered the outgassing and water absorption properties of all the materials in the unit. A drying cycle and a closure procedure have been devised which predict a dew point of less than  $-15^{\circ}\text{C}$  ( $+5^{\circ}\text{F}$ ) after 20 years at sea bottom at an external pressure of  $844\text{ kg/cm}^2$  ( $12,000\text{ psi}$ ).

#### IV. REPEATER ELECTRICAL DESIGN

##### 4.1 Configuration

As described in a companion article,<sup>2</sup> the repeater gain is provided by a pair of tandem amplifiers common to both transmission bands.

Table II contains a summary of the repeater electrical performance.

Table II — SG repeater electrical performance summary

Frequency (mHz)	Repeater Gain (dB)	Amplifier Gain (dB)	Network Losses (dB)	Repeater Noise Figure (dB)	Modulation Coefficients*		Repeater Return Loss	
					$M_{2E}^*$ (dB)	$M_{3E}^*$ (dB)	A end (dB)	B end (dB)
1	7.48	10.56	3.08	8.7	-112	†	34	25
2	10.37	12.13	1.76	8.0	-116	†	36	24
4	14.53	15.94	1.41	7.7	-110	†	33	22
8	20.50	22.07	1.57	7.0	-100	†	25	30
12	25.34	27.67	2.33	5.8	-84	†	22	17
13.75	27.20	30.64	3.44	5.8	-79	†	22	22
16.50	29.96	33.00	3.04	5.2	-77	-113	27	19
20	33.23	34.99	1.76	4.0	-73	-113	24	26
25	37.46	39.09	1.63	3.6	-71	-113	21	23
30	41.37	42.89	1.52	3.5	-70	-113	24	20

\* Defined at power amplifier output. The value of  $M_{3E}$  is that determined before installation of TAT-6. As discussed later in Section VII, this value is better than the actual repeater performance.

†  $M_{3E}$  is not a significant parameter in the low band.

## 4.2 Passive networks

### 4.2.1 Ground-separation filter

The ground-separation filters (GSFs) shown in Fig. 4 connect the cable to the directional filters. They were designed as high-pass filters. Coaxial capacitors ( $0.013 \mu\text{F}$ ) provide a low-impedance ground path for signal frequencies, while blocking the high dc voltage (up to 7 kV) which exists between the repeater unit (repeater ground) and the housing (sea ground). To prevent coupling between the repeater input and output, this impedance should ideally be zero. However, at low frequencies the reactance of the high-voltage capacitor becomes large, while at high frequencies inductive parasites dominate. The coaxial design virtually eliminates the inductance problem in the capacitor. A coaxial choke with a longitudinal inductance of  $250 \mu\text{H}$  reduces the unbalanced current in the GSF and thereby increases the isolation between the repeater input and output. Adequate GSF loop loss\* was achieved without building up the capacitance between the inner unit and the housing.

Powder core inductors carry the 657-mA dc line current to the amplifier biasing circuits. Each inductor along with the adjacent  $0.013\text{-}\mu\text{F}$  coaxial and low-voltage ceramic capacitors forms a full-section, 50-ohm, high-pass filter with a cutoff frequency of about 300 kHz.

### 4.2.2 Directional filters

The directional filter is a 50-ohm, four-port network with two high-pass and two low-pass filters. They are of conventional design using oppositely phased transformers in the two low-pass portions to help

\* GSF loop loss refers to stray transmission around the amplifier via the GSFs and the repeater's power path.



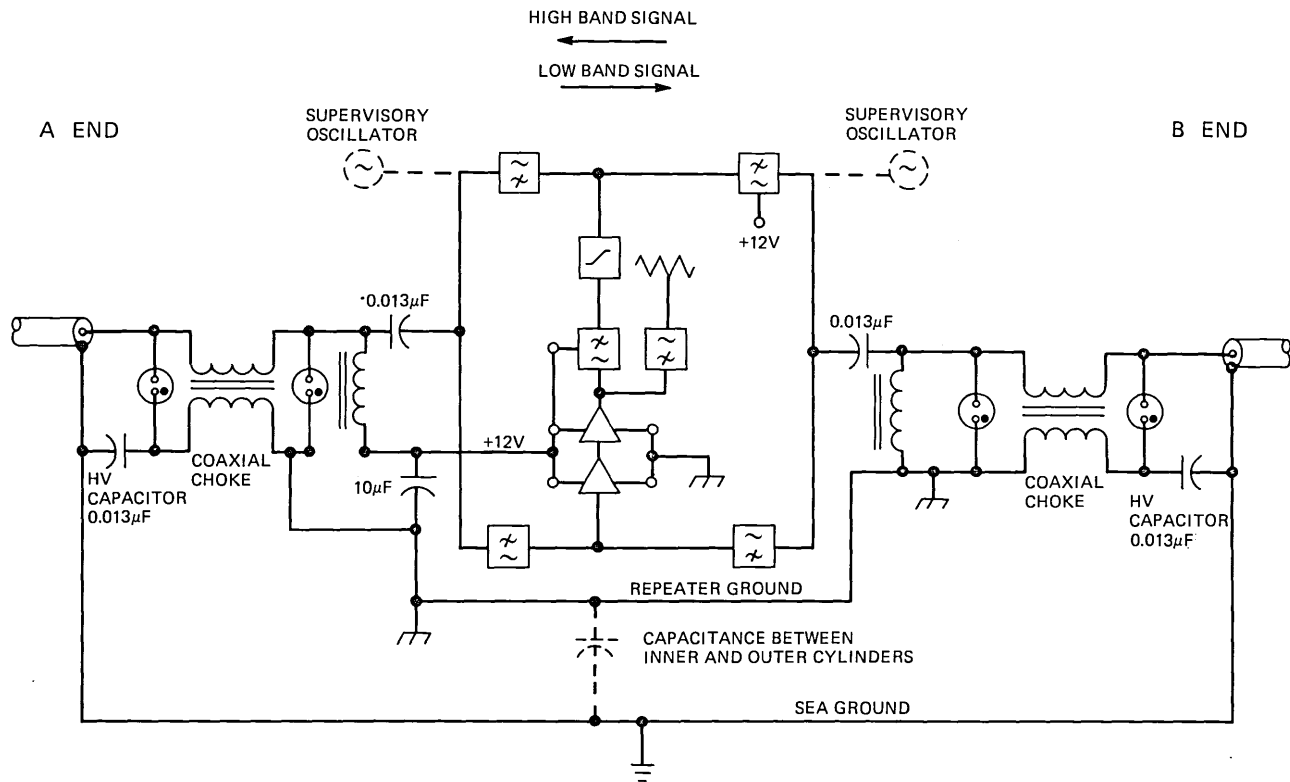


Fig. 4—SG repeater block diagram showing GSF circuit.

increase directional filter loop loss.<sup>†</sup> Figure 5 shows the rectangular arrangement and the individual shielded inductor compartments that provide ideal isolation between both sections and ports. All components are mounted on a single board and connected with printed wiring. The individual sections are tuned “in place” after all filter wiring is complete.

#### 4.2.3 Output network

The output network, shown in Fig. 6, contains surge protection diodes, a low-pass bandlimiting filter, a low-frequency loss equalizer, and a high-pass terminating filter. The filter pair was designed on a constant-R basis with a 3-dB crossover at 33.5 MHz. The low-pass filter increases the high-frequency loop loss around the amplifier and improves the noise margin<sup>4</sup> by suppressing the transmission of above-band noise. The high-pass section properly terminates the power amplifier at high frequencies, thereby maintaining a uniform and controlled stability margin.

A constant-R bridged-T equalizing network helps shape the repeater

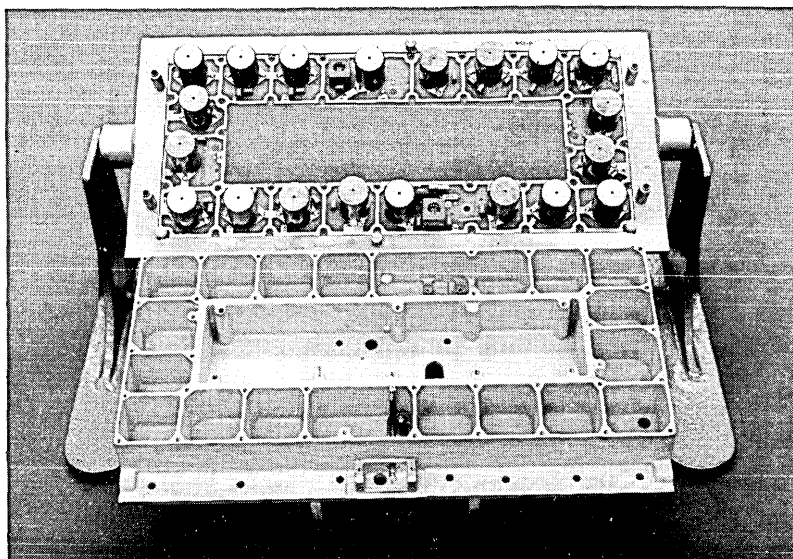


Fig. 5—Directional filter.

<sup>†</sup> Directional filter loop loss refers to the stray transmission around the amplifier via the tandem-paired filters, both high pass/low pass and low pass/high pass. Providing a phase reversal in one of the two paths increases the total loss because transmission via one path tends to cancel that via the other.

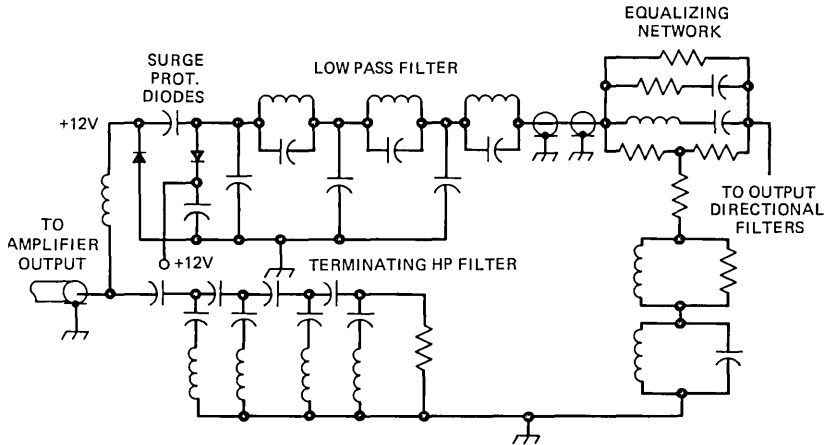


Fig. 6—Output network schematic.

gain and increases the output return loss and the external loop loss at low frequencies.

A pair of oppositely poled, reverse-biased diodes, whose capacitance is absorbed in the low-pass filter, provides surge protection for the power amplifier.

### 4.3 Amplifier

#### 4.3.1 Configuration

The amplifier (Fig. 7) consists of a two-stage preamplifier (PRA) and a three-stage power amplifier (PWA). Both PRA stages are common emitter while the PWA uses a common-base output stage, driven from a Darlington pair via a current step-up transformer. The gain is shaped with feedback. Shunt input, series output is used in the PRA, and shunt input, shunt output in the PWA. Feedback with hybrid-connected autotransformers actively terminate the amplifier input and output ports. The PRA, which has a high output impedance, is connected to the low-input impedance PWA with a resistor. This arrangement reduces the impedance interaction effect between the two at their respective loop gain and phase crossover frequencies and minimizes stability problems.

#### 4.3.2 Bias

The repeaters are biased at  $657 \pm 0.3$  mA with an average voltage of 11.9 V (at 2.5°C). Nominal operating points of individual transistors are listed in Table III. The input stage of the PRA is biased from the emitter of the second stage. During power turn-up, the first stage does not begin to conduct until the second-stage current reaches about 50 mA.

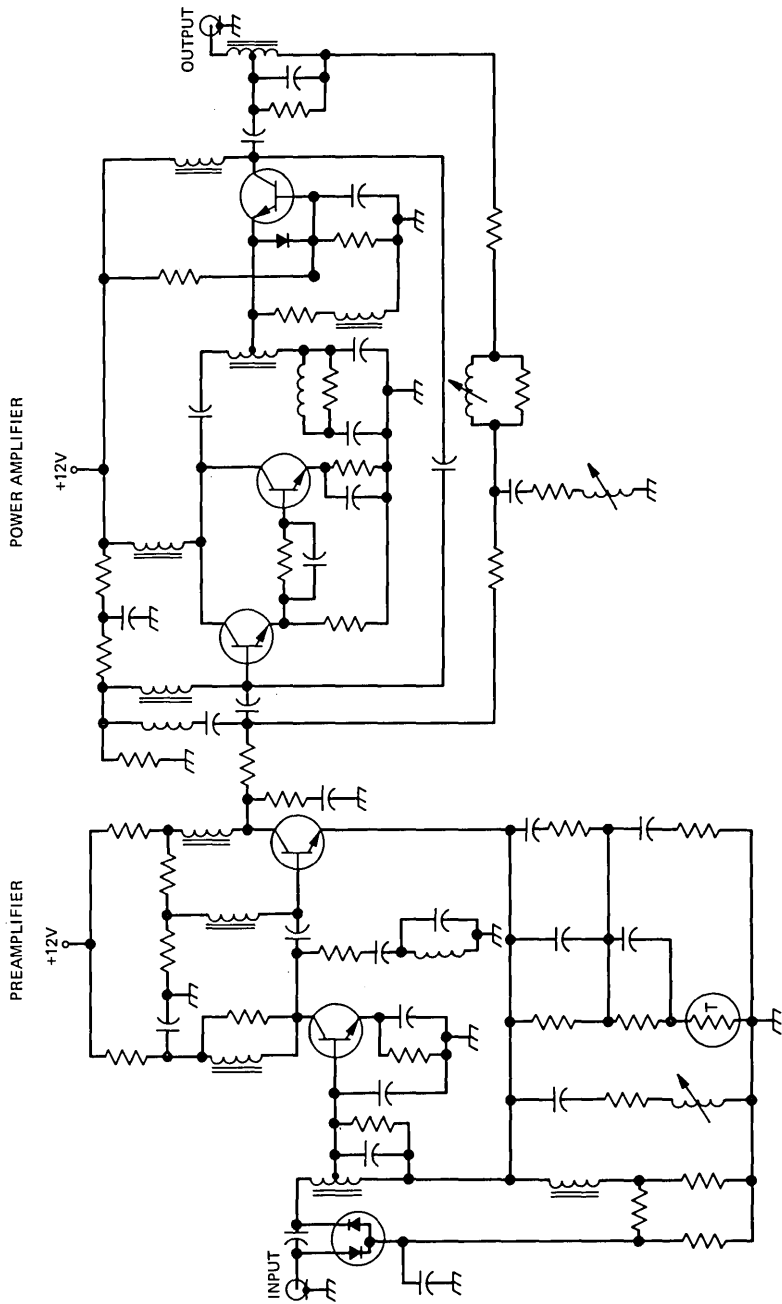


Fig. 7—SG amplifier schematic.

Table III — Nominal transistor operating points (2.5°C)

	Stage	Collector-Emitter Voltage (V)	Collector Current (mA)
Preamplifier	{ 1	9.44	49.8
	{ 2	9.24	153.1
Power amplifier	{ 3	9.16	50.2
	{ 4	10.05	147.2
	{ 5	9.99	147.2
Oscillator		8.05	9.2
Subtotal			556.7
Bleeder current (mA)			100.3
Total (mA)			657.0

Staggering the currents at which the two stages begin to develop gain avoids oscillation which can occur during power turn-on of feedback amplifiers. The dc-coupled Darlington pair in the PWA operates similarly.

#### 4.3.3 Gain

The amplifier gain objective equals the sum of:

- (i) The loss of 5.1 nmi of cable at 2.5°C, 2.5 kilofathoms.
- (ii) The loss of the repeater passive networks.
- (iii) The low-band gain boost.

The amplifier gain, 43 dB at 30 MHz, is divided approximately equally between the PRA and the PWA. It is controlled by the feedback circuits in both amplifiers. The repeater gain, which is further shaped by the bridged-T equalizer in the output network, was initially matched to within +0.03 dB of the objective.\* This necessitated extensive characterization of each component and the printed wiring boards. Component tolerances were assigned based upon both sensitivity studies and adjustment capability. The amplifier contains three adjustable inductors. Two are adjusted during the final repeater network testing stage along with an inductor in the output network and two in the directional filters.†

The shapes obtained with these final adjustments closely match the shapes of the three most significant sources of gain deviation:

- (i) Directional filter and output network loss variations.
- (ii) Miller capacitance of Darlington pair.
- (iii) Alpha sensitivity of the second stage in the Darlington pair.

The effectiveness of the gain control and adjustment techniques is

\* The low-frequency gain was later increased slightly to obtain more channels below 1 MHz at the expense of increasing the low-frequency gain deviation somewhat.

† This operation is discussed in Section 6.3.5.

indicated in Table IV, which is based upon the entire TAT-6 repeater production.

There are two basic types of SG amplifiers, fixed-gain and temperature controlled (TC). The latter, which are new to undersea cables, are used in those repeaters to be laid in shallow water areas where bottom temperatures change seasonally. The gain of TC repeaters is designed to increase with temperature, as does cable loss. Gain is controlled by an ambient temperature-sensing parallel-disk thermistor in the PRA feedback circuit. Figure 8 shows the repeater gain and the cable-loss change for a temperature rise from 2.5° to 10.1°C. Over this range, the repeater compensates for at least  $\frac{2}{3}$  of the cable loss change. The TC repeater is designed to have the same gain at 2.5°C as the fixed-gain repeater.

#### 4.3.4 Feedback

The achievable feedback is limited by both conventional and noise-generating stability considerations. As shown in Fig. 9, the nominal PRA feed-

Table IV — Repeater gain objective and average\* deviation (dB) at 2.5°C

Low Band				High Band			
Freq (MHz)	dB Gain Objective	Deviation without Terminations	Deviation <sup>†</sup> with Terminations	Freq (MHz)	dB Gain Objective	Deviation without Terminations	Deviation <sup>†</sup> with Terminations
0.75	6.404	-0.018	-0.018	16.50	29.950	-0.006	-0.017
1.00	7.346	0.092	0.092	16.75	30.190	0.001	0.026
1.50	8.935	0.094	0.094	17.00	30.430	-0.006	0.026
2.00	10.281	0.060	0.060	17.25	30.667	-0.005	0.026
2.50	11.469	0.044	0.044	17.50	30.904	-0.001	0.025
3.00	12.546	0.036	0.036	17.75	31.138	0.008	0.023
3.50	13.540	0.032	0.032	18.00	31.373	0.015	0.010
4.00	14.470	0.037	0.036	18.50	31.835	0.027	0.002
5.00	16.176	0.027	0.029	19.00	32.293	0.027	0.002
6.00	17.730	0.007	0.010	19.50	32.745	0.026	0.012
7.00	19.170	-0.019	-0.020	20.00	33.193	0.020	0.020
8.00	20.520	-0.047	-0.051	21.00	34.075	0.008	0.016
9.00	21.797	-0.063	-0.057	22.00	34.940	0.001	0.008
10.00	23.015	-0.044	0.046	23.00	35.788	-0.002	0.006
10.50	23.604	-0.030	-0.028	24.00	36.622	-0.007	0.006
11.00	24.182	-0.018	-0.019	25.00	37.441	-0.006	-0.003
11.50	24.751	-0.009	-0.003	26.00	38.248	-0.002	-0.029
12.00	25.309	-0.001	-0.014	27.00	39.042	0.008	-0.032
12.50	25.859	-0.009	-0.003	27.50	39.435	0.012	0.024
12.75	26.130	-0.015	-0.020	28.00	39.824	0.018	-0.001
13.00	26.398	-0.015	-0.030	28.50	40.211	0.023	0.026
13.25	26.665	-0.013	-0.024	29.00	40.596	0.024	0.045
13.50	26.929	-0.007	-0.007	29.50	40.978	0.016	0.048
13.75	27.192	0.001	0.009	30.00	41.357	-0.013	0.012

\* Based upon all the TAT-6 repeaters.

† Refers to armorless terminations.

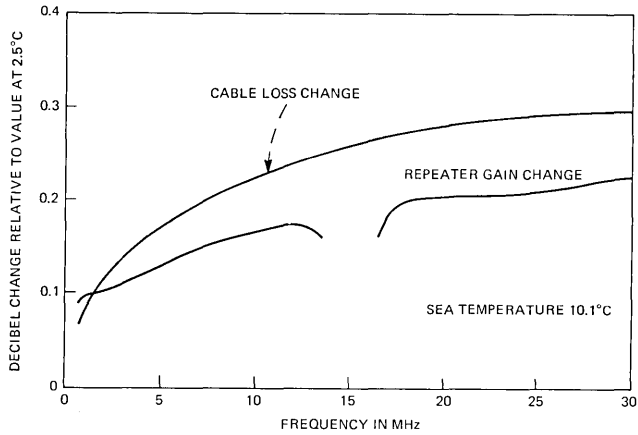


Fig. 8—Gain tracking of temperature-controlled repeater.

back ranges from 32 dB at 5 MHz to 11 dB at 30 MHz, while the PWA feedback is maximum at 1.5 MHz and decreases to 12 dB at 30 MHz. The repeater is stable for all combinations of open and short circuit terminations, for all possible combinations of transistors up to at least 45°C and at reduced currents, which occur during power turn-up. The

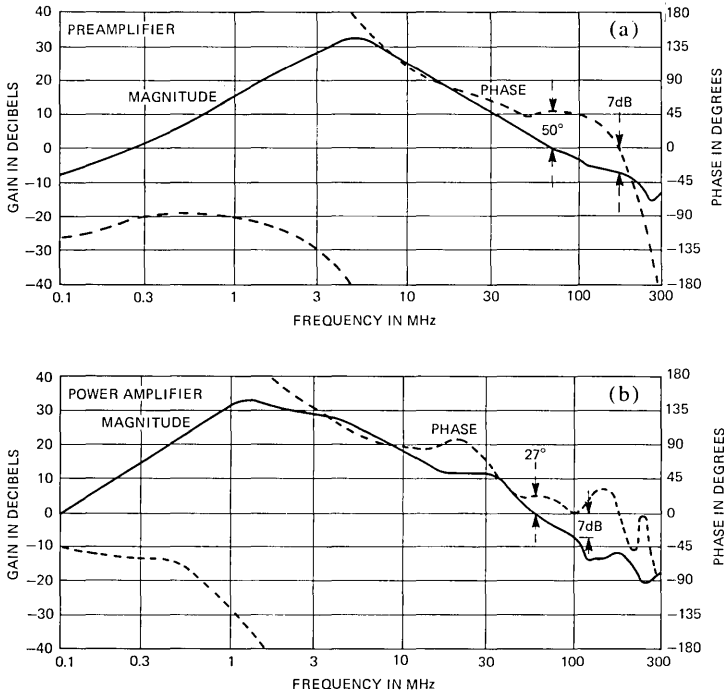


Fig. 9—Amplifier feedback.

noise-sing margin of the system is strongly influenced by the phase of both the inband and aboveband loop feedback of the PWA. Maintaining the phase characteristics near  $90^\circ$  across the high band and as large as possible aboveband resulted in significant improvement in the noise-sing margin.

#### **4.3.5 Thermal noise and intermodulation distortion**

The nominal repeater noise figure and intermodulation coefficients are shown in Table II. A 30-MHz noise figure of 3.5 dB was achieved by using a low-loss active termination and by selecting low noise-figure transistors for the input stage.

Second-order distortion coefficients range from  $-70$  dBm at 30 MHz to  $-112$  dBm at 1 MHz. The tandem amplifier configuration results in some fundamental frequency dependence in the coefficients. Because of the shaped gain in both amplifiers, the PRA second-order distortion contribution is significant for low-frequency fundamentals.

Third-order distortion products of the  $A + B - C$  type are the most important because of their number and their tendency to add in-phase from repeater to repeater. Measurements of many different products of this type during development and manufacture of the SG repeater indicated a value for  $M_{3E}$  of approximately  $-113$  dB in the high band.\* As discussed further in Section 7.2, the characterization of third-order distortion was misleading because a source of distortion existed that did not obey the usual rules.

#### **4.3.6 Overload protection**

Reverse current flow across the emitter-base junction of a silicon planar transistor can cause a change in the current gain. Although these junctions are forward-biased in the amplifier, abnormally large signal voltages can, in the output stage, produce voltages in the emitter-base breakdown region. Such abnormal signals can result from certain failures in the terminal equipment, or in the land facilities feeding the system, or from improper test procedures. The output stage of the PWA is protected against signal overload by a diode connected across the emitter-base junction. Additional protection is provided in the shore terminals.<sup>5</sup>

#### **4.4 Supervisory oscillator**

A single-transistor, crystal-controlled oscillator injects a unique frequency at the input of each repeater. These supervisory tones, which fall

---

\* Defined at amplifier output.



alternately in the high and low bands, are used for monitoring transmission levels and localizing faults on the system. A diode limiter and a thermistor-controlled attenuator maintain a stable tone power at the repeater output of  $-50$  and  $-40$  dBm in the low and high bands, respectively. The quartz crystals are circular, plano-convex, AT cut. They resonate in the fifth overtone thickness shear mode. Crystal characteristics are listed in Table V.

#### 4.5 Transistors

The 82-type transistor<sup>6</sup> used in the SG amplifier features a common design for all stages. It is a silicon planar epitaxial type with an  $f_T$  of 2.7 GHz designed to operate for 20 years at 1.5 W and a maximum junction temperature of  $65^\circ\text{C}$  with a maximum  $\alpha_0$  change of 0.0005. (Sample aging measurements to date indicate no discernible aging.)

Each transistor's small signal characteristics were determined at 10 V, 150 mA, and 9 V, 50 mA, the two nominal operating points. Two-port transmission parameters at 15 frequencies from 100 kHz to 400 MHz were computer-processed by an "on-line" circuit-modeling program to yield element values in the equivalent circuit of Fig. 10. Thus, each set of 60 complex transmission parameters was reduced to nine circuit elements. Noise figure and intermodulation coefficients at the two bias points were also measured. A transistor assignment program optimized the usage of a given lot of transistors by assigning each transistor to a stage in the repeater on the basis of its so-called "noise numbers." Five noise numbers were computed for each transistor. These numbers were proportional to the system noise which would be contributed by the transistor in each possible use.

The input stage noise number was proportional to the 30-MHz noise figure, while the output-stage noise number was dominated by the transistor third-order modulation coefficient. The program minimized the sum of the noise numbers, while yielding a required number of complete transistor sets. There were no grouping requirements based upon stability or gain deviation considerations. Table VI lists the median ac parameters of all transistors used in the TAT-6 link.

Table V — Crystal characteristics

	Low Band	High Band
Frequency band (MHz)	11.120–11.216	27.628–27.820
Spacing between tones (Hz)	200	400
Accuracy from nominal (Hz) (over 20 years and $0^\circ$ to $45^\circ\text{C}$ )	$-118, +40$	$-293, +98$
Resistance-min-max (ohms)	20–100	10–50
Shunt capacitance (pF)	4.25	8.4
Inductance (mH)	500	40
Q	350K to 1750K	140K to 700K

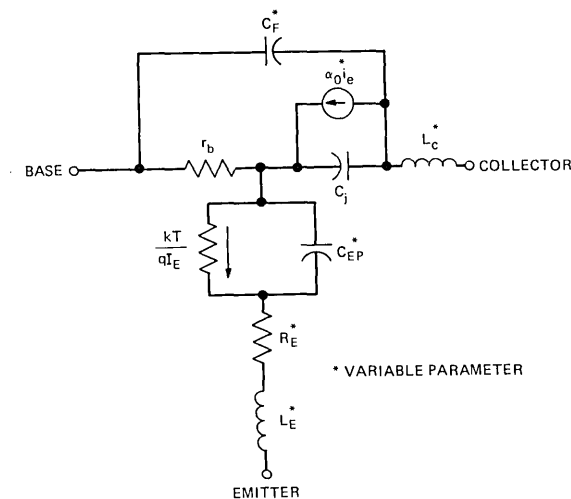


Fig. 10—Circuit model of 82-type transistor.

Table VI — Median transistor parameters

Transistor Type	Function	Bias		Median Parameter Values*				Stage Placement Criteria
		Volts	mA	$\alpha_0$	$R_E$ (ohms)	$C_F$ (pF)	$C_{EP}$ (pF)	
82A	Ampl. stage 1	9.4	50	0.9920	0.173	3.38	128	Noise figure and $\alpha_0$
82B	Ampl. stage 2	9.2	153	0.9892	0.192	3.29	376	
82C	Ampl. stage 3	9.2	50	0.9885	0.166	3.29	149	$C_F$
82D	Ampl. stage 4	10.0	147	0.9854	0.189	3.20	419	$M_2$ and $\alpha_0$
82E	Ampl. stage 5	10.0	147	0.9881	0.188	3.05	379	$M_3$ and $\alpha_0$
82F	Oscillator	8.0	9					$0.9780 < \alpha_0 < 0.9938$
82G	Oscillator	8.0	9					$0.9780 < \alpha_0 < 0.9890$

\* Refers to TAT-6 production. The median 30-MHz noise figure for the 82A was 1.87 dB. The median 28.9-MHz  $M_3$  for the 82E was 93.1 dB.

#### 4.6 Surge protection

Two gas-filled electron tubes in each GSF provide the first level of protection against the high-energy surges which accompany faults in the dc power path. These tubes break down at a voltage in the range of 75 to 600 v, depending on the rate of change of the incident surge voltage. Although the gas tubes prevent damage to the passive components, the transistors require a second level of protection which is furnished by reverse-biased diodes (Table VII).

Table VII — Repeater surge protection diodes

Location	No. of Diodes	No. of Diode Packages	Reverse Bias, Volts	Protection Function
Ground separation filter	3	3	12.0	Power path
Preamplifier	2	1	0.86	Amplifier input
Directional filter	2	1	4.0	Amplifier output
Output network	2	2	12.0	Amplifier output

Three Zener diodes in the GSF share equally (within 10 A) peak current surges of up to 160 A caused by the cable discharge, while limiting the voltage across the dc power path to the range  $-3$  to  $+19$  V.

The PWA output transistor proved to be very susceptible to damage from the surge's low-frequency components which pass through the low-band output directional filter. A pair of 4-V reverse-biased diodes placed across the directional filter reduced the surge and also improved the noise-sing stability margin by compressing gain at abnormally high low-band signal power.

Surge protection was probably the most elusive problem encountered in realizing an acceptable repeater design. The results of an extensive testing program in which hundreds of devices were repeatedly surged indicated that the average output stage transistor would survive 50 worst-case surges before failure. Achieving this degree of protection cost what appeared at the time to be a 3- to 4-dB increase in repeater third-order distortion. As further discussed in Section 7.3, the actual degradation was much greater.

#### 4.7 Corona noise

Because of the high voltage present in the repeaters and equalizers, it is possible that static discharges (corona noise) could either excessively degrade system noise performance or lead to an eventual component failure. The requirements adopted were based upon the possibility of insulation damage and failure and are about 20 dB more stringent than current requirements based on group band (48-kHz) data.

Each repeater and equalizer is backfilled with 4.4 atmospheres (50 psig) of dry nitrogen and tested for 21 hours at 7 kV. Broadband detectors, 0.1 to 30 MHz, record all corona "pops" which exceed 1 mV at the output of the repeater. Up to 12 counts exceeding this threshold are allowed in a 21-hour period.

#### 4.8 Passive components

A summary of the types and values of SG repeater passive components<sup>5</sup> is included in Table VIII.

All resistors are the tantalum film type on alumina substrates and have thermo-compression bonded leads.

NPO ceramic capacitors have replaced mica and paper types in all except high-voltage applications. The paper-castor oil high-voltage capacitors are of radically new design, featuring a coaxial structure to reduce parasitic inductance. Tantalum electrolytic capacitors are used for coupling and bypassing purposes where large values are needed.

Ferrite-core chokes, smaller air-core coils for filter networks, and a cavity-tuned inductor are all innovations from previous designs. Hybrid feedback at the amplifier's input and output ports is implemented by means of tightly controlled autotransformers wound on ferrite cores. An autotransformer is also used in the power amplifier to obtain a 2:1 current gain between the Darlington pair driver and the common-base output stage. In the ground-separation filters, coaxial longitudinal chokes help provide the necessary isolation between the amplifier input and output.

#### **4.9 Reliability**

As discussed in a companion article,<sup>2</sup> the design objectives for SG component reliability are 0.05, 0.5, and 1.0 FITs (failures in  $10^9$  device-hours) for passive components, diodes, and transistors, respectively. These levels of reliability have been achieved on previous systems.

Using the preceding reliability objectives and the repeater component count of Table IX results in a repeater failure rate of 21 FITs. (This excludes the oscillator, since its failure would not degrade system performance.)

#### **4.10 Terminations**

The cable-repeater terminations, described in detail in a companion article,<sup>3</sup> have a significant effect on system transmission. Although their actual insertion loss is small, about 0.13 dB per repeater at 30 MHz, they contribute a loss ripple due to impedance interactions with the repeater and cable. Reflections occur at each end of the "pigtail," the flexible coaxial transmission lead between the cable and repeaters within the termination. Because the insertion phase of the directional filter and output network varies rapidly with frequency (typically 360 degrees across the high band), the phase of the repeater reflection coefficient across the high band changes by about two revolutions. The reflection coefficient at the cable end of the termination results from excess capacitance in the transition area, 6 pF in the armorless and 3 pF in the armored terminations. The interactions between these two reflections, separated by the electrically long pigtail, causes a rapidly varying loss ripple whose magnitude approaches  $\pm 0.035$  dB in the high band (see Table IV).

Table VIII — SG repeater passive components

<i>Resistors:</i>					
Type	Values (ohms)	Tolerance (percent)	Dissipation (Watts)	Temperature Coefficient (PPM/°C avg)	20-Year Stability (max. percent)
Metal film	3-5000	±0.1 min.	1/16, 1/8	0-40	+0.05
<i>Capacitors:</i>					
Type	Values	Tolerance (percent)	Max. VDC	Temperature Coefficient (PPM/°C)	20-Year Stability (max. percent)
Coaxial H-V	0.013 μF	±3	8000	-40	+0.5
Ceramic	5 PF - 0.047 μF	±1 min.	15	±30	+0.02
Tantalum	1-10 μF	±7	15		
ESR	2 ohms at 2 MHz				
<i>Inductors:</i>					
Type	Values (μH)	Tolerance (percent)	Max. DC Current (mA)	Temperature Coefficient (PPM/°C)	20-Year Stability (max. percent)
Air core	0.1-44.3	±1 to ± 10	—	—	—
Torroidal powder core	12.9, 16.25	±3	700	-200	+0.5
Air core slug-adjusted	0.05-5.4	±2 (min. adj)	—	—	—
<i>Transformers:</i>					
Type	Remarks				
Longitudinal choke	Wound with 50-ohm coaxial cable, 250-μH minimum L to longitudinal currents, max. current 700 mA				
Phase reversing	1:1 and 1:-1, 50 ohms, 250 μH min. L, ferrite core				
Autotransformers	5:20 ohms and 33.3:50 + 100:150 ohms, ferrite core				
<i>Thermistors:</i>					
Type	Values (ohms)	Tolerance (percent)	Temperature Coefficient (ohms/ohms/°C)	20-Year Stability (max. percent)	
Parallel disks	13.83 at 11.2°C	±1	-0.044 at 25°C	+2	
Individual disk	29.0-34.0 at 25°C				

**V. EQUALIZER ELECTRICAL DESIGN**

For the first SG installation (TAT-6), two types of undersea equalizers were developed, a conventional ocean-block equalizer (OBE) and a special shore-controlled equalizer (SCE). The location in the system of these equalizers and their functions in the overall equalization plan are described in a companion article.<sup>2</sup>

The primary job of an OBE is to equalize the accumulated misalignment at the end of an ocean block. Such misalignment arises from design and manufacturing deviations in both repeaters and cable and from

Table IX — SG repeater component count

Component Type	Ground Separation Filters	Directional Filters	Output Network	Pre-amplifier	Power Amplifier	Oscillator		Subtotal
						HB	LB	
Resistors		4	8	19 or 21	17	9	9	59
Capacitors:								
Ceramic	4	36	19	12	8	6	6	85
Paper	2							2
Tantalum	1	1		6	8		2	16 or 18
Thermistor*				1				1
Inductors:								
Air core		20	11	2	4	3	3	40
Ferrite				4	4	1	1	9
Dust core	2							2
Transformers	2	2		1	2			7
Diodes	2	2		2	1	2	2	9
Transistors				2	3	1	1	6
Gas tubes	4							4
Crystals						1	1	1
Subtotal	17	65	38	51	47	23	25	†

\* Thermistor is used only in shallow-water temperature-controlled repeaters. It replaces two resistors.

† Total components: repeater with HB oscillator: 241; repeater with LB oscillator: 243.

uncertainties associated with predicting the overall transmission of the system in the ocean-bottom environment. The OBE is adjusted to its final setting aboard ship shortly before it is overboarded.

The primary job of the SCE is to compensate for transmission changes occurring in one sector over the life of the system. (For TAT-6, a sector is approximately one-fifth of the system length.) From the standpoint of the transmission path, both the OBE and SCE are passive. Gain for equalization is obtained by shortening the cable length between the two repeaters adjacent to an equalizer to a total of one mile (one-half mile on either side of the equalizer). In the lower part of the low band, additional equalization gain is provided by the repeater gain boost.

### 5.1 Ocean-block equalizer

The SG ocean-block equalizer design retained those features of the SF system OBE that proved so successful in equalizing that system, viz:

- (i) Independent equalization in the two transmission bands.
- (ii) Switchable networks—a set of 14 networks (7 per band), identical in all OBEs, that can be individually switched “in” or “out” of the transmission path.
- (iii) Mop-up networks—a series of up to seven tandem networks in each band that can be designed and fabricated late in the manufacturing cycle of an equalizer. These could be different for each OBE.

The switchable and mop-up equalization modes accomplish the primary OBE function and are discussed in detail in separate sections.

Figure 11 shows the OBE. Since there are no active electronics in the OBE, a power-separation filter (PSF) at each end bypasses the high-voltage direct current. This arrangement places the internal chassis ground at the same potential as the outer pressure housing (sea ground). (The repeater and SCE differ in having the internal chassis at center-conductor potential.)

Separation of the two transmission bands within the OBE is achieved through use of two directional filters, each consisting of a low-pass and high-pass filter paralleled at one end to form a three-port network.

A build-out network in each band centers the switchable network adjustment range around the nominal OBE loss, while preserving the maximum possible flat loss for mop-up network design. Nominal OBE total loss corresponds to that of 4.1 nautical miles of 1.7-in. SG cable at sea bottom plus a loss equal to the per-block repeater gain boost.

A coaxial transmission test lead exits the OBE housing through a high-pressure seal. This lead is used during tests of the assembled shipload of cable and repeaters prior to laying and during measurements between ship and shore while laying.

Within the OBE, the test lead terminates in a symmetrical 3-port splitting pad that can be switched "in" or "out" of the transmission path. After final adjustment on shipboard, the pad is switched "out." This disconnects the test lead and connects transmission straight through. Finally, the end of the external test lead is overmolded.

### **5.1.1 Switchable networks**

The insertion loss functions of the 14 switchable networks are given in Table X. Each network is realized by a constant resistance (50-ohm) structure. Three classes of shapes are identifiable, "root- $f$ ," "root- $f$  minus  $f$ ," and a broad "bump," whose peak loss is near the center of each band. (The latter two shapes have small amounts of root- $f$  loss added to make them physically realizable.) These three shapes are plotted in a companion article.<sup>2</sup> The frequency characteristics of 16 of the total of 128 settings obtainable in the low band are shown in Fig. 12. The switchable networks are capable of equalizing only smooth, relatively broad components of misalignment. (The more ripply components are handled by the mop-up networks.)

Of the three classes of switchable network shapes, the one with by far the largest range is root- $f$ . This is because repeater gain and cable loss, as well as changes in cable loss due to temperature and pressure effects, are approximately proportional to the square root of frequency. It follows, therefore, that residual differences in these parameters, including those due to inaccuracies in predicting sea-bottom temperature or depth

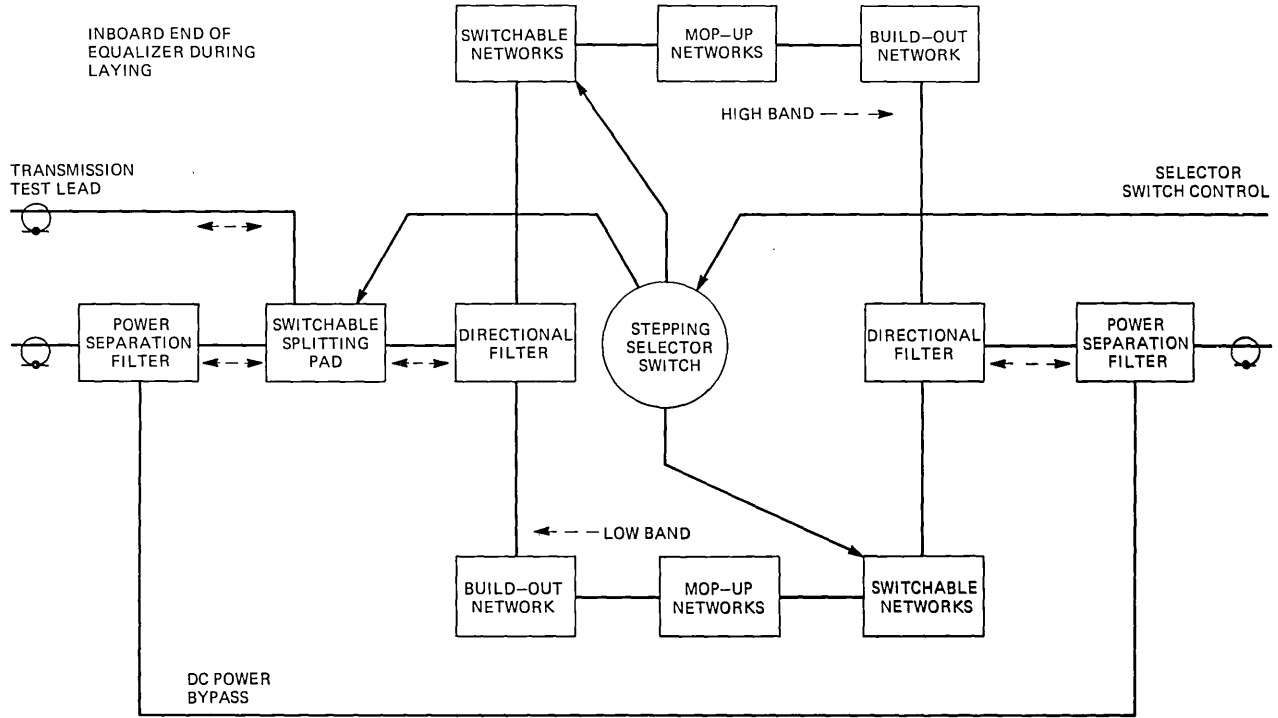


Fig. 11—Block diagram of ocean-block equalizer.



Table X — Ocean-block equalizer switchable loss shapes (dB)

Low Band	High Band
$8\sqrt{f/30}$	$8\sqrt{f/30}$
$4\sqrt{f/30}$	$4\sqrt{f/30}$
$2\sqrt{f/30}$	$2\sqrt{f/30}$
$1\sqrt{f/30}$	$1\sqrt{f/30}$
$8(\sqrt{f/14} - f/14) + 2\sqrt{f/30}$	$17.26(\sqrt{f/30} - f/30) + 0.5\sqrt{f/30}$
$4(\sqrt{f/14} - f/14) + \sqrt{f/30}$	$8.63(\sqrt{f/30} - f/30) + 0.5\sqrt{f/30}$
1.5-dB bump + $\sqrt{f/30}$	1.5-dB dump + $\sqrt{f/30}$

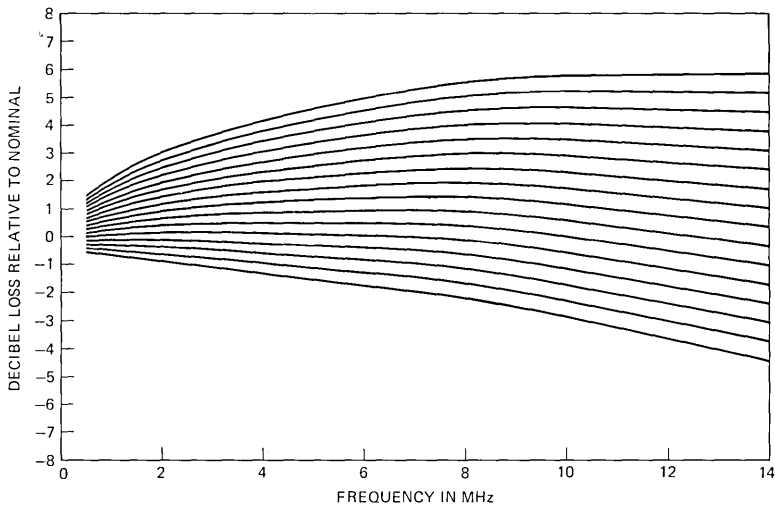


Fig. 12—One-eighth of the possible switchable network settings obtainable in the low band (nominal loss is equivalent to half the total switchable network loss).

produce transmission changes which are roughly proportional to root- $f$ .

The rationale behind giving the “root- $f$ -minus- $f$ ” shape the second largest range is more subtle. Consider the following: Cable loss per unit length,  $\alpha$ , can be expressed quite precisely as a function of frequency,  $f$ , by

$$\alpha = A\sqrt{f} + BDf, \quad (3)$$

where  $A$  and  $B$  are independent of frequency and  $D$ , the dissipation factor, is a measure of the loss due to the cable dielectric. Variations in nominal  $\alpha$  for manufactured cable that are due to variations in  $A$  are quite closely compensated for over the entire transmission band when each cable section is cut individually to a specified top frequency loss. Variations in  $B$  or  $D$ , on the other hand, are compensated for correctly only at the cutting frequency, because one is attempting to correct an

attenuation error that is directly proportional to  $f^*$  by varying a loss that is closely proportional to  $\sqrt{f}$ . (For SG cable, at 30 MHz the first term in eq. (3) is 94 percent or more of the total.) The resulting misalignment is compensated for reasonably well in the OBE by the root- $f$ -minus- $f$  switchable shape.

The third switchable shape, the broad bump, is the only one that is not specifically cause-associated. However, the root- $f$  shape has its greatest effect toward the top of each band, and the root- $f$ -minus- $f$  shape has its greatest effect near the bottom. Thus, the bump, whose effect is primarily in the middle of each band, provides a general-purpose equalization characteristic to the switchable networks.

Associated with each switchable network (and the test-lead splitting pad) is a small magnetic latching double-transfer relay. These relays are set to one of two possible states by means of a stepping selector switch. The stepping selector is operated by a series of pulses of either polarity applied to the switch control lead that enters the OBE housing at the end opposite the transmission test lead (Fig. 11). The selector is a single-pole, 16-position switch, each position associated with a particular relay and network, or with a reference condition. Each pulse applied to the switch control lead accomplishes two functions. First, it advances the selector one position (independent of pulse polarity). Second, a positive pulse switches the network (relay) associated with the new position "out," whereas a negative pulse switches the network into the transmission path.

### 5.1.2 Mop-up networks

In contrast to the switchable mode, two features of the mop-up networks worth noting are:

- (i) Their ability to provide fine-grain (i.e., ripply) compensation.
- (ii) The relatively short interval required between design of these networks and completion of manufacture of the OBE.

To achieve these features, each mop-up network uses a modular-design, constant-resistance (50-ohm) bridged-T configuration constructed from a predetermined stockpile of components and standardized hardware.<sup>†</sup> Parasitic circuit effects of components and hardware have been well-characterized in advance, because there is no time for the usual engineering development to assess and correct second-order effects. Specially written computer programs are used to expedite design and documentation effort. Network performance is computed taking into account the effects of parasites and discrete component values, and elec-

---

\* This is not strictly true for variations in  $D$  which can be frequency-dependent, but the point is still valid.

† This ensures that aged undersea cable quality components are available simultaneously with a network design.

trical test specifications are generated for both individual networks and tandem assemblies. The OBE is designed so that the complete equalizer, less mop-up networks and high-pressure housing, can be constructed and tested before mop-up design information is available.

An individual bridged-T network can provide a positive bump shape (loss vs frequency), a negative bump (dip), simple low- or high-pass shapes, or flat-loss. Networks can be connected in tandem (with minimum interaction due to the constant resistance design) to obtain combinations of these shapes. In practice, most mop-up networks are the bumps or dips, whose circuit configuration is shown in Fig. 13. For a fixed characteristic impedance,  $R_0$ , such simple shapes can be completely specified by peak (bump or dip) amplitude, center frequency, and stiffness (which can be defined as the ratio of upper half-loss frequency to center frequency).

The range chosen for the SG mop-up component stockpile is shown graphically in Fig. 14. The symmetry of this figure results from the nature of the bridged-T for bump and dip shapes which calls for a pair of LC resonance values that intersect equidistant from the horizontal  $R_0$  line along a vertical line corresponding to the center frequency. Similarly, the pair of shunt and series resistance values falls equidistant above and below the  $R_0$  line in Fig. 14. In some cases, when a network design calls for component values outside this range, a flat-loss network transformation can be applied which moves the required values inside the stockpile range. The resulting transformed network then has a loss which is the sum of the desired loss shape and additional flat loss.

The designer of mop-up networks must "spend" his flat loss wisely, because the available flat-loss is limited to 9.5 dB in the low band and 12.5 dB in the high band. The number of mop-up networks in a particular OBE could be less than the seven per band allowable from physical

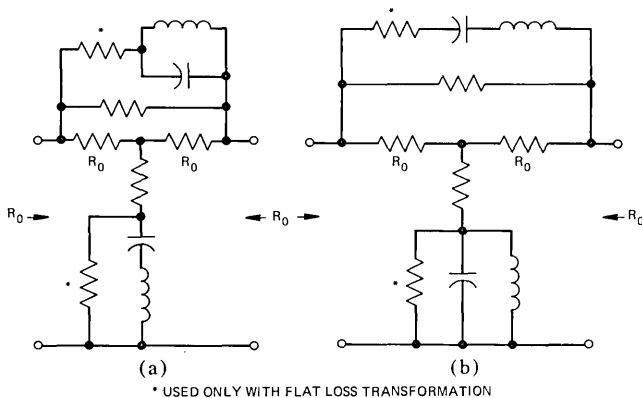


Fig. 13—Mop-up network configurations. (a) Loss dip. (b) Loss bump.

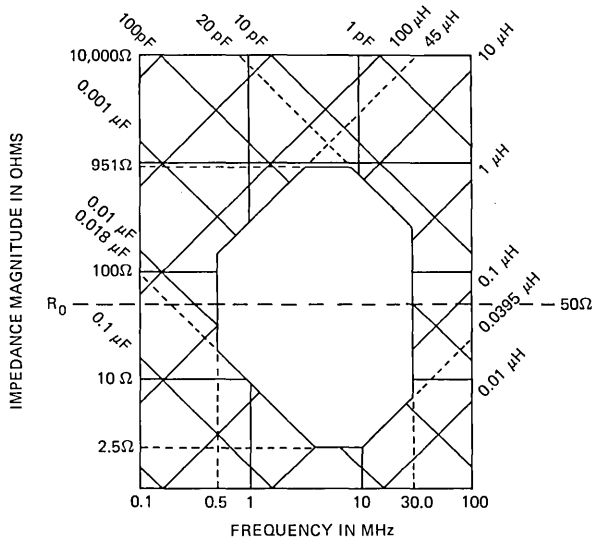


Fig. 14—Stockpile range.

Table XI — Passive OBE components

Component	Description	Value	Tolerance (percent)	Use
Resistor	Wirewound, vitreous enamel, power resistor	14.0 ohms	±1	Selector switch circuit
Capacitor	HV oil-impregnated, paper dielectric, housed in ceramic cylinder with metal end caps	0.02 μF	±3	PSF(A) and (B) assemblies
Inductor	Duolateral-wound over plastic form capable of continuous operation with up to 0.7 amperes through windings	1.0 mH	±5	PSF(A) and (B) assemblies
Selector-switch Relay	18-point, unidirectional switch “Crystal can” size, hermetically sealed, magnetic-latching relay containing two transfer break-before-make contacts with No. 1 contact metal. Relay has an H-shaped spring-supported armature-magnet assembly and an isolated, hermetically sealed coil chamber.			

constraints because of the limited amount of flat loss which is available.

### **5.1.3 Components**

With the few exceptions noted in Table XI, all components used in the ocean-block equalizer are identical in type with those used in the repeater, which have already been described.

### **5.2 Shore-controlled equalizer**

Because of uncertainty in the long-term stability of cable loss, plans for the earlier SD and SF systems had included shore-controlled equalizers (SCEs). In both cases, however, development effort on the SCEs ceased when adequate cable loss stability was assured. Based on this experience, the SG system development began assuming SCEs would not be required. In mid-1975, six months prior to the beginning of the first deep sea lay of TAT-6, cable loss changes noted in factory measurements<sup>3</sup> clearly indicated the necessity for installing SCEs. Development was started in August 1975, less than six months before the date the first unit was due to be shipped. This extremely short time interval required the use of readily available components.

#### **5.2.1 SCE realization**

The SCE has much in common with the OBE: directional filters, switched network configuration, and certain hardware. The OBE stepping-selector switch is replaced by an instrument-type 50-mW dc motor and gear train furnished by CIT.\* A modified repeater GSF replaced the PSF of the OBE, and a final gear reducer and wafer switch assembly were procured from commercial sources. Special filters, amplifiers, and rectifiers using available and aged SG components were designed to control the electromechanical switching operation.

#### **5.2.2 Method of control**

The SCE uses the same type of magnetic latching relays as the OBE for switching networks in or out of the transmission paths. Relay states in each SCE are controlled by two unique frequencies spaced 400 Hz apart in the 11.464- to 11.472-MHz band. As shown in Fig. 15, the two signals transmitted from the A terminal are selectively amplified and rectified in the SCE to produce two dc control voltages. The output of the motor channel powers the motor which turns the selector switch; the output of the relay channel, when present, serves as an "activate" signal for the latching relays as they are sequentially accessed by the selector switch. Position identification information is transmitted back to the A terminal by amplitude modulating the second harmonic of the motor channel frequency. Two adjoining selector positions are associated with each relay and network. One position corresponds to switching the network in, and the second corresponds to removing the network.

---

\* Compagnie Industrielle des Télécommunications.

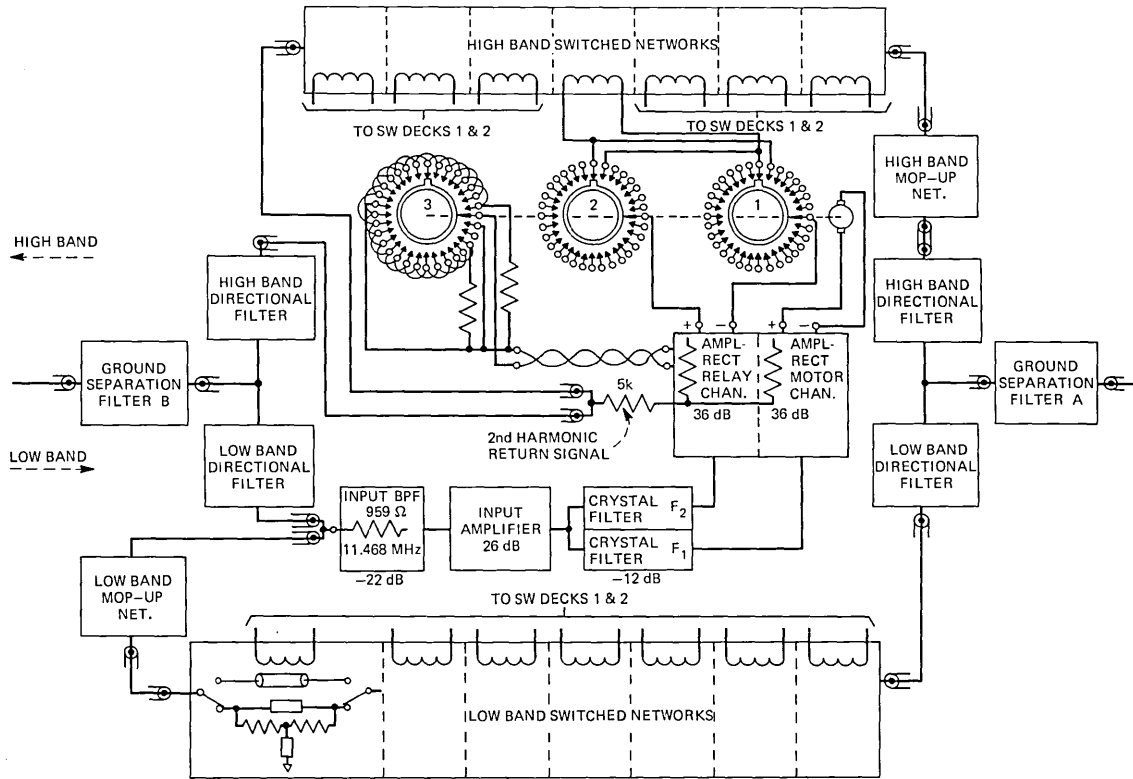


Fig. 15—Block diagram of SG shore-controlled equalizer.

Figure 16 is a chart recording of the second harmonic signal as received during an SCE-adjusting operation. The annotations indicate the loss shapes of the seven switchable networks in each band. Individual networks are switched in or out by transmitting a short burst (2–3 s) of the relay channel tone during the interval, typically 12 s, that the network coil is connected to the relay channel rectifier. By monitoring the level change of a supervisory tone which goes through the SCE, one can verify immediately that the network has switched.

Figure 17 shows the typical characteristics of the two control channels. The SCE is normally left in the index position after adjustment. In this position, the relay channel rectifier is connected to a diode rather than a relay coil. As the relay channel signal level is slowly increased, the second harmonic return increases smoothly until an abrupt step of about 20 dB occurs, indicating that the rectifiers have begun to conduct. This point serves as a reference level; a signal 12 dB above the reference will produce sufficient power to switch a relay. The motor channel characteristics are similar. The control tones are tuned to the precise center frequencies of their respective crystal filters by monitoring the returned second harmonic signal.

### **5.2.3 Control system design**

The control system of the SCE is a modified version of that used in the French S-25 system designed by Compagnie Industrielle des Télécommunications. The success of the accelerated SCE project is largely due to the cooperation of CIT in sharing their knowledge and experience and in furnishing the critical motor-gear train assemblies.

A number of measures prevent false operation of the SCE. The control frequency band, 11.464 to 11.472 MHz, is a space between supergroups normally used for noise monitoring. A band elimination filter at the A terminal blocks undesired incoming signals in this band. The operating level for the control tones was chosen sufficiently high, up to  $-6$  dBm at repeater output, to preclude the possibility of inadvertent operation. The second harmonic return signal exceeds the system background distortion by at least 20 dB. From the normal "rest" position of the controls, both  $F_1$  and  $F_2$  must be applied to change the SCE setting.

**5.2.3.1 Filters.** The input bandpass filter, centered at 11.468 MHz, is an LC type with a 4-dB bandwidth of 0.5 MHz and is designed to operate between 1000- and 50-ohm impedances. Together with the 959-ohm isolation resistor, it has a through loss of 22 dB and adds less than 0.2-dB bridging loss to the low-band transmission path.

Each crystal filter contains a single crystal of the same design used in supervisory oscillators. The crystal, with a series resistance of 20 to 36 ohms, operates in series between impedances of typically 5 ohms. Each filter provides at least 34 dB of adjacent channel suppression (400 Hz away) while adding 12 dB of flat loss.

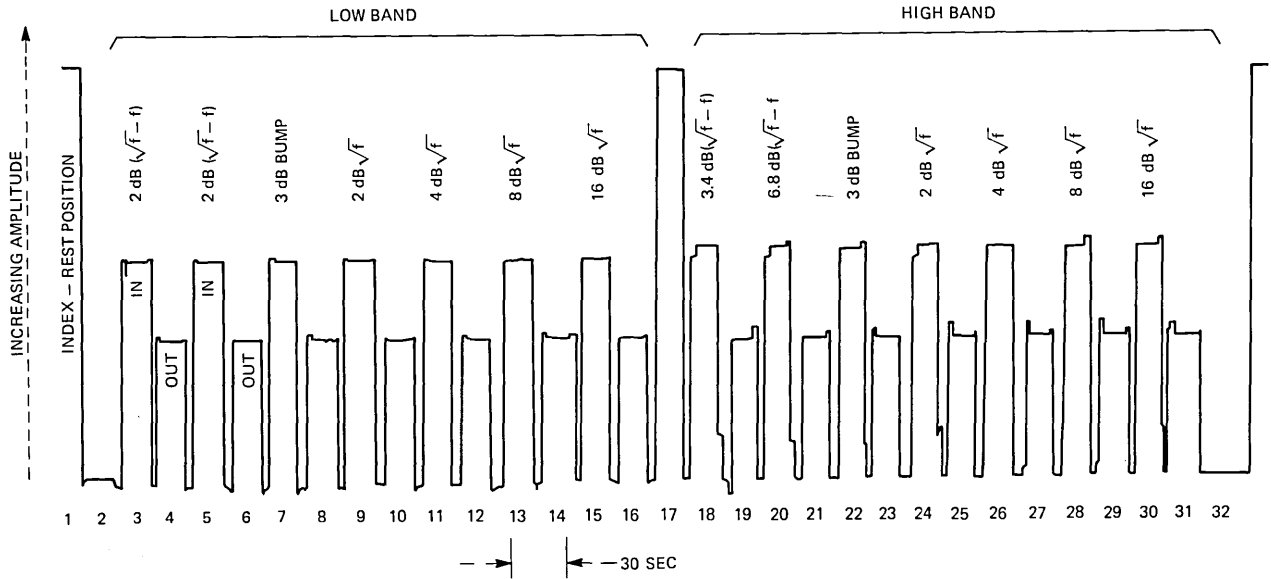


Fig. 16—Shore-controlled equalizer—second harmonic signal,  $2F_1$ , returned to shore during adjustment.



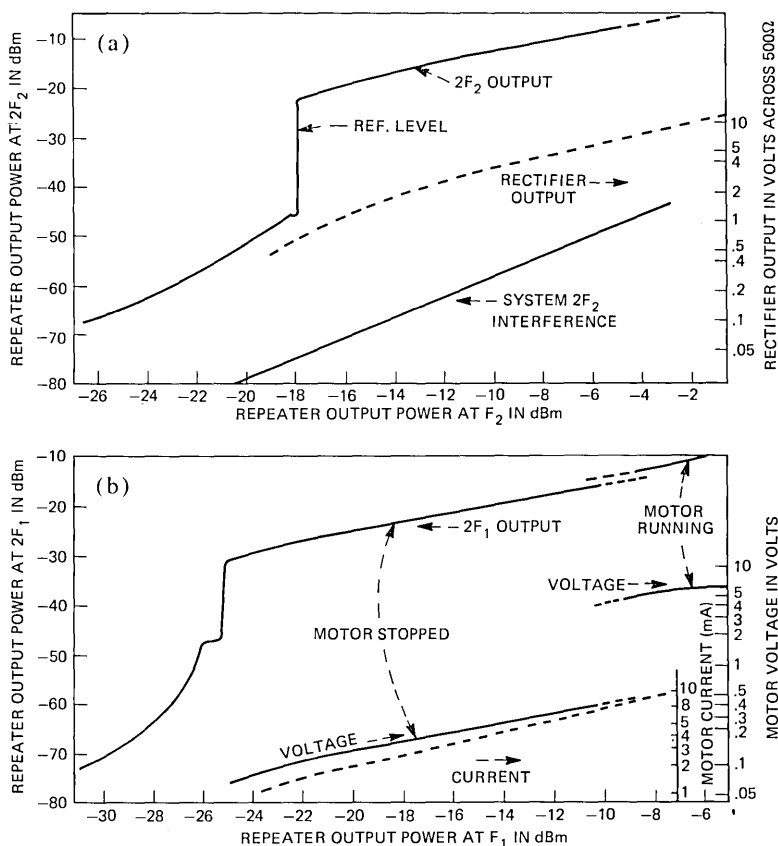


Fig. 17—(a) SCE relay-activate channel characteristics. (b) SCE motor channel characteristics.

**5.2.3.2 Amplifiers.** The three amplifiers are identical except for gain and terminations. Each has two common emitter stages with gain controlled by feedback and each is biased at 12 V, 219 mA. The input amplifier has 26-dB gain and 50-ohm input and output impedances. Each power amplifier provides a nominal gain of 36 dB. The power amplifier input impedances are low, as required by the crystal filters, and the outputs are tuned to operate efficiently into a voltage doubler-type rectifier. The actual gain of each power amplifier is tailored, by choice of feedback resistor, to accommodate the loss of its associated crystal filter. The gains and losses are arranged so that each rectifier will deliver 50 mW (5.0 V, 10 mA) to its load (motor or relay) when the signal power at the SCE input is  $-8$  dBm. Each amplifier rectifier will deliver a maximum output power of at least 200 mW.

**5.2.3.3 Electromechanical.** A precision-instrument-type, permanent magnet, dc motor drives an attached 2000:1 ratio gear train. A 15:1 worm

gear which connects to the wafer switch assembly provides the final reduction. Each of three identical switch wafers has a single pole and 32 positions, 31 of which are active. Two of the wafers connect to the relay coils. Each coil requires two positions, one for switching the network in and one for switching the network out. The third wafer is used as a four-level loss switcher which amplitude-modulates the power of the second harmonic return signal as the switch slowly turns. This return signal informs station personnel of the select switch position.

#### 5.2.4 Future improvements

Since completion of TAT-6, a solid-state circuit has been developed to replace the motor-switch assembly. The remaining components in the SCE are virtually unchanged.

#### 5.2.5 Switchable range

The switchable loss shapes available in the SCE are listed in Table XII. The networks are similar to those in the OBE except that the range and step sizes are twice as large. The SCE has no mop-up network capability.

### VI. MANUFACTURING

#### 6.1 Schedules and production rate

Repeater and equalizer final assembly and much of their manufacturing were done at a special factory in Clark, N.J. as with earlier repeaters for SD and SF.

Authorization to proceed with production was received in February 1972, with the first repeater scheduled for shipment in December 1974. Prior to the start of manufacturing, it was necessary to design new manufacturing and test facilities required to handle the SG hardware and the increased frequency range.

Because of the mid-1976 service date of TAT-6 and because the system called for over 800 repeaters and equalizers, it was necessary to achieve

Table XII — Shore-controlled equalizer switchable loss shapes (dB)

Low Band	High Band
$16 \sqrt{f/30}$	$16 \sqrt{f/30}$
$8 \sqrt{f/30}$	$8 \sqrt{f/30}$
$4 \sqrt{f/30}$	$4 \sqrt{f/30}$
$2 \sqrt{f/30}$	$2 \sqrt{f/30}$
$8 (\sqrt{f/14} - f/14) + 2 \sqrt{f/30}$	$34.52 (\sqrt{f/30} - f/30) + 2 \sqrt{f/30}$
$8 (\sqrt{f/14} - f/14) + 2 \sqrt{f/30}$	$17.26 (\sqrt{f/30} - f/30) + 0.5 \sqrt{f/30}$
3-dB bump + $\sqrt{f/30}$	3-dB bump + $\sqrt{f/30}$

production capacity of 16 units per week. Concurrently, it was necessary to maintain capacity for other systems at a rate of three units per week.

## **6.2 Environmental conditions**

All critical assembly operations are performed in “clean” rooms where temperature, humidity, and airborne contaminants are closely monitored. Objectives are less than 50,000 dust particles above 0.5 microns per cubic foot, temperatures of  $22.8^{\circ} \pm 1.1^{\circ}\text{C}$  ( $75^{\circ} \pm 2^{\circ}\text{F}$ ), and relative humidity of less than 40 percent. In the paper capacitor winding room, relative humidity is controlled to less than 20 percent. Dust counts on three sizes of particles (0.5, 1.0, and 2.0 microns) are monitored weekly for each clean room. Positive air pressures are maintained and monitored in all rooms and associated vestibules to prevent entry of contaminants.

## **6.3 Product development and manufacturing facilities**

The design of the SG system required improved manufacturing and test facilities. The purpose of these facilities was to enable the manufacture, aging, and testing of new components such as ceramic capacitors, to provide new transmission test facilities, and to provide new and improved facilities for closure type operations. Development work on facilities began at Clark, N.J. in February 1971.

### **6.3.1 Aluminum castings**

The large number of repeaters and the elimination of the hermeticity requirement for the electronics unit required that more economical procedures for making aluminum castings be investigated.<sup>7</sup> The investigation revealed that the castings should be made from the low-pressure permanent mold (LPPM) process and the cylinder should be extruded. Expensive machining operations were virtually eliminated with no sacrifices in quality. In addition, the separate, one-piece cylinder simplified the epoxy coating procedure and subsequent assembly with the main frame, which simply slides into the surrounding cylinder, where it is locked in place.

### **6.3.2 Ceramic capacitors**

Ceramic capacitors, new to undersea cable application, were substantially different from their predecessor,<sup>8</sup> the mica capacitors, both in physical appearance and electrical characteristics (Fig. 18). Their use in SG circuits was mandated by the need for smaller encapsulated units having negligible parasitic inductance. Replacement of mica with ceramic also reduced costs and avoided a serious procurement problem, that of purchasing top quality mica.

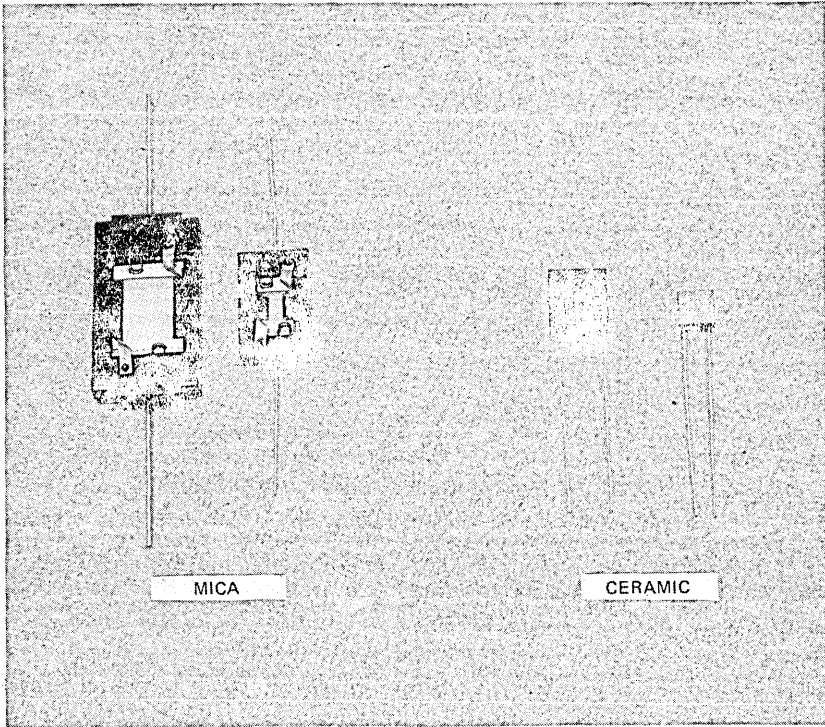


Fig. 18—Comparison of ceramic and mica capacitors.

Although ceramic capacitors are purchased from commercial suppliers, prior to manufacture of electronics, complete in-house qualification procedures had to be specified and implemented. Principal tests performed included insulation resistance, dielectric strength, capacitance, and conductance along with 17 weeks of voltage conditioning aging (see Fig. 19).

Because of its physical design, the ceramic capacitor was readily adaptable to automatic testing methods. Special test processing fixtures were provided onto which 25 capacitors were attached for processing through the full complement of tests. Flexibility was designed into the fixtures, enabling the capacitors to be tested individually for capacitance, conductance, and insulation resistance, or as a group of 25 as is required during aging and breakdown testing. Because of stringent tolerance requirements, 0.1 percent in some cases, test set accuracies and repeatability has to be in the order of 0.01 percent. Special design features such as gold-plated contact points on fixtures and shielding to eliminate stray parasitics were necessary.

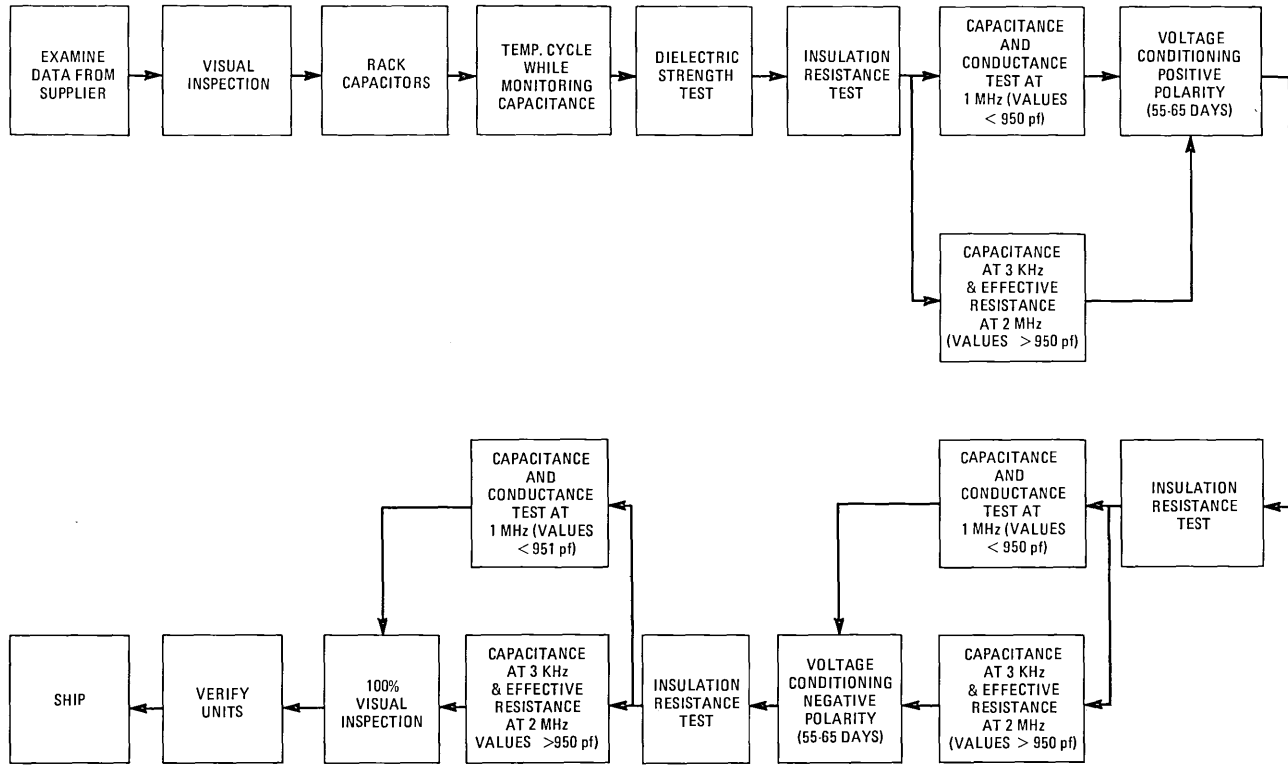


Fig. 19—Ceramic capacitor process flow chart.

### **6.3.3 Printed-wiring-board assemblies**

From a manufacturing viewpoint, one of the significant changes in physical design was the use of printed-wiring boards (PWB). PWB requirements and assembly techniques were developed with specific attention to component mounting procedures, fixturing, and soldering techniques. Overlays were provided to assist the technician in proper location of components. In addition, training programs were developed to acquaint the operators and inspectors with component identification, and to identify various component and board defects which could degrade reliability.

Detailed investigations were undertaken to establish improved board manufacturing processes and requirements. Plating procedures were revised and improved at printed-wiring board manufacturing locations. New visual standards to aid in judging dewetting of solder-coated circuit paths were also developed.

### **6.3.4 Seals**

The function of the high-pressure seal is to provide a dc power and signal transmission path into the high-pressure housing. It must withstand high dc voltage and full sea pressure, while maintaining a satisfactory coaxial transmission path. The seal chosen for the SG repeater and equalizer was a modified version of the 8-type seal manufactured at Western Electric's Burlington, N.C. plant. Its predecessor, the 3-type seal used in SF, did not have suitable transmission properties in the SG high band.

The primary sealing mechanism in both seals is the thin polyethylene gasket adjacent to the ceramic. In the 3-type, the ceramic is backed up by a large metal disk which provides satisfactory mechanical performance but introduces excessive capacitance with respect to the 50-ohm transmission impedance. The metal disk was eliminated in the design of the 8-type seal and a larger ceramic cylinder was used. This produced a suitable mechanical seal and at the same time reduced the capacitance to provide proper transmission impedance.

The 8-type seal (Fig. 20) was completely molded in one operation, including attachment of both pigtail leads, rather than three molding operations needed for the 3-type seal. This resulted in reduced cost and increased production capacity from each molding press.

The most severe problems encountered in developing the 8-type seal involved the feed-through assembly. The copper caps on the ends of the ceramic are provided to control electric field strengths. Initially, these were brazed to the ceramic to provide hermeticity in the assembly, but forces generated in the molding operation were sufficient to break the ceramic adjacent to the braze joint, destroying the hermeticity. This problem was overcome by making the conductor in two parts with the

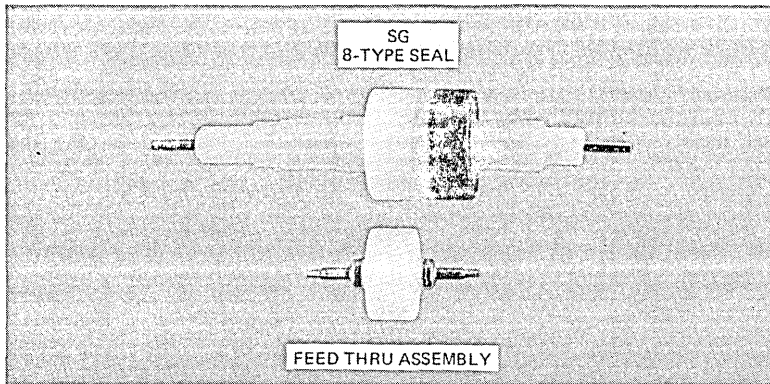


Fig. 20—High-pressure seal.

cap configuration integrally formed on each. These are assembled to the ceramic part (with small fluoroplastic washers between the ceramic and the caps) and screwed together with a coupling sleeve within the hole in the ceramic. A small slug of solder is included in this assembly. The unit is then heated to melt the solder into the threads and the threads are torqued hand tight. Upon cooling, the conductor parts are fused together. Differential thermal shrinkage compresses the fluoroplastic to form a hermetically sealed assembly.

This design change eliminated the need for metallizing the ceramic and brazing the caps to the ceramic, reduced the cost of the feed-through assembly, and produced a higher quality seal.

### 6.3.5 Subassembly and final repeater testing

Early in the planning, it was decided that the bulk of the transmission testing would be performed by a computer-operated transmission measuring set<sup>9</sup> (COTMS). Duplicate sets were provided. Choice of the COTMS was based on: (i) its ability to handle a measuring sequence automatically, including recording and interpreting results, and (ii) its precision, repeatability, and precision up to the prescribed top frequency. The COTMS has an accuracy with measurement-averaging of within 0.001 dB. Full utilization of the COTMS included time-sharing of the main measurement unit via remote stations, and formulation of programs specifically tailored to the product needs.

Software packages provided specific instructions to the tester so that type of unit, operation to be performed, and serial number could be double-checked prior to the start of testing. In addition, the software packages identified the proper sequence of test frequencies, checked test results at each frequency against specified limits, and stored a test history for each unit. CRT display units were used as input and output devices

to provide communications between the tester and the computer-monitored test facility. Data were collected on disk and later transferred to magnetic tape for analysis and storage. With the above programming and proper use of remote stations, a test capacity in excess of 20 repeaters per week was attained.

In addition to the COTMS facilities, a precision-adjusting test facility known as MINI-COTMS was also needed. Although called a MINI-COTMS, it bears little resemblance to the COTMS described above. Application of this facility was confined to repeater network and equalizer network tuning.

In the repeater network, five inductors are available for final tuning. Nominal gain for each of 118 discrete in-band test frequencies is stored in computer memory, while deviations from nominal for each frequency are visually displayed on the MINI-COTMS. A special program and adjusting procedure had been formalized which enabled the tester to minimize deviations at most in-band frequencies. The true value of this facility is readily apparent during adjustment, since some of the inductor adjustments interact with one or more others. In this situation, it is a great advantage to have the entire range of frequencies displayed on the CRT output. (Insertion loss measurements are displayed with a precision of  $\pm 0.015$  dB.) The CRT output, which includes the RSS value of the gain deviation, is observed by the tester while he is performing the final tuning operation. Maximum deviations allowable are of the order of  $\pm 0.05$  dB with the number of peaks being minimized. Hard copy output is obtained in two forms: values printed to the thousandth of a decibel and a plotted form. Optimum adjustment and use of results to apply corrective action led to minimum deviations among repeaters, which in turn led to a more readily equalizable system and more voice channels.

Equalizer adjustment procedures are similar to the procedures used to tune repeater networks but on a larger scale, with two parameters (insertion loss and return loss) being monitored. Over 70 inductors per equalizer are adjusted on this facility, with a maximum of 14 appearing on any one subassembly. Without a facility having the interactive capability and accuracy of MINI-COTMS, equalizer adjustment would have been virtually impossible.

Other facilities designed for network testing were the crystal oscillator test set, accurate to within 0.1 Hz in the 27-MHz frequency range, a noise and modulation test set, and coarse adjustment ( $\pm 0.1$  dB) test facilities.

### **6.3.6 Corona testing**

Repeaters have been designed to eliminate corona. However, disturbing "pops," or electrical discharges, can be generated under certain conditions. "Pops" above certain voltage levels can cause errors in data



transmission, degrade the quality of voice transmission, and deteriorate insulation.

For SG, extensive effort was spent on developing corona detection equipment and trouble-shooting techniques. A new wide-band detector was designed with the capability of detecting all possible wave shapes with uniform sensitivity across the 30-MHz transmission band. A 2.44-m × 3.66-m shielded room was constructed to provide for high production levels and stringent shielding requirements and to house the product during test. The capability of testing ground separation filters in a pressurized state was also provided. Experience obtained on previous projects proved that pressurizing tends to retard corona impulses. This is an acceptable procedure since final repeaters are pressurized with 4.4 atm (50 psig) of dry nitrogen. In actual production, 12 fixtures were provided and used with a majority of the ground separation filter testing performed with 1.68 atm (10 psig) of dry nitrogen applied to the product.

### **6.3.7 Closure**

Operations associated with closure of the repeater required some completely new facilities as well as an upgrading of existing facilities. Among the more significant changes were: introducing eB (electron beam) welding for joining the high pressure end covers to the copper beryllium housing, instituting a low-pressure test for checking the prime sealing surface of the seal, and modifying vacuum-drying facilities to enable this operation to be performed in the assembled repeater stage of production.

Seals were tested at low pressure to check the mating of the prime sealing surface of the high-pressure seal to the surface of the high-pressure end cover. In performing this test, an O ring and seal are assembled into a high-pressure cover under a small axial load. This relatively minor load, compared to the load when subjected to ocean-bottom pressures, permits the prime sealing surfaces to be tested without fear of the seal bulging to form a side or secondary seal. Helium at 7.8 atm (100 psig) is applied to the seal for two hours. The leak rate of helium past the O ring and prime sealing surfaces, plus migration through the polyethylene body of the seal or along the interface of the internal feed-through, is monitored with a mass spectrometer.

Because of the elimination of a sealed inner unit, the vacuum-drying operation had to be performed in the final stage of manufacture (unit sealed in its copper beryllium housing). This meant that existing facilities had to be modified to:

- (i) Include heating blankets that reduced the heat losses and were capable of heating the large copper beryllium housing to a temperature of 57°C (135°F).

- (ii) Handle a 500-pound (227 kg) repeater.

#### 6.4 Quality and verification of product

Manufacture of submarine cable repeaters and equalizers places emphasis on ensuring long-term stability and system reliability. To achieve this end, factors such as training personnel, maintenance of a clean work environment, and adherence to detailed processing specifications were stressed. A series of multiple inspections includes audits of procedures, methods, drawings, and product to assure conformance. These are all vitally important. For TAT-6, over 12,000 items of component performance data were transmitted on a daily basis to the data center for analysis, subsequent statistical manipulation, and finally storage.

As previously mentioned, transmission tests on the electronic subassemblies were performed and verified by the COTMS test facility. These measurements were immediately compared against specified limits, thereby providing instant feedback as to the acceptability of the unit tested. This instant feedback feature was important since it enabled engineering to investigate the cause of unusual test results while a unit was still in the original "fixtured" condition. Data were analyzed for trends so that impending out-of-limit conditions could be detected and compensating adjustments made before serious problems developed. Statistical data were also used as a basis for analyzing out-of-limit conditions and determining proper resolution.

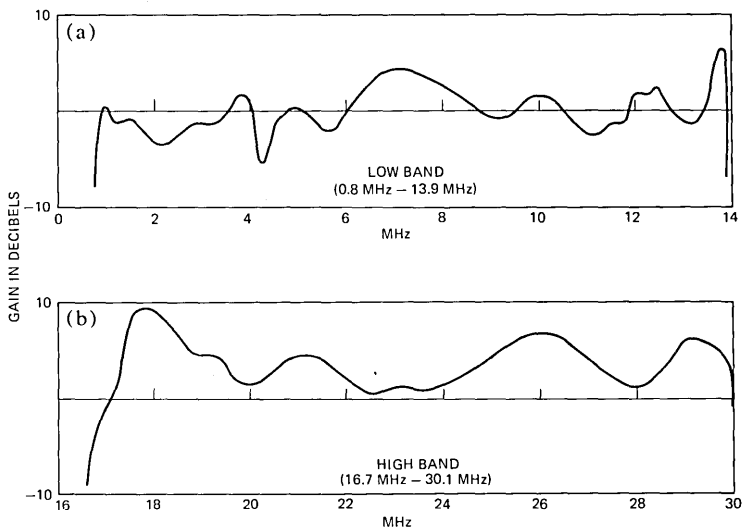


Fig. 21—TAT-6 undersea system misalignment.

Although the aging and testing program is time-consuming, it provides maximum assurance that system components will operate for their intended life.

Equally important with aging and test programs are the procedures which ensure that physical design requirements have been met and that accurate data have been transmitted. It is also necessary to insure that all operations, inspections, and deviations have been properly recorded. For these purposes, multiple inspection procedures are used. First, all operations, inspections, and tests are documented and verified by the signature of the person performing the operation. Second, product examiners verify that prior operations have been performed satisfactorily through entries on data sheets. Third, before any apparatus item (component or subassembly) can be shipped, inspection must verify that all operations have been properly performed.

All data pertinent to the assembly and test of a repeater likewise are compiled in a data book prepared for that specific repeater. This data book is verified for completeness and conformance by a Western Electric Auditor of Manufacturing Practices (AMP). The pertinent data (primarily electrical) are also checked by a resident Bell Laboratories engineer.

As an additional check of quality, the AMPS perform an independent random check of product previously accepted by product examiners.

The Quality Assurance Organization, independent of Western Electric product engineering, is responsible for preparing and performing quality surveys in collaboration with their Bell Laboratories counterparts. One such Bell Laboratories QA engineer is resident at Clark. QA surveys cover detailed investigations of compliance with specified procedures, methods, and drawings in all manufacturing areas.

## **VII. TAT-6 EXPERIENCE**

### ***7.1 Undersea system misalignment***

The net misalignment of the TAT-6 undersea system is shown in Fig. 21. The low and high bands contain 53 and 54 supergroups, respectively, including the frequency bands occupied by the order wire and supervisory tones. As indicated in a companion article,<sup>2</sup> the repeater level variation at some frequencies exceeds the end-to-end misalignment. The unpredicted repeater gain deviations arose largely from reflections between the repeater and the cable terminations. The design of the OBE mop-up networks was based upon transmission information obtained from measurements and computer simulation of prototype cable terminations. Evidently, the measured samples of terminations were not representative. With the completion of the first deep sea lay, it was obvious that a special OBE mop-up design would be required following each lay to maintain the misalignment within acceptable limits. Manufacture

of the first such special OBE was completed within a period of two weeks following availability of new mop-up network designs. The OBE was installed near the beginning of the second lay.

## 7.2 Noise performance

The measured thermal and second-order noise performance of TAT-6 was both satisfactory and consistent with predictions. Third-order intermodulation noise in the top part of the high band, however, exceeded our predictions by as much as 18 dB. The signal-to-noise ratios obtained by noise loading tests during commissioning are shown in Fig. 22. To minimize the total noise at high frequencies, repeater levels were lowered roughly 6 dB. Both the measured and the predicted 29.182-MHz signal-to-noise ratios are indicated in Fig. 23. Third-order intermodulation distortion normally increases 3 dB per 1-dB increase in signal level. On TAT-6, we observed a ratio that varied between 3:1 at low signal levels to 1.8:1 at high signal levels. Narrow-band noise loading tests (2 to 10 supergroups) indicated that most of the third-order distortion was generated by signals close to the frequency of the measured channel.

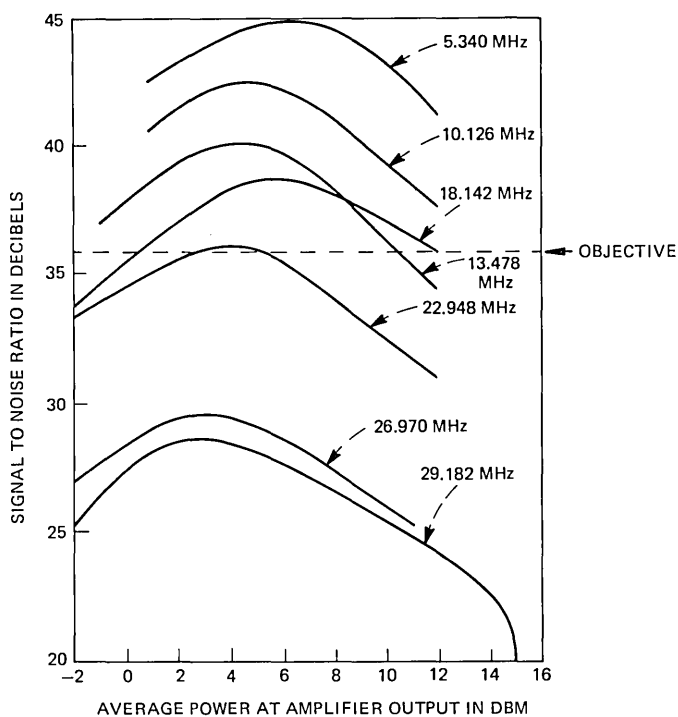


Fig. 22—TAT-6 measured signal-to-noise ratio.

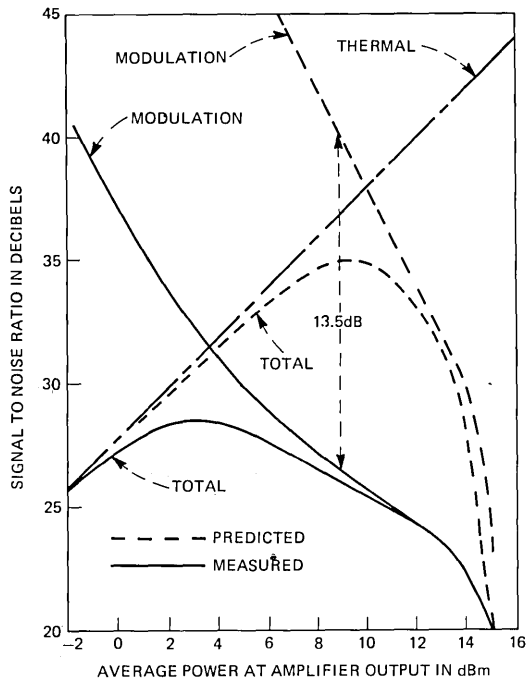


Fig. 23—TAT-6 measured and predicted 29.182-MHz signal-to-noise ratio.

### 7.2.1 Characterization of $M_{3E}$

Calculations of system intermodulation noise were based upon average repeater levels, repeater delay characteristics, and repeater modulation coefficients, each being a function of frequency. The modulation coefficients  $M_{2E}$  and  $M_{3E}$  were characterized in the same manner that had been successfully used in past systems.

A repeater is loaded with three or more fixed fundamental tones of frequencies  $A$ ,  $B$ , and  $C$ . Various product frequencies of the type  $A \pm B$  and  $A \pm B \pm C$  are measured. In the simplest case when the amplifier output stage is the dominant source of distortion, the coefficients  $M_{2E}$  and  $M_{3E}$  depend only on the product frequency and not on the specific fundamental frequencies. If there is significant dependence on fundamental frequencies, one must consider the effects of signal shaping and delay distortion in choosing the single most appropriate value of a particular modulation coefficient for use in calculating system noise.

In developing the SG repeater, the following fundamental frequencies were used to evaluate repeater intermodulation: 5.8, 14.5, 15.2, 16.6, 21.7, and 27.5 MHz. Nine different third-order and 17 different second-order product frequencies were measured in characterizing the repeater distortion coefficients. In addition, the distortion was measured at two different power levels, +5 and +12 dBm per tone.

Discovery of the excessive third-order intermodulation noise on TAT-6 triggered an intensive search for the source. Instead of measuring repeater distortion with fixed fundamental frequencies, fixed pairs of bandstop-bandpass product-frequency filters and continuously variable fundamental frequencies were used. A contour plot of the measured 3-tone ( $A + B - C$ ) distortion at 26.6 MHz and 2.5°C is shown in Fig. 24 with  $A$  and  $B$  as the independent variables. (Frequency  $C$  depends on  $A$ ,  $B$ , and the product frequency.) Frequency triplets that produce equal distortion are connected with "isomodulation contours." The distortion increases with the frequency of each fundamental and the product. Also the distortion tends to peak for products whose fundamentals are close to the product frequency. The latter are the same products which tend to add in phase from repeater to repeater and thus dominate on long systems. These "significant" distortion products increase in power by about 6 dB between room and sea-bottom temperatures, while those which were measured during development and manufacture decrease about 1 dB over the same temperature range.

### **7.2.2 Source of excess third-order distortion**

Because of the frequency, power level, and temperature dependence of repeater third-order distortion, the initial characterization was inadequate and misleading. Improved measurement techniques indicated that the two surge-protection diodes in the output network increased the repeater distortion by about 12 dB. Distortion caused by these diodes cannot be explained in terms of conventional behavior involving nonlinear resistance and capacitance. The distortion can, however, be explained semi-quantitatively in terms of nonlinear MOS (metal-oxide-semiconductor) capacitance and conductance effects. In addition, tests have shown that when the reverse-biased output network diodes are replaced with reverse-biased MOS capacitors, the resulting distortion contours have characteristics similar to those of Fig. 24. The distortion, while of third-order type, is actually produced by second-order interaction; second-order products are generated and modulated again with the fundamental signals. At the time of this writing, it is not clear in detail how the MOS-type nonlinearity is produced in the surge-protection diodes. Figure 25a is a block diagram of a nonlinear network whose calculated isomodulation contours have the same characteristics, Fig. 25b, as those measured on an SG repeater.

### **7.2.3 Future noise improvement on TAT-6**

Following the successful analytical modeling of the repeater third-order distortion, an experimental post-distorter network was designed, built, and tested. The distorter, consisting of diodes and linear networks, achieved 15 to 20 dB of third-order distortion reduction on a single repeater over a 10-dB dynamic range.

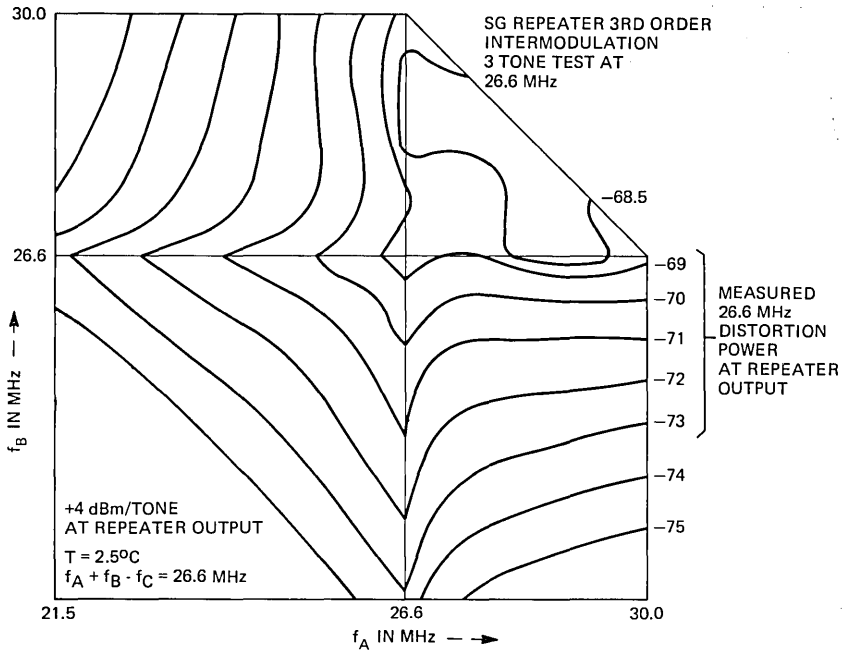


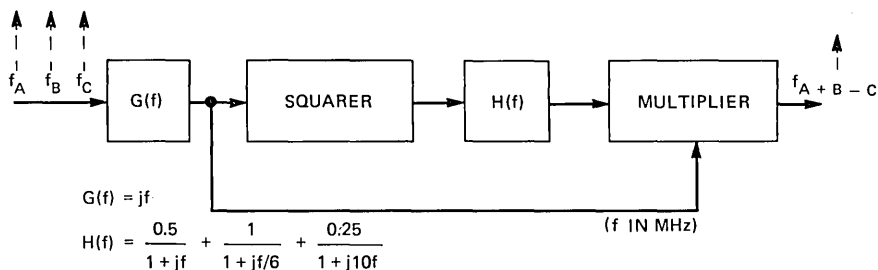
Fig. 24—Isomodulation contours of SG repeater with surge protection diodes.

It was further successfully tested as a possible noise canceler on TAT-6 by noise-loading single supergroups in the portion of the high band where delay distortion is relatively small.

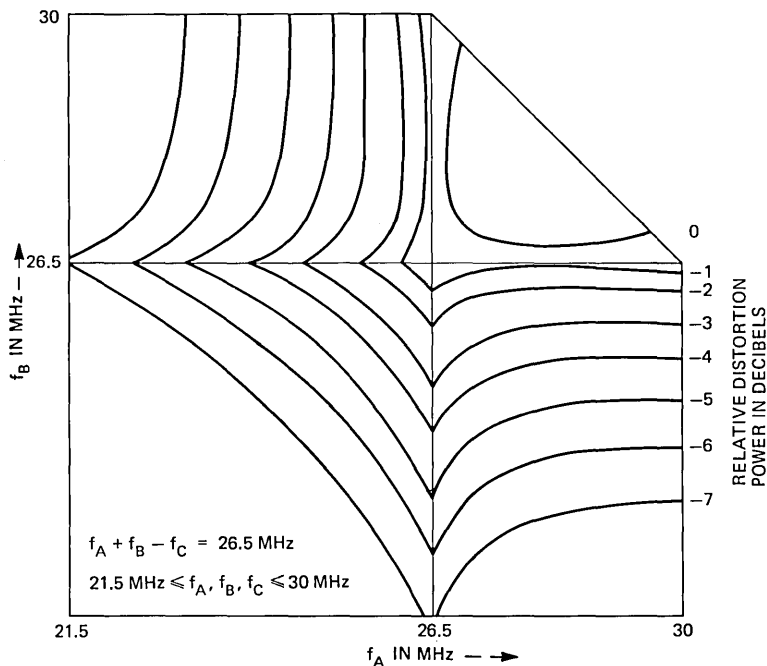
A post-distorter is presently being constructed for the three top hypergroups of TAT-6. It consists of 34 tandem distorter networks connected by loss equalizers, phase equalizers, and amplifiers. Each distorter network will cancel the distortion produced by one block of 20 repeaters. A 13-dB suppression of third-order distortion is expected, which should reduce total noise by the 6 dB required to meet the original system design objectives. The loss equalizers in the post-distorter are adjustable to track the system loss change with time.

#### 7.2.4 Noise improvement on future SG systems

Prior to completion of TAT-6, the design of the 82-type transistor had been modified to improve its ability to withstand surges. The new "double epitaxial" design features a two-step collector impurity profile which increases the collector-emitter breakdown voltage while maintaining exceptional linearity. This improvement allowed removal of the two surge-protection diodes in the output network and one gas tube in each GSF. Since the semiconductor diodes contributed nearly all the excess third-order intermodulation noise, most of the necessary im-



(a)



(b)

Fig. 25—(a) A fundamental frequency dependent third-order distorter. (b) Computed 26.5-MHz response of distorter.

provement in repeater linearity was achieved before the problem was discovered.

Further investigation of transistor third-order distortion revealed that it had two characteristics of the diode distortion, unusual power level and fundamental-frequency dependence. It was discovered that these characteristics could be essentially eliminated by changing the crystal orientation of the transistor from the  $\langle 111 \rangle$  axis to the  $\langle 100 \rangle$  axis. It



appears that the MOS capacitance associated with metallization and the oxide passivation layer is the source of the unusual distortion. Third-order distortion measurements ( $A + B - C$  type products) on samples of MOS capacitors have shown that capacitors built on a  $\langle 111 \rangle$  crystal orientation generate 13- to 17-dB more distortion than those built on  $\langle 100 \rangle$  crystals. This difference in distortion is probably proportional to the difference in interface energy state densities for the two orientations.<sup>10</sup> Semiconductor distortion studies are being continued in an effort to more fully understand and characterize the physical mechanisms which produced this unforeseen behavior. The results of these studies will be published when they have been completed.

## REFERENCES

1. "SF Submarine Cable System," B.S.T.J., 49, No. 5 (May-June 1970), pp. 601-798.
2. S. T. Brewer, R. L. Easton, H. Soulier, and S. A. Taylor, "SG Undersea Cable System: Requirements and Performance," B.S.T.J., this issue, pp. 2319-2354.
3. G. E. Morse, S. Ayers, R. F. Gleason, and J. R. Stauffer, "SG Undersea Cable System: Cable and Coupling Design," B.S.T.J., this issue, pp. 2435-2469.
4. C. D. Anderson, "Overload Stability Problem in Submarine Cable Systems," B.S.T.J., 48, No. 6 (July-August 1969), pp. 1853-1864.
5. M. Brouant, C. Chalhoub, P. Delage, D. N. Harper, H. Soulier, and R. L. Lynch, "SG Undersea Cable System: Terminal Transmission Equipment," B.S.T.J., this issue, pp. 2471-2496.
6. W. M. Fox, W. H. Yocum, P. R. Munk, and E. L. Sartori, "SG Undersea Cable System: Semiconductor Devices and Passive Components," B.S.T.J., this issue, pp. 2405-2434.
7. J. V. Milos and P. A. Yeisley, "Manufacturing Aluminum Castings and Extrusions for use in SG Submarine Cable Repeaters," Western Electric Engineer, July 1975.
8. A. T. Chapman et al., "Manufacture of Submarine Cable Repeaters and Ocean Block Equalizers," B.S.T.J., 49, No. 5 (May-June 1970), pp. 663-681.
9. W. J. Geldart, et al., "A 50 Hz-250 mHz Computer-Operated Transmission Measuring Set," B.S.T.J., 48, No. 5 (May-June 1969), pp. 1339-1381.
10. P. V. Gray and D. M. Brown, "Density of  $\text{SiO}_2$ -Si Interface States," Appl. Phys. Lett., 8 (1966), pp. 31-33.



## **SG Undersea Cable System:**

# **Semiconductor Devices and Passive Components**

By W. M. FOX, W. H. YOCOM, P. R. MUNK,  
and E. F. SARTORI

(Manuscript received September 28, 1977)

*In this paper we describe the active devices and passive components used in the SG undersea cable system for the TAT-6 link between Green Hill, Rhode Island, and St. Hilaire de Riez, France. We explain reasons for component choice and present information about design, performance, screening, and reliability.*

### **I. INTRODUCTION**

Traditionally, in high-reliability communication systems such as undersea telephone cables, well-established component and device designs and manufacturing processes are used. But with the development of the SG undersea cable system, this conservative approach has been challenged by the need for devices of higher performance. This requirement resulted, in some cases, in sophisticated device designs that border on "state-of-the-art" concepts. For example, the increase in channel capacity or bandwidth requires high-frequency transistors incorporating design and processing features that are relatively new. Nevertheless, new features were carefully evaluated so that they would meet the system reliability requirements. In general, reliability is the governing criterion for the selection of components and devices for the undersea cable system. This concept and how it applies to passive components and active devices are covered in the following subsections: II, transistors; III, diodes; IV, gas tubes; V, resistors; VI, capacitors; and VII, inductors and transformers. Each subsection is complete for each component or device and covers: (i) choice and requirements, (ii) design and construction, (iii) characterization and screening, and (iv) aging.

## II. TRANSISTORS

### 2.1 Requirements

Although there are seven transistor codes, six in each repeater, all are the same basic design. This, of course, is a very desirable arrangement for simplicity and economy of manufacture. The basic development code is a passivated npn silicon planar transistor and is divided into: (i) the 82A for the input stage, selected chiefly for low noise; (ii) the 82B and 82C as intermediate-stage devices selected for high gain and low capacitance, respectively; (iii) the 82D and 82E as driver and output transistors, which are optimized for low second- and low third-order modulation coefficients, respectively; and (iv) the 82F and 82G for low- and high-band oscillators. Table I shows assignment of the transistor codes to the various functions and their most critical characteristics.

### 2.2 Design

The design of the transistor draws on the epitaxial, planar, and noble contact metallurgy technology commonly used in contemporary discrete and integrated devices.

#### 2.2.1 Thermal considerations

Being a power high-frequency transistor, the transistor's active element is in essence an array of conventional, small, high-frequency devices electrically connected in parallel on the same silicon chip. Packing a large number of these small devices close together (to keep capacitance low) naturally creates a thermal problem. And where both reliability and low distortion performance are important, this problem becomes critical. For a long service life, the transistor must operate at as low a temperature as possible, and at the same time all parts of the active element must be

Table I — Location and characteristics of transistors

Transistor Code	Circuit Designation	Function	Operating Voltage	Stage Placement Criteria (Median)
82A	Q201	Input stage	$V_{CE} = 9.2V$ $I_C = 50mA$	$NF = 1.87$ $a_o = 0.992$
82B	Q202	Intermediate stage	$V_{CE} = 10V$ $I_C = 150mA$	$a_o = 0.0990$
82C	Q301	Intermediate stage	$V_{CE} = 9.2V$ $I_C = 50mA$	$C_F = 3.20$
82D	Q302	Driver stage	$V_{CE} = 10V$ $I_C = 150mA$	$M_{2E} = -54.2$ $a_o = 0.986$
82E	Q303	Output stage	$V_{CE} = 10V$ $I_C = 150mA$	$M_{3E} = -93.1$ $a_o = 0.988$
82F	Q601	Low band oscillator	$V_{CE} = 10V$ $I_C = 10mA$	$0.978 < a_o < 0.98$
82G	Q501	High band oscillator	$V_{CE} = 10V$ $I_C = 10mA$	

uniform in temperature so that low levels of distortion are achieved. This is accomplished by grouping the emitters into four quadrants of nine emitters each, with appropriate spacing between (see Fig. 1). A thermal profile of the 82-type transistor indicates the temperature uniformity across the active element is within a range of 3°C.

### 2.2.2 Impurity distribution

A unique feature of the transistor manufacture is that each individual silicon wafer of starting material is carefully profiled for the impurity distribution of its epitaxial layer. Poon<sup>1</sup> showed that intermodulation distortion could be reduced by properly shaping the transistor doping profile in the collector region. In practice, optimum low-distortion performance is obtained by grading the epitaxial layer so the concentration of impurity atoms gradually increases in the epitaxial layer in a direction approaching the substrate (see Fig. 2). In processing, the epitaxial profile seen in Fig. 2 is readily achieved by a combination of processing temperature and an appropriately shaped profile at the start. During sub-

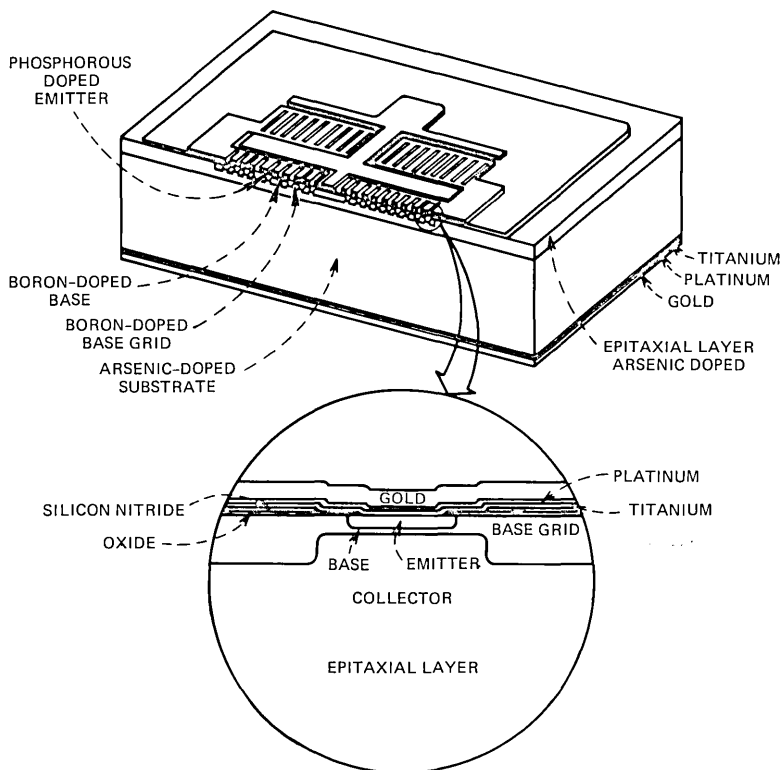


Fig. 1—Cross section of transistor chip. Insert shows enlarged view of a single emitter.

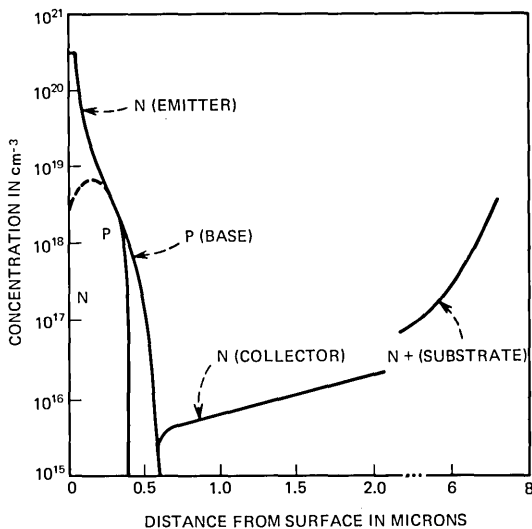


Fig. 2—Transistor impurity profile, with concentration as a function of depth from the surface.

sequent high temperature operations, a redistribution of impurity atoms occurs in just the right amount to produce the desired collector impurity distribution. Intermodulation coefficients represented by  $M_{3E}$  below  $-100$  dBm have been realized in this manner. However, early transistor models which were optimized for low distortion by using epitaxial layers  $5 \mu\text{m}$  thick were found to be vulnerable to transient surges. Therefore, to improve transistor surge capability, a  $7\text{-}\mu\text{m}$  thickness of the epitaxial layer was found to be necessary. An inherent problem associated with silicon microwave transistors is that the device may go into secondary breakdown in some modes of operation. Use of the thicker epitaxial layer tends to shift the onset of secondary breakdown to higher voltages. This compromise in epitaxial layer thickness resulted in a slight penalty in the third-order modulation coefficient.

Emitter and base impurity distributions shown in Fig. 2 are achieved by straightforward diffusion processes adjusted to meet the transistor's electrical requirements.

Finally, the silicon substrate through which the collector current flows is made thin and is heavily doped with arsenic. Consequently, low collector series resistance, low collector contact resistance, and low thermal resistance are achieved.

### 2.2.3 Active element

The active element (Fig. 1) consists of 36 emitter stripes. Each emitter is  $2.5 \mu\text{m}$  wide and  $65 \mu\text{m}$  long and is separated by  $12.5 \mu\text{m}$ . The number and size of the emitters were chosen to provide the necessary power

dissipation, low intermodulation distortion, and a flat gain-current characteristic over the operating current range.

A band of deep diffused boron surrounds each emitter and forms a  $p^+$  grid-like structure over the entire active element. This diffusion serves as both a gettering diffusion and as a means of lowering the base resistance between the emitter stripes and at the base contact itself. A combination of a relatively large base contact area and a high surface concentration provides a low base contact resistance ( $r_b''$ ), necessary for low noise performance. Similarly, a combination of very narrow emitter stripes and stripe spacing and the boron grid provide a low base resistance ( $r_b'$ ). The active base region is also boron-diffused and is tailored to provide a gain range of  $45 < h_{FE} < 160$ , an emitter breakdown voltage greater than 5 volts, and a base layer width of  $0.23 \mu\text{m}$ . In summary, the above provides the necessary vertical and horizontal geometry for a gain bandwidth cutoff frequency ( $f_T$ ) of 2.7 GHz.

The contact metallization used is the Bell System standard titanium, platinum, and gold system. Emitter and base areas are contacted by overlays which lead to wire-bonding pads outside the active element. Collector contact is made through a metallized layer on the back side of the chip.

The titanium-platinum-gold metallization makes use of a new sputter-etch process. This process was first devised by Herb and Labuda<sup>2</sup> and later applied to the transistor manufacture as the first production device sputter-metallized. Even though this appears inconsistent with the policy of using only well-established processes for undersea cable devices, early results were so encouraging it was decided to proceed with the process. In practice, this process is remarkably uniform in quality and manufacturing yields when compared to the older plating process.

Briefly, the process consists of depositing uniform layers of Ti, Pt, and Au; masking the contact areas with nickel plate; and then rf sputter-etching away those areas not wanted. The mechanism depends on the relative etch rates of the various materials used.

#### **2.2.4 Device stabilization**

Traces of metallic impurities are always present in semiconductor starting materials and sometimes are introduced in subsequent processing steps. They are known to degrade electrical properties of semiconductor junctions and upon their removal the junction characteristics are restored. Any scheme which removes or immobilizes these impurities is considered a gettering process.

Two such processes are successfully used in the transistor processing. The first makes use of a high concentration, deep, and highly stressed diffusion region in the transistor's active element. As mentioned earlier, a deep boron-diffused grid-like structure is formed in the base area to

create a  $p^+$  region in the proximity of each emitter stripe. A diffusion such as this is known to have two important properties: (i) the enhanced solubility of metallic impurities in a p type diffusion, and (ii) the high density of dislocations associated with this type of boron diffusion.<sup>3</sup> Both these effects, as well as their close proximity to the emitters, result in a very effective gettering mechanism. Junction leakage currents have been reduced several orders of magnitude to a few hundredths of a nanoampere. Furthermore, the transistor exhibits a very flat gain-current characteristic at low currents (Fig. 3) which can be attributed to the reduction in the number of recombination sites in the gettered base region.

The second gettering process is used on both transistors and diodes, which contain silicon dioxide and nitride layers. Because stability of surfaces is so important in establishing reliable device operation, these layers are, in addition to other functions, used where appropriate in passivation techniques for controlling semiconductor surface potentials. However, silicon dioxide is known to be porous to alkali metals, particularly sodium ions. These ions can migrate to the silicon surface and alter the electrical characteristics of the device. Every effort possible is exerted in manufacture to eliminate these contaminants but, as a precautionary step, the device is protected by a silicon nitride coat which is placed over the oxide as a permanent seal. In addition, immediately before the nitride coat is applied, the underlying layers of oxides are given a gettering treatment to rid them of possible ionic contamination.

The final step in device stabilization is a high temperature anneal of each completed transistor wafer to relieve any stresses introduced during the metallization operations.

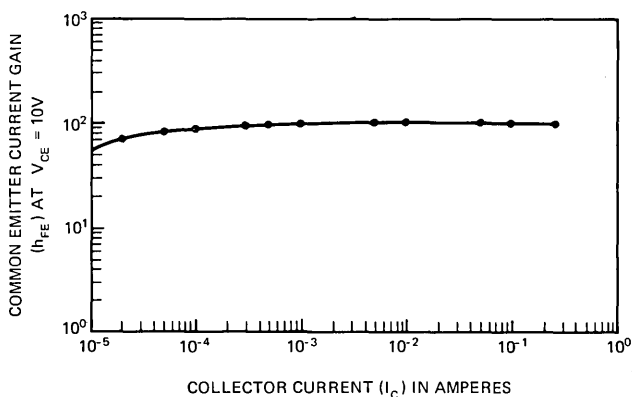


Fig. 3—Common emitter current gain characteristics, with transistor gain as a function of collector current.



### 2.2.5 Encapsulation

Because operating temperature is so important a factor in establishing device reliability and performance, a significant amount of effort is invested in the design of low thermal impedance packages. Furthermore, these packages are required to remain vacuum tight over substantial excursions of temperature and time. They must consist of materials that do not introduce excessive stress on the fragile semiconductor chip.

The structure chosen for the transistors and diodes is a hermetically sealed encapsulation which provides alumina ceramic isolation for low parasitic capacitance and inductance, stud mounting, and low thermal resistance. The transistor combination of the active element and package has a thermal derating factor of less than  $24^{\circ}\text{C}$  per watt. This is consistent with the thermal objectives of the system, whose goals are based on a maximum operating junction temperature of  $65^{\circ}\text{C}$ . Although the package was developed specifically for the transistor, it is also used for diodes to simplify manufacture.

The encapsulation features are also based on providing the transistor or diode with the best possible environment during its lifetime, even with the device active element itself equipped with a passivated design. Charge accumulation is enhanced by the presence of water vapor and electrolysis contributes to degradation of internal structural members; therefore, all semiconductor devices are hermetically sealed. Also high temperature baking of piece parts and cold-weld closures minimize the chance of residual gas evolution inside the enclosure after the seal is made.

Figure 4 is an illustration of the package. This encapsulation consists of two subassemblies (a header assembly and a stud can assembly). These assemblies are joined together by a cold-welding process after the semiconductor chip is bonded to the header and the connections to the feed-through leads have been made.

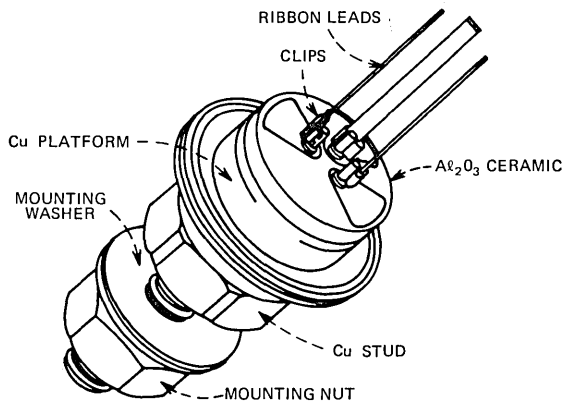


Fig. 4—Semiconductor device encapsulation. Diodes and transistors are hermetically sealed in this package.

The header assembly consists of a number of separate piece parts brazed together. The welding flange of the header assembly is fabricated from oxygen-free high-conductivity copper using cold forming operations. The molybdenum platform, upon which the semiconductor chip is mounted, is punched from special material which will not delaminate during fabrication. Ceramic insulators consist of an aluminum oxide disc metallized with a mixture of molybdenum and manganese, over which a thin layer of copper is plated. Feed-through terminals are made of Kovar lead wire and Kovar washers. All parts are brazed together simultaneously using special brazing alloys, and the final assembly is then finished with layers of nickel and gold plate.

Can assemblies are also made of separate piece parts. The stud is cold formed of an alloy of copper selected to meet the torque requirements necessary to ensure good thermal contact to the repeater housing. The can is formed from oxygen-free copper and is ultrasonically welded to the stud. The assembly is finished with a nickel and a gold plate.

To ensure reliability and integrity for the package, a number of tests and examinations are performed during assembly and upon the completed package. Some are destructive sampling tests and designed to determine failure limits. An example is hydrostatic pressure testing until rupture occurs. Another test is a lead push test, in which force is applied axially to the end of the lead of the header until it is pushed through the ceramic.

As part of the final screening of devices, the package is again scrutinized for mechanical defects by exposing the devices to acceleration tests, shock tests, and particle tests as well as detailed visual examination.

### **2.3 Characterization**

Electrical characterization of underseas cable semiconductor devices is, of necessity, a detailed and exacting process. The high system performance objectives and the rigorous reliability goals require testing procedures not usually applied to ordinary devices. For example, the reliability objectives for the transistor demand that a change in common emitter current gain ( $h_{FE}$ ) be no more than 2.5 percent over the service life of the transistor. This is equivalent to a change in small signal current gain ( $a_o$ ) of less than 0.0005 over a 20-year period. Therefore, these devices must not only be designed to meet such stability requirements, but must be characterized to such a degree that it can be determined that such minute changes can be detected. Toward this end a battery of tests is performed, some of which are repeated many times during the screening program.

Characterization is in two parts: dc tests primarily determine the reliability qualities of the device, RF tests show mostly the circuit perfor-

mance capabilities. In addition to conventional dc tests, several of which are performed at multiple bias points, special tests such as pulse tests and surge capability tests are conducted. Transistor current gain measurements are made at several levels of collector current on each individual device.

Two tests are made at use conditions (50 and 150 mA), one test is made at a level very sensitive to transistor changes (5 mA) to monitor aging and selection, and another is made at high current (250 mA), which is a good indicator of whether all emitters are properly functioning. Each candidate transistor must be able to meet the gain-current characteristic shown in Fig. 3.

Another example of special testing is the test placed on the transistor's emitter junction. The quality of the emitter junction is particularly critical because of its exposure in service to noise overload which may momentarily push the emitter into reverse conduction, its exposure to residual surges which act similarly on the device and stem from cable fault, and its exposure to inverse bias which may occur temporarily during fault monitoring. Therefore, the shape of the emitter reverse voltage-current characteristic is critical and must be determined for each device. Table II shows typical dc characteristics of the transistor.

RF testing consists of four noise figure measurements, ten intermodulation coefficient measurements, and "on-line" transistor modeling of each device. On-line modeling is transmission characterization performed on a computer-operated test system which produces a circuit model for each transistor. The S parameters of each transistor are measured at the two use conditions and at 15 frequencies from 0.1 MHz to 436.8 MHz. These data are automatically fed into a computer and by means of a circuit-oriented model (Fig. 5) reduced to six basic parameters. The model is constructed so that it fixes the values of those transistor elements which are not likely to vary widely in manufacture. Fixed values shown in Fig. 5 are calculated from the geometry, impurity concentration, etc., for a typical transistor. The variable elements are (i) small signal current gain  $a_o$ , (ii) capacitance associated with  $a_o$  cut-off frequency  $C_{ep}$ , (iii) collector/base capacitance less inner capacitance  $C_F$ , (iv) total emitter resistance  $R_e$ , (v) total emitter inductance,  $L_E$ , and

Table II — Some typical DC characteristics

$I_{EBO}$ ( $V_{EB} = 2V$ )	<0.35nA
$I_{EBO}$ ( $V_{EB} = 3V$ )	<10nA
$I_{EBO}$ ( $V_{EB} = 4V$ )	<235nA
$I_{CBO}$ ( $V_{CB} = 10V$ )	<0.07nA
$I_{CEO}$ ( $V_{CE} = 10V$ )	<0.09nA
$BV_{CBO}$ ( $I_C = 100 \mu A$ )	>60V
$BV_{EBO}$ ( $I_E = 100 \mu A$ )	>5V
$V_{CB}, V_{EB}$ ( $I_E = -100mA$ )	>0.91V
$h_{FE}$ ( $I_C = 150mA, V_{CE} = 10V$ )	$50 < h_{FE} < 160$

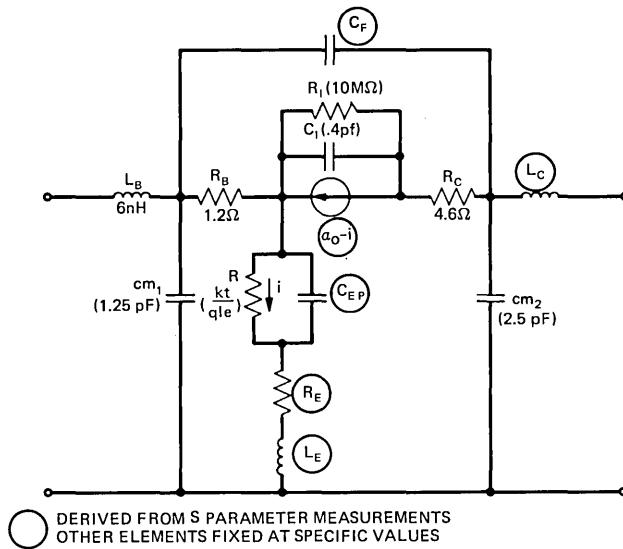


Fig. 5—Circuit-oriented model used to establish transistors' behavior in a repeater set. Circled elements are varied to match data. Other elements are calculated from geometry and impurity distribution.

(vi) total collector inductance  $L_c$ . Distributions of all RF parameters are compiled, and each transistor is assessed with respect to its relative position in the total population. It is then assigned to a specific repeater set where it has a unique and optimized function. Table III illustrates how tightly the model parameters are controlled for TAT-6.

#### 2.4 Screening and aging

Although, in essence, mechanical screening begins at the very onset of manufacture, a series of mechanical evaluations is performed on all completed devices to confirm the integrity of the device's structure. Electrical screening begins with environmental stresses such as channel aging, overstress power aging, and high temperature stress, and ends with long-term aging.

Channel aging is done on a 100-percent basis and serves to eliminate inferior devices that, despite all the precautions taken in manufacture, may still have some surface charge accumulation. This is accomplished by holding each device at elevated temperature with its junction at reverse bias for a period of one week.

Accelerated power aging is a shakedown test. Each transistor is power-overstressed at a level three times its operating level (4.5 W) for a period of one week. This test is well within the capability of the transistor structure and enables detection of devices with marginal quality and incipient failure modes.

Table III — 82 type transistor—AC model parameter data

	82A*		82B†	
	-2σ	+2σ	-2σ	+2σ
$a_o$	0.9894	0.9932	0.9842	0.9926
$R_e(\Omega)$	0.1530	0.1962	0.1729	0.2156
$C_F(\text{pF})$	3.035	3.863	3.011	3.679
$C_{EP}(\text{pF})$	111.2	151.3	292.3	462.0
$L_E(\text{nH})$	6.535	6.833	6.565	6.891
$L_C(\text{nH})$	6.024	6.689	6.314	6.892

	82C*		82D†	
	-2σ	+2σ	-2σ	+2σ
$a_o$	0.9818	0.9926	0.9808	0.9900
$R_e(\Omega)$	0.1455	0.1956	0.1712	0.2176
$C_F(\text{pF})$	3.131	3.452	3.015	3.529
$C_{EP}(\text{pF})$	120.2	202.3	340.3	486.6
$L_E(\text{nH})$	6.543	6.868	6.554	6.892
$L_C(\text{nH})$	6.010	6.674	6.348	6.848

	82E†	
	-2σ	+2σ
$a_o$	0.9814	0.9925
$R_e(\Omega)$	0.1669	0.2155
$C_F(\text{pF})$	3.085	3.745
$C_{EP}(\text{pF})$	317.8	466.4
$L_E(\text{nH})$	6.566	6.889
$L_C(\text{nH})$	6.318	6.814

\* ( $V_{CE} = 9.2\text{V}$ ,  $I_C = 50\text{ mA}$ ).

† ( $V_{CE} = 10\text{V}$ ,  $I_C = 150\text{mA}$ ).

The high-temperature stress technique is a sampling test based on the observation that semiconductor device life is related to the magnitude of the stressing temperatures. A sample of every lot of transistors is stressed at three different time intervals and three junction temperatures. Distributions of failure based on the reliability goals ( $\Delta h_{FE} < 2.5\%$  in 20 years) are then made for each time and temperature combination. From these data, the commonly known Arrhenius Failure Distribution (Fig. 6) is made which provides a convenient method of determining the failure rate for any time-temperature combination. Inspection of these acceleration life curves reveals that the sigma of the failure distribution remains constant at various stress levels; therefore, we may extrapolate the curves in Fig. 6 to long-time, low-stress-level conditions. Note in Fig. 6 that the intersection of the 20-year objective with a 65°C use condition (these being the reliability objectives) is coincident with a value of sigma of the transistor failure distribution, which is extremely small. This establishes the confidence level or percentage of failure to be expected. With six transistors in each repeater of the 700-repeater system, these extrapolations indicate that in 20 years one would anticipate less than one transistor failure in the entire system.

Finally, the devices are placed on six-month long-term age at maxi-

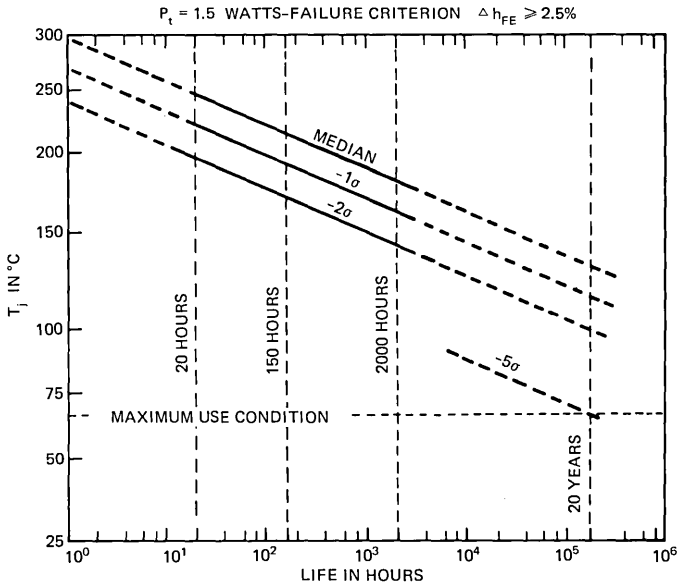


Fig. 6—Pattern of accelerated aging for transistors.

imum operating conditions. During this time, devices are tested at regular intervals, the results of which are observed for trends. These data are statistically extrapolated over a 20-year period, with the objective of assuring a 20-year life in the repeater. Figure 7 is a graph of how a group of SG transistors age. The graph contains a plot of the median as well as the standard deviation in the population. After initial stabilization, no further trends are evident.

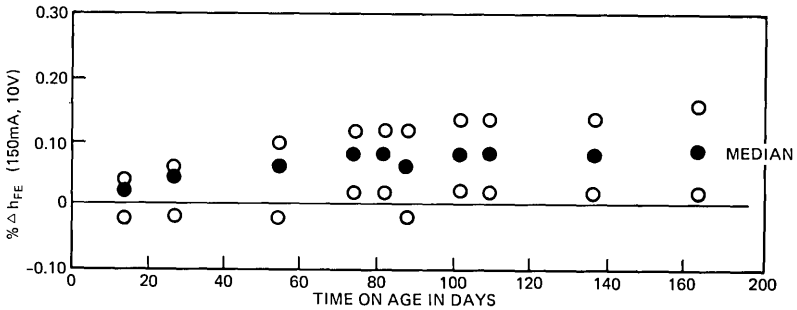


Fig. 7—Stability of a group of transistors during long-term aging.

## **2.5 Transistor improvements for future systems**

Upon completion of transistor manufacture for TAT-6, several important design improvements were made to the 82-type transistor. The transistor's surge capability was significantly upgraded by fabricating the device in double epitaxial silicon, where the normally lightly doped thin epitaxial layer is separated from the heavily doped substrate by a thick epitaxial layer of intermediate doping level. Use of the double epitaxial layers shifts the onset of secondary breakdown to higher power levels while still maintaining good linearity and high frequency performance. A compromise in epitaxial thickness as reported in Section 2.2.2 is no longer necessary. Furthermore, unexpected high distortion near the upper end of the transmission band was markedly reduced by changing the orientation of the starting silicon material from  $\langle 111 \rangle$  to  $\langle 100 \rangle$ . Experimental devices indicated interface surface effects were the cause of this anomalous behavior. Moreover, a recent study by Olson<sup>8</sup> shows surface effects can contribute to intermodulation distortion.

Another important change concerns the semiconductor device encapsulation. Gold-plated piece parts that make up the package have been replaced by unplated nickel parts at a considerable cost savings with no penalties in reliability or integrity of the encapsulation. And finally, additional high-temperature annealing of the assembled transistors prior to final sealing has further enhanced the transistor's stability. The slight change in gain during the initial period of aging under operational conditions (Fig. 7) is no longer evident, so that now the transistor is essentially stable from the very beginning.

## **III. DIODES**

### **3.1 Requirements**

A total of seven diode codes are used to obtain the required protection for each repeater. They consist of three basic types, two of which are similar to those used in the SF system.

The 522 is a silicon planar diode used for signal overload protection and is new for the SG system.

The 523B,C,D,E, and F are silicon mesa-type diodes. Specifically, the 523B acts as an amplitude control for the oscillator, the 523C furnishes input protection for the preamplifier, and the 523E is used for signal path surge protection and is located in the directional filter.

The 524A is also a silicon mesa-type diode and is used as a voltage limiter for power path surge protection in the ground separation filter. They are used in a set of three in parallel, packaged as the 532A. In the event of a cable break or large transient through the repeater, these diodes must regulate the peak voltage across the repeater during the transient. Table IV shows the diode complement.

Table IV—Location and characteristics of diodes

Diode Code	Circuit Designation	Function	Operating Voltage	Critical Characteristic
522A	CR-301	Output transistor signal overload protector	-0.8V	$C < 10$ pf series resistance 10 to 13 $\Omega$
523B	CR-501	High/low band oscillator amplitude limiters	0V	max. C/pkg. = 20 pf
523C	CR-201	Signal path surge protectors	-0.85 (each chip)	max. C/pkg. = 8 pf chip $\Delta = < 1$ pf
523D	CR-401	Signal path surge protectors	-12V	max. C/pkg. = 4.8 to 5.8 pf
523E	CR-101	Signal path surge protectors	-4V (each chip)	max. C/pkg. = 11.6 to 12.6 pf
523F	CR-402	Signal path surge protectors	-12V (one chip)	max. C = 4.8 to 5.8 pf
532A	CR-701	Power path surge protector	-12V	forward characteristic matched to within 0.1V @ 75A/set of 3 $V_{BR} = 15V @ 10mA$

### 3.2 Design

New for the SG system, the 522A employs a planar technology similar to that of the transistor, including silicon nitride passivation. The design is tailored to provide protection during signal overload to the emitter-base junction of the output transistor of the power amplifier. Signal overload can result in reversing the bias of the emitter-base junction, causing it to go into breakdown. This is known to degrade stability characteristics of the transistor. Diode characteristics which will provide this protection during signal overload and which would not alter the current during normal signal levels are seen in Fig. 8.

To meet these requirements, a small gold-doped silicon chip was designed. Small area keeps the capacitance low, and gold doping controls the slope of the forward V-I curve after forward conduction begins. The diode junction is formed by boron diffusion and protected by a silicon nitride layer. To achieve the required forward V-I characteristic, a thin layer of gold is evaporated on the back of the wafer and diffused into the silicon. This lowers the lifetime of the minority carriers and increases the series resistance of the diode. Contact metallization is provided to the chip by a nickel-gold overlay.

The chips for the 523 and 524 diode types are similar in design to 468A and 467A used in the SF system<sup>4</sup> and include a silicon dioxide passivation layer over the junction area.

The 522A chip is mounted in the same SG package as the transistor. The 523 type chips are also in the same package but are mounted in series, two to a package. The 524A is mounted in a slightly modified one-lead version of the basic SG package and then mounted on a heat sink as a matched group of three diodes (Fig. 9).



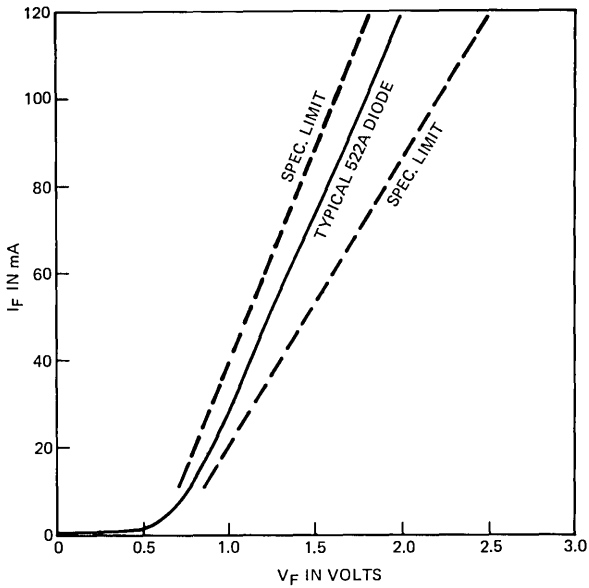


Fig. 8—Forward characteristics of a 522A diode.

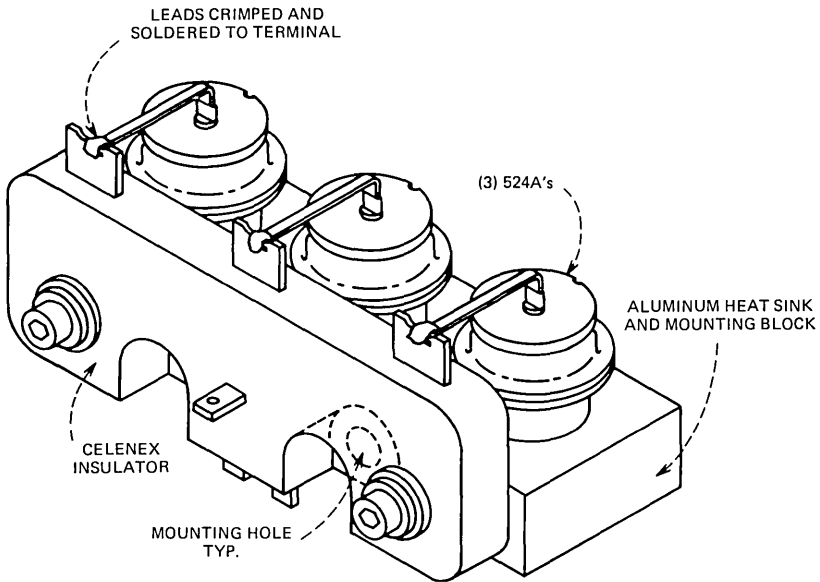


Fig. 9—Matched diodes mounted on a heat sink and connected in parallel.

### 3.3 Characterization

A battery of tests is performed, some of which are repeated many times during the course of the screening program. In addition to the normal diode tests of saturation current, forward and reverse voltages, surge

tests, etc., specific tests are performed on the various codes. For instance, the diode characteristic curve in Fig. 8 is ensured for each 522A by measuring the forward voltages and currents at a number of operating levels. The 523 family of diodes which contains two chips is characterized for each chip and the combination of the two chips, and then fitted to the specific protective functions (see Table IV).

Finally, the 524A which is the basic building block for the 532A surge protector is characterized by measuring the individual diode breakdown voltages during a 75A surge and then matching them to within 0.1 V for the three diodes set.

### **3.4 Screening and aging**

Screening consists of channel age tests, accelerated age, and operational aging at use conditions. The channel age test consists of holding the diode at reverse bias for 16 hours at 150°C and at 80 percent of the breakdown voltage. The accelerated age test consists of holding the diodes at high temperature for 144 hours. Devices that behave differently from the main populations are discarded, and the remaining diodes are aged for six months at maximum use conditions. Those diodes that exhibit the most stable characteristics are then selected for use in the repeater.

The aging characteristics of SG diodes are similar to those of the SF system, in which many years of accumulated data indicate unprecedented reliability.<sup>5</sup>

### **3.5 Device manufacture**

The manufacture of semiconductor components makes use of the principles devised for the devices used in earlier undersea cable systems. To reduce the possibility of unforeseen sources of device instability, all manufacturing operations are meticulously performed under stringent conditions. All the crucial operations are performed in a clean room environment. Raw materials and piece parts are inspected to assure conformance to the design intent. Thorough records of all inspections are kept, to create an atmosphere of quality consciousness and to provide diagnostic information in the event of deviant behavior of devices or device lots. Control charts are used to monitor the uniformity of the processes, and inspections take place at every step in the manufacture to prevent introduction of incipient failures. Pedigree data on each device is stored so that any particular device is traceable from its material point of origin throughout its history in the manufacturing shop.

In the SG program, many new and sophisticated pieces of apparatus were used to improve precision and control. Furnace operations such as oxidation, diffusion, and annealing are all performed in an automatically controlled furnace complex. This system achieves with fine pre-

cision the processing repeatability and uniformity required for device manufacture. Process variables such as gas flow, temperature, insertion and withdrawal times, speed, and other related parameters no longer involve human variability. Vacuum deposition stations used in metalization operations are similarly automated. Wafer separation is accomplished by laser-beam cutting. Finally, a specially constructed, scanning electron-beam microscope is used to inspect each individual device before it is sealed in its encapsulation.

#### **IV. GAS TUBES**

Primary signal path surge protection is accomplished by four WE 469A gas tubes similar to those used in early undersea cable systems.<sup>6</sup>

#### **V. RESISTORS**

##### **5.1 Choice**

Tantalum nitride film resistors were chosen for the SG system because of their stability, the predictability of their aging characteristics, and their low parasitic effects. In addition, their performance in the Bell System as well as in the SF undersea cable system<sup>7</sup> has been excellent.

##### **5.2 Requirements**

Resistors are used in bias networks, current limiting, feedback networks, wave shaping, equalizers, impedance matching, and level adjustment. Tolerances range from  $\pm 15$  percent for some of the low-valued resistors to  $\pm 0.1$  percent for others in critical applications.

Two sizes of resistors are required. Type 265 resistors are rated at  $\frac{1}{8}$  W but are operated at a maximum of  $\frac{1}{16}$  W, at which power the film temperature is such as to guarantee end-of-life tolerances well below those required by the system. Type 266 resistors are used in the repeater output stage and are rated at  $\frac{1}{2}$  W but are operated at a maximum of 0.3 W to keep end-of-life tolerances well within system requirements. There are fifty-nine 265-type resistors and fifteen 266-type resistors in the repeater. A typical ocean-block equalizer may contain one hundred nine 265-type resistors, of which twenty-two are used for "mopping up." Resistor patterns range from 0.6 square to 250 squares. Although the SF system used resistors formed on sapphire (the 243-type), considerable experience since has demonstrated that resistor films on bare alumina substrates possess more than sufficient stability for the SG application. In addition, the use of alumina substrates amounts to a considerable cost saving.

### 5.3 Construction

Resistors range in value from 3 to 10,000 ohms and are fabricated using as-sputtered sheet resistances ranging from 4.5 to 25 ohms/square.

Both 265- and 266-type resistors are made by sputtering the appropriate tantalum nitride film onto  $9.52 \times 11.43$  cm ( $3\frac{3}{4}'' \times 4\frac{1}{2}''$ ) ceramic substrates, followed by evaporated layers of titanium and palladium, over which is plated  $3 \mu\text{m}$  of gold. Resistors are patterned photolithographically and are laser-scribed into "mini" substrates 2.54 cm (1 inch) square. These squares contain ten 265- or four 266-type resistors which are then pre-anodized, heat-treated, and then final-anodized to value. Then the squares are sawed apart into discrete resistors, and leads are attached by thermal compression bonding. A pre-stamped polyvinylidene fluoride sleeve is shrunk over the resistor for protection. The stamped information on the sleeve includes the sputter run number, the substrate number in the run, the "mini" number, and the individual resistor number from the "mini," thus allowing complete traceability for each individual resistor. Complete resistors are shown in Fig. 10.

The resistors are assembled by gold-to-gold thermocompression bonding, thus precluding whiskers and other possible intermetallics.

### 5.4 Screening and reliability

The resistors are heat-treated in "mini" form for two weeks at  $150^\circ\text{C}$  to determine resistor film quality. Then assembly of the resistors is

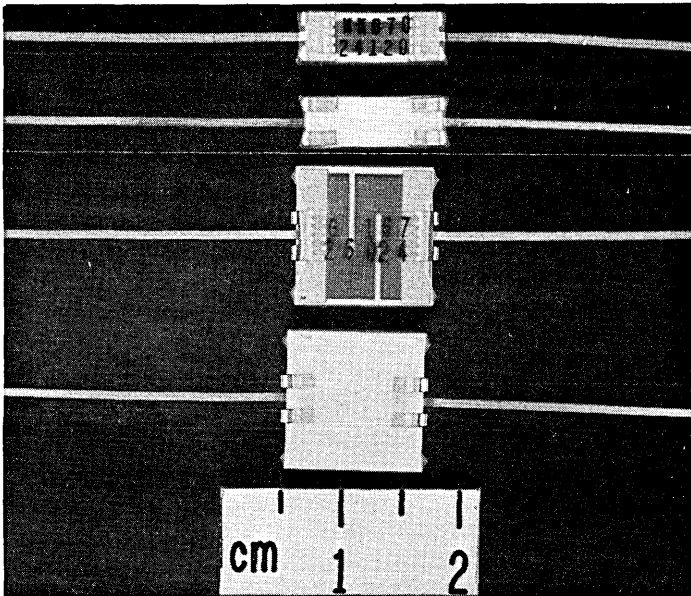


Fig. 10—Thin film resistors.

completed, and they are shipped to the repeater assembly location where each resistor is visually examined, a sample of the product is voltage-surge tested, then all resistors are baked 24 hours at 105°C, followed by five temperature cycles from -40° to +85°C. After that, each resistor sustains a short-time overload of 6.25 times rated power for 5 minutes. This is followed by 1,500 hours at rated power to screen out any resistors with anomalous behavior and, after a final resistance check and noise measurement, the resistors are ready for assembly. Overall yield after screening and testing is 75 percent.

## **VI. CAPACITORS**

### **6.1 High-voltage paper capacitors**

As described elsewhere in this publication, the coaxial cable supplies dc power at constant current to operate each repeater, as well as carrying the composite carrier signals being transmitted in both directions. To separate the dc power from the carrier signals, power separation filters are included on each side of the repeater amplifiers (see Fig. 11). Sufficient dc power is tapped off to power the repeater, and the dc current is returned to the cable. The major source of destructive high frequency feedback around the repeater results from the series inductance in the path between the “sea” ground and the internal repeater ground. It is possible to eliminate this inductance by making the signal path a completely coaxial structure in which the outer conductor comprising a coaxial capacitor is used to “connect” the two grounds (see Fig. 11).

#### **6.1.1 Choice of capacitor materials**

The coaxial capacitor must be able to stand the full cable voltage (7 kV) plus any anomalous spikes generated during fault conditions. Consequently, castor-oil impregnated kraft paper capacitors were chosen for this service, as they have been for earlier submarine cable systems, with excellent results.

#### **6.1.2 Requirements**

The maximum voltage sustained by these capacitors at the shore ends of the system is 7 kV. Capacitance value is 13 nF  $\pm$ 3 percent. The smallest physical size together with the required coaxial structure and voltage rating dictated the unit shown in Fig. 12. Notice the tube with expansion bellows to allow for the expansion of the castor-oil-impregnant, particularly during the high-temperature processing which the repeater undergoes. Coaxial construction plus near-perfect axial electrical symmetry reduces series inductance to 20 nH.

#### **6.1.3 Construction**

As can be seen in Fig. 13, this capacitor is actually two capacitors in

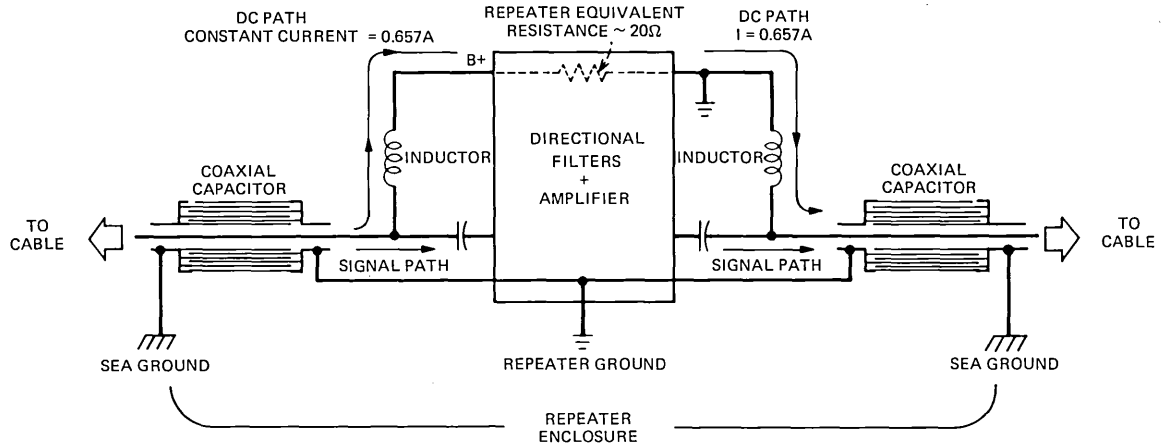


Fig. 11—Diagram showing how coaxial capacitors are used to “connect” the “sea” ground and the repeater ground.

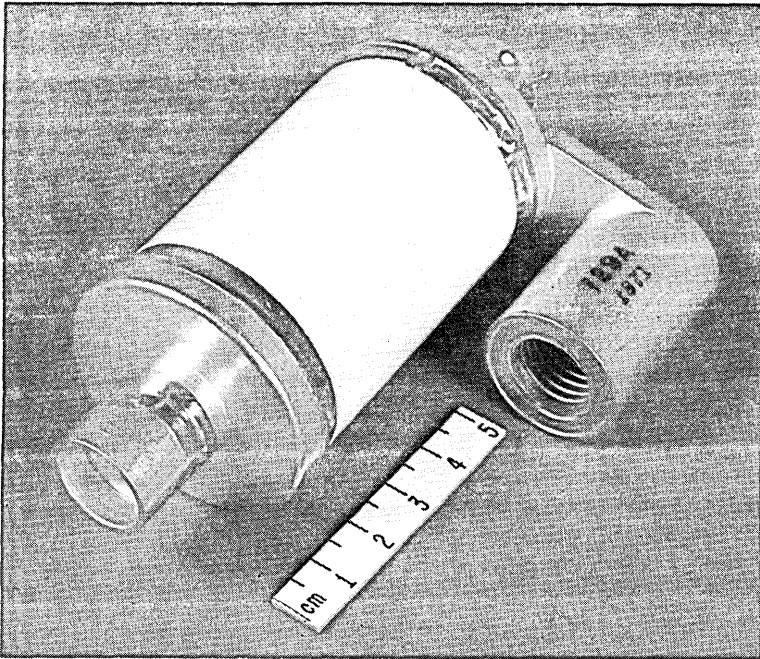


Fig. 12—Completed coaxial capacitor used in ground separation filter. Note expansion bellows.

series. Notice how the conducting foils are interleaved so that there is a “floating” foil not attached to the external connections. The capacitor is wound on a hollow alumina ceramic tube with metal ferrules soldered to it at both ends. The floating foil plus the connected foils are separated by 5 layers of 25- $\mu\text{m}$  (1-mil) paper. Foils are approximately 6- $\mu\text{m}$  ( $1/4$ -mil) thick aluminum. This combination of papers and foils is wound to the appropriate diameter (and capacitance value) with conductor “flags” attached to the outside foils at positions that are axially symmetrical and 90 degrees apart around each end of the capacitor. This symmetry is necessary to keep the series inductance of the structure as low as possible. The capacitor is completed by enclosing the paper-foil unit in a ceramic housing which is soldered in place. One ferrule is equipped with the expansion bellows plus a filling tube where the oil enters the unit. After a vacuum bake, the capacitor is impregnated with pure castor oil and sealed. All external metal parts are nickel + gold plated for solderability and to eliminate corrosion. Nickel is included as a diffusion barrier.

Other high-voltage capacitors used in the equalizers are constructed in a similar manner, but are not in a coaxial configuration.

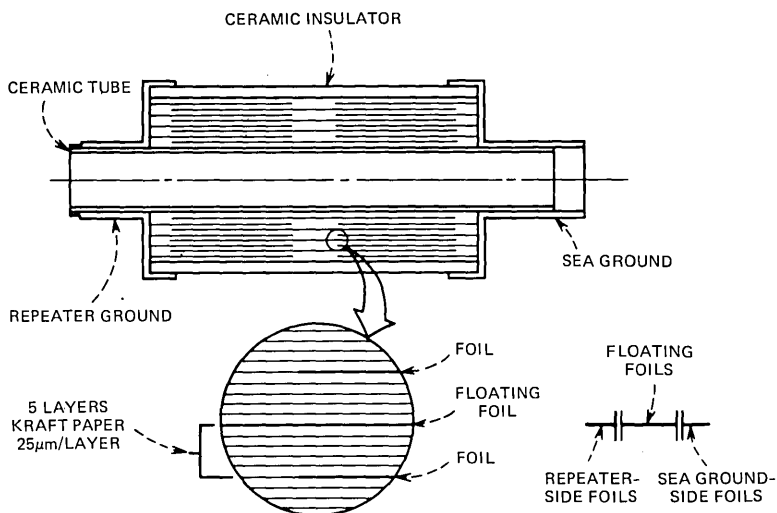


Fig. 13—Diagram showing cross section of coaxial capacitor (expansion bellows not shown).

#### 6.1.4 Qualification and testing

Every roll of capacitor paper purchased is qualified for use by testing capacitors made from the paper. These test capacitors are wound and impregnated with castor oil, tested for 25 days at 66°C and more than twice-rated voltage. Capacitance and insulation resistance shifts are checked as well as catastrophic failure.

Ten percent of all manufactured product is sacrificed for a similar test, and all product is screened for 6 months at sea-bottom temperature (4°C) and at higher than rated voltage. During these tests, all significant electrical parameters must remain within tight limits.

Capacitance tolerance for this application is  $\pm 3$  percent, with a total shift during life of perhaps 0.5 percent. Capacitors are initially stabilized by temperature cycling between  $-18^{\circ}\text{C}$  and  $+66^{\circ}\text{C}$ , and capacitance shifts are again held to tight limits. Insulation resistance and effective series resistance at 100 kHz (a measure of internal, stable, electrical continuity) are both held to absolute values; the change in those parameters during processing and aging is also held to tight limits.

## 6.2 Ceramic capacitors

### 6.2.1 Choice

Previous submarine cable systems used mica capacitors because of their excellent trouble-free history of providing stable, reliable operation at sea-bottom temperatures. The parasitic performance of mica capacitors at SG frequencies, however, precludes their use. Ceramic capacitors were chosen instead, although their long-term reliability had to be es-



tablished as part of the program. Results of testing and screening to date have shown this choice to have been a good one.

### **6.2.2 Requirements**

As Western Electric does not manufacture ceramic capacitors, the required units are purchased from outside suppliers under specification KS-21013. Required values range from 3 pF to 0.047  $\mu$ F, with 80 percent of the values less than 1000 pF. Tolerances range from  $\pm 5$  percent to  $\pm 0.2$  percent, with the majority of applications requiring  $\pm 1$  percent. Ceramic capacitors are available in a range of temperature coefficients but, for this application, NPO (zero temperature coefficient) capacitors are used because their capacitance stability with temperature averages better than  $\pm 0.02$  percent. There are no applications where the less temperature stable, high-K dielectric capacitors would suffice, in spite of their smaller size.

### **6.2.3 Construction**

Ceramic capacitors use a thin (37  $\mu$ m), modified titanium dioxide ceramic as a foundation onto which are screen-printed palladium electrodes. The ceramic sheets are piled up and punched into stacks which are pressed and fired. The resulting "chip" with alternating electrodes emerging from each end is coated on the ends with a fritted silver, which is then fired, thus connecting alternating electrodes together (see the cross section in Fig. 14). The completed chip is measured for capacitance and other parameters and then sorted into a "post office" of graded values, which are then paired to give the correct total value. Leads are soldered to the paired chip which is then mounted into a molded diallyl phthalate case and encapsulated with a silicone rubber potting material (see Fig. 15). After testing, capacitors are finally mounted into the appropriate printed wiring board.

The copper wire leads are nickel- and gold-plated to keep them cor-

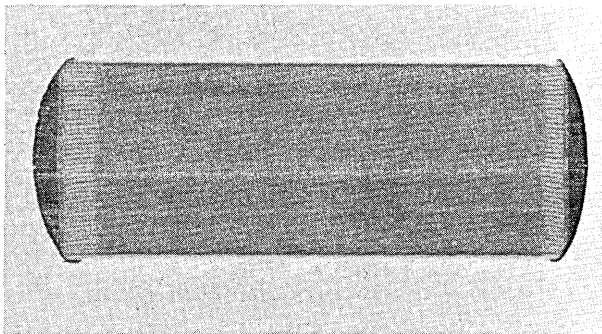


Fig. 14—Cross section of ceramic capacitor.

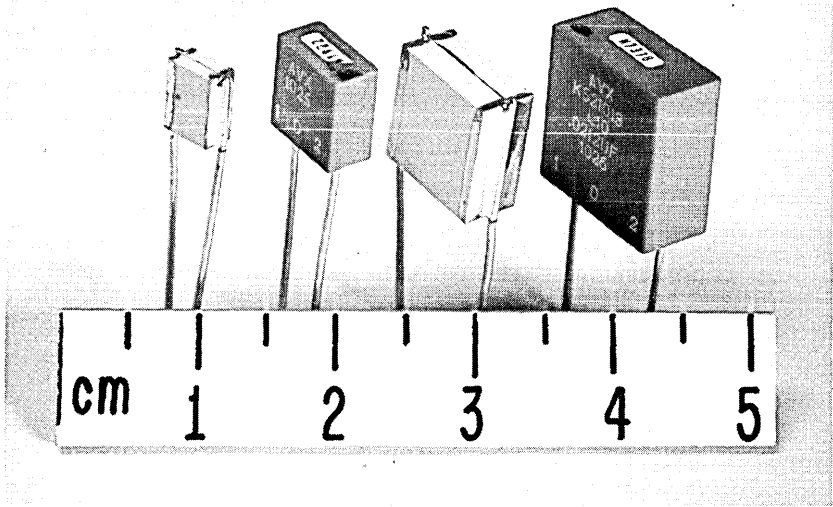


Fig. 15—Ceramic capacitors.

rosion-free and solderable. The nickel is used as a diffusion barrier between the copper and gold.

#### **6.2.4 Screening procedures**

With the application of voltage, ceramic dielectric undergoes an electrochemical degradation which eventually results in breakdown. The preliminary accelerated life testing of 3500 capacitors of the type to be used under a variety of conditions led to the conclusion that under sea-bottom conditions their average life would be over 100,000 years, but that it would be necessary to screen out atypical capacitors that might fail much earlier.

All capacitors undergo a rigorous testing program by the supplier, and a sample of each lot is subjected to destructive electrical and mechanical tests to determine the capability of the lot.

After delivery to Western, the capacitors are subjected to additional testing. To screen out any which may have an intermittent internal connection, each capacitor is cycled over the entire operating and storage temperature range ( $-20^{\circ}$  to  $60^{\circ}\text{C}$ ) twice while it is continuously monitored for capacitance. The capacitors are also life-tested at voltages ranging, according to dielectric thickness, from 150 to 450 V dc. Electrical parameters are monitored and compared before test, after two months of test, and after four months of test. Both fixed and statistical limits are placed on the values and the changes in value, to screen out any units which could be peculiar.

### 6.2.5 Reliability

In 96,702 capacitors screened, 8 short-circuited on the four-month life test. Assuming that the failure rate is proportional to the third power of the applied voltage, they would short-circuit at the rate of 0.005 FIT\* in the system.

## 6.3 Solid tantalum capacitors

### 6.3.1 Introduction

Solid tantalum capacitors were used extensively for the first time in the SF submarine cable system. They are particularly useful because of their large capacitance density. Twenty solid tantalum capacitors are in each SG repeater: fifteen 1- $\mu$ F and five 10- $\mu$ F units (see Fig. 16). They are used exclusively as coupling and bypass elements, since their characteristics do not allow their use as elements in frequency-sensitive networks.

### 6.3.2 Screening procedures

All capacitors are measured for capacitance value, series resistance, and leakage current as they enter the Western Electric, Clark, New Jersey shop. Then, at specified periods during nine months of screening, they are measured for the same parameters four more times. Screening

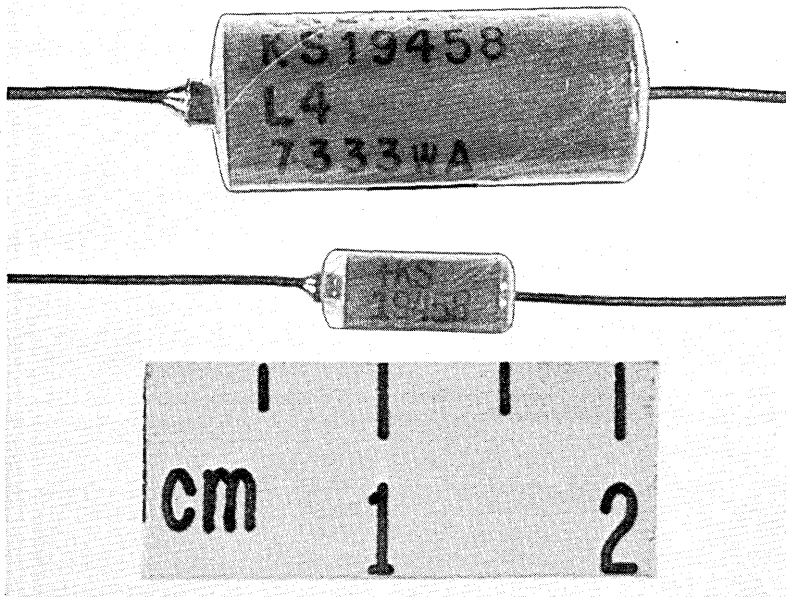


Fig. 16—Tantalum capacitors.

\* Number of failures in  $10^9$  hours.

consists of temperature cycling, pulsing, surge testing, and life testing for three 60-day periods at elevated temperature and voltage.

After these tests, any unit displaying a  $\pm 0.5$ -percent change in capacitance is rejected. The absolute differences in successive readings of series resistance and leakage current are limited to fixed maximum values. In addition, the results are looked at statistically, so that any units showing absolute differences outside  $3.5\sigma$  for either parameter are rejected.

## VII. INDUCTORS AND TRANSFORMERS

### 7.1 Transformers

Transformer designs for undersea cable systems are influenced profoundly by the ratio of highest-to-lowest transmitted frequency. The SB, SD, and SF systems all maintained a ratio of about 12:1. In the SG system, however, this ratio has been increased to 50:1. The 30-MHz top frequency requires smaller designs to reduce parasitics, but sizes should not be so small that the low-frequency characteristics are degraded or the reliability is compromised.

Figure 17 shows the signal transformer designs. The 2678B/C is used either as an input or output transformer, while the 2678A is used for interstage coupling. All are "transmission line" transformers, and the input and output units are designed as hybrids. All use the same toroidal

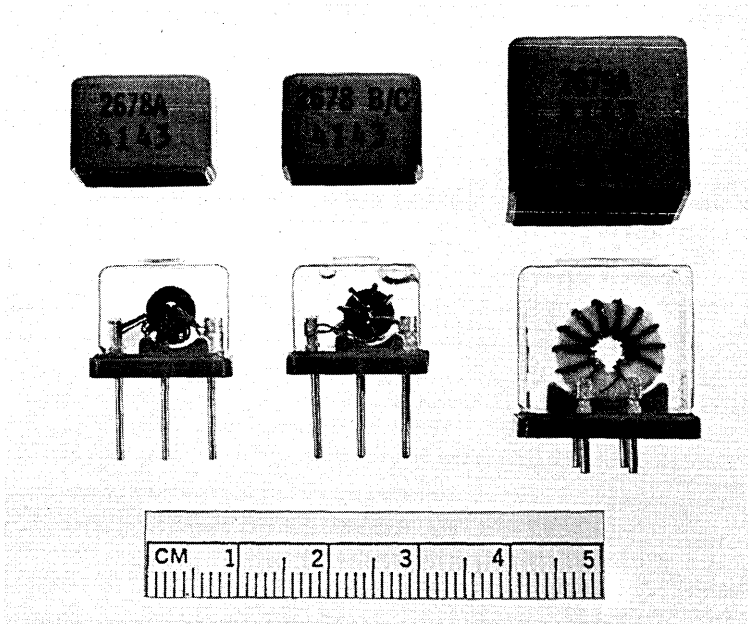


Fig. 17—Signal transformers.

core material, a newly developed manganese-zinc ferrite. The electrical integrity of these units must exist well outside the system's bandwidth, where overall gain and phase of the feedback amplifier continue to be important.

The 2679A transformers are used in such a way that their parasitic capacitance and short-circuit inductance become elements in the directional filter. Consequently, this puts a premium on the reproducibility and stability of these components. This is achieved by making the winding from a pair of wires, twisted under controlled tension at a specified number of turns per inch.

Figure 18 shows the 2680A longitudinal choke whose purpose is to suppress longitudinal currents while remaining transparent to the transverse signal voltages with no more than a 2-percent reflection coefficient. Its self-inductance is part of the power separation network; as such, it must carry the 0.657-A cable current. It is designed to withstand the 8-kV surge which could appear between the windings in the event of an accidental cable cut near shore. This combination of re-

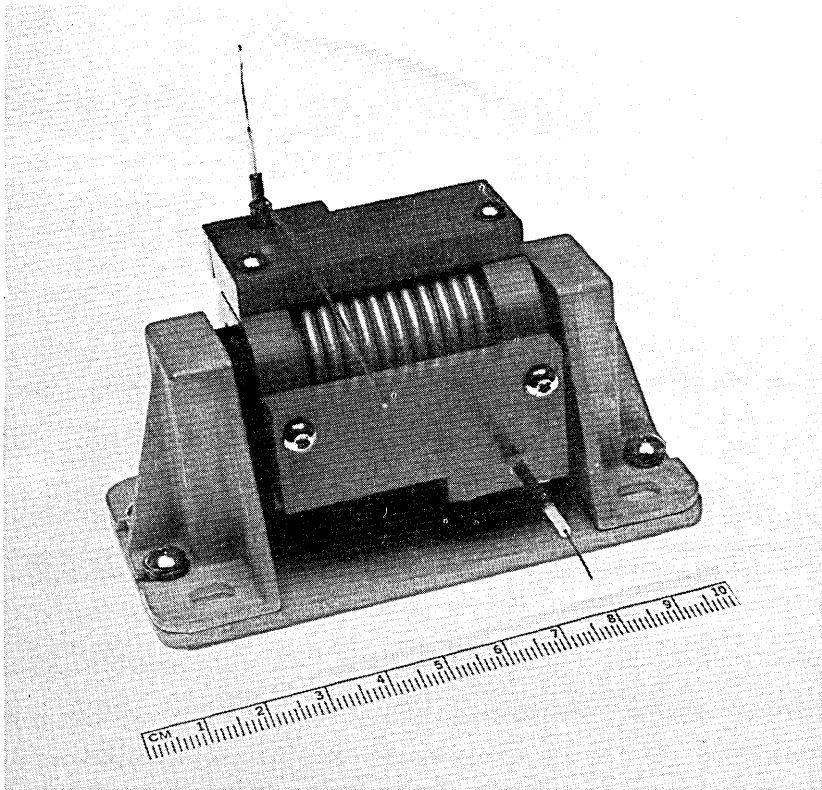


Fig. 18—The 2680A longitudinal choke.

quirements has resulted in the development of a special coaxial cable which comprises the winding and in the use of manganese-zinc ferrite core material. The compromise between permeability and coercive force appears to be appropriate.

### 7.2 Inductors

Eight inductor structures were developed and are shown in Fig. 19. Of the 68 codes using these designs, 27 are adjustable and form a stockpile of continuous inductance (0.0395 to 45  $\mu\text{H}$ ) for adjusting the mop-up filters. The remaining codes range up to 1000  $\mu\text{H}$ . Wherever possible, designs have used the highly reliable procedures and materials developed for earlier systems. A new glass-bonded mica formulation with lower dielectric constant has been developed to lower distributed capacitance. New completely shielded designs have been necessary because of the tighter packing of components. Lower inductance units feature precisely spaced solenoidal windings, which are wound under tension and varnished in place. Higher inductance values are achieved by using varnish-coated, multiple-pie, duolateral windings.

The 1714A unit, shown in Figs. 19 and 20, is the most crucial inductor in the group. It measures 3.85  $\mu\text{H}$  and is adjustable over a range of  $\pm 2.5$  percent. It is used to control repeater gain by varying  $\beta$  in the feedback amplifier. The length-to-diameter ratio is optimized to produce the

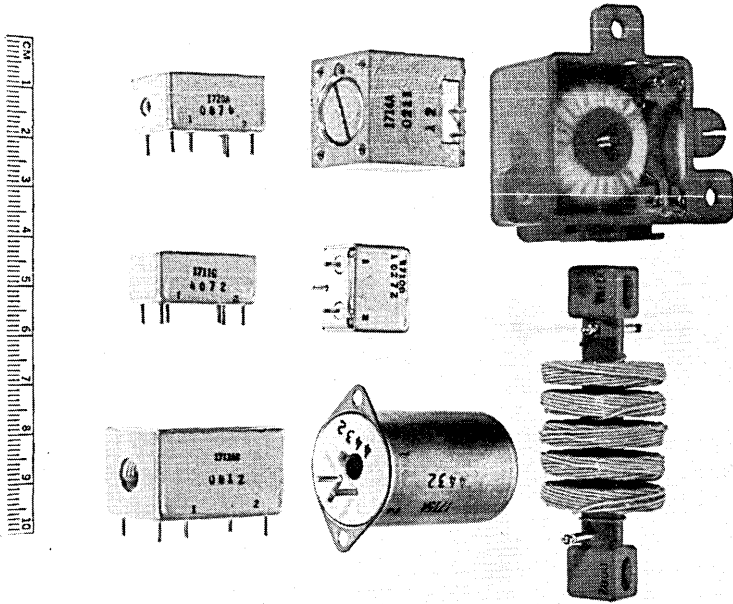


Fig. 19—Inductors.

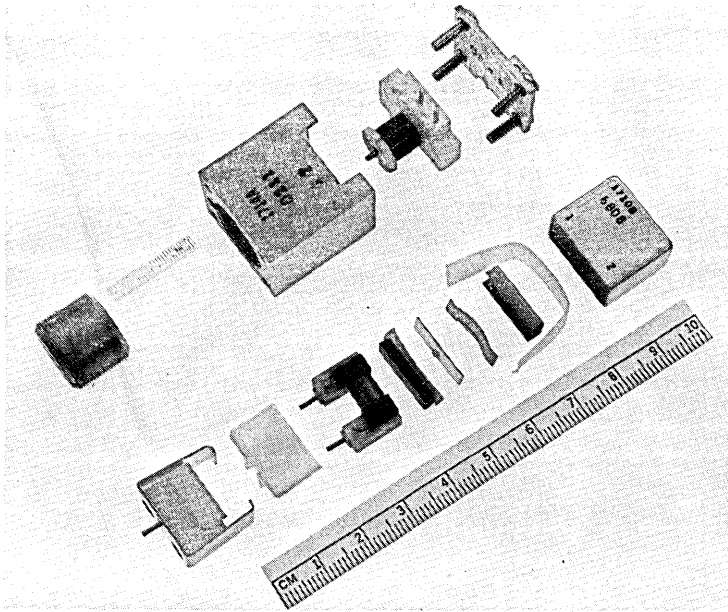


Fig. 20—Exploded view of 1710B and 1714A inductors.

highest possible principal resonance consistent with the attainment of high impedance at 200 MHz. Shielding is achieved by enclosing the winding in a brass block. Inductance is varied by turning a hollow brass plug in and out of the cavity to modify the inductor's magnetic field.

The 1710A and 1710B transistor feed chokes are  $56 \mu\text{H}$  with  $\pm 5$  and  $\pm 2$  percent tolerances, respectively. Besides some initial adjustment capability, their first resonance (parallel resonance) must be at a high frequency and must exhibit high impedance. Also, the in-band third-harmonic products must not exceed  $-115 \text{ dBm}$  when both fundamentals are at  $+10 \text{ dBm}$ . These requirements have resulted in the design shown exploded in Fig. 20. The magnetic circuit consists of a small ferrite bar, separated from the ferrite winding spool by a mica shim to give a precise air gap. This ferrite bar is moved relative to the core to give the correct value of inductance. The position of the ferrite bar is maintained securely by spring-loaded clamps until the bar can be bonded in place.

The 1719A inductor shown in Fig. 19 is designed to produce  $1 \text{ mH}$  with the  $0.657\text{-A}$  dc cable current through the winding. Because the unit must be corona-free to ground at  $7,000 \text{ V dc}$ , a magnetic core is not practical. As this inductor is in shunt with the signal path, it must maintain a specified minimum impedance up to  $60 \text{ MHz}$ . This is accomplished by winding the inductor as a duolateral coil of five sections. The *shunt* resonance (high impedance point) due to the overall inductance tuned by the effective capacitance is broad and occurs at  $3 \text{ MHz}$ . The first *series*

resonance due to magnetic coupling between the winding pies and the distributed capacitances occurs above 60 MHz, thus achieving the required minimum impedance of 1000 ohms over the band of interest.

### **7.3 Screening and reliability testing for transformers and inductors**

To ensure that the inductive components would not be degraded after a long period of use, only materials were considered which had been thoroughly tested and which were determined to be suitable candidates for the proposed applications. All raw materials and piece parts were subjected to inspection, cleaning, and testing procedures before they were used. As a means of verifying and justifying the choice of material as well as methods of construction, all inductive components were subjected to artificial aging and stabilization.

This was accomplished by temperature cycling each component over the range from  $-18$  to  $+66^{\circ}\text{C}$ . The temperature cycles served two purposes: they accelerated aging changes and they established a trend line. Components were considered acceptable only if, after a series of temperature cycles, parameter changes were within permissible limits and the changes after each series of cycles were becoming smaller so that the extrapolated end-of-life changes would also be within the accepted limit.

### **REFERENCES**

1. H. C. Poon, "Implications of Transistor Frequency Dependence," *IEEE Trans. Elec. Devices*, *ED-21*, No. 1 (January 1974), pp. 110-112.
2. G. K. Herb and E. F. Labuda, "Semiconductor Device Fabrication Using Nickel to Mask Cathodic Etching," U.S. Patent 3,808,108, applied for December 1971, issued April 1974.
3. M. R. Poponiak, W. A. Keenan, and R. O. Schwenker, "Gettering of Biopolar Devices with Diffused Isolation Regions," H. Huff and R. Burgess, eds., *Semiconductor Silicon* (1973), pp. 701-708.
4. A. J. Wahl, W. McMahon, N. G. Lesh, and W. J. Thompson, "Transistors, Diodes, and Components," *B.S.T.J.*, *49*, No. 4 (May-June 1970), pp. 683-698.
5. A. J. Wahl, "Ten Years of Power Aging of the Same Group of Undersea Cable Semiconductor Devices," *B.S.T.J.*, *56*, No. 6 (July-August 1977), pp. 987-1005.
6. V. L. Holdaway, W. Van Haste, and E. J. Walsh, "Electron Tubes for the SD Submarine Cable System," *B.S.T.J.*, *43*, No. 4 (July 1964), pp. 1759-1782.
7. Ref. 4, pp. 683-698.
8. H. M. Olson, unpublished work.



## ***SG Undersea Cable System:***

# **Cable and Coupling Design**

By G. E. MORSE, S. AYERS, R. F. GLEASON,  
and J. R. STAUFFER

(Manuscript received May 26, 1978)

*This paper describes 1.7-in. SG submarine cable and cable terminations and compares their mechanical and electrical performance with the design objectives. At 30 MHz, transmission loss in the cable is very sensitive to variation in dielectric loss. Precautions required to prevent excessive dielectric loss change during cable manufacture and subsequent system life are discussed. Sea-bed temperature and pressure coefficients are reviewed in the light of TAT-6 experience, and an estimate is made of possible attenuation change over a 20-year interval.*

### **I. INTRODUCTION**

As discussed in the preceding papers, the British Post Office (BPO) had primary responsibility for cable development for the SG system and Bell Telephone Laboratories (BTL) was responsible for the repeater-to-cable coupling design.

A number of factors ruled out the use of 1.5-in. diameter-over-dielectric (DOD) SF<sup>1</sup> cable for the SG system; not least of these was its high loss. The channel capacity chosen for SG required an upper frequency of approximately 30 MHz. At this frequency, the attenuation of SF cable for a transatlantic system would have reached a formidable 32,600 dB but, by using a low-loss dielectric at an increased diameter, 1.7 in. DOD SG cable reduced this total by 5000 dB. This saved 123 repeaters and reduced the system power feed voltage.

However, cable attenuation remained far higher than on any previous system. This was reflected by: an increased sensitivity to manufacturing tolerances, significant attenuation changes with time (cable aging), and increased importance of laying effects and sea-bed temperature and

pressure coefficients. Of particular concern was the control and characterization of dielectric loss behavior. Surprisingly, the adoption of a low-loss dielectric seems to have compounded the difficulties and eventually came to dominate the cable development. This may be understood in part when it is appreciated that a change in dielectric loss-angle of 1 microradian on all the cable would cause a change of 26 dB at top frequency on TAT-6.

## II. DESIGN OBJECTIVES

Many factors influence the design of a new cable. These include system costs, the development schedule, manufacturing capability, considerations of shipboard handling and maintenance, and compatibility with the repeater, its housing, and termination.

Early considerations of the possible lines of development indicated that, in the available time, a series of objectives based largely on modifications to the SF design would be the best approach. Economic studies showed that, for an upper frequency of 30 MHz, a more expensive cable with lower attenuation would reduce the total system cost in addition to increasing system reliability by reducing the number of repeaters.

The following improvements to the SF design were therefore set as general objectives.

(i) Reduce the cable attenuation at 30 MHz by the use of a larger cable and a lower-loss dielectric.

(ii) Reduce the dc resistance of the inner conductor by some 50 percent to offset the increased line current required by the SG repeater.

(iii) Increase the strength of the deep water cable to exceed, by at least 20,000 lb<sub>f</sub> (88.96 kN) the weight in water of 3000 fathoms (5486 m) of cable plus three repeater bodies.

(iv) Improve the handling performance in terms of the minimum safe bending radius and the number of reverse bends before the inception of a crack in the outer conductor.

Work in conjunction with Imperial Chemical Industries Ltd. (ICI) and Standard Telephones and Cables Ltd. (STC) showed that a dielectric material with a loss angle of 47  $\mu$ rad at 30 MHz could be extruded satisfactorily at a diameter of 1.7 in. (43.18 mm), the cable dimension giving minimum system cost. The inner conductor retained the SF geometry with the diameter increased to 0.478 in. (12.14 mm) to meet the other essential requirements. This dimension gave the cable the convenient impedance of 50 ohms, which is very near to the value for minimum attenuation and provides a value of attenuation negligibly greater than the minimum.

With these basic parameters fixed, the more detailed objectives were formulated, and development concentrated on providing a detailed

specification for all stages of material supply, cable manufacture, and testing.

### III. DESCRIPTION OF CABLE

A number of different cable designs are required to meet the wide range of laying stresses and operational risks that a long-distance, deep-water system must survive. To satisfy these requirements, five versions of 1.7 in. (43.18 mm) cable were developed: an armorless cable for deep water use, a light armored transition cable, a heavy single-armored cable, a heavy double-armored cable, and a screened cable.

#### 3.1 Armorless deep sea cable

The main system cable (Fig. 1) is an armorless design protected by a polyethylene sheath and provided with an internal strength member. It is suitable for use in deep water where there is little risk of damage by fishing trawls, clam dredgers, and ships' anchors, or of disturbance and abrasion by ocean currents on a rocky sea bed. Cable to this design constituted 93 percent of TAT-6.

##### 3.1.1 Inner conductor assembly

The strength member of the composite inner conductor consists of a 41-wire, high-tensile steel strand in which three layers of wires are arranged, all with a left-hand lay, around a central king wire. The design, shown in Fig. 2, is essentially a scaled-up version of the SD/SF strand with the wire sizes increased to give a nominal diameter of 0.4305 in. (10.93 mm). The previous distribution of bending stresses was retained at the increased diameter by increasing the lay length to  $9.10 \pm 0.35$  in. ( $231.1 \pm 8.9$  mm). If steel wire with a tensile strength of 300,000 lb<sub>f</sub>/-

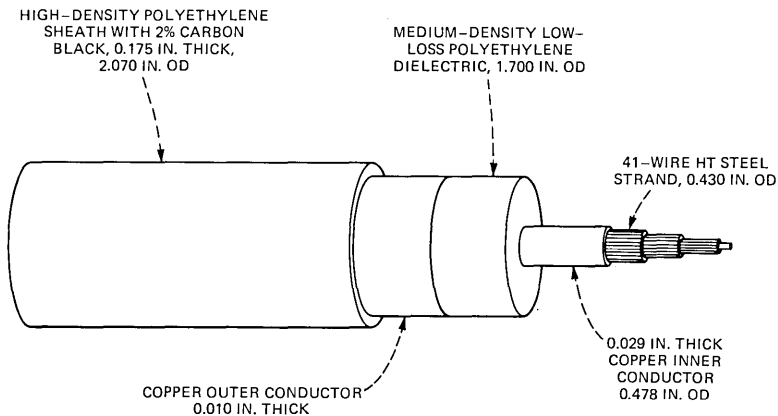


Fig. 1—Armorless SG ocean cable.

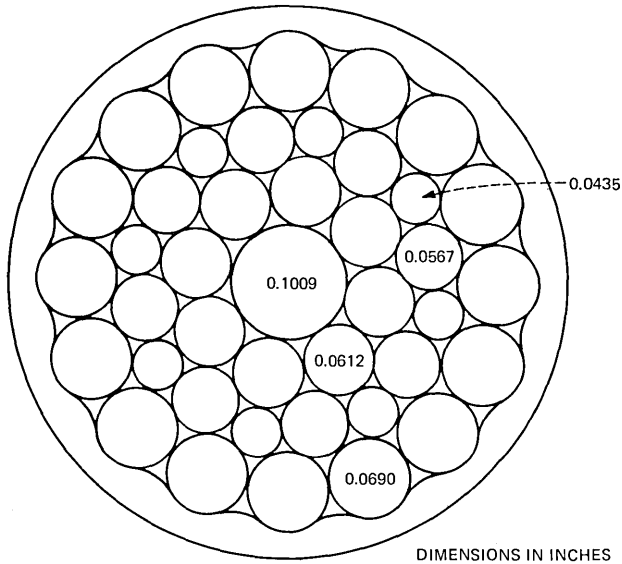


Fig. 2—Cross section of inner conductor. The tolerance on the wires is  $\pm 0.0005$  in., except for the center wire, where it is  $\pm 0.0010$  in. The wire is high tensile steel, 291,200 to 336,000  $\text{lb}_f/\text{in}^2$  (2008 to 2317 MPa).

$\text{in}^2$  (2068.5 MPa) is used, the strand has a strength of 37,000  $\text{lb}_f$  (164.6 kN). Based on an estimated weight in water of 3500  $\text{lb}_f$  (15.57 kN) per nautical mile, this gives the cable a strength-to-weight modulus\* of 10.6 nmi (19.67 km). The immersed weight of a repeater body is 550  $\text{lb}$  (2446 N) so when three bodies are supported at a depth of 3000 fathoms the excess strength of the cable is nearly 25,000  $\text{lb}_f$  (111 kN). This exceeds the design target by 25 percent without including the strength contribution of the other materials outside the steel strand.

The inner conductor is formed from a 0.029-in. (0.737 mm) thick, fully annealed, high-conductivity copper tape. It is wrapped around the strand, in tandem with the strand-forming operation, to produce an oversize tube. The tape edges are closed in a longitudinal butt joint which is seam-welded with an inert gas arc. The conductor is completed by drawing the tube tightly onto the strand to give a finished diameter of  $0.478 \pm 0.001$  in. ( $12.14 \pm 0.025$  mm). The previous practice of specifying oxygen-free high conductivity copper was relaxed to allow the use of a cheaper high conductivity electrolytic tough pitch copper. To maintain weld quality and reliability, a minimum purity of 99.9 percent and maximum oxygen content of 0.05 percent were specified. A further

\* The modulus of a cable is equal to the strength divided by the weight per nautical mile in sea water.

control was placed on the maximum size (0.0014 in., 0.036 mm) and dispersion of oxide grains. The minimum conductivity allowed was 100.8 percent as defined by the International Annealed Copper Standard (IACS).

To ensure that the copper-to-steel interlayer shear strength is sufficient to transfer laying and recovery stresses to the strength member, the copper is heavily swaged into the interstices of the strand. The thickness of copper immediately over the wires is reduced to 0.024 in. (0.61 mm), but the effective thickness of the conductor is held at 0.029 in. (0.737 mm) by suitable adjustment of the difference between tape feed rate and line speed. As a result of cold forming, the conductor tape is work-hardened, and its conductivity is reduced on an average by 1.2 percent. This is later offset by approximately 0.35-percent increase due to a partial anneal during core extrusion. In the design model, a final conductivity of 99.5 percent IACS was assumed. This value was set low to ensure that sufficient repeaters were ordered. In TAT-6, the mass conductivity, determined from 119 samples of finished inner conductor, was 100.2 percent IACS. This result assumes a value of 8.89 g/cm<sup>3</sup> for the density of copper. If account is taken of the true density, then the volume conductivity would appear to have been slightly higher at about 100.4 percent IACS. The design value for the inner conductor resistance was 0.911 ohms per nautical mile at 10°C. Cable manufactured for TAT-6 in fact came out slightly higher at 0.931 ohms per nautical mile because the conductivity of the steel was lower than expected.

### **3.1.2 Dielectric**

As system bandwidths are increased, the dielectric loss becomes more significant. Its contribution to cable attenuation is proportional to the product of loss angle and frequency and is independent of cable size, whereas the contribution from the conductor loss is inversely proportional to cable diameter and, once skin effect is established, is substantially proportional to the square root of frequency. The effect of dielectric loss at high frequencies is to increase cable attenuation and accentuate the deviation from a root frequency law, particularly in large diameter cables, thus complicating the compensation of manufacturing deviations by length adjustment.

In cable used for SF at 6 MHz, the dielectric was responsible for only 3 percent of the total loss at the top of the band, but using this polyethylene in SG cable increases the proportion to 10 percent at 30 MHz. To gain a worthwhile improvement, it was necessary to halve the dielectric loss while maintaining the other essential properties. Two UK suppliers, ICI and Bakelite Xylonite Ltd (BXL), met this requirement during the development stage and UBE Industries of Japan was approved during TAT-6 cable production.

Table I — Loss angle requirements

Frequency (MHz)	Loss Angle in Microradians at 23°C	Change from 23° to 3°C
30	47 ± 6	11 ± 2
	Loss angle expressed as a proportion of the loss angle at 30 MHz, 23°C	
1		0.62 ± 0.14
6		0.77 + 0.10
		-0.14

The selected dielectric is a high molecular weight polyethylene characterized by a low contamination level, a precisely controlled permittivity, and a low dielectric loss. The reduction in loss was achieved by raising the density to 0.930 g/cm<sup>3</sup> (thus reducing the amount of amorphous material contributing to the loss), reducing the concentration of polar groups, and controlling more closely other impurities and adventitious contamination. Although approximately 3 μrad of the reduced loss angle was offset at 30 MHz by an increase in permittivity caused by the increase in density, the shift from SF to SG polyethylene is responsible for a net reduction in TAT-6 cable loss of 1300 dB at 30 MHz. The nominal\* SG polyethylene loss angle is shown in Table I.

The tolerance at 1 and 6 MHz was expressed as a proportion of the 30-MHz value to control the shape of deviations in the linear frequency loss term while, at the same time, allowing the material suppliers a reasonable margin. A control on the loss-angle change with temperature was specified to limit the uncertainty in sea-bed loss at 30 MHz and to avoid a multiplicity of cable coefficients.

To allow for some small variation among sources of material, the quality assurance control was related to the nominal values of each material as determined during the type approval process. However, in approving alternative polyethylenes, the need to process them under similar conditions was appreciated; hence, close controls were placed on those properties affecting extrusion characteristics. Thermal oxidation was controlled by the low-loss antioxidant used in SF cable—Ethyl Antioxidant 330 [1, 3, 5 trimethyl-2, 4, 6 tri (3, 5-ditertbutyl 4-hydroxy-benzyl) benzene]. As a further protection against thermal oxidation, the granule feed hopper to the extruder screw was flooded with nitrogen. The increased density and crystallinity of the low-loss material led to a reduction in its stress crack resistance, but the level achieved was considered acceptable in view of the protection provided by the sheath and outer conductor and the absence of any record of a service failure due to stress cracking.

\* The nominal loss angle of SG polyethylene at 30 MHz is based here on the value obtained with the Bell Laboratories Murray Hill test set. The Bell Laboratories set was used as the reference against which the dielectric test sets at the polyethylene suppliers and the two cable factories were calibrated by a careful exchange of plaques.

The polyethylene is pressure-extruded over the inner conductor and cooled in a series of water troughs which successively reduce the core temperature to the factory ambient (further details are given in Section V). The rate of cooling is arranged to prevent retraction of the core from the inner conductor. By this means, the interlayer adhesion required to transfer longitudinal laying stresses to the inner strength member is maintained. During development, the interlayer shear strength over a 3-in. length of conductor typically varied between 500 and 1000 lb<sub>f</sub> (2225 and 4450 N) and occasionally reached 2000 lb<sub>f</sub> (8900 N). However, under production conditions, the adhesion achieved over the same length varied between 250 and 500 lb<sub>f</sub> (1112 and 2225 N). The required adhesion was 225 lb<sub>f</sub> (1000 N). After extrusion, the dielectric is shaved to a diameter of  $1.700 \pm 0.003$  in. ( $43.18 \pm 0.076$  mm) at a temperature of 20°C. The eccentricity of the inner conductor is limited to 0.020 in. (0.51 mm).

### **3.1.3 Outer conductor and sheath**

The outer conductor is fabricated from an annealed copper tape,  $0.010 \pm 0.0005$  in. ( $0.254 \pm 0.0127$  mm) thick by  $5.630 \pm 0.010$  inch ( $143.0 \pm 0.254$  mm) wide, having essentially the same properties as the inner conductor tape. It is wrapped tightly around the shaved core at a temperature of  $20 \pm 1^\circ\text{C}$  with the edges overlapped longitudinally by approximately 0.25 in. (6.35 mm). The maximum stretch permitted in the forming process is 0.5 percent. To provide the conductor with support and protection, it is oversheathed in a tandem operation with high-density polyethylene to a diameter of  $2.07 \pm 0.03$  in. ( $52.58 \pm 0.76$  mm). To ensure adequate bending performance and avoid alignment problems when jointing, the minimum sheath thickness was limited to 0.150 in. (3.81 mm) and maximum eccentricity to 0.020 in. (0.51 mm).

In the design model, a conductivity of 100.5 percent IACS was assumed for the outer conductor, but during TAT-6 production an average mass conductivity of 100.8 percent IACS was measured on 121 samples. This figure becomes 101.0 percent IACS if a correction is made for the error in assumed density. The average dc resistance for the entire production run was 0.836 ohms per nautical mile at 10°C.

During development, the bending performance of three outer conductor thicknesses, 0.008, 0.010, and 0.012 in. (0.203, 0.254, and 0.305 mm), was examined in combination with three sheath thicknesses, 0.125, 0.150, and 0.165 inch (3.175, 3.81, and 4.19 mm). A wide variation was found among cable samples having the same outer conductor and sheath thickness, which made comparison difficult. In general, the resistance to buckling and cracking improved as the conductor and sheath thicknesses increased, but the thicker the conductor the more pronounced the effect of the sheath. Each combination was assessed from flex tests but the extent of bending damage was very dependent on the test rig

used. There was also a marked improvement in bending performance when the bending diameter was increased from 9 to 10 ft (2.74 to 3.05 m). These differences were considered sufficient to justify setting 10 ft (3.05 m) as the bending limit for 1.7-in. (43.18 mm) cable.

The performance of the 0.008-in. outer conductor was very marginal at a bending diameter of 10 ft (3.05 m) and it failed to survive 50 reverse bends in every test at 9 ft (2.74 m) irrespective of sheath thickness. The selected combination of 0.010/0.165 in. (0.254/4.19 mm) was also slightly marginal, but the risk was thought to be acceptable provided the minimum sheath thickness did not fall below 0.150 in. (3.81 mm).

The sheath material was a high molecular weight, high-density ethylene copolymer, containing 2.6 percent by weight of carbon black. The density specified was slightly higher than that required in SF cable. This increased the flexural modulus which increased the hoop stress applied to the outer conductor by the sheath, thus improving the reverse bend performance. Four sources of sheath material were approved, although only three were used in TAT-6. Towards the end of production, the inclusion of carbon black as protection against actinic radiation was discontinued except for cables ordered as repair lengths. Ironically, the removal of carbon black brought a substantial improvement in bending performance. In continuous loop tests, where cable is driven in a figure eight between two sheaves, the onset of cracking at 6-ft (1.83 m) diameter changed from 20 to 40 reverse bends and at 10 feet (3.05 m), cracking did not occur before 100 reverse bends. Clearly, the use of a natural sheath material opens up the prospect of a useful cost saving in future systems from the use of a thinner conductor/sheath combination. However, those responsible would be well advised to retain the original dimensions for repair lengths containing carbon black. In the final design, the weight in sea water was 1.6 tons\* per nautical mile and in air 5.7 tons per nautical mile. The strength was 16.5 ton<sub>f</sub> and the modulus 10.5 nmi (19.5 km).

### **3.1.4 Jointing**

Shipboard and factory joints were developed along separate lines to take account of differences in the conditions and equipment available for their preparation. For example, while both share a common standard for tensile strength and bending performance, completion of a shipboard joint is required in the shortest possible time.

Both methods use a swaged steel ferrule to make a joint in the inner conductor assembly, and each type of joint has a minimum strength of 15 ton<sub>f</sub>. In the factory, this is achieved using a 6.5-in. (165.1 mm) long ferrule pressed to a mean diameter of 0.82 in. (20.8 mm) and in a repair by swaging a 4.5-in. (114.3 mm) long ferrule to a diameter of 0.87 in. (22.1 mm). With these dimensions, there is little to choose between them

---

\* 1 ton = 2240 lbs, or 1016 kg.



electrically. The factory ferrule has a return loss at 30 MHz of 20 dB compared with 21.5 dB for the shipboard version.

The dielectric is restored using an injection molding process, and both versions must be capable of withstanding 200 kV dc for 1 minute in type approval tests. All core joints are examined radiographically for voids, cracks, and inclusions. Each joint made in the factory must also withstand a production test of 100 kV dc for 1 minute without failure. In a shipboard joint, the outer conductor is connected through by the insertion of a split copper wire braid soft-soldered to the parent outer conductor. While this technique has a superior bending performance to the SF outer conductor restoration, lingering doubts regarding its long-term electrical stability have prevented its adoption for factory use. To improve the flexibility of the outer conductor restoration, instead of spot-brazing a split copper tube directly to the outer conductor as in SF, three helical copper tapes are spot-brazed to the split tube and to the outer conductor. This provides a semiflexible connection which, in a complete joint, is capable of withstanding 50 reverse bends at a diameter of 10 ft (3.05 m) without loss of continuity. In the factory, the joint is completed by fusing a split section of sheath to the cable and sealing it with a longitudinal seam weld. The hoop stress of the sheath is restored by a tight, close-wound binding of  $\frac{1}{16}$  in. (1.59 mm) galvanized iron wire for a distance of 5 ft (1.52 m) over the joint. For the shipboard joint, the sheath is restored by a polyethylene sleeve slipped on the cable and located over split sheath sections placed as packing over the braid. The ends of the sleeve are fused to the sheath in an injection mold and reinforced with a galvanized wire binding.

### **3.1.5 Pre-formed dead ends for holding armorless cable (stoppers)**

When holding armorless cable during a repair, it is necessary to grip the cable by a method that transfers the load from the inner strength member to the dead end without causing damage to the cable. This is arranged using a dead end manufactured by Preformed Line Products (GB), Ltd, Andover, England. In essence, thirteen 0.212-in. diameter high tensile steel wires are formed into a helical tape 26 ft long. The wires are fixed together with a vinyl adhesive and coated on the inside of the helix with aluminum oxide. By reversing the lay of the helix at the middle of the tape, the ends may be folded into a hairpin which, when wrapped around a cable, leaves a convenient loop for the attachment of a shackle.

A single dead end is capable of holding armorless cable at tensions up to 18 ton<sub>f</sub> but, if cable is held at the bow of a ship for long periods, tension, bending, and vibration fatigue may cause premature outer conductor failure well below this value. Since a splice may take several hours to complete, the use of two dead ends in tandem, linked by an equalizing sling to spread the load, is essential.

With careful protection of the cable at the eye of each dead end, it is possible to hold SG cable for 12 hours under a cyclic load of 1 to 7 tonf with a period of 6 seconds. However, if the tension range is increased to 1 to 9 tonf, the time to develop fatigue cracks in the outer conductor is halved.

### **3.2 Armored cable**

In shallow water, additional protection is required to prevent cable failure due to abrasion or disturbance by fishing trawls and ships' anchors. This may be achieved by the provision of a suitable armor or by cable burial depending on the circumstances. Since the TAT-6 route was suited to cable burial using a plow, it was planned to maximize protection by laying heavy single-armored cable to a depth of 1000 fathoms (1829 m) and by burying the cable at depths less than 500 fathoms (914 m). Clearly, the description "shallow water" is something of a misnomer, but the need for protection is real. Fish are now caught at 800 fathoms (1460 m), and a trawl fault has occurred at a depth of 735 fathoms (1340 m). In TAT-6, the plow was used to a maximum sea-bed depth of 350 fathoms (640 m), while the transition to armorless cable was made at 750 fathoms (1372 m). However, a short length of single-armored cable was successfully laid at 1100 fathoms (2012 m) when the depth briefly increased after the transfer from armorless to armored cable on completion of the deep sea lay.

When low attenuation is not a prime requirement, operational constraints during laying and repair favor the choice of a small diameter coaxial for the armored cable. However, during the SG development the feasibility of armoring the main system cable was demonstrated and on a sea trial this cable was laid and recovered without serious difficulty. Indeed, the feasibility of using a heavy double-armored 1.7-in. cable was also demonstrated. The 1.7-in. cable was selected because its greater strength and weight provided increased protection from trawler attack and also because its use reduced the number of repeaters required.

#### **3.2.1 Single-armored cable**

To reduce the risk of an insulated break in the inner conductor and the attendant difficulty in location, it is customary in the design of armored cables to provide a ductile conductor that more than matches the elongation characteristic of the armor. In SG, the continued use of solid copper was prohibitively expensive, but there was insufficient time to develop an alternative\* structure with high elongation before TAT-6 was laid. As a result, the TAT-6 armored cable used the high tensile steel strand inner conductor assembly of the armorless cable. It was therefore

---

\* See possible alternatives in Section 3.2.3.

necessary to select the armor material with some care. The use of Grade-65 (British Standard abbreviation) medium tensile steel wire armor gives a residual strength\* well below the minimum strength of the strand at a strain equal to the yield strain of the strand. In practice, the strand yields at approximately 1 percent strain when the armor has a residual strength of 11 ton<sub>f</sub>. Since the minimum strength of the strand is 16.5 ton<sub>f</sub>, its failure under load will cause a cable break and exposure of the inner conductor to the sea. The armor has a minimum strength of 68 ton<sub>f</sub>; therefore, taking into account the contribution from the strand, the effective strength of the cable is 73.5 ton<sub>f</sub>. In proving trials, the inner conductor integrity was demonstrated at tensions up to 79 ton<sub>f</sub> with failure occurring at approximately 0.8 percent strain.

The single-armor design is shown in Fig. 3. It comprises 25 wires of  $0.291 \pm 0.004$  in. ( $7.391 \pm 0.102$  mm) diameter, medium tensile galvanized steel applied with a left-hand lay of  $36.5 \pm 1.0$  in. ( $927 \pm 25$  mm) over a bedding of 75-pound (34 kg) jute. The armor is coated with bitumen and bound with two servings of 3-ply, 28-pound (12.7 kg) jute applied in opposite directions and coated with a bituminous compound to a finished diameter of 3.05 in. (77.5 mm). The cable specification in fact allowed the use of an approved alternative to jute and, since the completion of TAT-6, synthetic yarns have replaced it as the preferred bedding and serving material.

The single-armored SG cable has a weight in sea water of 15 tons per nautical mile and a weight in air of 24 tons per nautical mile. It is clearly not a cable that a small repair ship could handle easily but, provided the serving remains intact, it is relatively docile and can be coiled in a tank to a diameter of 12 ft (3.66 m) and drummed without difficulty at a diameter of 10 ft (3.05 m).

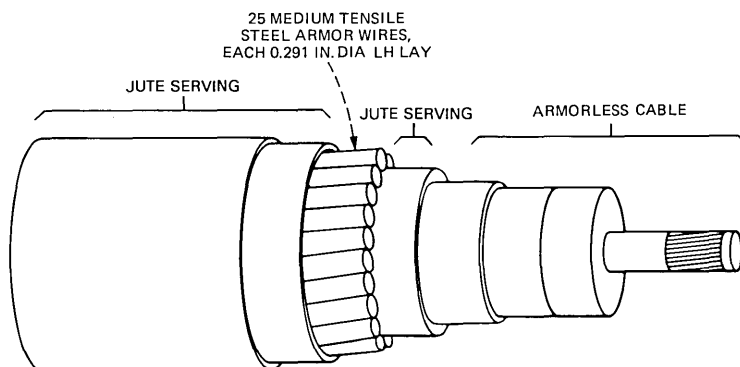


Fig. 3—Single-armored SG cable.

\* Residual strength is the difference between breaking strength and the strength at a particular value of strain.

### 3.2.2 Transition cable

Since the static weight in water of single-armored cable at 1000 fathoms (1828 m) approaches very nearly the strength of the armorless cable, a light-armored transition cable is required at a transfer from armored to armorless cable. In the absence of previous experience of laying heavy-armored cable at this depth, it was considered advisable to provide a double-armored transition cable with a neutral torque characteristic. The design strikes an optimum strength-to-weight modulus of 2.6 nmi (4.82 km) for the armorless cable with respect to the transition cable and for the transition cable with respect to the single-armored cable. (That is, the armorless cable has strength to support the weight in water of 2.6 nmi of transition cable and, similarly, the transition cable has strength to support the weight in water of 2.6 nmi of single-armored cable.)

The transition cable is shown in Fig. 4. Each layer of armor has 48 Grade-65 galvanized steel wires coated with polyvinyl chloride to space the wires uniformly around the cable. In the first layer, the wires are  $0.085 \pm 0.001$  in. ( $2.159 \pm 0.025$  mm) diameter applied with a left-hand lay of  $42 \pm 1$  in. ( $1067 \pm 25$  mm) and in the second layer they are  $0.078 \pm 0.001$  in. ( $1.981 \pm 0.025$  mm) diameter applied with a right-hand lay of  $54 \pm 1$  in. ( $1372 \pm 25$  mm) over an intermediate serving comprising two opposing layers of  $3 \times 17$  pound (7.7 kg) jute coated with bitumen. The cable is completed with an outer serving of two opposing layers of  $3 \times 28$  pound (12.7 kg) jute flooded with a bituminous compound to an overall diameter of 3.17 in. (80.5 mm). Its weight in sea water is 5.9 tons per nautical mile, and its weight in air is 15.5 tons per nautical mile.

The armor strength varies from 21 to 25.8 tonf, depending on the quality of steel, but because the inner conductor fails at 1-percent strain, only about 88 percent of the potential strength is realized. The combined strength of the armor and strand therefore varies from 35 to 39.2 tonf.

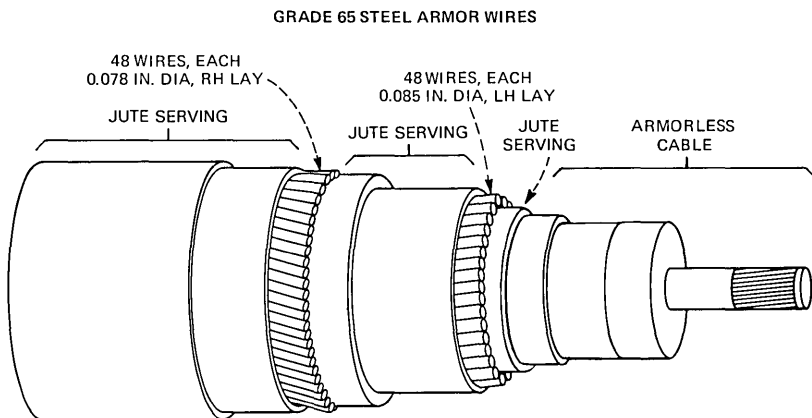


Fig. 4—Transition cable.

In proving trials, failure occurred at 39 ton<sub>f</sub> with an extension of 0.84 percent. No rotation of the armor was observed.

### **3.2.3 Double-armored cable**

As stated previously, the feasibility of laying a double-armored SG cable was demonstrated but such a cable was not adopted for TAT-6. The bedding and first armor pass is as for the single-armored cable. Then, with coatings of bituminous compound under and over each layer, two intermediate servings of 3-ply 17-lb (7.7 kg) jute are specified with opposing lays. This is followed by a second armor pass of 33 wires,  $0.291 \pm 0.004$  in. ( $7.391 \pm 0.102$  mm) diameter, Grade-65 medium tensile galvanized steel, applied with a left-hand lay of  $48 \pm 1$  in. ( $1219 \pm 25$  mm). The second pass is served with two opposing layers of 3-ply 28-lb (12.7 kg) jute coated in bituminous compound to ensure that the serving adheres firmly to the armor. The finished cable has a weight of 32.8 and 46.8 tons per nautical mile in sea water and air respectively and an overall diameter of 3.8 in. (96.5 mm). It has a tensile strength of 162 ton<sub>f</sub>.

The tremendous strength of this cable rules out the use of a composite inner conductor with a high tensile steel strand if an insulated inner conductor break is to be avoided. However, preliminary trials of a 19-wire mild steel strand and of copper-clad aluminum rod indicate that either could be used, the former with virtually no further development.

### **3.3 Screened cable**

At shore ends and in land sections, additional screening is required against electromagnetic interference in the low-frequency band. In SG, the primary concern is with the radio broadcast band, 0.55 to 1.6 MHz. At these frequencies, adequate protection is given by increasing the outer conductor thickness to 0.030 in. (0.762 mm). This was shown to be practicable towards the end of SG development and may be used in future systems, but in TAT-6 a modified version of the SF screened cable<sup>1</sup> was used. The cable impedance was converted to 50 ohms by increasing the inner conductor diameter to 0.281 in. (7.137 mm). Corrosion-prone neoprene-covered armor wire was replaced by a conventional armor, protected with tar and jute servings.

## **IV. ELECTRICAL CHARACTERIZATION**

To enable the system to be equalized, the level of uncertainty in the predicted attenuation of laid cable must be reduced to that which can be corrected by the ocean-block equalizer (OBE). While many factors contribute to uncertainty, some tend to be random while others are systematic. The random factors include manufacturing variations and measurement error. An error in the temperature or pressure coefficient, on the other hand, will cause a systematic deviation from the predicted

sea-bed loss. In the OBE, provision was made for the correction of cable misalignment amounting to  $\pm 2.5$  dB systematic and  $\pm 1.5$  dB random per ocean block at 30 MHz. In a 20-repeater block, this corresponds to a total of  $\pm 0.48$  percent of cable loss.

Since cable and repeater development proceeded simultaneously, predictions of cable loss and laying coefficients were required in advance of the manufacture of experimental cable sections. The initial estimates were provided from theoretical consideration of the physical properties and dimensional behavior of cable material based on experience with SD and SF systems and supplemented as necessary by experimental data of dielectric loss at frequencies up to 30 MHz. Uncertainties in sea-bed estimates were narrowed in the light of experience gained from sea trials and refined again as experimental data led to a better understanding of the results. The objective was the characterization of cable typical of large-scale production rather than the accurate description of experimental lengths.

#### 4.1 The effect of variation in manufacture

Strict control of material properties, cable dimensions, and manufacturing processes is exercised through the cable specification, in order to limit the variation in cable loss. Table II shows the potential magnitude of variations due to raw material and dimensional tolerances. In the case of conductivity, no advantage is to be gained from an upper limit, so the anticipated variation is shown. A similar situation exists with the

Table II — Effect of variation in material properties and cable dimensions on cable attenuation

Parameter	Tolerance	Effect on Attenuation in Percent		
		1 MHz	6 MHz	30 MHz
Inner conductor:				
Diameter	$\left\{ \begin{array}{l} \pm 0.001 \text{ in.} \\ (\pm 0.025 \text{ mm}) \end{array} \right.$	$\pm 0.00$	$\pm 0.00$	$\pm 0.00$
Thickness	$\left\{ \begin{array}{l} \pm 0.0005 \text{ in.} \\ (\pm 0.013 \text{ mm}) \end{array} \right.$	$\pm 0.00$	$\pm 0.00$	$\pm 0.00$
Conductivity	$\pm 0.4\%$	$\mp 0.15$	$\mp 0.15$	$\mp 0.15$
Core insulation:				
Diameter	$\left\{ \begin{array}{l} \pm 0.003 \text{ in.} \\ (\pm 0.076 \text{ mm}) \end{array} \right.$	$\mp 0.18$	$\mp 0.18$	$\mp 0.17$
Relative permittivity	$\pm 0.004$	$\pm 0.09$	$\pm 0.09$	$\pm 0.09$
Loss angle: 30 MHz				
6 MHz	$\left\{ \begin{array}{l} \pm 6 \mu\text{R} \\ + 5.5 \mu\text{R} \\ - 7.4 \mu\text{R} \end{array} \right.$	—	—	$\pm 0.57$
1 MHz	$\left\{ \begin{array}{l} \pm 7.4 \mu\text{R} \end{array} \right.$	—	$+0.24$ $-0.33$	—
Outer conductor:				
Air gap	$\left\{ \begin{array}{l} \pm 0.0006 \text{ in.} \\ (\pm 0.015 \text{ mm}) \end{array} \right.$	$\mp 0.11$	$\mp 0.10$	$\mp 0.10$
Thickness	$\left\{ \begin{array}{l} \pm 0.0005 \text{ in.} \\ (\pm 0.013 \text{ mm}) \end{array} \right.$	$\pm 0.00$	$\pm 0.00$	$\pm 0.00$
Conductivity	$\pm 0.4\%$	$\mp 0.04$	$\mp 0.04$	$\mp 0.04$

air gap\* between the core and outer conductor. Although it cannot be quantified by the specification, every attempt is made to control and regulate its size. It is perhaps worth commenting that the limits on diameter and permittivity variation were met in every cable section manufactured for TAT-6 (the former by a fair margin), and that the polyethylene core material met the loss angle requirement in more than 97 percent of the cable sections.

#### 4.2 Control of deviation from design

With one exception, the effect of individual tolerances is small, but when combined they amount to a total deviation of  $\pm 1.2$  percent at 30 MHz. Half of this is due to the dielectric loss, but since its effect at low frequencies is far less, equalization at 30 MHz by length adjustment will cause a significant deviation from design in the low band. This was thought to be sufficient justification for a further control on the final characteristic. When the first experimental cable lengths were produced, another reason emerged.

Attenuation measurements on trials cables revealed an enhanced loss which had every appearance of being due to the dielectric but which proved difficult to confirm from dielectric loss measurements on samples prepared from extruded core. The apparent<sup>†</sup> increase in loss angle was 7 to 8  $\mu\text{rad}$  at 30 MHz. Since this had a significant impact on attenuation, it was incorporated into the design model. It became necessary therefore to provide a means of checking that the effect remained constant during production. This was achieved by extracting the apparent loss angle of the cable at 30 MHz from an examination of the ratio of the losses at 30 and 1 MHz using the following expression:

Apparent loss angle at 30 MHz =  $57 + 188(R - 5.756) \mu\text{rad}$ ,  
where

$$R = \frac{\text{measured insertion loss (dB) at 30 MHz}}{\text{measured insertion loss (dB) at 1 MHz}}$$

It can be shown from consideration of the transmission equations that the ratio  $R$  is proportional to the loss angle at 30 MHz but relatively independent of it at 1 MHz. It is also virtually unaffected by deviations in loss which are "cable shape." Combining errors from all sources, including test equipment, the technique is considered accurate to  $\pm 1.7$  microradians at 30 MHz. By smoothing the measured data, it is possible

---

\* The outer conductor does not conform precisely to the surface of the dielectric; the term "air gap" refers to the space between the outer surface of the dielectric and the inner surface of the outer conductor. The thickness of the air gap is the average value of the separation between these surfaces.

<sup>†</sup> The apparent increase in loss angle is now thought to be due in part to a calibration error of 5  $\mu\text{rad}$  in the reference dielectric test set. It is hypothesized that the remainder is due to oxidation or contamination of the polyethylene during core extrusion.

to reduce this uncertainty to  $\pm 1$  microradian. Given that the dielectric as supplied remains within tolerance, then the apparent loss angle should not vary by more than  $\pm 8 \mu\text{rad}$  from a nominal value of  $62 \mu\text{rad}$  at  $10^\circ\text{C}$ . This proved to be the case, but it was soon found that a tolerance of this magnitude allowed large variations in the change of dielectric loss between raw material and finished cable resulting from differences in manufacturing conditions. Since this had an adverse effect on subsequent loss stability, the control was placed instead on the processing change. This was implemented by restricting the change between raw material measured at  $23^\circ\text{C}$  and finished cable measured at  $10^\circ\text{C}$  to  $14 \pm 4$  microradians. To give an early warning of approaching trouble so that immediate remedial action could be taken, the use of moving range control charts showing the dielectric process change was made mandatory toward the end of TAT-6 production.

Having extracted a value for the dielectric loss at 30 MHz, the combined deviation of the cable shape components of cable loss can be estimated and controlled. A tolerance of  $\pm 0.5$  percent was specified which encompassed the total production deviation from the mean characteristic at each factory.

It is evident from Table II that small variations in the air gap could be responsible for a sizeable "laying effect," i.e., the amount by which the cable misses its sea-bed design loss. To check that the application of the outer conductor was under control, one section in 10 was required to be repanned (removed from one storage pan and coiled into another) after the factory transmission tests and then remeasured. A large increase in loss as a result of handling the cable would point to a slack outer conductor and the need for adjustment of the forming mill.

In the final design loss for factory measurements at  $10^\circ\text{C}$ , shown in Fig. 5, an air gap of 0.0020 in. (0.051 mm) was assumed. In repanning operations, the air gap collapsed on the average by 0.0007 in. (0.018 mm) after a single turnover and by a further 0.0002 in. (0.005 mm) following a second turnover. However, the degree of scatter was fairly large and appeared to be related to previous storage conditions and the time elapsed before turnover.

#### **4.3 Sea-bed coefficients**

Laying coefficients to allow correction for temperature, pressure, and handling effects were obtained from 18 nmi (33.4 km) of prototype SG cable manufactured by STC. The trials cable was produced in four equal lengths, half with ICI and half with BXL low-loss polyethylene. The temperature coefficient was determined from transmission measurements of individual and paired lengths at five equally spaced temperatures varying from  $22^\circ$  to  $4^\circ\text{C}$ .

At high frequencies, the cable temperature coefficient is increasingly



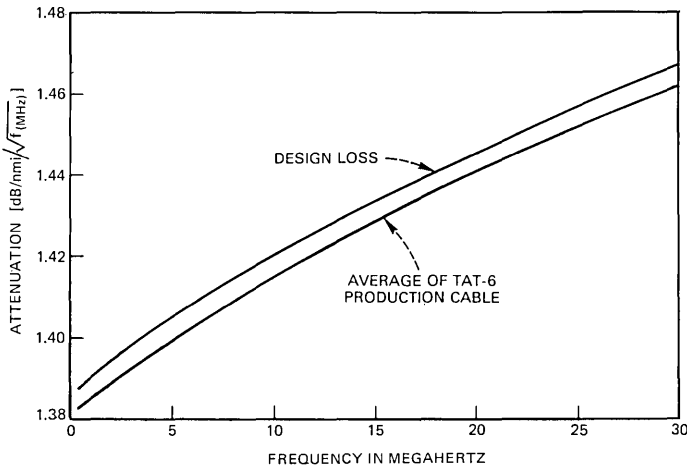


Fig. 5—Attenuation at 10°C and 0 fathom. An air gap of 0.002 in. between the outer conductor and core was assumed in the calculation.

dependent on the dielectric loss, but there was little evidence of difference among the SG dielectrics. The mean of the trials cable coefficients is compared in Fig. 6 with the final design coefficient. This is split into two parts to allow for laboratory evidence which suggested that the rate of thermal expansion of the dielectric differed over the temperature ranges 2.5° to 10°C and 10° to 20°C. However, a measured temperature coefficient was liable to apparently substantial but quite illusory modification by small variations in outer conductor behavior. If the direction of temperature change was from low to high, then the outer conductor did not move until the air gap closed. This caused an apparent increase in the temperature coefficient by overriding part of the dielectric contribution. An apparently nonlinear coefficient was readily caused by excessive delay between two measurements at successive temperatures. This allowed additional collapse of the outer conductor as the sheath very gradually contracted. A similar effect could be produced by successively overshooting and overcorrecting several times before reaching a stable temperature. The time constant of these effects was far longer than that required for dc resistance stabilization.

#### 4.4 Sea trial

Having established the temperature coefficient, a sea trial was conducted in June 1973 by Cable Ship *Alert* to determine the pressure coefficient of the armorless cable and to assess the handling characteristics of the armored cable. The two 9-nmi (16.7 km) lengths of armorless cable were laid at depths of 1500 and 2500 fathoms (2743 and 4572 m) in the form of a hairpin, keeping both ends on board to facilitate trans-

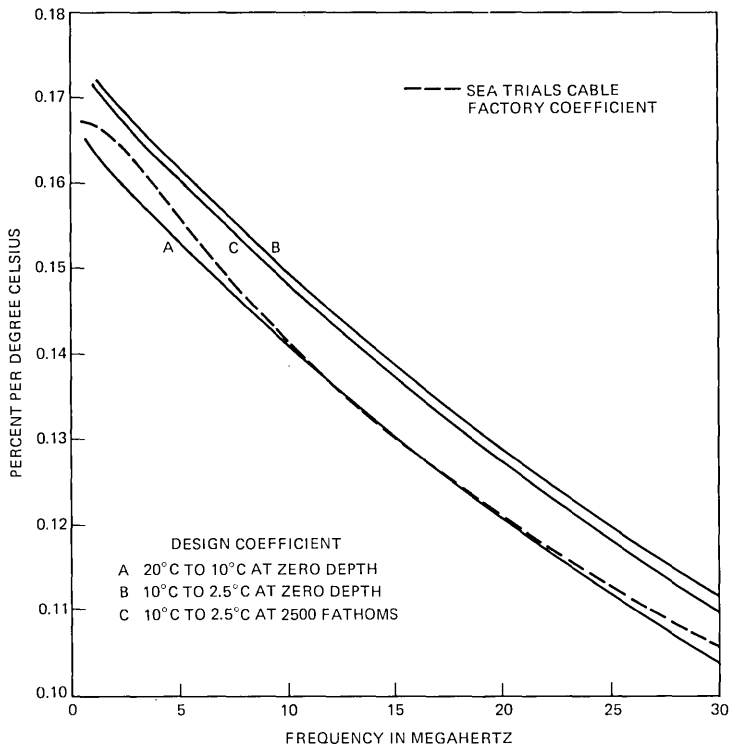


Fig. 6—Attenuation temperature coefficient for 1.7-in. SG cable.

mission tests. The design coefficient shown in Fig. 7 was based on the two points obtained from each cable measurement. The depth coefficient increased with frequency due to the increased influence of the dielectric. The coefficient obtained from the ICI cable was smaller than that from the BXL and, at 1 MHz, was 0.12 percent lower than the computed value for SF cable. It was therefore decided to bias the SG design coefficient towards the BXL characteristic with a value slightly above the SF design at 1 MHz.

The curve in Fig. 7 labeled "Mean Sea Trials Cable Coefficient" was calculated using additional depth information gained from downrunner\* measurements. These were taken when the cable just reached the sea bed at each depth. The sea-trial cable coefficient is the average of a linear fit through the four points thus obtained for each length. Treated in this way, the ICI and the BXL data confirm the previous ICI two-point coefficient. The data also indicate the presence of a large air gap in the BXL cable which is consistent with the attenuation change seen during handling operations.

\* The downrunner is the portion of cable between the ship and the sea bed.

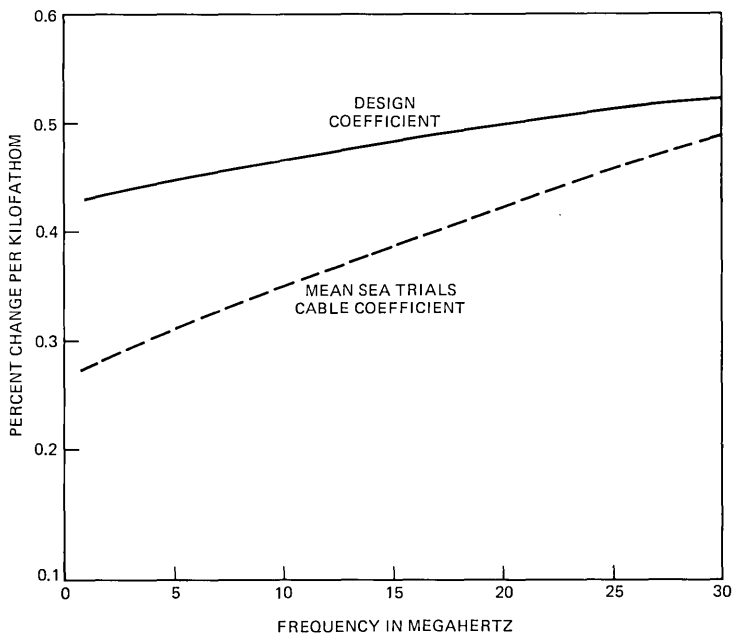


Fig. 7—Attenuation pressure coefficient for 1.7-in SG cable.

The essentially non-depth-dependent component of the pressure coefficient due to closing the air-gap under the outer conductor was modeled from air-gap behavior determined from laboratory measurement and sea trials results. The design value was set at 0.37 percent flat with frequency.

After the sea trials, both cables were streamed (laid out on the sea bottom), one at each depth, with a view to recovery at a later date to assess their stability over the intervening time period. This was undertaken in June 1975 by Cable Ship *John W. Mackay*. During the two-year interval, the cable which had been manufactured under conditions closest to those approved for TAT-6 production had increased in loss by the equivalent of 1  $\mu$ rad at 30 MHz.

#### V. ANOMALOUS DIELECTRIC LOSS INVESTIGATION DURING TAT-6 CABLE PRODUCTION

When cable production started at CDL\*, it was found that some freshly produced lengths exhibited excessively high apparent loss angles at 30 MHz, 20 to 30  $\mu$ rad above nominal. It was quickly discovered that the effect was related to extruding core into an initial trough of water

\* Cables de Lyon, Calais, France.

at 105°C† instead of the then accepted value of 95° to 97°C, as shown in Fig. 8. The higher temperature had been chosen to maintain adhesion and freedom from voids at increased extrusion line speeds. As a result of the investigation described below, the subsequent extruded core was chilled in a first water trough having a temperature of 92°C.

The high apparent loss angle of the affected cable continued to increase with time in the factory, appearing to reach a peak value after three to six months and then showing signs of slowly decreasing. When the temperature of the water in the first trough was reduced to 97°C, cable was produced within specification but some changes in apparent loss angle with time still remained (see Fig. 9). This resulted in lengthy investigations into the effects of water on polyethylene.

Freshly produced core, extruded into water at 97°C, was rushed from the factory to the laboratory and water measurements were made on three concentric layers. The outer layers were found to contain up to 200 parts per million (ppm) of water, while the other layers contained close

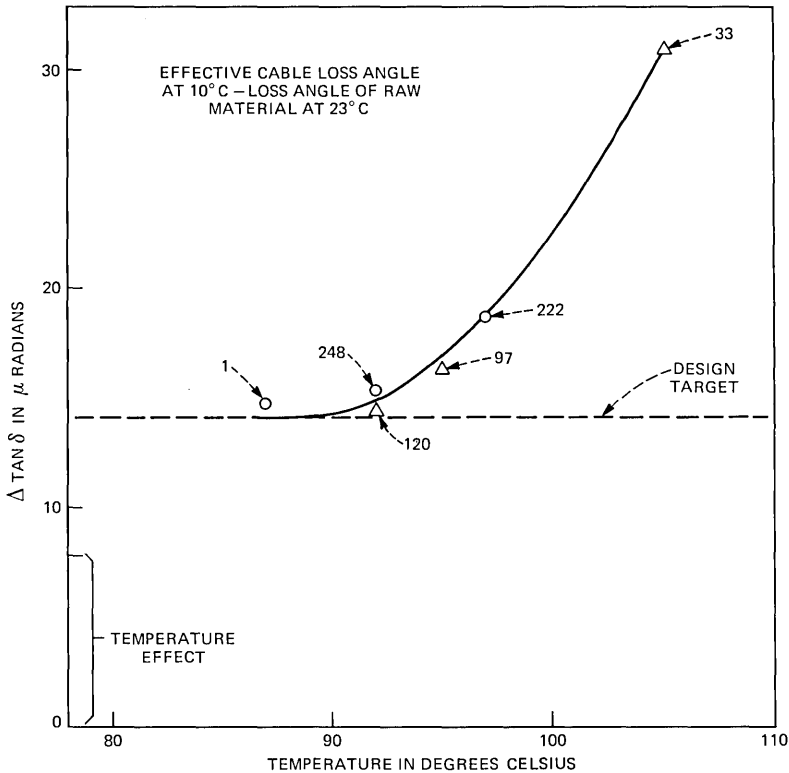


Fig. 8—Core extrusion cooling temperature versus loss angle change. Number of cable sections represented by each plot is shown on the curve.

† Pressurized cooling troughs allow temperatures above the atmospheric pressure boiling point.

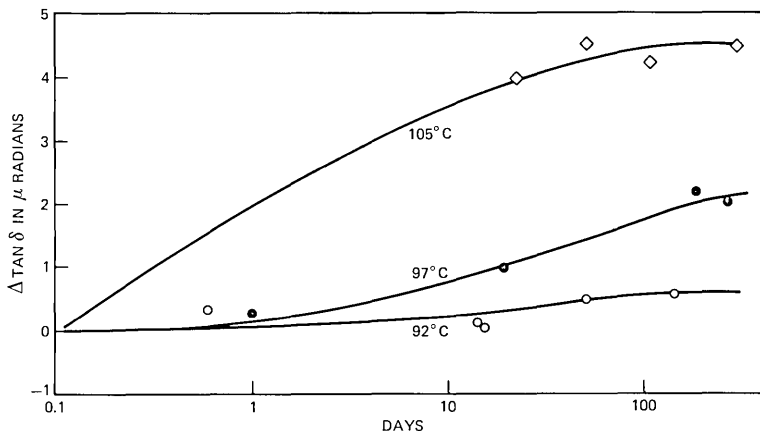


Fig. 9—Typical factory aging characteristic for cable core cooled at different temperatures. Change in apparent cable loss angle with time at 30 MHz and 10°C.

to the normal saturation levels of about 10 ppm at room temperature. Plaques were also molded from material from these three layers and the loss angles determined at several frequencies. Plaques from the outer layers of the core initially showed enhanced loss angles with an excess of 20 to 30  $\mu$ rad at 30 MHz, but the values decreased quite rapidly with time, recovering to expected values within 24 hours.

### 5.1 Water measurements

As a result of this initial work, techniques were developed for examining the quantity and nature of the water trapped in the core. A cutter was produced which could remove a cylindrical plug from a cable core without affecting the distribution of water. If six of these plugs were used and sliced into thin disks, the radial distribution of the water in the core could be measured using a DuPont moisture analyzer to an accuracy of  $\pm 5$  percent or  $\pm 2$  ppm for small quantities of water. The distribution of water through a fresh core of SG polyethylene is given in Fig. 10. Most of the water is concentrated in the outer layers and is far in excess of normal saturation levels. It was suspected that the excess water was clustered in the form of microdroplets in small voids less than 1  $\mu$ m in size. A Perkin-Elmer scanning calorimeter was used to confirm this theory of clustering. By cooling samples to  $-55^\circ\text{C}$  and then monitoring them while gradually heating to  $30^\circ\text{C}$ , a peak in heat capacity was observed at  $0^\circ\text{C}$  caused by the melting of ice crystals formed where the water had clustered. The quantity of clustered water was calculated from the enthalpy of fusion of frozen water. Attempts to see the microdroplets under a microscope proved unsuccessful, although clusters 2  $\mu$ m in diameter were detected when plaques were subjected to high-pressure steam and quenched in water at  $23^\circ\text{C}$ . This supports the suggestion that

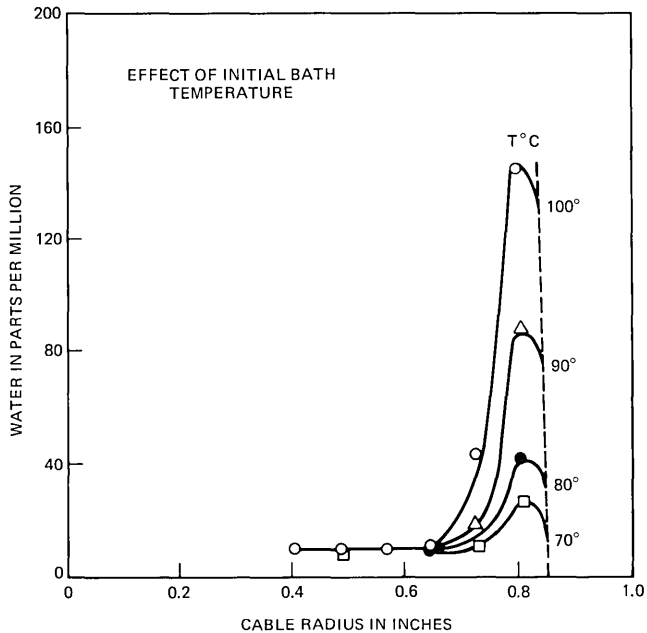


Fig. 10—Distribution of water through an SG cable core.

the microdroplets produced under normal, less severe conditions are smaller than  $1 \mu\text{m}$ .

The techniques described above were used to determine the quantity of both the total and clustered water in samples saturated at temperatures between  $4^\circ$  and  $100^\circ\text{C}$ , with samples saturated above  $23^\circ\text{C}$ , then quenched in water at  $23^\circ\text{C}$  (see Fig. 11). Within the limits of detection (10 ppm), no clustered water melting at  $0^\circ\text{C}$  was observed in samples saturated at or below  $50^\circ\text{C}$ .

### 5.2 Exploration of water trapped during core extrusion

The polyethylene core is extruded at about  $190^\circ$  to  $200^\circ\text{C}$  and is then cooled by traversing a series of water troughs starting at temperatures of  $80^\circ$  to  $100^\circ\text{C}$  and descending in temperature to  $20^\circ\text{C}$ . When the molten core enters the first trough, water vapor diffuses into the polyethylene to produce a concentration of 100 to 200 ppm near the surface, reducing to about 10 ppm at a depth of 0.2 in. As the temperature of the polyethylene drops below approximately  $105^\circ\text{C}$ , crystallization starts and it is hypothesized that noncompatible materials (polar groups, antioxidant, and water) are swept ahead of the crystallizing surfaces. When the temperature decreases further, the clustering of these impurities triggers the precipitation of globules of water near the outer surface of the core. The globules contain traces of water-soluble salts and antiox-

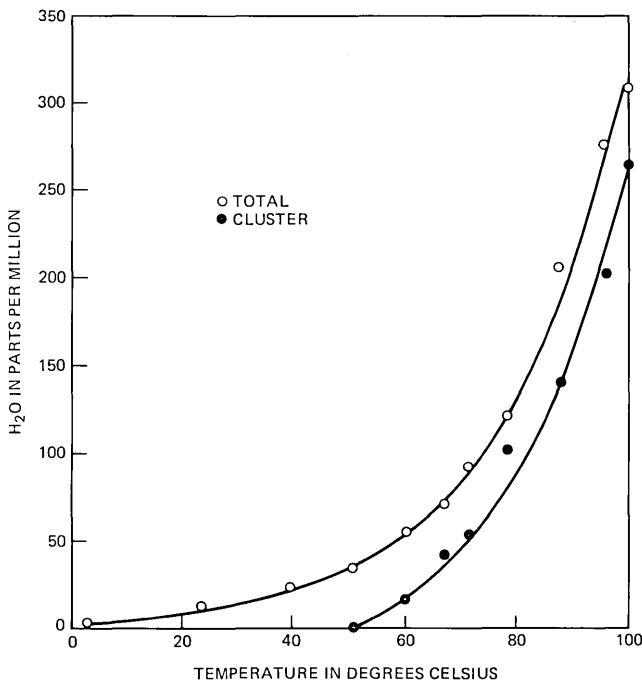


Fig. 11—Saturation content in SG cable.

ident and attract to the polyethylene-water interface any polar groups in the vicinity. Thus, the water droplet conditions its surroundings and produces some small water-filled voids with hydrophilic surfaces. The diffusion coefficient drops sharply with temperature, and very little of the precipitated water can escape from the cable before it reaches room temperature. When the core is exposed to the atmosphere prior to sheathing, the trapped water slowly dries out and if it is left for longer than one week in the air, it will usually recover to a low water content. However, many of the voids will be left with hydrophilic surfaces so that, if exposed to water on the sea bed, they can refill, causing changes in the dielectric loss.

The standard procedure of shaving 0.070 in. (1.78 mm) from the outside of the core removes the more heavily contaminated material but is insufficiently deep to remove all the damaged polyethylene.

### 5.3 Effects of water on dielectric loss

To determine the effects of water on the dielectric loss of the polyethylene core, numerous experiments have been carried out both on cable and on plaques simulating cable core. It was found that, although water in the vapor phase has a small effect on the dielectric loss below the microwave range, microdroplets as small as 0.1  $\mu\text{m}$  in diameter can have

considerable influence on the loss in the megahertz region. They act as small regions of high permittivity and finite resistivity dispersed in a low-loss dielectric medium. The dielectric response of such a system is governed by relaxation equations and in the simplest case will exhibit a single Debye-type peak whose frequency is mainly dependent on the permittivity and resistivity of the small regions. In the case of the microdroplets, the resistivity of the water will be modified by the presence of soluble impurities such that the peak occurs in the megahertz range. The general behavior is known as the Maxwell-Wagner effect. In practice, there may also be a small increase in loss in the megahertz region due to water in the vapor phase causing an enhancement of the gamma process,<sup>2</sup> which is centered around 1 GHz in polyethylene.

Typical behavior is illustrated in the results of the following experiment, shown in Fig. 12. To simulate the conditions in the outer layer of the core immediately after extrusion and cooling, a series of plaques (2 mm thick) was molded at 180°C. The molten plaques, attached to metal backing sheets, were then dropped into baths of water at 95° to 70°C for 30 minutes. The dielectric loss was measured at frequencies up to 30 MHz as a function of drying time at 23°C and 35-percent relative humidity. The effect of the water on the polyethylene was found by normalizing the times and plotting the excess loss over that for a normal molded plaque cooled in air. A typical example simulating a first cooling trough at 95°C is given in Fig. 12; the initial effect is large, with a peak

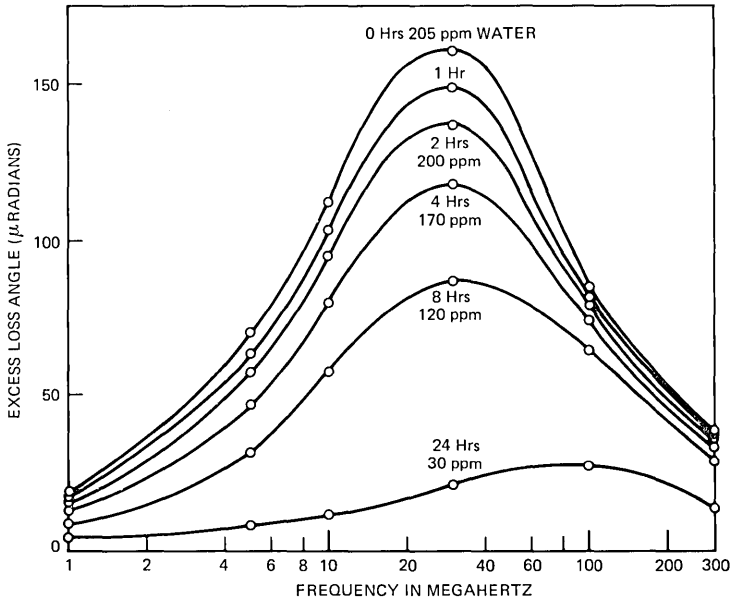


Fig. 12—Increase in loss angle caused by immersing molten plaques in water at 95°C for 30 minutes, plotted as a function of drying time.



excess loss of approximately 160  $\mu\text{rad}$  at 3 MHz for a water content of 245 ppm. The effect decays quite fast so that, after eight hours, the peak excess loss is down to approximately 85  $\mu\text{rad}$ ; after twenty-four hours, the peak has shifted up to 8 MHz and is approximately 25  $\mu\text{rad}$  high for a water content of 30 ppm. The experiments on plaques highlight the effect of clustered water on polyethylene, but luckily the influence on the overall attenuation of finished cable is heavily diluted by a number of factors.

The behavior of plaques represents only the outer layers of the core. The inner layers are free from clusters and contain water to the normal saturation level of about 10 ppm. This level remains substantially constant while the outer layer dries down. So whereas the effect of water on the dielectric loss of the outer layer of freshly extruded core is initially very large, the rest of the core is scarcely affected, and the dielectric loss integrated over the whole cross section shows only a small increase. As a rough rule of thumb, the overall change in dielectric loss integrated over the entire SG cable core is about  $\frac{1}{10}$  the excess loss of a plaque simulating its outer layer. Taking as an example the results of the plaque experiment given in Fig. 12, the plaque initially exhibited an excess loss of 37 microradians at 30 MHz, decreasing to 12 microradians after 24 hours. The dielectric loss of an equivalent SG core would be increased initially by 3.7 microradians; this would then drop to 1.2 microradians.

In terms of overall cable attenuation, the effect is further diluted by the fact that, at low frequencies, the dielectric loss contributes only a very small proportion of the total loss; even at 30 MHz it contributes only 6 percent. Even so, a 1- $\mu\text{rad}$  change at 30 MHz is equivalent to 26-dB change in an overall system of 3400 miles which, if it occurred on the sea bed, would require that the system be re-equalized at several points along its length.

## VI. CABLE AGING

The effects of water introduced during the extrusion process and the changes in loss observed on cable lengths monitored in the factory raised questions about the long-term loss stability of the cable in service. Prior to laying the cable, there were only conjectures of the likely behavior on the sea bed but, in spite of inadequate evidence, it was essential to make some estimate of the possible changes in loss over the 20-year life of the system so that an adequate equalization strategy could be formulated. The only piece of evidence available from measurements on sample cable was that a piece of SG sea-trials cable, laid at 1500 fathoms for 2 years, had aged by 1  $\mu\text{rad}$  at 30 MHz. Using this information and results based on other work, it was predicted that the dielectric loss of the SG cable system would age by  $-1$  to  $+3$   $\mu\text{rad}$  in 20 years. (That is, the uncertainty embraced possibilities ranging from a 1- $\mu\text{rad}$  decrease to a 3- $\mu\text{rad}$  increase in 20 years.)

As predicted, the TAT-6 system is slowly aging on the sea bed: 346 days after commissioning, the phase delay had increased by about  $3.5 \mu\text{s}$  and 583 days after commissioning the attenuation of the deep-water sections had increased by 21.6 dB at 27.5 MHz. The change of attenuation with frequency is approximately linear. The Requirements and Performance paper in this issue of the B.S.T.J. discusses the time behavior of the observed aging and the use of shore-controlled equalizers to compensate for it.

It is hypothesized that water is entering the TAT-6 cable on the sea bed at the repeater terminations and is traveling along the cable causing compression of the core and expansion of the sheath. The resulting sea-water film between the core and outer conductor acts as a lossy dielectric in series with the polyethylene. This, together with the dimensional changes of the cable structure, will cause an increase in attenuation and a change in phase delay.

It is further hypothesized that, in addition to aging from this cause, water in contact with the core will gradually diffuse into the polyethylene and refill some of the dried microvoids. The rate of diffusion will be very slow at deep-sea pressure and temperature. To confirm that polyethylene with dried cluster sites will reabsorb water, laboratory experiments were carried out on a series of plaques similar to those described in Section 5.3. The plaques were allowed to dry under laboratory conditions for a week (simulating the average time between extruding and sheathing the core), by which time their water contents were less than 10 ppm. They were then exposed to approximately 98-percent humidity, and the resulting changes in loss angle as a function of exposure time were plotted for frequencies up to 30 MHz. The results for a plaque initially conditioned in  $95^\circ\text{C}$  water are given in Fig. 13. After exposure for 28 days, the plaque had about 60 ppm of water in it. The experiments are still continuing.

The results have been expressed in Fig. 14 in terms of overall attenuation for a complete cable length of 3400 nmi. The curves illustrate how aging from this cause initially might appear linear with frequency and subsequently change shape. In the case of the cable on the sea bed, the effect of exposure to water will proceed at a considerably slower rate than that observed in the experiments. The rate will be limited by the construction of the cable, the longer diffusion paths, and the effects of increased pressure and reduced temperature. Attempts have been made to account for these effects; using data from experiments on short cable samples, they predict similar shapes but about  $\frac{1}{3}$  the magnitude of the aging shown. Reabsorption of water into cluster sites will not change the phase delay significantly.

While neither of the two aging mechanisms described above can individually account for all aspects of the observed cable changes, com-

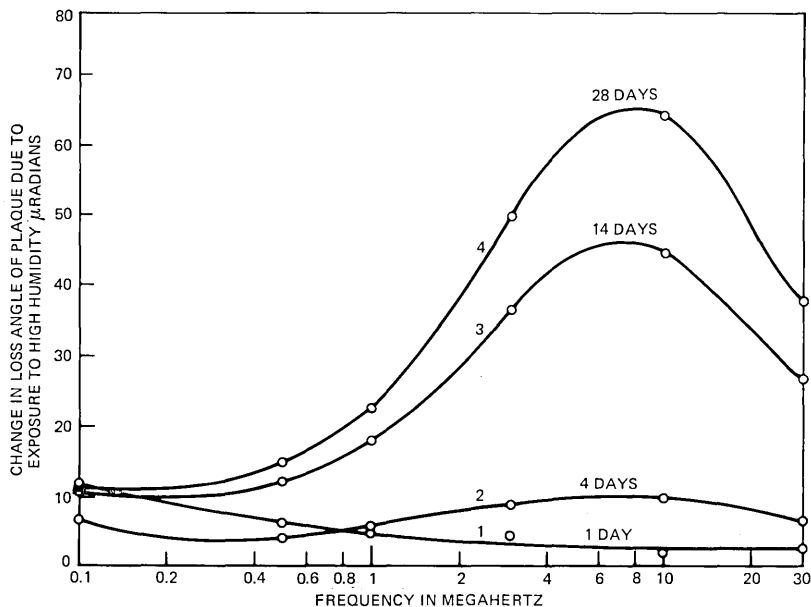


Fig. 13—Change in loss angle of plaque on exposure to high humidity after drying for one week.

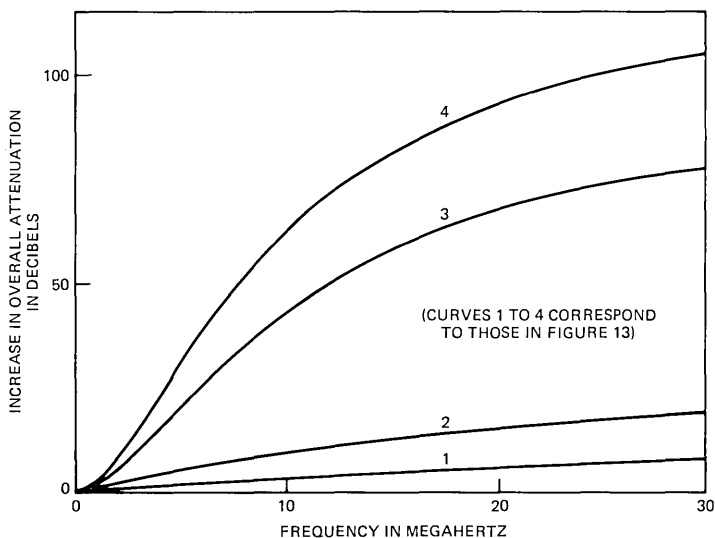


Fig. 14—Calculated attenuation changes in a 3400-nmi 1.7-in. SG cable assuming dielectric changes due to water.

binations of the two mechanisms can be made to fit the data, including the rate of loss change with time. However, the long-term aging prediction cannot be confirmed without better knowledge of (i) the relative movements of core and outer conductor on the sea bed and (ii) the effects

of reabsorption of water on the dielectric loss under deep-sea conditions.

## VII. LAYING EFFECT

Laying effect is the difference between predicted and actual sea bed transmission losses at the time of lay. Predictions are based on cable and repeater factory measurements that are corrected for estimated sea-bed conditions. A non-zero laying effect can result from errors in factory or shipboard measurements, from cable aging during the period between these measurements; from errors in cable temperature, pressure, and handling coefficients, and from differences between predicted and actual sea-bed conditions at the time of lay. It can also be caused by imperfect knowledge of repeater and equalizer termination losses and impedance discontinuities at the cable-pigtail and the repeater-pigtail interfaces.

In TAT-6, the observed laying effect was remarkably consistent among the several cable lays. It was possible to differentiate between shallow and deep water lays and between cable from different manufacturers. A typical result is shown in Fig. 15 for the first deep water lay. Laying effect was essentially zero at 30 MHz but reached + 0.45 percent at the bottom of the low band. This may be interpreted as a constant cable shape component of + 0.45 percent, which is offset at 30 MHz by a dielectric loss angle at sea bottom which is  $4 \mu\text{rad}$  higher than predicted.\*

The average cable shape and linear-loss components of the deep-water laying effect were, from Table III, +0.42 percent and  $+ 4.4 \mu\text{rad}$ , respectively. Because these errors cancelled at 30 MHz, the resulting misalignment remained well within the equalization range of the OBE but their magnitude is sufficient to warrant an explanation. The difference between the design and the mean sea trials cable pressure coefficient, shown in Fig. 7, suggests a starting point. At 1 MHz, this is +0.16

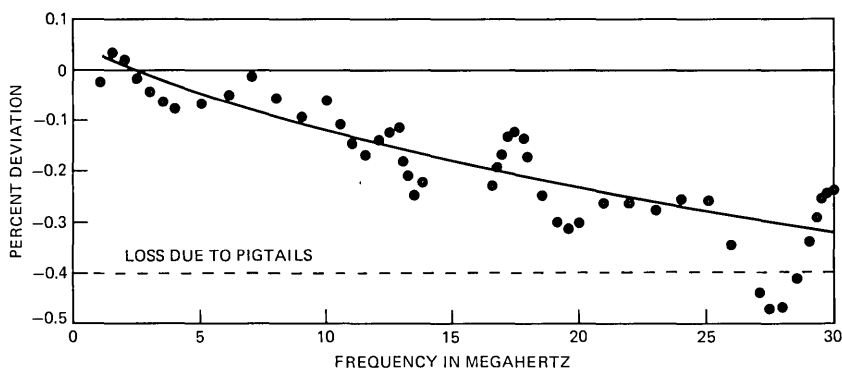


Fig. 15—Lay 1 (deep water) laying effect including 0.4 percent pigtail loss.

\* Positive laying effect corresponds to gain relative to prediction.

Table III — TAT-6 cable laying effect

Lay	Cable Length and Supplier (nmi)	Mean Annual Sea-Bed Temperature (°C)	Mean Sea-Bed Depth (kF)	Cable Shape Laying Effect (%)	Linear Loss Laying Effect at 30 MHz ( $\mu$ rad)
Green Hill burial	111 STC/SWC*	10.4†	0.045	+0.30	+1.5
Lay 1	605 STC	2.6	2.19	+0.45	+4.0
Lay 2	634 CDL	2.3	2.67	+0.34	+4.0
Lay 3	640 STC	2.3	2.39	+0.47	+5.5
Lay 4	640 STC	2.9	1.83	+0.51	+4.5
Lay 5	640 STC/CDL	2.6	2.45	+0.31	+4.0
St. Hilaire burial	114 STC	12.8	0.068	+0.44	+2.0

\* Cable manufactured by STC and armored by Simplex Wire and Cable Co.

† Actual temperature during the Green Hill burial operation is thought to have been about 2°C higher than annual mean.

percent per kilofathom, enough to explain +0.37 percent of the cable-shape laying effect in deep water. The difference in slope is equivalent to 1.3  $\mu$ rad per kilofathom at 30 MHz, enough again to account for 3  $\mu$ rad of the deep water linear-loss laying effect. This leaves only 0.05 percent cable shape and 1.4  $\mu$ rad of excess loss angle to account for. Together, they correspond to a misalignment of less than  $\pm 0.1$  percent across the band.

Any further attempts to explain the remaining laying effect are probably not justified by the accuracy of measurement that was possible. However, the loss-angle component could be accounted for by in-factory aging. At least half the cable used in TAT-6 was extruded and cooled under conditions which could cause an increase in loss angle of 2  $\mu$ rad after 6 months' storage (see Fig. 9). The remaining cable shape effect could also be accounted for quite easily by an error in the air-gap coefficient. Analysis of factory transmission measurements, including study of any change due to cable turnovers, suggests that the average air-gap at 10°C was less than the figure of 0.002-in. (0.051 mm) adopted for the final design. Assuming there is no air gap present when the cable is on the sea bed, then the change in air gap from ship to sea bed will be less than expected and could reduce the cable-shape laying effect by as much as 0.2 percent.

## VIII. CABLE TERMINATIONS

Terminations, frequently called couplings, are used on each end of each cable section to interface the cable to the repeater or equalizer. They must perform the following functions:

(i) Transfer tensile loads from the strength member of the cable to the repeater or equalizer end cone.

(ii) Provide a signal path between the cable and the coaxial pigtail wire which connects the termination to the repeater or equalizer.

(iii) Provide sufficient flexibility to permit handling over 9-ft diameter drums and sheaves on cable ships.

(iv) While performing the functions above, be capable of withstanding full sea-bottom pressure and the full system dc operating voltage.

Terminations used on armorless cable differ somewhat in requirements and configuration from those used on armored cable, so it is useful to discuss them separately.

### 8.1 Terminations for armorless cable

The 8G coupling is used on armorless cable. The specific performance requirements to achieve the functions listed above are:

(i) 40,000-lb<sub>f</sub> (177.9 kN) tensile capability.

(ii) 600 in.-lb<sub>f</sub> (67.8 m-N) torque capability at maximum tensile load.

(iii) At least 35-dB structural return loss from each end.

(iv) Capability to allow at least a 45-degree angle between the cable and the repeater or equalizer axis.

(v) 7000-V dc capability at both possible polarities with no breakdown and no noise generation in the transmission band.

(vi) Capability to withstand 12,000 pounds per square inch (816 atmospheres) sea pressure.

Figure 16 illustrates the design of the 8G coupling. The center strand strength member of the cable is terminated in epoxy in the termination cone. This in turn is glued to a ceramic ring, and the entire assembly is encapsulated in polyethylene. This molded unit is then placed inside the cone housing which attaches to the gimbal mechanism. The gimbal in turn attaches to the gimbal housing and clamp ring, which threads onto the end cone of the repeater or equalizer. In this way, a tensile load in the cable strand is transferred to the repeater or equalizer housing.

Two half-slots are formed in the polyethylene which encapsulates the strand termination. Two keys, part of the cone housing cap, engage these slots to prevent rotation of the anchor mold assembly and provide the required torque capability.

The molded polyethylene layer between the ceramic of the termination assembly and the cone housing is dimensioned to be thin enough to

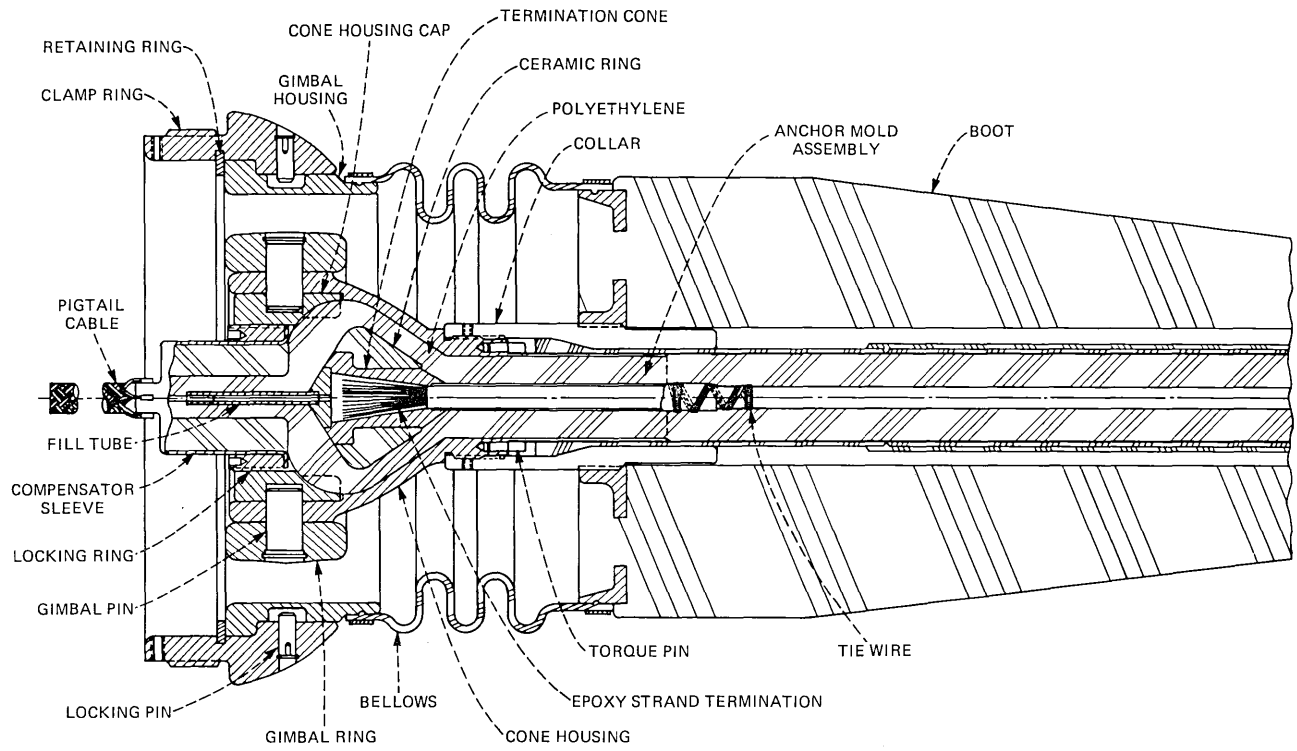


Fig. 16—SG armorless cable coupling.

support the required tensile load and thick enough to provide the high-voltage capability stated above. Within these constraints, it was not possible to achieve the required return loss in the anchor mold assembly as molded. The structure showed excessive capacitance with respect to 50 ohms, so more inductance was needed. To provide this, the large polyethylene sleeve was added at the end of the anchor mold assembly.

The tube on the end of the termination assembly opposite the strand is used for introducing the terminating epoxy into the cone; thus, it must be kept open until the termination is attached to the cable. Since the anchor mold assembly is provided to the cable factory in overmolded condition, the tube must extend outside the molded volume. For this reason, the compensating sleeve could not be made a part of the anchor mold assembly. Instead, it is a separate part which is added after the epoxy termination is complete. The inner conductor of the coaxial pigtail cable is crimped and soldered into the end of the tube and the joint overmolded.

On the opposite end of the anchor mold assembly, the inner conductor of the cable is attached to the conductor tube of the assembly by three turns of three wires to allow for some axial motion under load without loss of continuity. The outer conductor is dimensioned to maintain the 50-ohm cable characteristic impedance up to the termination assembly.

By careful impedance control where possible and by use of the compensating sleeve, the return loss requirement was satisfied.

The gimbal mechanism is so designed that it provides slightly more than 45 degrees of motion between the cable and the repeater or equalizer axis. The bellows is provided to accommodate the gimbal motion while keeping foreign material out of the gimbal mechanism.

The entire termination outside the molded polyethylene is open to sea water, so the sea pressure produces only an additive hydrostatic compression in the various parts. Similarly, the molded assembly is essentially solid so that sea pressure has no detrimental effect.

All the metal parts are made from either copper or copper-beryllium to prevent electrolytic corrosion in sea water.

The large rubber boot serves to limit cable bending radius at the termination and to help guide the whole assembly through the cable machinery on the cable ship.

## **8.2 Terminations for armored cable**

Requirements for the couplings for armored cables differ from those stated above primarily in the tension and torque values. Both the 1-inch (25.4 mm) shielded armored and the 1.7-inch (43.2 mm) single-armored cables have strengths well in excess of 100,000 lb<sub>f</sub> (445 kN). After careful



analysis, it was decided that the kind of coupling structure necessary to make the coupling as strong as the cable was unreasonable from both a fabrication and a cost standpoint. Consequently, it was decided to limit the coupling capability to:

(i) 100,000 lb<sub>f</sub> (445 kN) tension.

(ii) 25,000 lb<sub>f</sub>·in. (2825 N·m) torque.

In addition, in the couplings for armored cable, the tensile load must be carried from the steel armor wires to the copper-beryllium repeater housing. To prevent corrosion in sea water, special attention must be paid to electrically isolating these two materials from each other at some point while maintaining the tension and torque-carrying capability.

Figure 17 shows the 8N coupling which is used with 1.7-in. (43.2 mm) single-armored cable. The 8P coupling, which is used with 1.0-in. (25.4 mm) shielded-armored cable, is very similar to the 8N, differing only in the details in the round nut assembly that must change with cable diameter.

As in previous cable systems, double-armored cables are terminated as single-armored, the outer armor layer being lashed off outside the coupling.

The strength termination is achieved by crimping a ferrule onto the end of each armor wire. The terminated wires are then placed into the slots of the armor ring against which the ferrules bear. The load is transferred by a yoke arrangement through plastic insulators from the steel armor ring to the copper-beryllium armor housing. The plastic insulators prevent electrolytic corrosion between the dissimilar metals.

To carry the required torque, the armor housing is threaded into a copper-beryllium bushing and secured with a key in the threads. The outside of the bushing is hexagonal in shape and mates, through a plastic insulator, with the hexagonal interior profile of the steel armor ring housing. Similarly, the interface surface between the armor ring housing and the armor ring is hexagonal for torque transfer.

Since most of the strength is in the armor wires, a strength termination is not required for the strand. A direct connection is thus made between the cable inner conductor and the coaxial pigtail inner conductor. The joint is overmolded to provide a transition from the cable to the pigtail outer diameter. The round nut assembly provides a connection between the cable outer conductor and the special outer conductor insert designed to accommodate the diameter transition. This transition joint provides the required return loss.

Other features of the armored coupling such as the gimbal, the bellows, and the rubber boot serve the same functions as described in connection with the armorless cable coupling.

In summary, using the designs described above, the 8G, 8N, and 8P couplings met or exceeded all design requirements.

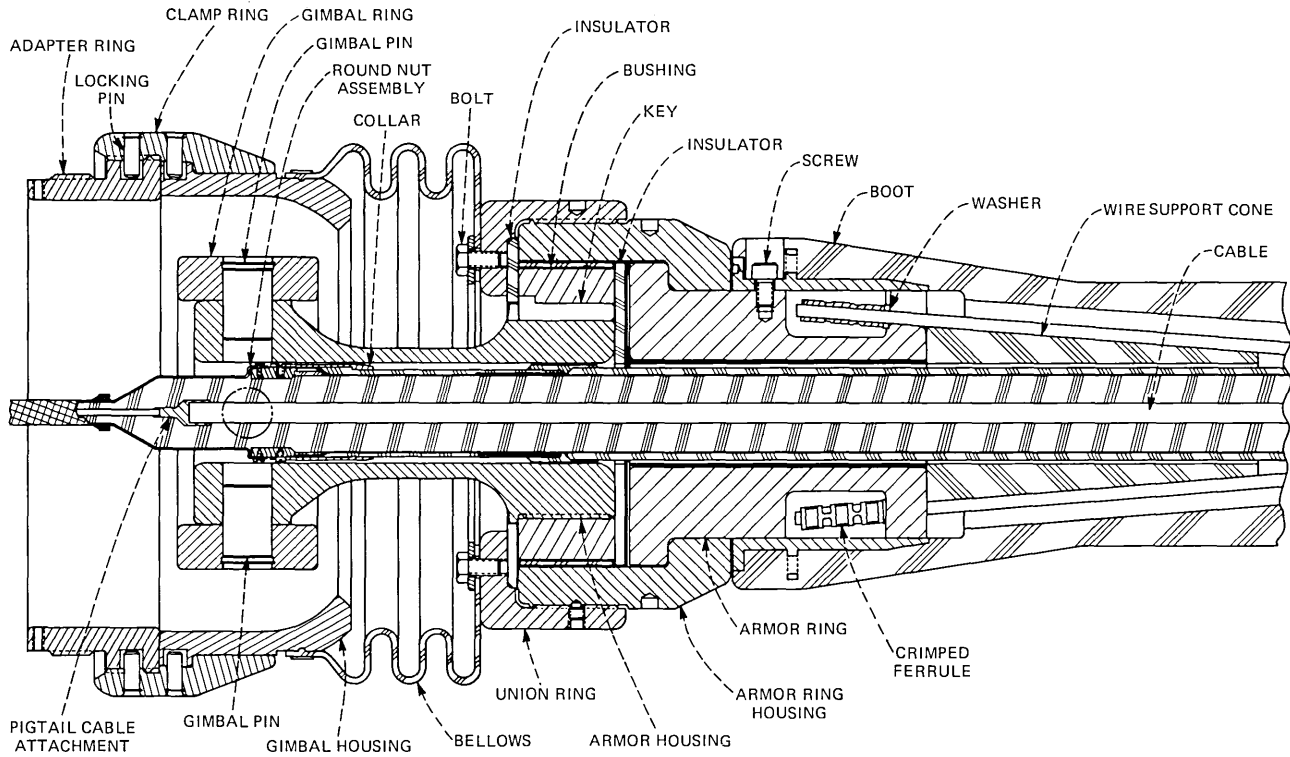


Fig. 17—Typical SG armored cable coupling.

### **8.3 Pigtail cable**

The coaxial pigtail cable mentioned above, which connects the terminated cable to the repeater, has an outer diameter over the insulation of 0.500 in. (12.7 mm) and an inner conductor diameter of 0.146 in. (3.71 mm). These dimensions, used in standard formulas, do not provide a 50-ohm structure. The outer conductor is a copper braid with 0.020-in. (0.51 mm) diameter wires. These wires are much larger than those used in standard braids (typically, 0.007 in. (0.18 mm) diameter), but are required to allow for some loss of material due to corrosion while maintaining continuity. Because these larger wires are used, the outer conductor current is effectively approximately 0.010 in. (0.25 mm) outside the outer surface of the polyethylene insulation. The 0.146-in. (3.71 mm) inner conductor compensates for this effective increase in outer diameter. The braid is covered with heat-shrinkable tubing to hold it in place and to limit water flow for corrosion protection.

When the pigtail is placed in sea water, the conductivity of the water causes a small reduction in the effective coaxial outer diameter, which changes the characteristic impedance of the structure. This change must be accounted for when correlating "wet" and "dry" transmission measurements.

## **IX. ACKNOWLEDGMENTS**

Many individuals within Bell Laboratories and the British Post Office contributed to the development of SG cable. Their efforts are gratefully acknowledged here. In particular, mention must be made of the considerable efforts made by E. F. S. Clarke and E. E. L. Winterborn (both now retired) who were successively responsible for coordinating the development program.

Acknowledgment is made to the Director of Research of the British Post Office for permission to publish this paper.

## **REFERENCES**

1. "SF Submarine Cable System," *B.S.T.J.*, 49, No. 5 (May-June 1970), pp. 601-825.
2. N. G. McCrum, B. E. Read, and G. Williams, *Anelastic and Dielectric Effects in Polymeric Solids*, New York: Wiley, 1967, Chapter 10.



## **SG Undersea Cable System:**

# **Terminal Transmission Equipment**

By M. BROUANT, C. CHALHOUB, P. DELAGE, D. N. HARPER,  
H. SOULIER, and R. L. LYNCH

(Manuscript received October 7, 1977)

*Terminal transmission equipment has been developed for the SG cable system that, compared to similar equipment for land analog facilities, makes more efficient use of the transmitted bandwidth and provides superior continuity of service. Although economy of development effort dictated the use of existing equipment and conventional design techniques wherever possible, many new designs were required to achieve the desired features. Means for protecting the undersea repeaters from gross signal overload and a carrier generating scheme for hypergroup and wideband-line frequency-translation equipment are examples of new designs that proved particularly challenging. Duplication of higher-level multiplex equipment coupled with automatic changeover switching is the means used to obtain the desired service continuity. In this regard, much care was required to limit amplitude and phase differences between duplicate transmission paths to insure "hitless" maintenance changeover switching. Other features of the terminal include an on-site equalizer design and construction capability at the wideband line and supergroup levels, a separate 3-channel order-wire facility, individual supergroup signal limiters, and the ability to operate with 3-kHz as well as 4-kHz/spaced message channels. Mechanical design follows the current French standard for such equipment. CIT-Alcatel in France carried out the detailed design.*

## **I. INTRODUCTION**

The terminal transmission equipment (TTE) for the SG Undersea Cable System provides the vital interface between the inland telephone network and the undersea link. Interconnection to the domestic network is at the basic supergroup level; thus, the TTE consists of *frequency-di-*

vision multiplex and wideband line equipment (including a directional filter that provides a physical 4-wire to equivalent 4-wire conversion) (Fig. 1). The transmitting multiplex serves to frequency-translate fifty-plus basic supergroups, combining them to form what we call the "baseband." The receiving multiplex performs the inverse operation.

The wideband line equipment provides its customary functions of signal preemphasis and deemphasis, equalization, level adjustment, and the like. Following the conventional equivalent 4-wire undersea cable terminology, the terminal stations at opposite ends of the system are designated A and B. Low-band transmission in the A-to-B direction is at baseband frequencies directly. In the opposite direction, the high band is formed by one further stage of frequency translation of the baseband, which takes place in the wideband line equipment.

The principal system parameters influencing TTE design are summarized below:

- (i) Nominal frequency band (corresponding to 4000 3-kHz voice channels):
  - Low band 800 to 13,300 kHz,
  - High band 16,700 to 29,300 kHz.
- (ii) Possible extension to:
  - Low band 500 to 13,900 kHz,
  - High band 16,100 to 29,500\* kHz.
- (iii) Operation with either 3- or 4-kHz voice channels, or a combination of the two.
- (iv) Design load per channel:  $-13$  dBm0.
- (v) Terminal noise contribution (both stations): No more than 250 pW0p (24.5 dBnc0) in the worst channel, with the system fully loaded and with all transmission levels at their nominal values.

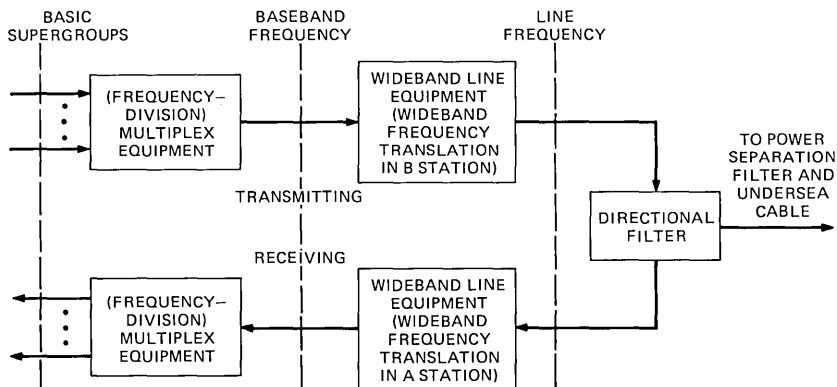


Fig. 1—Summary diagram of the SG terminal transmission equipment.

\* Experience gained with the first SG system installation, TAT-6, has led to an upward translation in the extended high band by about 500 kHz (Fig. 4b).

Of course, 3-kHz spaced channel operation is common on long-haul undersea cable routes. It has also been traditional that undersea system design loads be higher than those for similar inland carrier systems for, among other reasons, the potential application to them of speech concentrators such as TASI or CELTIC.

The reason for nominal and extended frequency bands is quite simple. During development, it was not possible for us to be sure of the exact transmission band that would ultimately be achieved. This depends on the degree to which repeater gain can be trimmed to match cable loss at the band edges, and on the degree of success of mop-up equalization in the ocean-block equalizers.<sup>1</sup> We chose to design for the extended bands to encompass the largest bandwidth that optimistically could be achieved, so that the TTE would never restrict channel capacity of the overall system.

Conceptually, we were guided in the design of the TTE for the SG system by two main principles:

- (i) The available frequency band should be used to the fullest.
- (ii) The failure of an active device should not cause a loss of service of more than the equivalent of one supergroup.

In addition to the capability of 3-kHz operation, the first principle resulted in a unique multiplex frequency allocation that, in turn, required development of new modulation equipment. The second principle, one of reliability, we achieved largely through automatic protection switching between duplicated equipments.

## II. FREQUENCY ALLOCATION

The frequency plan for the SG system was chosen primarily to achieve efficient use of the available transmission band and secondarily to minimize the degree to which standard multiplex equipment and techniques of other undersea and inland systems would have to be modified. For example, the ease with which new carrier frequencies could be produced was a factor in our plans. From the outset, our desire to achieve a high traffic-band efficiency factor (defined as the ratio of the actual frequency spectrum devoted to traffic to the total transmission band) forced us to reject standard CCITT\* or Bell System frequency plans developed for inland carrier systems of comparable or greater bandwidth than the SG baseband, e.g., 12- and 60-MHz CCITT international systems and the L4 and L5 systems.<sup>2,3</sup> The traffic-band efficiency factor for the 12- and 60-MHz terrestrial systems is 0.89 and 0.78, respectively, and

---

\* The International Telegraph and Telephone Consultative Committee.

that of the basic Bell System mastergroup itself is only 0.87, whereas that for the SG plan is greater than 0.95.\*

### 2.1 Baseband assignment

The SG baseband comprises six *hypergroups* (HG) numbered 1 through 6 in ascending frequency, as shown in Fig. 2. The term *hypergroup* is British Post Office (BPO) terminology that refers to an arbitrary number of supergroups<sup>†</sup> assembled in a contiguous frequency band. Hypergroup 1 is direct-formed by supergroup translating equipment (Fig. 3). Positions of the 14 supergroups are those of supergroups 3 through 16 of the standard CCITT 4-MHz system, or equivalently, those of the CCITT basic 15-supergroup assembly.<sup>4-6</sup> Hypergroups 2 to 6 each contain 10 supergroups and together occupy the band 4032 to 16,424 kHz. They are formed in two steps of frequency translation. First, a *basic hypergroup* is formed by supergroup translation (CCITT supergroups 4 through 13), and then by hypergroup translation (Figs. 3 and 2, respectively).

Note that all the carrier frequencies are odd multiples of 124 kHz, a desirable feature from the point of view of carrier generation. Thus, the conventional 8-kHz gap between supergroups within hypergroups, which permits through-supergroup connection, is preserved between hypergroups as well. One exception is the HG 1-HG 2 gap of 4 kHz, an offset

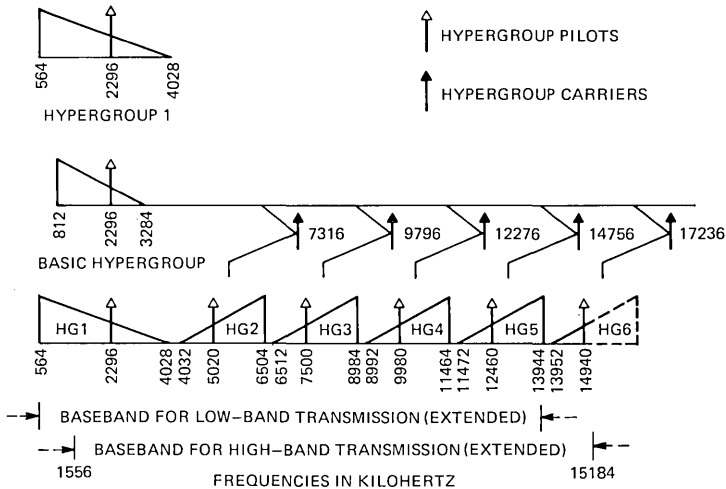


Fig. 2—Frequency allocation—SG basebands.

\* At present, the line-to-terminal cost ratio of terrestrial carrier systems relative to their undersea cousins naturally leads to frequency allocations that, while not optimum in traffic-band efficiency, nevertheless achieve an overall efficiency due to less severe terminal filtering needs which facilitate pilot monitoring, automatic gain regulation, and circuit distribution (e.g., blocking and reinserting of large bundles of voice circuits).

<sup>†</sup> Each supergroup corresponds to 60 4-kHz or 80 3-kHz voice channels.



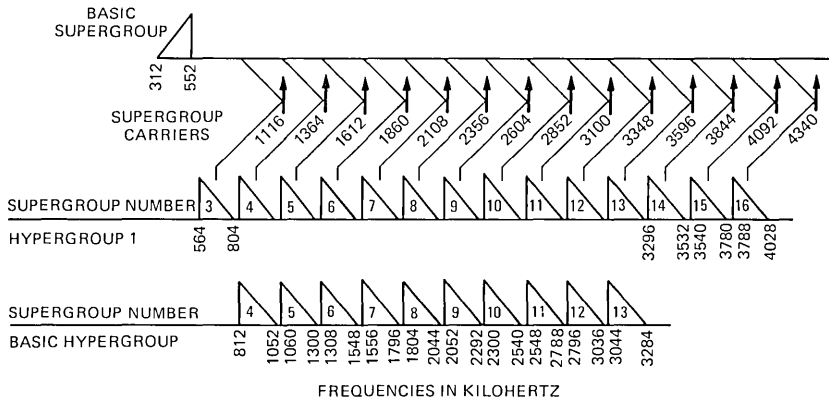


Fig. 3—Frequency allocation—basic hypergroup (and hypergroup 1).

needed to retain the 124-kHz integral multiple characteristic of hypergroup carriers. A secondary advantage of this choice is that all hypergroup carriers fall between voice channels for either 3- or 4-kHz spacing, thereby easing carrier leak requirements.

Several comments are in order concerning the makeup of hypergroups. First, we did not retain supergroup 3 in the basic hypergroup primarily to ease design complexity of, and reduce group-delay distortion caused by, the hypergroup modulator band filter, which must reject the carrier and upper sideband while passing the lower sideband. Next, we included supergroups 14 to 16 in HG 1 (but not in the basic hypergroup) to ease design of the HG 2 modulator band filter, which must reject the basic hypergroup band (because of leakage across the modulator) in addition to carrier and upper sideband. Furthermore, our choice of a 10-supergroup basic hypergroup limits to five the number of new designs of hypergroup translation units.

Although we have spoken of the SG baseband, one can, in fact, distinguish two slightly different spectra as evidenced in Fig. 2. The low-band baseband is simply hypergroups 1 through 5, whereas the high-band baseband includes hypergroups 2 through 5 plus part of hypergroups 1 (supergroups 7 through 16) and 6 (supergroups 9 through 13). The latter allows sufficient separation between the wideband-translation carrier frequency of 31,620 kHz and the upper edge of the high band at line frequency so that design of the associated modulator band filter is easily realizable. Note that this carrier is also an odd multiple of 124 kHz.

In summary, we believe that the SG frequency allocation is a good compromise between the objectives of efficient use of bandwidth and minimum development of new frequency-translating and carrier-generating equipment.

## 2.2 Order-wire and supervisory-tone band assignment

The order-wire and repeater supervisory-tone band assignments<sup>1</sup> are shown in Figs. 4a and 4b, for the low and high bands, respectively. One can see that both assignments fall within those of the multiplex, so that particular channels in hypergroup 1, supergroup 16, i.e., (1, 16) and (4, 5) in the low band and (1, 16) in the high band, cannot be used for commercial traffic.

## 2.3 Pilot assignment

A *hypergroup pilot* is inserted at the input of each transmitting hypergroup at a frequency of 2296 kHz, midway between supergroup 9 and 10, to facilitate measurement. (Line-frequency assignment of these pilots is given in Figs. 4a and 4b.) Due to its near-central location within each

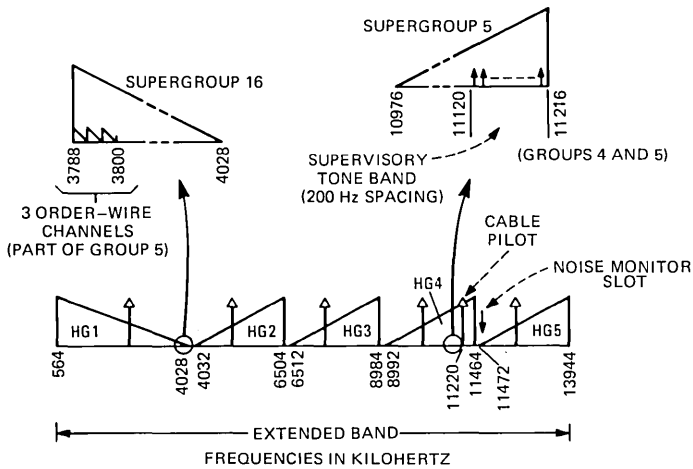


Fig. 4a—Frequency allocation—low band.

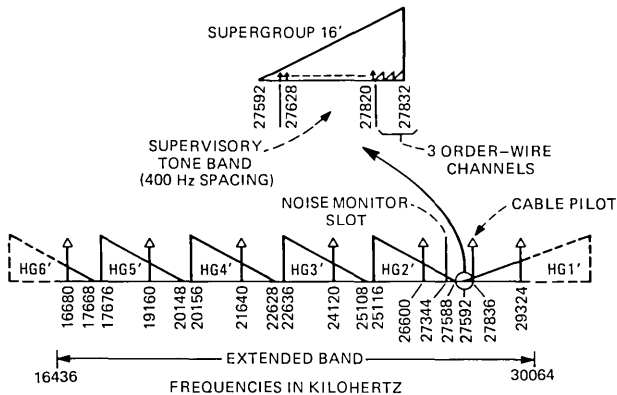


Fig. 4b—Frequency allocation—high band.

hypergroup, it should be representative of the overall transmission level of the hypergroup.

There are no separate assignment of *line* (or *system*) *pilots*, i.e., those which provide information about the behavior of the wideband link (wideband line plus undersea). Instead, the HG 2 and 5 pilots provide this function by being monitored at the input of the transmit and output of the receive wideband line equipment. This is illustrated in Fig. 5.

One additional pilot in each direction of transmission, the *cable pilot*, is inserted and measured as close as practical, from a transmission standpoint, to the undersea system to furnish information about the behavior of only this part of the wideband link. The cable-pilot frequency in the low and high bands was chosen to be near that of the supervisory tones and to fall between supergroups.

The power level of all pilots is  $-20$  dBm0.

### III. CONFIGURING THE TTE FOR RELIABLE OPERATION

#### 3.1 Reliability criterion

As mentioned before, the layout of the TTE is such that failure of an active component will not involve loss of more than the equivalent of one supergroup of traffic (80 3-kHz or 60 4-kHz channels). The object of this section is to examine the ramifications of this principle on the configuration of the TTE; in particular, the extent of equipment duplication and automatic changeover switching.

#### 3.2 Features common to transmit and receive

Generally speaking, the supergroup equipment itself (including supergroup signal limiters, modulators, and equalizers, all of which are discussed later) need not be duplicated to meet the above criterion. On the other hand, failure of a supergroup carrier would affect five or more supergroups. Thus, supergroup carrier generators are completely duplicated with automatic protection switching at the outputs for each in-

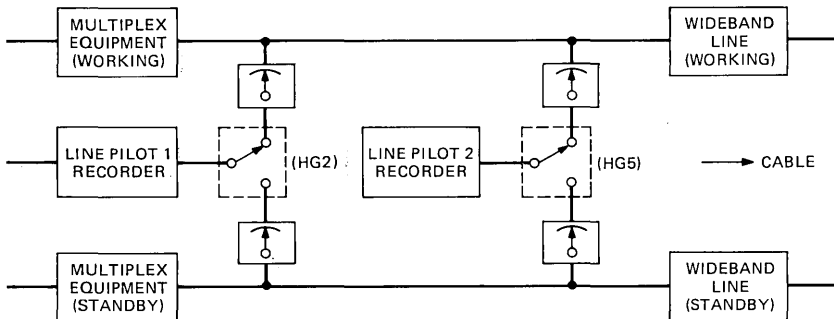


Fig. 5—Line-pilot monitoring (transmit and receive).

dividual carrier. Of course, duplicate sources of the master oscillator frequency of 124 kHz are required.

Referring to Fig. 6, we see that the transmission path between supergroup couplers\* and the directional filter is duplicated. In the transmitting direction, this involves hypergroup translation and wideband line equipment. The same is true in the receiving direction but with the addition of hypergroup regulators. The duplicated paths in each direction are called *Path I* and *Path II*. At any one time, the particular paths that connect the directional filter to the supergroup equipment are referred to as *working* and the others as *standby*. If a working path fails, the two are interchanged.

Naturally, hypergroup and wideband translation carrier generators are duplicated, and are referred to as *generator 1* and *generator 2*.† Connection to the translating equipment is not the same as to the supergroups, because hypergroup and wideband line equipment is itself duplicated and protected by automatic changeover switching. Duplicate generators for each hypergroup carrier can be connected to the transmission paths in the combinations shown in Table I by means of patch links.

The 2296-kHz hypergroup pilot supply is duplicated. Pilot supplies are connected to the transmission paths by means of patch links that allow combinations similar to those in Table I.

The directional filter unit (which includes the receiving path-splitting coupler) is passive but, because a failure here could affect the entire wideband path, we considered it prudent to provide a “built-in” spare which can be quickly interchanged manually for the working unit, albeit not without momentarily interrupting traffic.

### 3.3 Special transmitting features

Working and standby hypergroup pilots on the transmitting side are monitored at the output of the wideband line equipment just after the changeover switch but prior to the directional filter (Fig. 6). The changeover logic control recognizes pilot *failure* as a change in amplitude from nominal of between 2 and 3 dB. Failure of a working pilot initiates a path changeover provided there is not a concurrent standby pilot failure. Additionally, an alarm inhibit capability is provided on an individual hypergroup pilot basis which, if operated, removes that particular pilot from consideration by the changeover logic.

The cable pilot is introduced through a passive coupler after the transmit changeover switch but prior to the directional filter (Fig. 6),

---

\* The couplers themselves are passive and therefore not duplicated.

† Roman numerals I and II are reserved for the duplicated transmission paths protected by automatic changeover switching. All other duplicated equipment is designated 1 and 2.

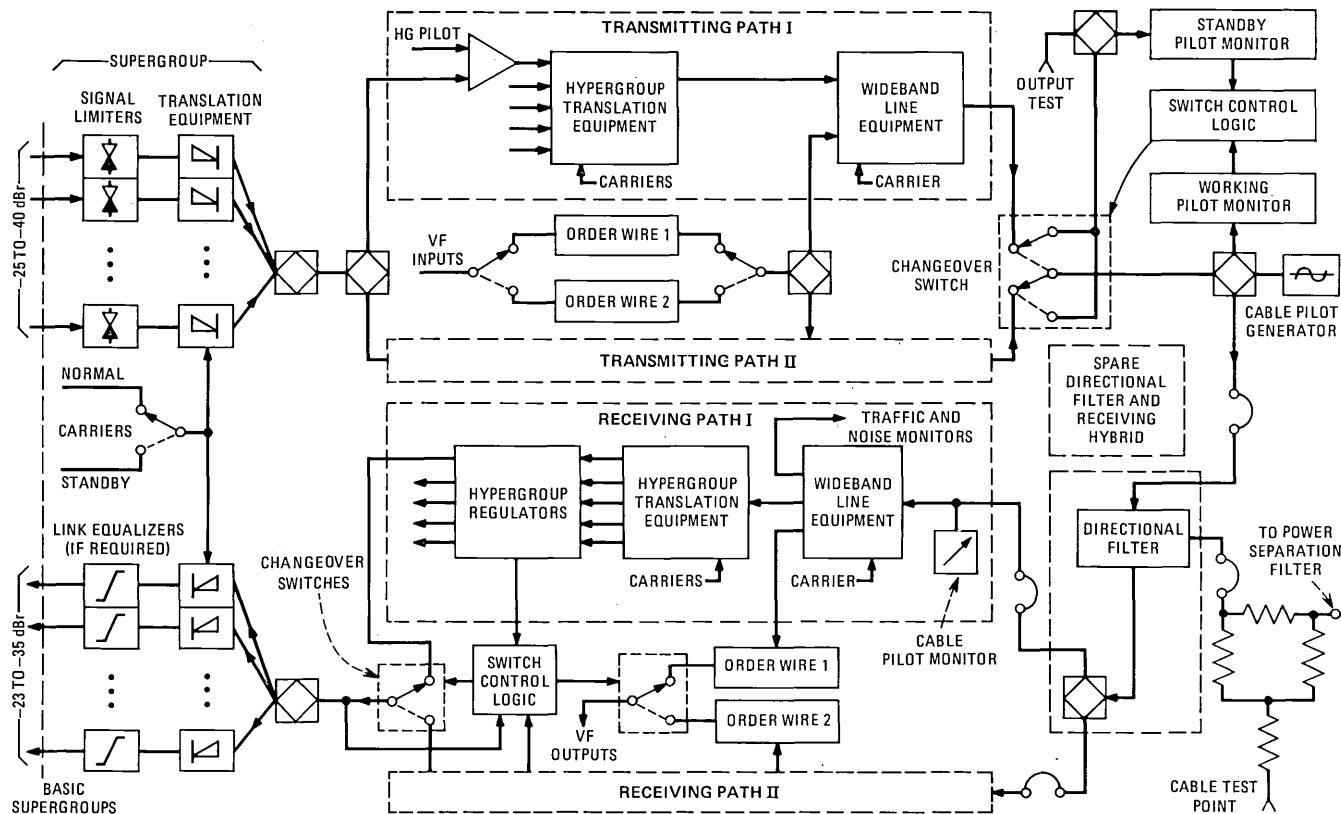


Fig. 6—Overall configuration of the SG terminal transmission equipment.

Table I

Combination No. 1 (normal operation)	Combination No. 2 (source and load paralleled)
Generator 1 → Path I Generator 2 → Path II	Generator 1 $\rightarrow$ Path I Generator 2 $\rightarrow$ Path II
Combination No. 3 (interchange of source)	Combination No. 4 (two loads from single source)
Generator 1 $\rightarrow$ Path I Generator 2 $\rightarrow$ Path II	Generator 1 $\rightarrow$ Path I Generator 2 $\rightarrow$ Path II

thereby assuring that its level is independent of all adjustments in the transmitting paths.

### 3.4 Special receiving features

In the receiving terminal, the cable pilot is monitored just after the directional filter and path splitting coupler so that its level is independent of receiving path adjustments.

Although there is a receive changeover switch for each hypergroup, all are activated simultaneously by the receive path-changeover-logic-and-control unit when it detects a fault affecting even one hypergroup. There are minor advantages to individual hypergroup changeover switch operation, but we felt they are more than counterbalanced by the complexity of maintenance that would result if some working hypergroups were on Path I while others were on Path II.

Inputs to the receiving changeover-logic-and-control unit are from five sources:

- (i) and (ii) Hypergroup pilot level at the output of Paths I and II regulators.
- (iii) and (iv) Gains of Paths I and II regulators.
- (v) Working hypergroup pilot levels just beyond the changeover switches.

Switching occurs for either of the following conditions:

- (i) At a changeover switch output, the absolute difference between measured and nominal pilot level becomes greater than 1 dB, whereas at the standby path regulator output the corresponding difference is less than 1 dB.
- (ii) The difference in gain of corresponding Path I-Path II regulators is more than about  $2\frac{1}{2}$  dB, in which case the path whose regulator is providing the smaller correction becomes the working path.

Just as for the transmitting changeover switches, the receiving switches themselves are not duplicated, but pilot monitoring beyond the switches measures their performance as well. Individual pilot-alarm-inhibit capability is also provided.

### 3.5 Final comment on TTE configuration

The preceding description of TTE duplication and changeover switch operation brings to light the high degree of interdependence of multiplex and line terminal equipment. This is in contrast with most inland systems where multiplex and line terminals constitute separate families of equipment having little in common except impedance and transmission level at their interface. The intimate character of the association is underscored by the lack of separate line pilots in the SG wideband equipment.

## IV. WIDEBAND LINE EQUIPMENT

The wideband line equipment (WLE) provides transmission between the multiplex and the terminal *power separation filter*.<sup>7</sup> Figure 7 is a simplified block diagram of the WLE. Aside from the conventional line functions of amplification, preemphasis, deemphasis, equalization, and the like, the SG WLE is designed to:

- (i) Monitor performance of the undersea link.
- (ii) Initiate changeover switching, in event of a failure, between duplicate terminal transmission paths.
- (iii) Protect the undersea repeaters from high-level signal overload.
- (iv) Provide adjustment capability to compensate for (a) that part of the shallow-water cable loss change with seasonal temperature, which is not equalized by temperature-controlled repeaters,<sup>1</sup> and (b) that part of transmission aging of the undersea link, which is not compensated for by shore-controlled equalizers.<sup>1</sup>

In some cases, accomplishing these functions provided us with interesting design problems that we had not encountered during development of terminals for earlier undersea systems.<sup>8,9</sup>

### 4.1 Amplitude and phase equality of duplicated paths

We have designed the changeover switching in such a way that maintenance switching (i.e., that which does not result from a transmission path failure) will not even momentarily disturb transmission more than a negligible amount.\* To appreciate how this is accomplished, refer to the schematic in Fig. 8. If the amplitude and phase of the signals on each path are equal, closing of contacts B1 and B2 has no effect. Subsequent opening of contacts A1 and A2 (in either order) will interchange paths and loads without disturbance.

To evaluate the influence of path amplitude and phase differences, consider the following. The ratio in decibels of power delivered to the load in two cases, (i) separate paths ( $P_0$ ) and (ii) parallel paths ( $P_1$ ), is

---

\* So-called hitless switching.

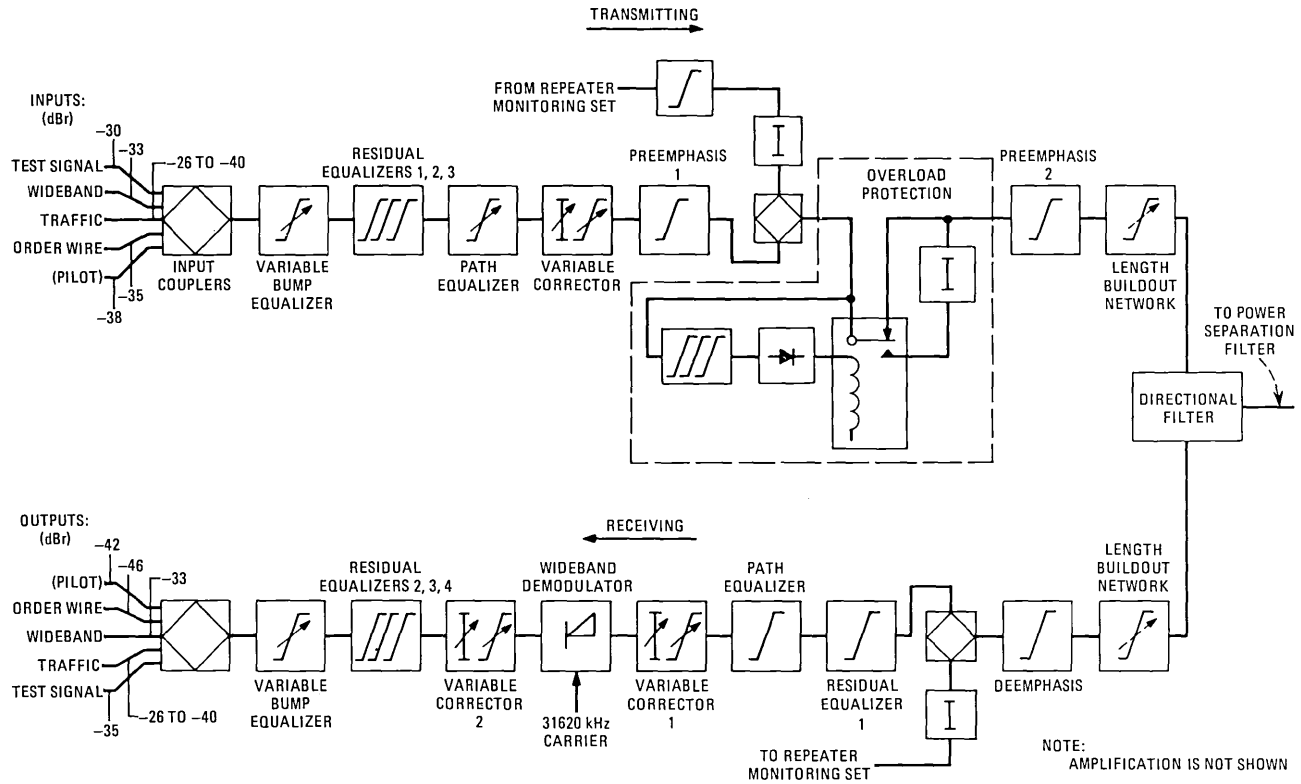


Fig. 7—Wideband line equipment-A station (B station is similar except frequency translation is in the transmitting line and only one preemphasis network is used).



$$e_1 = E_1 \cos \omega t$$

$$e_2 = kE_1 \cos(\omega t + \phi)$$

$$A_{dB} = 20 \log_{10} \frac{2}{\sqrt{1 + 2k \cos \phi + k^2}}$$

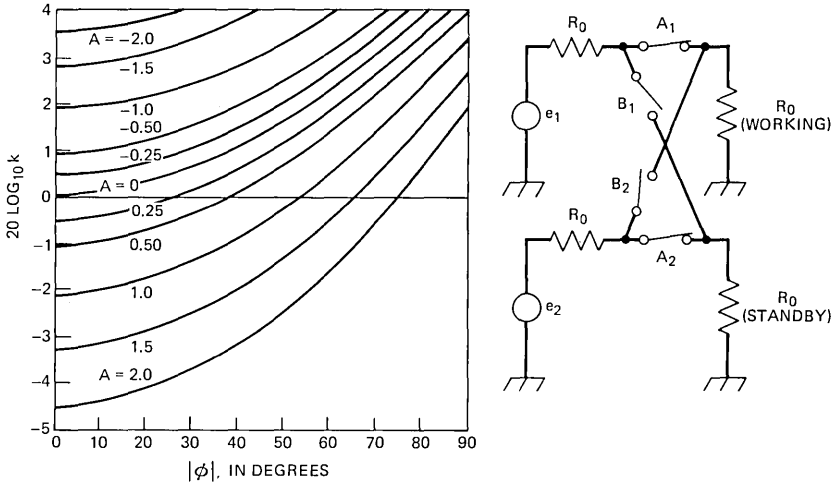


Fig. 8—Effect of path amplitude and phase differences on changeover switching.

$$A = 10 \log_{10} \frac{P_0}{P_1} = 20 \log_{10} \frac{2}{\sqrt{1 + 2k \cos \phi + k^2}},$$

where  $k$  and  $\phi$  are defined in Fig. 8. In that figure, contours of constant  $A$  are plotted as functions of  $k$  and  $\phi$ . One sees that, provided  $\phi$  is not too large, the change in magnitude at paralleling is less than that for complete transfer. For example, if  $|20 \log k| < 0.5$  dB and  $|\phi| < 30^\circ$ ,  $A$  is always less than about half a decibel. The phase disturbance at paralleling is

$$\tan^{-1} \frac{k \sin \phi}{1 + k \cos \phi},$$

and is always less than for complete transfer.

#### 4.2 Protecting repeaters from signal overload

The peaks of a sufficiently high signal voltage applied to an SG repeater can, in time, cause a change in current gain of the output transistor. We decided, therefore, to limit to a safe value the maximum signal that can be applied to the undersea link from the terminal. This function is accomplished by the *wideband overload protection unit*, shown schematically in Fig. 7. The wideband signal is monitored at the output of the last active circuitry in the transmitting line and shaped with an equalizer before it is amplified and measured by a pseudo-quadratic detector. Should the detected signal exceed a predetermined threshold, a high-loss pad is switched in series with the transmission path. The ideal

frequency weighting in the detection path would be one so that a change in spectral density\* of the signal at the input of the overload protection unit has the same effect on the mean power of the signal at the detector as it does at the output transistor in the highest level repeater in the link.

To avoid insertion of the pad for a momentary signal overload, the time constant of the detector is approximately 1 second. On the other hand, once the pad is inserted, it can only be reset manually.

We anticipate that operation of this unit will be extremely rare, because of the action of the supergroup limiters (described in Section 5.1.3), and probably due only to an equipment failure or adjustment error within the TTE itself. (Operation of the overload protection unit in the working transmitting line would, of course, cause changeover to the standby path.)

### **4.3 Pilot generation and measurement**

As explained in Section 2.3, hypergroup and cable pilots serve to monitor operation of the multiplex, line, and undersea links, to initiate automatic protection switching, and to control the gain of receiving hypergroup regulators.

In principle, hypergroup and cable-pilot generators are identical designs, i.e., a quartz oscillator generates a stable frequency that is amplified and clipped to assure level stability. The signal is then filtered to remove harmonics and other spurious energy that could disturb traffic. The generator output is monitored (displayed on a front-face meter) and fed to a test jack so it can be checked with external equipment. An alarm is initiated for changes from nominal of a sufficient amount.

Pilot measuring units are also similar. A narrow-band 2296-kHz quartz filter is located at the input of those units monitoring the basic hypergroup (and hypergroup 1) pilot, and is followed by amplification and detection. On the other hand, for those units monitoring hypergroup pilots at baseband frequencies (except HG 1); this circuitry is preceded by a demodulator whose carrier frequency was chosen to restore the pilot to 2296 kHz. For the cable-pilot measuring units, a demodulator is not used; instead, a narrow-band quartz filter at cable-pilot frequency (11220 and 27836 kHz in the low and high bands, respectively) precedes amplification and detection. For all units, the pilot level is displayed on a front-face meter. A test jack provides access for an independent check of pilot level, and an alarm is initiated for sufficiently large level changes from nominal.

---

\* Peak-to-mean-power ratio remaining constant.

#### 4.4 Traffic and noise monitors

A continuous indication of undersea system noise is furnished by a unit connected near the output of the receive wideband line equipment that measures noise in a frequency slot, which is about the bandwidth of a voice channel, and is located between two supergroups in the neighborhood of the supervisory-tone band. Refer to Figs. 4a and 4b. The measuring apparatus itself consists of a quartz filter centered at 4276 kHz (A terminal\*) and at 11,468 kHz (B terminal) followed by amplification and a pseudo-quadratic detector. Noise power is displayed on a meter whose scale is  $\pm 7$  dB. Preceding this apparatus in the measuring path is a variable attenuator of  $\pm 10$  dB in 1-dB steps. Fixed levels are such that a zero meter reading can correspond to noise in the range of about 28 to 48 dBm. An alarm is initiated if the measured noise power exceeds the nominal value (zero meter reading) by more than 5 dB.

Also connected near the receive wideband line output is a traffic measuring unit similar to the noise measuring unit except that it is broadband (because it measures the complete traffic band) and is not alarmed. An attenuator adjustment on the front face (0 to 15 dB in 5-dB steps) permits the zero meter reading to correspond to 8, 13, 18, or 23 dBm. (4200 channels at  $-13$  dBm/channel corresponds to a broadband power per band of 23.2 dBm.)

Traffic as well as noise measurements are necessary to monitor an analog transmission system such as SG whose signal-to-noise performance is intermodulation rather than overload limited.

#### 4.5 Alarm and maintenance features

As we have seen, behavior of the transmission link is monitored by means of pilot, noise, and traffic measurements. Pilot generating and measuring apparatus and noise measuring apparatus give visual indication of variations from nominal and initiate alarms when variations exceed specific limits. Upon initiation, alarm lamps on the front face of a unit and at the top of the bay containing that unit are lit, and the alarm is extended to the station alarm equipment which is expected to provide audio as well as visual indications. In this way, a technician is directed to the source of the trouble. A two-position switch on the face plate of the unit, when in the *cutoff* position, inhibits the station alarm as long as the source of the alarm remains. When the trouble is cleared, the alarm is reactivated until the switch is returned to the *normal* position. Finally, an output from pilot, traffic, and noise measuring units can be connected to a chart recorder (12 recorders are provided in a separate bay). This arrangement permits a continuous record to be obtained, when and if it is desired.

---

\* The A station noise monitor is positioned after wideband translation to baseband.

#### 4.6 Principle of primary frequency comparison

From the point of view of carrier generation, an undersea cable link often acts as an interface between national frequency standards. To insure that the frequency offset between terminals is within performance limits (no more than 2 parts in  $10^8$  for an SG link), it is necessary to compare master oscillator frequencies (primary frequency supplies). Comparison between the two terminals is accomplished in the following manner. Let us designate:

$f_g$ —primary frequency (nominally 124 kHz) (from which all TTE carrier frequencies are derived) at the A terminal.

$f'_g$ —Similarly at the B terminal.

$N_1 f_g, N_2 f_g$ —Carrier frequency for hypergroups 2 and 5, respectively, at the A terminal ( $N_1 = 59, N_2 = 119$ ).

$N_1 f'_g, N_2 f'_g$ —Similarly for the B terminal.

$f_1$ —Basic hypergroup pilot frequency (nominally 2296 kHz) at the A terminal.

$f'_1$ —Similarly for the B terminal.

$f_t$ —Wide-band translation carrier (nominally 31,620 kHz) at the A terminal.

$f'_t$ —similarly at the B terminal.

The A terminal transmits the HG 2 and 5 pilots at line frequencies of  $(N_1 f_g - f_1)$  and  $(N_2 f_g - f_1)$ , respectively. At the B terminal, each is demodulated by the corresponding hypergroup carriers,  $N_1 f'_g$  and  $N_2 f'_g$  to obtain  $f_1 + N_1(f'_g - f_g)$  and  $f_1 + N_2(f'_g - f_g)$ . The frequency difference between these recovered pilots,  $(N_2 - N_1)(f'_g - f_g)$ , is displayed directly on an analog meter (pointer movement proportional to the frequency difference) at the B terminal. Additionally, an A terminal reference frequency is made available in the B terminal, which is the difference frequency between received HG 2 and 5 pilots at line frequency, i.e.,  $(N_2 f_g - f_1) - (N_1 f_g - f_1) = (N_2 - N_1) f_g$ , nominally 7440 kHz.

A similar arrangement provides a frequency-difference display and a B terminal reference signal in the A terminal, even though additional frequency translations by  $f_t$  and  $f'_t$  are involved.

#### 4.7 Equalizers

We can make the following distinctions with regard to wideband line equalizers:

- (i) Fixed equalizers meant to achieve the best overall signal-to-noise ratio for an ideal system in the sense of one with no undersea misalignment.
- (ii) Equalizer networks designed and fabricated on site during commissioning<sup>10</sup> to compensate for actual misalignment measured after completion of installation.
- (iii) Adjustable equalizers which, during commissioning, can be used

to achieve the best overall signal-to-noise ratio for an actual link with undersea misalignment, and, after commissioning, can be used to compensate for transmission changes resulting, for example, from temperature changes on the continental shelves and, in conjunction with the shore-controlled equalizers,<sup>1</sup> from cable aging.

The terminal equalization plan is discussed in more detail in a companion article.<sup>10</sup>

#### **4.7.1 Fixed equalizers**

In the category of fixed equalizers are the *line buildout*, *preemphasis*, and *deemphasis networks*, and the *path equalizers*. The line buildout networks in the transmit and receive paths are fixed for each terminal in that the effective electrical length to the first repeater from the terminal is equal to three-quarters of the loss of a nominal repeater section. In this way, flexibility is maintained in placement of the first repeater, while at the same time reasonably standard terminal equalization is preserved.

Path equalizers compensate for small misalignment unavoidably introduced in the wideband path, by interconnecting cabling and the like, and differences between nominally identical paths.

Given the nominal line equipment, the preemphasis network (transmit) provides the calculated loss shape to optimize overall s/n as mentioned in Section 4.7, item (i), above. The deemphasis network (receive) compensates for the preemphasis loss shape as well as for that of the last section of undersea cable (which is not compensated for by the gain of a repeater).

#### **4.7.2 Equalizers fabricated during commissioning**

To achieve final alignment of an SG link in a minimum of time after installation, we developed a *residual equalizer unit*. In a single unit, up to five bridged-T<sup>11</sup> networks can be mounted and connected in tandem. The frequency-loss characteristic of each network can be a bump, dip, or slope of wide ranging selectivities. Several such units are used in both transmit and receive paths (Fig. 7). A kit of components (inductors, capacitors, and resistors) covering specific ranges of values, as well as other hardware, is supplied with the WLE. After link misalignment has been measured, bridged-T networks are designed (with the aid of a computer) and constructed on site, and inserted into the wideband line.

### 4.7.3 Adjustable equalizers

Both broad- and fine-grain equalization capability is provided by the front-panel-adjustable networks which facilitate initial performance optimization and subsequent realignment following undersea loss variations. Broadband adjustment at line frequency is provided in both the transmit and receive paths by a so-called *variable corrector* that contains four types of circuits: slope, curvature, flat, and  $\sqrt{f}$ . At the frequency of maximum excursion (e.g., the peak of the curvature shape), each is adjustable in 0.3-dB steps over a range of  $\pm 3$  dB (slope and curvature) or  $\pm 6$  dB (flat and  $\sqrt{f}$ ). A second type of variable corrector, used only in the receive path, provides additional flat and  $\sqrt{f}$  adjustable gain range.

Among other functions, the variable correctors must be able to compensate for certain fault conditions in the undersea link, i.e., those whose effect on transmission is not so severe that service cannot be maintained, albeit at reduced performance, until repair operations commence.

A *variable bump equalizer*<sup>12</sup> permits narrow-band adjustment in the vicinity of a series of discrete baseband frequencies related by geometric progression. Selectivity is such that adjustment at one of these frequencies involves negligible change at adjacent ones. Because of the slightly different basebands, 16 bumps are available in the low band, but only 12 in the high-band direction of transmission.

### 4.8 Order-wire facilities

The line terminal is equipped with three order-wire circuits, each terminated at voice frequency with a unit permitting two- or four-wire operation and signaling. The frequency-translation circuitry is distinct from the regular multiplex equipment. Each channel undergoes translation to 24 to 28 kHz, as in the French Post Office (PTT) Type 70 12-channel equipment,<sup>13</sup> before the three are contiguously assembled at 60 to 72 kHz, the bottom quarter of the standard group baseband. The final two stages of translation correspond to placement in group 5 of supergroup 16 (see Figs. 4a and 4b).

The order-wire equipment is duplicated; in the transmit direction, either equipment can be connected by a manual switch to the transmitting paths. In the receiving direction, order-wire signals are selected from the working path through an automatic switch controlled by the receive changeover logic. See Fig. 6.

One of the three channels is equipped as a local order wire (i.e., for exclusive use between terminals), with an operator panel containing headset jacks plus ring and call-cutoff pushbuttons.

## V. MULTIPLEX EQUIPMENT

The multiplex portion of the TTE is located between supergroup distribution frames and the wideband line equipment (Figs. 1 and 6). It includes supergroup and hypergroup translating equipment (STE and HTE) with the associated carrier generators, hypergroup regulators, supergroup limiters (transmit), and supergroup equalizers (receive). Typically, this circuitry constitutes a link between domestic inland facilities (at basic supergroup) and the wideband line equipment (at SG system baseband).

Design of the multiplex equipment allows it to operate with 3- or 4-kHz spaced channels, with a per-channel load of  $-13$  dBm0 in either case.

The supergroup and hypergroup frequency assignments have already been discussed in Section II. Refer to Figs. 2 and 3.

### 5.1 Supergroup equipment

#### 5.1.1 Frequency translation

Supergroup translation equipment is derived from standard PTT domestic equipment,<sup>14</sup> which already conforms to CCITT recommendations,<sup>6</sup> but special care was given to reduce carrier leaks. Unfortunately, supergroup carrier frequencies, which are multiples of 4 kHz, do not necessarily fall between channels when operating with 3 kHz spacing as they do with the more conventional 4-kHz spacing. The disturbance level of an ensemble of spurious tones must be less than  $-65$  dBm0/channel, so we felt it prudent to hold the power of a single spurious frequency to no higher than  $-70$  dBm0.

Performance requirements for the supergroup translating equipment are summarized below:

- (i) Carrier-leak,  $\leq -70$  dBm0 transmitting,  $\leq -40$  dBm0 receiving.\*
- (ii) Thermal and intermodulation noise (for  $+6.0$  dBm0/supergroup loading),  $\leq 30$  pW0p ( $15.3$  dBmnc0) transmitting or receiving.
- (iii) Return loss at all ports,  $\geq 25$  dB.
- (iv) Crosstalk ratio (single frequency)  $\geq 85$  dB.

#### 5.1.2 Carrier generation

The supergroup carrier generating equipment is of conventional design, a harmonic generator (fed from a 124-kHz master oscillator) driving a parallel string of LC bandpass filters, each selecting the appropriate harmonic for a particular supergroup, followed by a gain-regulated drive amplifier. Suppression of unwanted carrier frequencies at each output is greater than 80 dB. As mentioned in Section 3.2, the supergroup carrier

---

\* Receive carrier leaks fall outside the transmission band.

generating equipment is duplicated, with a changeover switch at the outputs for each carrier. Signal detection permits automatic changeover operation and alarm initiation in case of failure in the working equipment.

### 5.1.3 Supergroup signal limiters

Application of sufficiently high-powered signals to analog transmission systems will cause excessive intermodulation noise<sup>15</sup> that interferes with traffic and, in a severe case, causes overload which can result in the loss of all traffic. To prevent this situation from occurring on the SG system, we decided to equip each input of the transmitting STE with a signal limiter (Fig. 6). The limiter is transparent (fixed attenuation) to signals in the normal operating range. Should the applied signal exceed preset amplitude limits, however, a controlled amount of attenuation is introduced in a variable loss network in the signal path.

Two monitoring circuits are used to control loss insertion, (i) a peak level monitor, and (ii) a mean-power level monitor. Refer to Fig. 9. Response of the peak monitor is relatively fast but consistent with maintaining within acceptable limits the generation of unwanted wideband energy. In practice, operation and restoration times of about 1 and 5 ms, respectively, are used. Response time of the mean-power monitor is, on the average, much slower than this, but depends on the magnitude of its overload, i.e., the higher the overload the shorter the response time.

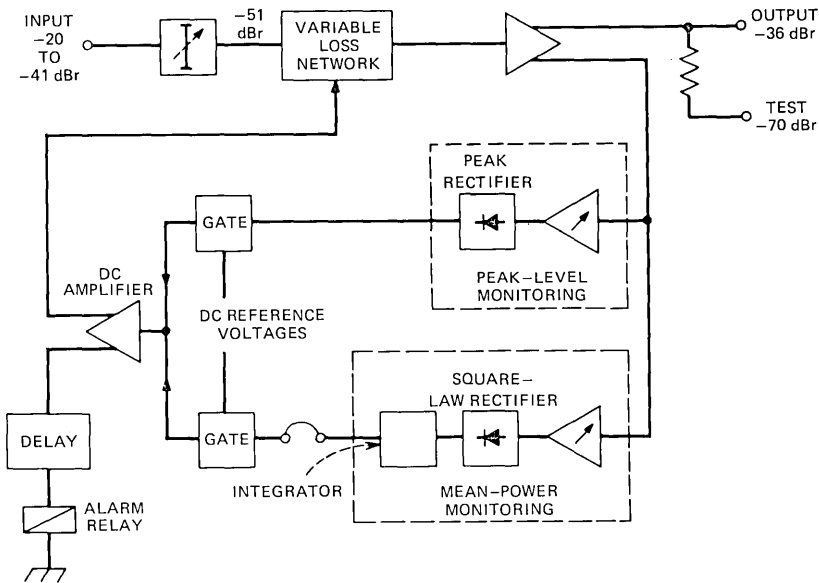


Fig. 9—Supergroup signal limiter.



To allow for differing types of traffic and the actual performance of the undersea link, the operating point of the peak and mean-power limiter circuits are separately adjustable by means of attenuators in each amplifier/detector input. The dc output of each monitor is compared with a reference voltage. When exceeded, the difference voltage is applied (after amplification) to the variable loss network; the larger the difference voltage, the greater the loss increase. A second output from the dc-amplifier energizes an alarm indicative of limiter operation, but a delay network suppresses the alarm if the limiter is activated only momentarily.

An input attenuator to the limiter unit is adjusted at the time of installation for differences among administrations with regard to transmission level at the supergroup input.

The supergroup signal limiter used in the SG terminal is a slight modification of the British Post Office (BPO) limiter<sup>15</sup> as manufactured by GEC, Ltd, and is constructed under SOTELEC 70 equipment practice to conform to the remaining TTE equipment manufactured by CIT-Alcatel of France.

#### **5.1.4 Narrow-band-elimination filters**

To assure a clear slot between particular supergroups for subsequent insertion of hypergroup and cable pilots, and to facilitate undersea noise monitoring, narrow-band-elimination filters centered at 308- and 556-kHz are inserted between signal limiter and modulator in certain transmitting supergroups, and between demodulator and equalizer in the corresponding receiving supergroups.

#### **5.1.5 Supergroup link equalizers**

Although the primary means of compensating for undersea misalignment in the terminal are the residual equalizers in the WLE, we decided nevertheless to have available for use a supergroup-link equalization capability if needed to satisfy the CCITT recommendation regarding amplitude distortion,<sup>16</sup> viz., no greater than  $\pm 1.5$  dB relative to a midband frequency which itself must be  $\pm 0.1$  dB of nominal. When used, an equalizer is placed after the supergroup demodulator as shown in Fig. 6.

A simplified circuit diagram of the equalizer is given in Fig. 10. It is essentially an amplifier whose gain in the 312- to 552-kHz band is determined by damped resonant R-L-C circuits inserted as shunt elements in the feedback network. Up to five such circuits per amplifier can be used. Just as for the residual wideband line equalizer, a specific kit of components is provided for on-site construction, during commissioning, of the feedback and other gain controlling elements.

A sophisticated computer program is used to determine the number

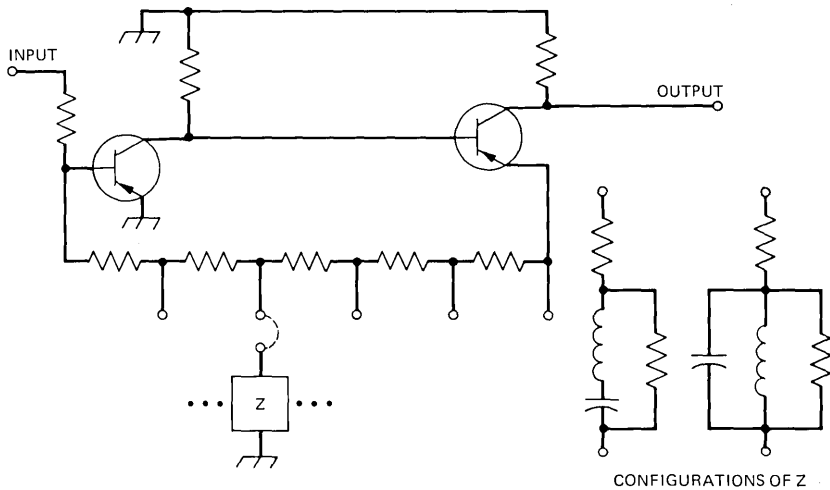


Fig. 10—Supergroup-link equalizer.

and configuration of the feedback circuits and the value of all variable components. The program uses an iterative trial-and-error process which continues until the computed link gain after equalization is within a specified tolerance. If equalization proves particularly difficult, e.g., for those supergroups near the edge of the wideband, a second amplifier can be placed in tandem with the first.

## 5.2 Hypergroup equipment

### 5.2.1 Frequency translation

A new design of hypergroup translating equipment is justified for use with undersea systems to achieve high traffic-band efficiency. Moreover, the tight phase and amplitude difference constraints made the new design an interesting one.

Most subassemblies of the HTE are of conventional design. Negative feedback amplifiers are made up of transistor pairs, the modulators use fast diodes in a ring configuration between ferrite core transformers, and the filters are LC type using ferrite inductors and mica capacitors. Solder-adjustable resistive pads permit level alignment. Coupling of the hypergroups is at a low input impedance amplifier on the transmit side and at a low output impedance amplifier on the receive side.

A departure from conventional practice was the addition of a series LC circuit at the input of each carrier amplifier. Tuning the capacitor permits adjustment of carrier phase over a sufficient range to compensate for phase differences between duplicate HTE paths for each hypergroup.

Performance requirements for the hypergroup translating equipment are summarized below:

- (i) Carrier leak,  $\leq -55$  dBm0 at transmitting,  $\leq -40$  dBm0 at receiving.
- (ii) Thermal and intermodulation noise (for +16.0 dBm0/hypergroup loading),  $\leq 20$  pW0p (13.5 dBm0) transmitting or receiving.
- (iii) Return loss at all ports  $\geq 25$  dB.
- (iv) Crosstalk ratio (single frequency)  $\geq 85$  dB.

### 5.2.2 Carrier generation

Design of the hypergroup (and wideband) carrier generating equipment was particularly challenging. The conventional scheme of harmonic generator followed by selective filters was not capable of producing sufficient carrier purity because the ratio of carrier frequency to master oscillator frequency is so large. (In the extreme case of the wideband carrier, the ratio is 255.) Furthermore, it was necessary to maintain the phase difference between corresponding carriers from the duplicated generators to within a few degrees to be consistent with hitless change-over switching between transmission paths as well as hitless manual patching at the duplicated generator outputs, whose combinations are illustrated in Table I.

The arrangement chosen to do the job is shown in Fig. 11 in block form. Notice the harmonic-generator, selective-filter combination is still present, but the desired harmonic of 124 kHz is only used to phase-lock

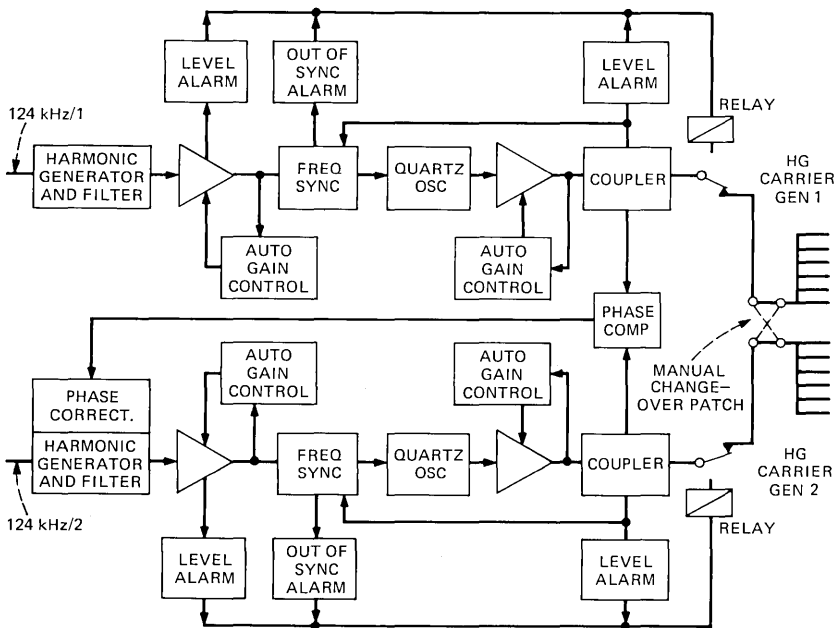


Fig. 11—Hypergroup carrier generation.

a quartz oscillator which is the actual carrier source. The necessary carrier purity is achieved by means of a first-order low-pass filter within the phase-locked loop whose cutoff frequency is only a few Hertz (except during capture). This arrangement produces, in effect, an extremely narrow-band-pass filtering action at the carrier frequency.

A phase comparator monitors the difference between corresponding generators and controls a corrector which automatically compensates phase deviations.

Performance requirements for the hypergroup (and wideband) carrier generating equipment are summarized below.

- (i) Frequency stability of the master oscillator is preserved.
- (ii) Output level stability:  $\pm 1$  dB.
- (iii) Carrier-to-noise ratio: at least 100 dB in 3-kHz band.
- (iv) Phase difference between duplicate generators:  $< 5$  degrees.

### **5.2.3 Hypergroup regulators**

The hypergroup regulator is a conventional design, i.e., an amplifier whose gain is pilot-controlled. A narrow-band quartz filter in the regulation loop extracts the hypergroup pilot from the traffic band at the amplifier output. This signal is then amplified, rectified, and compared to a dc reference voltage. The resulting difference signal controls the temperature of a thermistor located in the feedback path of the amplifier. The regulator has a compression ratio greater than 10 over an input range of  $\pm 2.5$  dB about its nominal gain.

Lamps on the front panel of the unit indicate when regulation exceeds  $\pm 1$  dB and  $\pm 3.5$  dB, and the latter can be transferred to the station alarm, as is the loss-of-pilot alarm which is initiated if the amount of regulation exceeds 7 dB. Input and output test points are also provided on the front panel.

## **VI. MECHANICAL ARRANGEMENT**

The SG system terminal transmission equipment is produced under a mechanical specification standardized in France under the name SO-TELEC 70,<sup>17</sup> whose basic elements are the *frame*, a simple mechanical support for *shelves* which contain a number of plug-in *units*. This total arrangement constitutes a *bay*. Units are provided with a front face plate on which are located labeling, test points, meters and other indicators, and in-service adjustment facilities. The rear face supports a connector that mates with its shelf-mounted partner. Mechanical locking is assured either by the connectors themselves or by a screw on the face plate. All shelves are the same width and depth, but their height can be a multiple of a modular unit of 44.5 mm.

Interconnection of units within a shelf (and occasionally between shelves) is done at the rear. Input and output access to a shelf is through vertical terminal strips, one on each front side of the shelf.

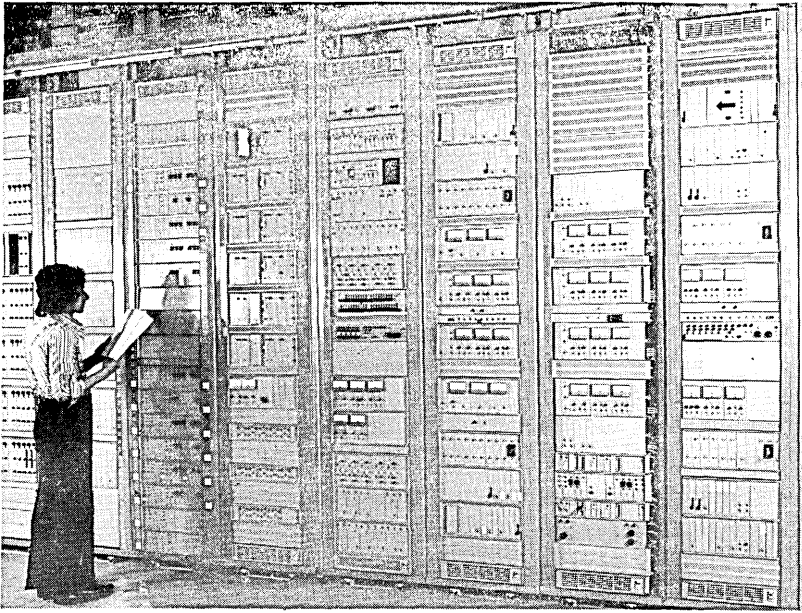


Fig. 12—Typical bay lineup of SG terminal transmission equipment.

A frame supports the shelves, and is in turn held to a base fixed to the floor. Wiring between shelves generally follows along the inside of the vertical frames and connects to the terminal strips.

A typical bay line-up for a terminal is pictured in Fig. 12. Although variations from this bay layout are possible, one must be careful to limit length differences of many intra-bay cabling runs in order to preserve phase equality of duplicate paths. The high degree of functional interdependence of line and multiplex terminal equipment dictates that they be physically close.

## VII. CONCLUSIONS

Achieving and maintaining maximum use of the undersea link have been our prime objectives from conception through production of the SG terminal transmission equipment. Accomplishing these ambitious objectives has led in some instances to complex designs whose development has been challenging because of, on the one hand, technological difficulties associated with the relatively high frequencies used (compared to earlier undersea system designs), and on the other the multiplicity and diversity of required functions. In four years it has been necessary to plan for and then design, develop, and produce no fewer than 263 different types of units. Undertaking the work in this interval constituted a wager that could only be won by exerting an all-out effort.

Everyone who has participated in this task confidently believes that the SG terminal transmission equipment will render all the service we have the right to expect from it.

### VIII. ACKNOWLEDGMENTS

Many individuals from organizations on both sides of the Atlantic were involved in TTE development from planning through installation as part of the first SG system implementation, TAT-6. Representatives from the Network Planning Department of the British Post Office Telecommunications Headquarters, the National Center for Telecommunications Studies and the Submarine Branch of the French Post Office, the Ocean Cables group of the Long Lines Department, American Telephone and Telegraph Company, and the Undersea Systems Department of Bell Laboratories helped guide development, but the lion's share of the work was carried out most commendably by members of Compagnie Industrielle des Télécommunications (CIT-Alcatel) in France.

### REFERENCES

1. C. D. Anderson, W. E. Hower, J. J. Kassig, V. M. Krygowski, R. L. Lynch, G. A. Reinold, and P. A. Yeisley, "SG Undersea Cable System: Repeater and Equalizer Design and Manufacture," *B.S.T.J.*, this issue, pp. 2355-2402.
2. F. H. Blecher, R. C. Boyd, F. J. Hallenbeck, and F. J. Herr, "The L-4 Coaxial Systems," *B.S.T.J.*, 48, No. 4 (April 1969), pp. 821-839.
3. F. C. Kelcourse and F. J. Herr, "L5 System: Overall Description and System Design," *B.S.T.J.*, 53, No. 10 (December 1974), pp. 1901-1933.
4. Recommendation G338, "4-MHz Valve Type Systems on Standardized 2.6/9.5 mm Coaxial Cable Pairs," Volume III.1 of CCITT Green Book.
5. Recommendation G343, "4-MHz Systems on Standardized 2.1/4.4 mm Coaxial Cable Pairs," Volume III.1 of CCITT Green Book.
6. Recommendation G233, "Recommendations Concerning Translating Equipments," Volume III.1 of CCITT Green Book.
7. E. T. Calkin, I. Golioto, W. J. Schatz, R. E. Schroeder, D. S. Shull, "SG Undersea Cable System: Undersea System Power," *B.S.T.J.*, this issue, pp. 2497-2522.
8. R. L. Lynch, J. L. Thomas, and C. A. Von Roesgen, "SF System: Shore Terminal Facilities and Fault Location," *B.S.T.J.*, 19, No. 5 (May-June 1970), pp. 721-748.
9. A. Bianchi, M. Dubois, R. Salvador, and H. Soulier, "La Liaison Sous-Marine Marseille-Alger II," *L'Echo des Recherches*, July 1973.
10. D. N. Harper, B. O. Larson, and M. Laurette, "SG Undersea Cable System: Commissioning: Final System Alignment and Evaluation," *B.S.T.J.*, this issue, pp. 2547-2564.
11. O. J. Zobel, "Distortion Correction in Electric Circuits with Constant Resistance Recurrent Networks," *B.S.T.J.*, July 1928, pp. 438-534.
12. J. Oswald and C. Chalhoub, "L'Égalisation," *Câbles et Transmission Ann.*, 16, No. 3 (July 1962).
13. G. Duval, J. Grollemund, and J. C. Duval, "Organes Fonctionnels de Ligne Avec Appel à Fréquence Zéro," *Câbles et Transmission Ann.*, 25, No. 4 (October 1971).
14. G. Laguerie, M. Louboutin, and M. Knapp-Ziller, "Modulation de Groupe Secondaire, etc.," *Câbles et Transmission Ann.*, 25, No. 4 (October 1971).
15. N. P. McKay, "Wideband Signal-Limiters," *P.O.E.E.J.*, 62, Part 4, January, 1970.
16. Recommendation M46, "Bringing International Group, Supergroup, etc., Links into Service," Volume IV.1 of CCITT Green Book.
17. G. Laguerie, M. Lagarde, and J. Menu, "Structure Mécanique du Matériel SOTELEC 70," *Câbles et Transmission Ann.*, 25, No. 4 (October 1971).

## **SG Undersea Cable System:**

# **Undersea System Power**

By E. T. CALKIN, I. GOLIOTO, W. J. SCHATZ, R. E. SCHROEDER,  
and D. S. SHULL

(Manuscript received July 21, 1977)

*The power-feed equipment for the SG cable system is of the type that regulates the output current and limits the output voltage. It energizes the serially connected repeaters in the TAT-6 undersea system. This paper describes the power-feed equipment in general terms and, in more detail, several new power techniques. These new techniques include inductive-input inverters in the main power train, pulse-position-modulation in the control and monitoring circuits, precise digital metering of output current and voltage, vacuum switch elements in the transfer switch, and special new components and design concepts in the power separation filter needed to achieve SG-wide-band-transmission objectives in the presence of the high, TAT-6, power-feed voltages.*

## **I. INTRODUCTION**

The SG power-feed equipment is similar in system configuration to that which powers the SD<sup>1</sup> and SF<sup>2</sup> undersea cable systems previously developed and installed by the Bell System. As examples: (i) power-feed redundancy is achieved by connecting two load-sharing, independent, direct-current sources in series, with provision for the automatic assumption of the full load by the survivor should one current source fail, (ii) the cable is powered at each end with opposite polarities and a sea-ground power return, and (iii) the power supplies at both ends operate

as current sources with their maximum output voltages restricted to be less than the voltage standoff capabilities of the repeaters.

Despite the conceptual similarities among the SD, SF, and SG power-feed systems, the techniques used to realize the system features have changed as the performance requirements have become successively more stringent and new circuit and physical design technologies have become available, or have been invented, to meet the performance requirements. Representative SG requirements are summarized in Table I.

In this paper, we describe the SG power-feed system as applied to TAT-6, emphasizing the following new circuit and physical design features:

- (i) Inductive-input inverters in the power stages of the main power train.
- (ii) Pulse-position-modulation in the control and monitoring circuits.

Table I — Representative SG power-feed performance requirements for TAT-6

Output current:	
Nominal	657.00 mA
Set point resolution	$\pm 0.10$ mA ( $\pm 0.015\%$ )
Variation within 24 hours	$\pm 0.33$ mA ( $\pm 0.05\%$ )
Variation resulting from a $\pm 1000$ -V load change	$\pm 3.30$ mA ( $\pm 0.5\%$ )
Variation resulting from the failure of one of the two converters	$\pm 3.30$ mA ( $\pm 0.5\%$ )
Output voltage:	
Nominal voltage	5200 V/station
Maximum voltage	7500 V/station*
Tolerable earth potential	2300 V/station*
Shutdowns:	
Current	+6% of nominal current (circuit duplicated)
Voltage	9250 $\pm$ 750 V (static) 10800 V, maximum (dynamic)
Alarms:	
Cable current	$\pm 1\%$ (minor), $\pm 3\%$ (major), fixed
Cable voltage	$\pm 5\%$ (minor), $\pm 15\%$ (major), adjustable to bracket the cable voltage
Noise:	
Inverter harmonic tones	$< 0.17$ $\mu$ V in any 3-kHz band from 0.3 MHz to 30 MHz
Impulse (signal transmission path)	Maximum of one pop per 15-min period that exceeds $-10$ dBmO in any 48-kHz channel (requirement of the entire shore station including the power separation filter)
Power separation filter transmission requirement:	
Return loss	$\geq 20$ dB, 0.5 to 30 MHz

\* In normal operation, the voltage-limiting-inception level would be set approximately 1000 V above the zero-earth-potential operating level, e.g., at 6200 V in TAT-6 stations. Hence, a readjustment is necessary to take advantage of the total voltage capability of the power supply.



- (iii) Precise, digital metering of the current and voltage in the high-voltage output circuits.
- (iv) Vacuum switches in the "hot transfer" switch circuits and vacuum relays in the wideband, signal-transmission path of the shore-station power separation filter.
- (v) New, high-voltage, wideband, signal-transmission components and a low-pass, skin-effect filter in the power separation filter.
- (vi) Physical design techniques to control radiated and conducted electromagnetic interference (EMI) within and from the power supply and into the power separation filter.

## II. GENERAL DESCRIPTION OF THE POWER-FEED SYSTEM

Figure 1 displays the power-feed and signal transmission connections to the TAT-6 cable. The A terminal (Green Hill, Rhode Island) power supply provides a current of 657 mA at a nominal, positive voltage of 5200 V with a maximum capability of 7500 V. The 657 mA is joined to the signal transmission path within the power separation filter, and together they are routed into the center conductor of the cable. As the current passes through each repeater (as shown in Fig. 1), sufficient voltage is dropped to power its active circuits. At the B terminal (Saint Hilaire de Riez, France), the power-feed arrangements and equipment are identical to those at the A terminal, except that the power supply's output voltage is negative. The maximum end-to-end cable voltage capability of the SG power-feed equipment is 15,000 V. Maximum capability would be exercised only on long cables in the face of adverse earth potentials. Note also that the 7500-V capability of each power supply permits continuance of TAT-6 cable operation with a high-impedance, shunt fault, in the cable or in a repeater, as close as 2900 V to one station (7500 V from the other station) until a repair ship arrives and begins the repair operation.

The power-return-current path is routed from the power supply through the power separation filter and the ocean-ground panel to specially constructed ocean-ground grids.<sup>3\*</sup> Potential differences of as much as 2.7 kV have been observed between the ocean-ground grids in the TAT-1 system.<sup>4</sup> The power supplies at each end of the TAT-6 cable are adequately regulated to absorb potentials of similar magnitude while maintaining control of the cable current.

The manually operated transfer switch and adjustable test load, both located in the load transfer bay (Fig. 1), permit the cable to be transferred between power plants without taking the cable out of service. This simple, but important, circuit is also part of the interlock system where

---

\* Although Reference 3 is related to an earlier British system, it provides details of the problems encountered in designing, installing, and operating ocean-ground grids.

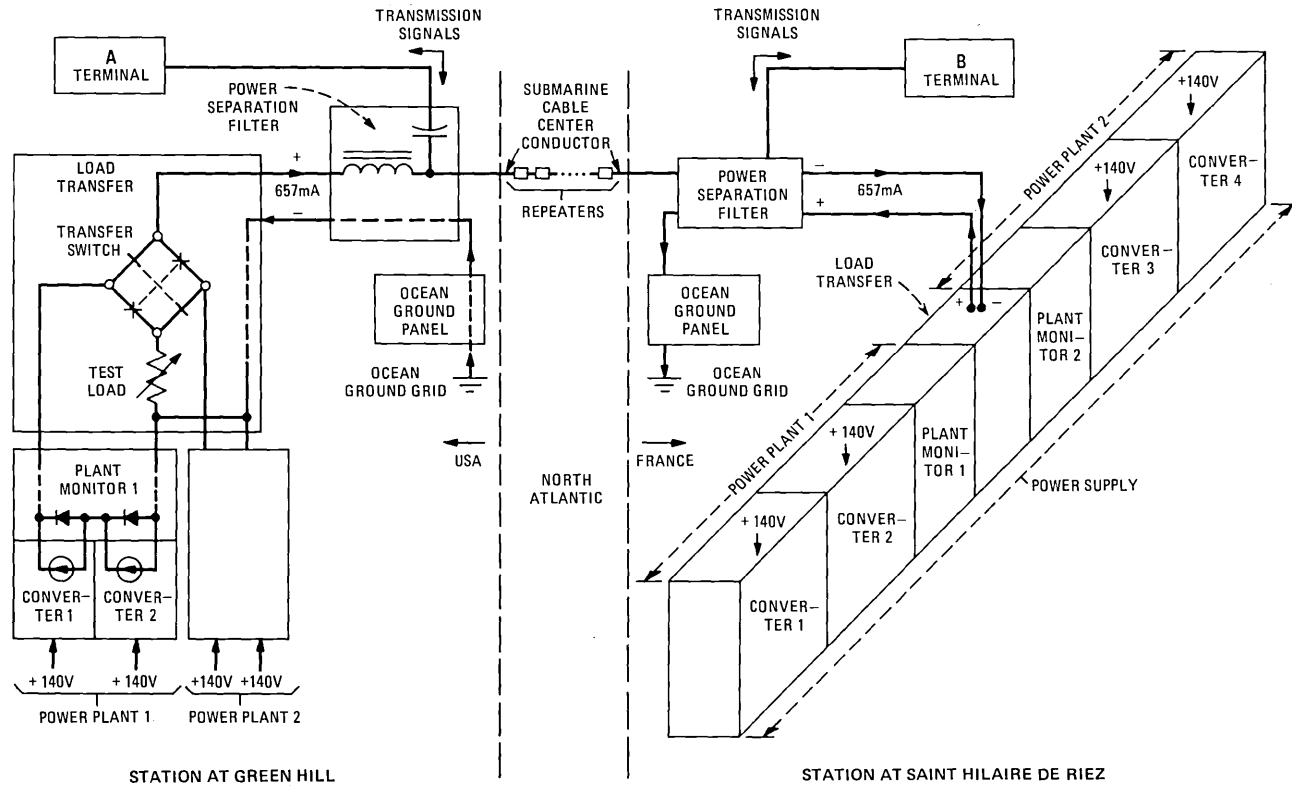


Fig. 1—Power-feed and signal transmission connections to the TAT-6 cable.

it differentiates between energized and unenergized high-voltage areas and permits access to the unenergized parts of the equipment for maintenance and inspection.

Previous Bell System power-feed equipment relies on conservatively designed, mechanically simple, transfer switch mechanisms. Although very rugged mechanically and proven reliable in many existing systems, these transfer switch mechanisms are physically large and cumbersome to operate. Hence, the SG-power-feed equipment makes use of a reliable, smaller, lighter, and simple-to-operate transfer switch.<sup>5</sup> The switch, shown in Fig. 2, has two cams that rotate with the handle of the switch. The cams operate plungers in four vacuum interrupters.

Figure 3 displays an annotated photograph of the seven-bay power supply. The bays are approximately 2.13 m (7 ft) high, approximately 0.71 m (28 in.) deep, and either approximately 0.79 m (31 in.) or approximately 1.14 m (45 in.) wide. The power supply ensemble is approximately 6.86 m (22.5 ft) wide.

Each of the seven bays contains low-voltage and high-voltage spaces. The low-voltage spaces contain alarm, monitoring, and control circuit components that are mounted in plug-in modules. Plug-in modules are

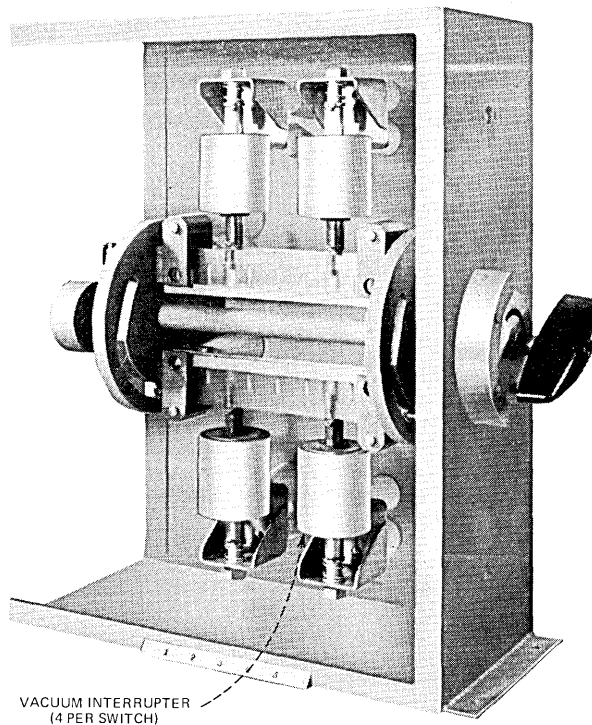


Fig. 2—Transfer switch.

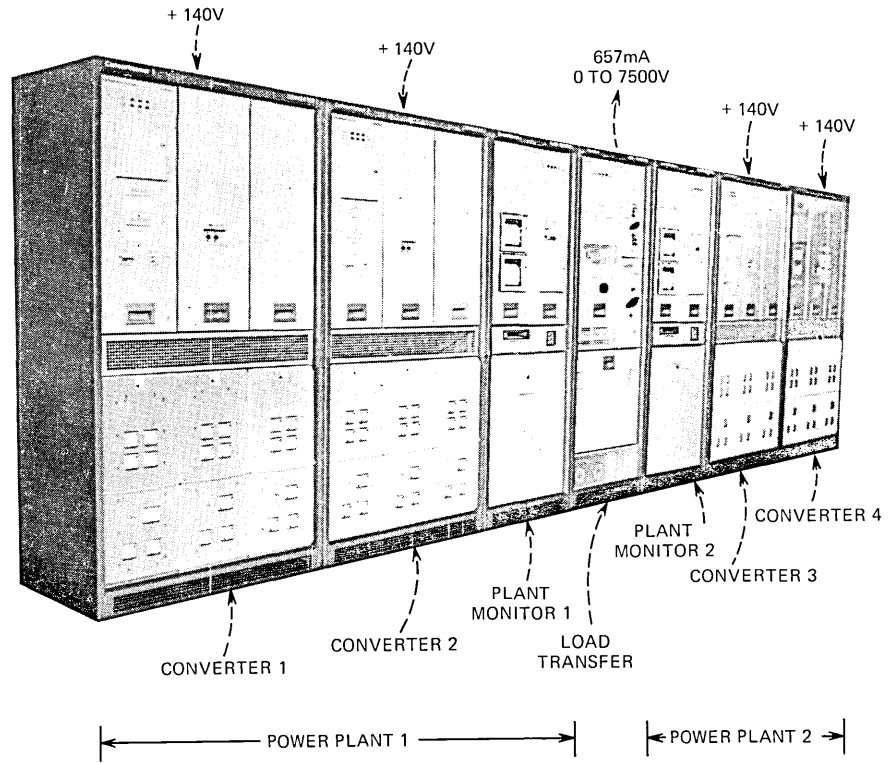


Fig. 3—SG power supply for one end of a long-haul, undersea cable.

located in pull-out slides to provide easy access for both normal operation and maintenance. The high-voltage circuits in the seven bays of the power supply and the high-voltage circuits in the power separation filter are contained in compartments that can be accessed only after appropriate manipulation of the key-controlled, safety-interlock system to assure the disconnection of the input power to the high-voltage space being accessed.

All interbay wiring in the seven-bay power supply is routed through connectors, except for the high-voltage leads, to minimize installation effort and errors. The center conductor and inner shield of a triaxial (shielded coax) cable provide the high-voltage and power-return paths, respectively, between the power supply output and the power-separation-filter bay. The outer shield is useful in reducing EMI conduction from the power supply to the power-separation-filter bay.

The power conversion systems are powered from +140-V battery systems.\* In addition, 115-V, 50/60-Hz power is required by the digital meters in the plant monitor and load transfer bays and the test load cooling fans. The 115-V inputs are not shown in Fig. 1.

### III. POWER CONVERSION TECHNIQUES

The process of converting power from the +140-V source into a precisely controlled, 657-mA, constant-current level suitable for energizing SG-type cables, at up to 7500 V, is accomplished in the converter bay. The cable-powering requirements are far more demanding than those of previous cables. For example, the 5.0-kW, nominal output capability of each SG converter bay represents a more than eight-fold increase over the capability of the most recent, previous, comparable Bell System converter. The power-train circuits follow the SF system practice of switching at ultrasonic frequencies† to:

- (i) Minimize the stored energy in filter capacitors.
- (ii) Avoid generation of high-level, audible noise.
- (iii) Minimize the physical size of magnetic apparatus.

The increase in power level and the more demanding regulation requirements prompted the use of a pulse-width-control technique instead of the saturable-reactor-type power control used in several previous undersea cable systems. The pulse-width-control technique is used to control switching-regulator transistors in the power path.

The increase to 5.0 kW of converter output power required efficient utilization of the state of the art in power transistor technology. High current (25 A), medium voltage (200 V), and fast switching speed (0.75- $\mu$ s

---

\* A description of the primary power arrangements including the commercial power connections, the rectifier-floated battery systems, and the automatic-or-manual-start, standby engine-alternator systems is beyond the scope of this article.

† The SF power-feed equipment was the first to use static converters switching at ultrasonic frequencies to power long-haul underseas cables.

rise-and-fall times) devices were selected as appropriate to operate with the +140-V input voltage and to minimize the number of required power stages. The +140-V input was selected to minimize current levels. The nominal current drain from the +140-V input for a converter bay is less than 36 A instead of over 100 A if a 48-V input had been used. The lower input current results in:

- (i) Less  $I^2R$  losses, thereby providing greater efficiency in the primary power path.
- (ii) Lower-strength magnetic fields emanating from the inverter's switching circuits.

The basic dc-to-dc power conversion unit, referred to as a "power stage," operates at 20 kHz (inverter) and 40 kHz (switching-regulator) to develop an output current of up to 690 mA at voltages of up to 2500 V from the +140-V input. Each converter bay contains up to three of these power stages with their outputs connected in series to obtain up to a 7500-V output. During normal operation in a TAT-6 station, six power stages (three in each converter bay) are powering the cable with each power stage operating at less than half its power capability. Figure 4 shows a converter bay with one power stage extended from the bay on its slide and with its EMI-containment covers removed.

A power stage is self-starting and requires only +140-V power, an oscillator-synchronizing signal, and the pulse-width-control signal as inputs for normal operation. Both high-power switching and low-level-control-and-monitoring circuits are incorporated in this plug-in package. Each power stage contains its own base-drive generator rather than receiving base-drive from an external, common generator in the converter bay. This feature assures that the loss of a base drive generator will not cause multiple power train damage. Also, the distribution of switching currents, and the resultant EMI noise radiation within and from the bay, is minimized.

Operation of the power switching transistors to near their maximum current capability requires the use of fast-responding, monitoring-and-protection circuits to prevent damage during load transients. Among the monitoring circuits are those that detect excessive switching currents and sense the high-voltage-output level.

### **3.1 Description of the power path**

The interconnections among the principal elements in the power stage are shown in Fig. 5. The regulator transistor (Q5) switches at 40 kHz to control the power flow from the +140-V input to the inductive-input inverter (Q1, Q2, Q3, and Q4), using a conduction range from 0 to 90 percent. The ratio of Q5 "on" time to the time of a single switching period provides the required average output voltage from the regulator in response to one of the current or voltage control systems in the power plant.

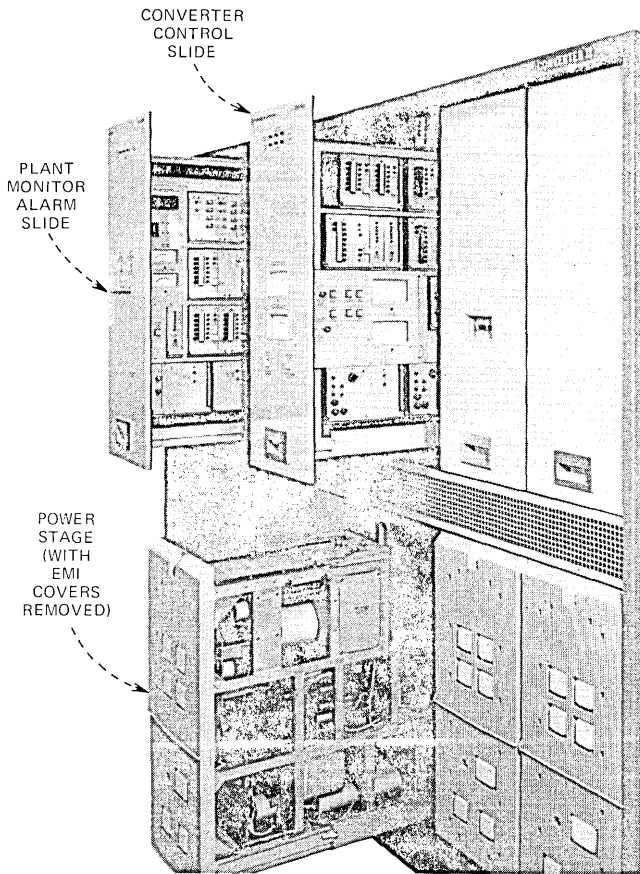


Fig. 4—Power stage extended on its slide from a converter bay.

Identical pulse-width-control signals are applied to all power stage regulators in a converter bay to force each power stage to support an approximately equal share of the load voltage.

The inductor L1, located between the regulator's output and the inverter's input, smoothes the voltage pulses from the regulator to establish a regulated direct-current flow into the inverter. This current flow is inverted into a regulated-amplitude, alternating current by the 20-kHz commutation of the Q1-Q2-Q3-Q4 bridge circuit. The bridge output is applied to a step-up transformer, full-wave rectified, filtered, and applied toward the external load. The inductor L1 is strategically located in the power path to limit the rate of rise of the current in the power semiconductors. The advantages of this special connection between the regulator and inverter in the power path are that it:

- (i) Permits safe operation of all power semiconductors close to their maximum ratings.

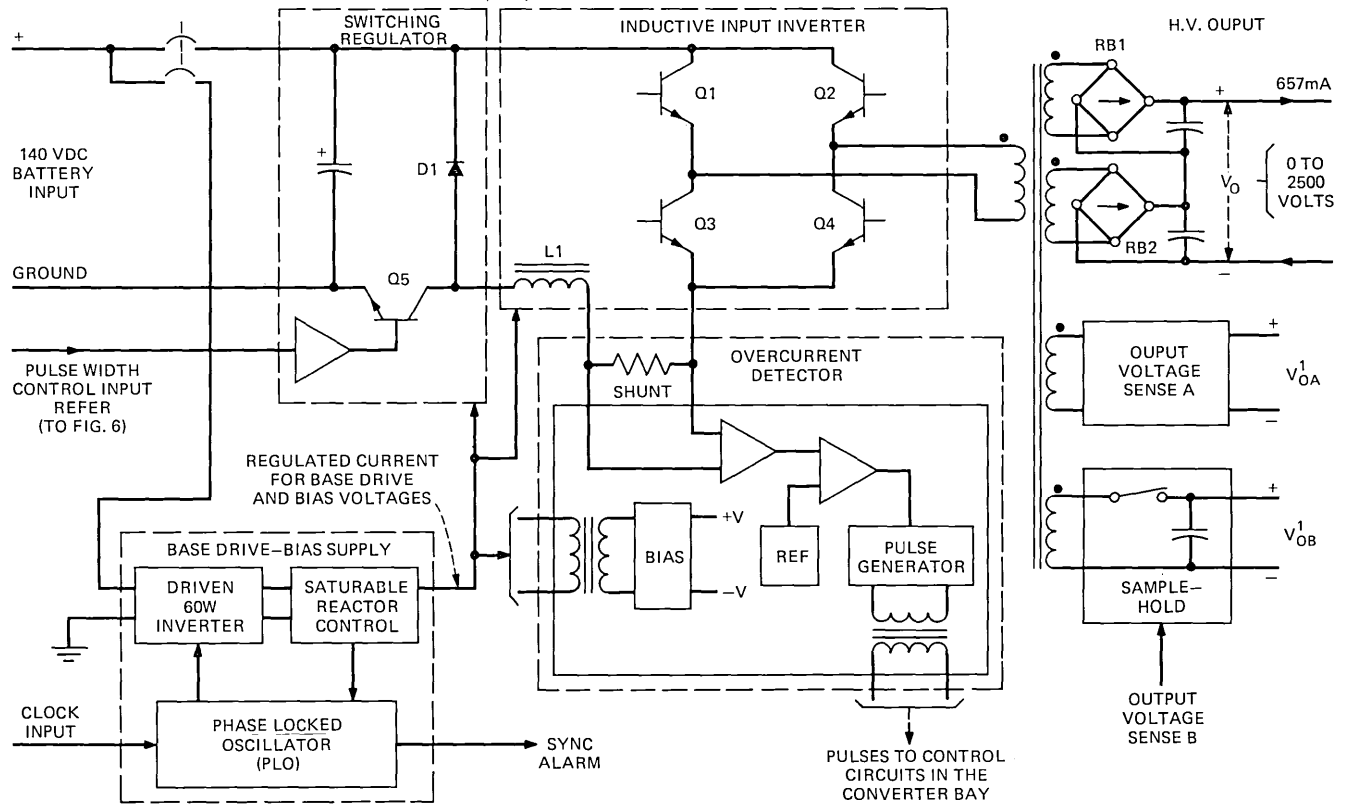


Fig. 5—Principal elements of a power stage circuit.



- (ii) Controls peak currents in the bridge inverter even during commutation.
- (iii) Allows easy adaptation of switching-loss-reduction networks which greatly reduce the transistor-peak-power dissipation and improve the efficiency by reducing the average switching loss.

The design and operational details of the basic power circuit topology, described above in general terms, have been documented.<sup>6-10</sup> Hence, the following discussion is concerned primarily with describing the overcurrent protection, the voltage sensing, the base-drive and bias supply, the physical realization, and EMI suppression.

### **3.2 Overcurrent protection**

A fast-responding, overcurrent detector monitors the L1 inductor current that is the input current to the inverter (Fig. 5). The L1 inductor controls the rate of change of current in all semiconductors in the main power path. Thus, only a single overcurrent detector is required in each power stage. The overcurrent detector works in conjunction with the converter bay's control system. This combination limits the peak current in all power switches to be no more than 20 percent above normal under transient conditions, including those occurring in response to the application of a direct short circuit on the output.

The overcurrent detector consists of a shunt, an amplifier to raise the shunt's voltage level by 21 dB, a stable, direct-voltage reference, and a fast-slew-rate comparator that switches a pulse generator to the "on" state if the shunt current exceeds a predetermined threshold. The overcurrent detector has transformer isolation both in the output-pulse signal path and bias-power input path. This is required because the entire overcurrent detector circuit experiences common mode voltage excursions of 200 V at a 1000 V/ $\mu$ s rate during power switching. More details of the overcurrent detector can be found elsewhere.<sup>11</sup>

When the overcurrent detector's pulses are issued from a power stage, the control system in the converter bay halts conduction in the regulators in all power stages in the bay. This blocks further energy flow from the +140-V source to the inverters. Once this control loop becomes active, the cutoff intervals of the regulators are controlled to the proper duration to allow excess stored energy in the power path's magnetic components to be dissipated into the load. As a consequence, the switching currents in the inverter are reduced to normal levels before further regulator conduction is permitted.

### **3.3 Isolated output voltage sensing**

Precise determination of a power stage's output voltage is required by the converter bay's regulation, alarm, and shutdown circuits. Each power stage contains sensing circuits that monitor the output transformer's voltage with sense windings. Direct sensing of the high voltage output is not desirable, since the secondary circuits may operate at several kilovolts above common. (This is a consequence of the series connection of the high-voltage outputs of the power stages.)

Unfortunately, a sense winding does not provide a voltage signal that has an ideal rectangular waveform, but one with large ringing transients and voltage notches at each polarity transition during inverter commutation. These aberrations vary considerably with load. They typically occur in power inverter circuits and cannot be completely avoided.

These disturbances excluded the use of conventional rectifier and passive filter circuits in this accurate, linear, sensing application. Instead, a unique application of a zero-order type sampling circuit is used to synchronously sample the voltage during a brief interval of the positive half-cycle of the sensed waveform midway between the commutation events. The sample switch is then held "off" to ignore the voltage ringing notches associated with commutation and the complete negative half-cycle. The charge stored on the "hold" capacitor maintains a relatively constant voltage across the high impedance load during the nonsampling part of the cycle.

Using this sampling scheme, tracking accuracy between the sense output and high-voltage output is better than  $\pm 1$  percent of full scale over the 2500-V output range. The sensing circuits are duplicated in each power stage for improved reliability.

### **3.4 Internal base drive and bias supply**

An efficient, 60-W, saturable-reactor-controlled, 20-kHz, quasi-rectangular-wave current source operates from the +140-V input to provide a  $\pm 2$ -A, regulated current to the inverter power transistors for base drive, to the regulator driver as a source for its base drive, and to the bias voltage supply in the overcurrent detector (Fig. 5). This  $\pm 2$ -A source determines the inverter commutation but not the regulator switching, since that is controlled by the converter bay's control circuits through the pulse-width-control input.

A phase-locked oscillator (PLO) operates with the base-drive source in a feedback system to minimize the variable, phase-shift error introduced by the saturable reactor. The PLO synchronizes the inverter's noisy commutation interval to the converter bay's clock with a phase-shift error of less than  $\pm 0.2$  radian. The commutation transient always occurs during the "off time" of the regulator transistor and therefore does not contribute jitter to either the leading or trailing edge of the conducting period. An alarm is issued if synchronization fails to occur.

This synchronization feature prevents beat frequencies from appearing in the converter bay's output and other anomalous effects. Synchronization of all high-power switching also reduces the possibility of random noise tones exceeding the stringent power-plant-output-noise requirement of less than  $0.17 \mu\text{V}$  for any single frequency in any 3-kHz band from 0.3 MHz to 30 MHz. Note, however, that loss of synchronization would not necessarily result in an increase in EMI.

### **3.5 Physical realization of and EMI control in the power stage**

The power stage is physically realized as a completely shielded plug-in module that has input and output, hand-operated connectors and weighs approximately 56.7 kg (125 pounds). It is also key-interlocked and cannot be removed from its location at the bottom of the converter bay (Fig. 4) unless the high-voltage circuits within the modules are de-energized.

Shielding is utilized to minimize the effects of the radiated EMI noise produced by power-switching semiconductors within the unit. The shielding includes individually shielded compartments within the power stage as well as solid heat sinks on the front and rear of the unit, solid side covers with EMI gasketing, and honeycombed shields on the top and bottom of the unit.

The switching semiconductors, which are the main heat sources, are mounted on a heat sink that serves as the front panel of the unit. This takes advantage of both natural convection and radiation modes of heat transfer. Top and bottom honeycomb shields permit air flow through the power stage for internal cooling.

The transformer that connects the inverter output to the high-voltage rectifier was specially developed for this application. The high-current, low-voltage terminals are located on one side of the transformer, with the low-current, high-voltage terminals on the opposite side. The transformer is mounted on a solid wall separating two shielded compartments with its high-voltage terminals protruding through the wall, thus providing the output rectifier compartment of the power stage with minimum noise contamination from the inverter's switching circuits.

## **IV. PULSE POSITION MODULATION AND DEMODULATION**

A major design problem in power-feed equipment providing regulated currents at high voltage is the implementation of current sensing in the high-voltage side. Very accurate current sensing is necessary for feedback control of the current as well as for alarm, shutdown, and metering functions. Analog magnetic amplifier technology has been successfully employed in previous high-voltage supplies. However, the need in the SG system for high precision (on the order of 0.01 percent) and the desire for less complex and lower cost apparatus made it necessary to develop a new technique for sensing current at high voltages.

The objectives of the new technique are to:

- (i) Generate a signal that is an accurate linear function of the current being sensed.
- (ii) Provide dc isolation in coupling the signal from the circuits referenced to the high-voltage side, where the current is sensed, to the signal-processing circuits referenced to the ground side.
- (iii) Process the received signal to perform various control, alarm, shutdown and metering functions.
- (iv) Provide operating power to the sensing circuits located in the high-voltage side, without employing an auxiliary power supply having high-voltage isolation.

The pulse-position-modulation (PPM) method<sup>12</sup> is used for current-sensing and information-coding. The PPM circuits convert a sensed analog signal into pulses whose position in time is varied relative to the occurrence of a trigger pulse. Pulse transformers couple the pulse from the PPM circuits, referenced to the high-voltage side of the power plant's output, to processing circuits referenced to the ground side. The pulse transformers are the only link between the PPM and processing circuits. To minimize EMI susceptibility, a low-impedance, balanced transmission line, terminated at each end with pulse transformers, is used to carry the pulse signals between the PPM circuit and the signal processing circuits.

The PPM method provides excellent signal-to-noise characteristics. Superimposed random noise has little effect on the time position of the pulse carrying the modulated signal. The PPM method is therefore well suited for interbay transmission of signals within various wire cables without appreciable reduction of the signal-to-noise ratio.

#### **4.1 Regulation**

The basic PPM circuit is used as the control element in multiple feedback loops controlling the output current and voltage of the power plant.

The principal feedback loop regulates the cable current at 657 mA. Figure 6 includes the current control loop. The switching transistor (Q5)\* in the regulator section of each power stage is controlled by the state of a set/reset-type flip-flop in the power-stage-control circuit. Each switching transistor is turned on by a start-pulse signal originating at the 40-kHz clock. The start-pulse signal is applied, through isolation transformers, to the set terminal S of the flip-flop, setting it to a state that supplies a base-drive signal from the Q output to the switching transistor in each power stage.

---

\* Same Q5 as in Fig. 5.

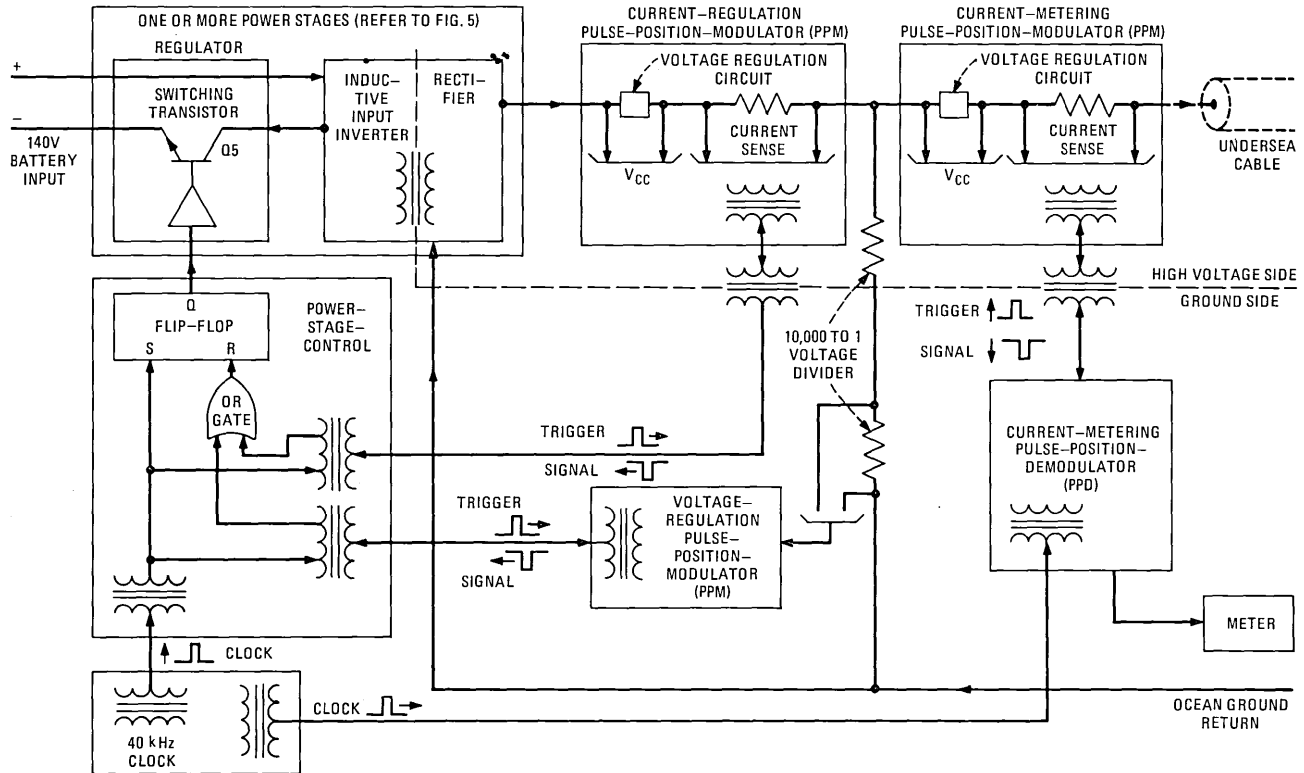


Fig. 6—Simplified circuit showing output-regulation and metering systems using pulse-position modulators.

At the same time, a positive-polarity trigger pulse is also transmitted from the 40-kHz clock to the current-regulation PPM circuit in the high-voltage side. The trigger pulse synchronizes the PPM circuit to the start of the switching-transistor-base-drive pulses. The signal pulse returned from the PPM circuit has a negative polarity. The trigger pulses and signal pulses share a common transmission path. The signal pulse is routed through an OR gate to the reset terminal R of the flip-flop. The flip-flop output is reset by the signal pulse to a state that terminates the base-drive pulse at the output Q. As a consequence, the regulator transistor in each power stage is turned off. The duty cycle (ratio of the time lapse between the trigger and signal pulses to the period of the trigger-pulse train) of the PPM output signal determines the width of the voltage signal to the output of the regulator and, ultimately, the current supplied to the cable.

Power to operate the current-sensing PPM circuits is obtained from the voltage ( $V_{cc}$ ) developed across the voltage-regulation circuit in the PPM circuits, as shown in Fig. 6. The voltage drop across the voltage-regulation circuit in the PPM circuit is used to furnish 12 V to the PPM circuits. Sixty-mA line current is needed to power the PPM circuits. This permits the PPM circuits to effectively regulate the cable current at any value greater than 60 mA. The voltage-regulation circuit in the PPM circuit bypasses current in excess of 60 mA. The networks required to obtain closed-loop stability are inserted across the error amplifiers (not shown in Fig. 6) located within each PPM.

The current regulation loop has control of the cable current during normal operation. After an initial 5-hour warmup period, the maximum 24-hour current drift is less than  $\pm 0.05$  percent if the ambient temperature variation stays within  $\pm 5^\circ\text{C}$ . This represents a change of  $\pm 0.33$  mA when the cable current is set to 657 mA.

The voltage-regulation loop is a secondary control loop designed to limit the output voltage to a preset level. Figure 6 illustrates one of the voltage-regulation PPM circuits. The power plant's output voltage is sensed by means of the 10,000-to-1 voltage divider.\* A signal pulse is sent from the voltage-regulation PPM circuit through the isolation transformers and the OR gate to the set/reset flip-flop within the power-stage-control circuit. The OR gate, and hence the flip-flop circuit, reacts to the first pulse that arrives at the OR gate during each cycle of operation.

The voltage regulation loop has a combined setability and maximum drift of  $\pm 25$  V.

---

\* Note the contrast between the direct voltage sensing used in the power plant's output where the circuit common is close to earth potential and the indirect voltage sensing previously described for the converter bay's output where the common of one bay is the high-voltage side of the other.

#### 4.2 Alarms and shutdowns using PPM circuits (not shown in Fig. 6)

The basic PPM circuit is also used in conjunction with pulse-sequence detection and decoder circuits to generate alarm and/or shutdown signals. Alarms of  $\pm 1$  and  $\pm 3$  percent are obtained from one PPM circuit sensing the cable current. The PPM circuit receives a trigger pulse from the clock circuit every  $25 \mu\text{s}$  (a 40-kHz rate) and generates a signal pulse in the middle of the time period under normal conditions when the cable current is at its nominal value. The PPM circuit has a negative transfer function. Hence, an increase in the cable current shortens the time delay between the trigger and signal pulses. The signal pulse is sent to four sequence-detection circuits. Each circuit compares the occurrence of the signal pulse to a marker pulse generated by feeding a 2.5-MHz clock frequency\* into a decoder circuit that quantizes the period between trigger pulses into 32 discrete time slots, each with a duration of  $0.8 \mu\text{s}$ . Marker pulses are obtained at time slots 4, 12, 20, and 28. The marker pulse occurring at time slot 4 is generated  $3.2 \mu\text{s}$  ( $4 \times 0.8$ ) after the trigger pulse. The marker pulses at time slots 12, 20, and 28 occur at  $9.6 \mu\text{s}$ ,  $16 \mu\text{s}$ , and  $22.4 \mu\text{s}$  after the trigger pulse. The PPM circuit has an active range of  $\pm 4$  percent around the nominal cable current. As a consequence, each time slot is equivalent to 0.25 percent ( $8 \text{ percent} \div 32$ ) change in the sensed cable current.

No alarms will occur when the cable current is at 657 mA, and the signal pulse appears at time slot 16. When the sensed output current begins to increase, the PPM circuit will send a signal pulse to the sequence-detection circuit earlier than time slot 16. When the signal pulse appears earlier than the marker pulse occupying time slot 12, the sequence-detection circuit will generate a +1 percent current alarm. If the cable current continues to increase until the signal pulse appears before the marker pulse occupying time slot 4, a +3 percent current alarm is generated. Current alarms of  $-1$  and  $-3$  percent are generated when the sensed current decreases enough to cause the signal pulse to appear after the marker pulses occupying time slots 20 and 28, respectively.

Means are provided for in-service checking of the proper functioning of these alarms. Techniques used to check all four alarm circuits in a single operation are described elsewhere.<sup>12</sup>

With slight modifications, a PPM circuit can be used to sense either cable current or cable voltage with an active range suited to detect and send out alarm and/or shutdown signals for any desired percent change in the cable current or voltage.

---

\* A single 2.5-MHz clock is used to provide, by division, the 40-kHz clock signal that synchronizes all clocks in the power supply.

### **4.3 Metering using PPM and PPD circuits**

Figure 6 also includes a pulse-position-demodulation (PPD) circuit used with a PPM circuit to provide a metering function. The PPD circuit converts the time-delayed pulses from the PPM circuit into an analog signal after the pulse signals pass through the isolation transformers into the ground-side circuits.

A synchronizing trigger pulse is sent from the clock through the PPD to the PPM. The resulting PPM signal is a narrow pulse, linearly controlled in time delay by the amplitude of the sensed cable current. The signal pulses are sent to the PPD where they are used to set and reset a flip-flop circuit within the PPD. The output of the flip-flop is a rectangular-wave signal having a width proportional to the time delay of the signal pulse. This rectangular-wave signal is applied to an averaging filter producing a direct current output. The amplitude of the direct current output signal is a linear function of the time delay of the signal pulse. This direct current output can be used for either digital or analog metering.

Expanded-scale meter PPM and PPD circuits are used with digital meters to provide greater accuracy. The circuits have an active range of 16 mA centered around the nominal 657-mA cable current. The overall measurement accuracy at the 657-mA current is  $\pm 0.33$  mA ( $\pm 0.05$  per cent).

A technique for employing a PPD in the feedback loop of the PPM circuit to linearize its transfer function and render the system insensitive to timing errors is described elsewhere.<sup>12</sup>

### **4.4 Physical design considerations for PPM circuits**

The operation of the PPM circuits with narrow pulses and consequentially broad frequency spectrum in a high-electromagnetic-interference and high-electrostatic-voltage environment required that considerable care be exercised in the physical design of both the PPM circuits and the bays where they are mounted.

The components of the PPM circuits are mounted on three-layer printed-wiring boards and are located, with their associated pulse transformers, in the high-voltage areas of the converter and plant monitor bays. The components of the low-voltage PPD circuits are also mounted on three-layer, printed-wiring boards. Several of these boards comprise a low-voltage plug-in module, located in one of the pull-out equipment slides in a converter or plant monitor bay. Access to PPM circuits located in high-voltage areas is possible only when the circuits are deenergized, while the low-voltage PPD circuits located in the ground-side areas are always available to the operator.

The three-layer boards provide the PPM and PPD circuits with two layers of interconnecting paths and a third layer that is used as a ground



plane. The ground plane consists of very wide ground paths to all integrated circuits, thus providing a low-impedance ground that aids in reducing susceptibility to noise pulses.

Figure 7 displays the location of the four PPM circuits (one current-regulation, two alarm and shutdown, and one current-metering) in the high-voltage area of a converter bay. Two PPM circuit boards are mounted on each metal base plate with a perforated metal covering over both boards. This cover and the metal base plate are electrically con-



Fig. 7—Pulse-position-modulators shown in the high-voltage area of a converter bay.

nected to the high-voltage circuit to form an equipotential electrostatic field that surrounds the integrated circuits in the modulators. This arrangement prevents any damage to the integrated circuits by eliminating the possibility of large voltage gradients in the surrounding field. The cover and base plate also reduce electrostatic coupling of EMI into the PPM circuits.

The current-regulation PPM in a converter bay is equipped with coarse and fine cable-current-adjust potentiometers, that are electrically at high voltage. These potentiometers are adjusted from the front of the converter bay by means of long, nonconducting shafts.

## V. SHORE STATION POWER SEPARATION FILTER

The shore station Power Separation Filter (PSF) bay is so named because it is the bay in which the wideband signal transmission path and the high-voltage dc power path, which share the undersea cable's center conductor, are separated for connection to their respective terminal equipment. Viewed in simplified form, the PSF circuit is a three-port filter, with an all-pass port for connection to the undersea cable, a high-pass port for connection to the wideband line transmission equipment (WLE),<sup>13</sup> and a low-pass port for connection to the power supply.

There are two fundamental but diametrically opposite design requirements for the PSF circuit: (i) to pass the wideband signal with some minimum acceptable values of return loss and insertion loss, which requires that components be small and circuit paths short; and (ii) to keep high-voltage partial discharge activity ("corona") below some appropriate threshold that requires that components be large and circuit paths widely spaced and long, in order to minimize destructive charge transfer in dielectrics and to satisfy transmission impulse noise objectives. For the SG system, with an upper frequency of 30 MHz and a maximum operating voltage of 7500 Vdc, the resulting dilemma was formidable and required extensive changes in the electrical and mechanical configurations compared to shore station PSFs of earlier undersea cable systems.

In addition to separating the power and signal paths, the PSF bay performs a number of important additional functions in the operation, maintenance, and safety of the cable system. Specifically, it provides: (i) proper electrical and mechanical termination of the undersea cable, (ii) a 75:50-ohm impedance match between the WLE and the cable, (iii) extensive shielding and filtering to prevent EMI from reaching the wideband signal path, (iv) facility for quick metallic connection of test equipment to the undersea cable center conductor, (v) an adjustable, 5-kW, auxiliary load that can be connected to the power supply in lieu of the undersea cable system, (vi) extensive high-voltage protection for

equipment and personnel, and (vii) in conjunction with the power supply, a key-interlocked safety system that synchronizes their mode of operation and controls access to hazardous voltage compartments.

A simplified diagram of the PSF circuit is shown in Fig. 8. The broken lines represent copper compartments, which serve the dual purpose of EMI shielding and high-voltage protection. The end of the undersea cable connects to the cable compartment, and the wideband signal path is separated from the high-voltage power path by C1 and L. The signal path proceeds from C1 through the transmission compartment to the WLE port. From L, the high-voltage power path goes through the wall of the inner compartment to switch S, through filter network N, to the power supply port. Switch S is a large, key-interlocked, rotary power switch that controls the mode of operation of the PSF and access to its high-voltage compartments. Auxiliary contacts (not shown) operate vacuum relay K.

The dominant requirement on the design of the signal path is a return loss of  $\geq 20$  dB over the entire SG band. This requires that impedance discontinuities be kept to a minimum. These occur primarily in the cable compartment, where high voltage considerations require large clearances, resulting in significant structural variations from the desired signal path impedance. The 20-dB return loss requirement is equivalent to a voltage reflection coefficient  $|\rho| \leq 0.1$ , since return loss =  $20 \log |1/\rho|$ . For a cable of characteristic impedance  $Z_0$ , terminated in an impedance  $Z_T$ ,

$$\rho = \frac{Z_T - Z_0}{Z_T + Z_0}.$$

Let the PSF be represented by its equivalent series impedance  $Z_S = R_S + jX_S$ , and let each signal port be terminated in its characteristic impedance,  $Z_0$  (both ports referred to the same impedance level). Then the reflection coefficient at either port is:

$$\rho = \frac{(Z_S + Z_0) - Z_0}{(Z_S + Z_0) + Z_0} = \frac{Z_S}{Z_S + 2Z_0}.$$

The series resistance is small, and at the higher frequencies lead inductance dominates, so that

$$\rho = \frac{jX_S}{2Z_0 + jX_S},$$

whence for

$$|\rho| \leq 0.1, X_S \leq \sqrt{4/99} Z_0 \simeq 0.2 Z_0.$$

This result provides a means of estimating the maximum allowable lead length through the cable compartment. At the undersea cable port,  $X_S = 0.2 \times 50 = 10 \Omega$ , and at the top frequency of 30 MHz, an allowable

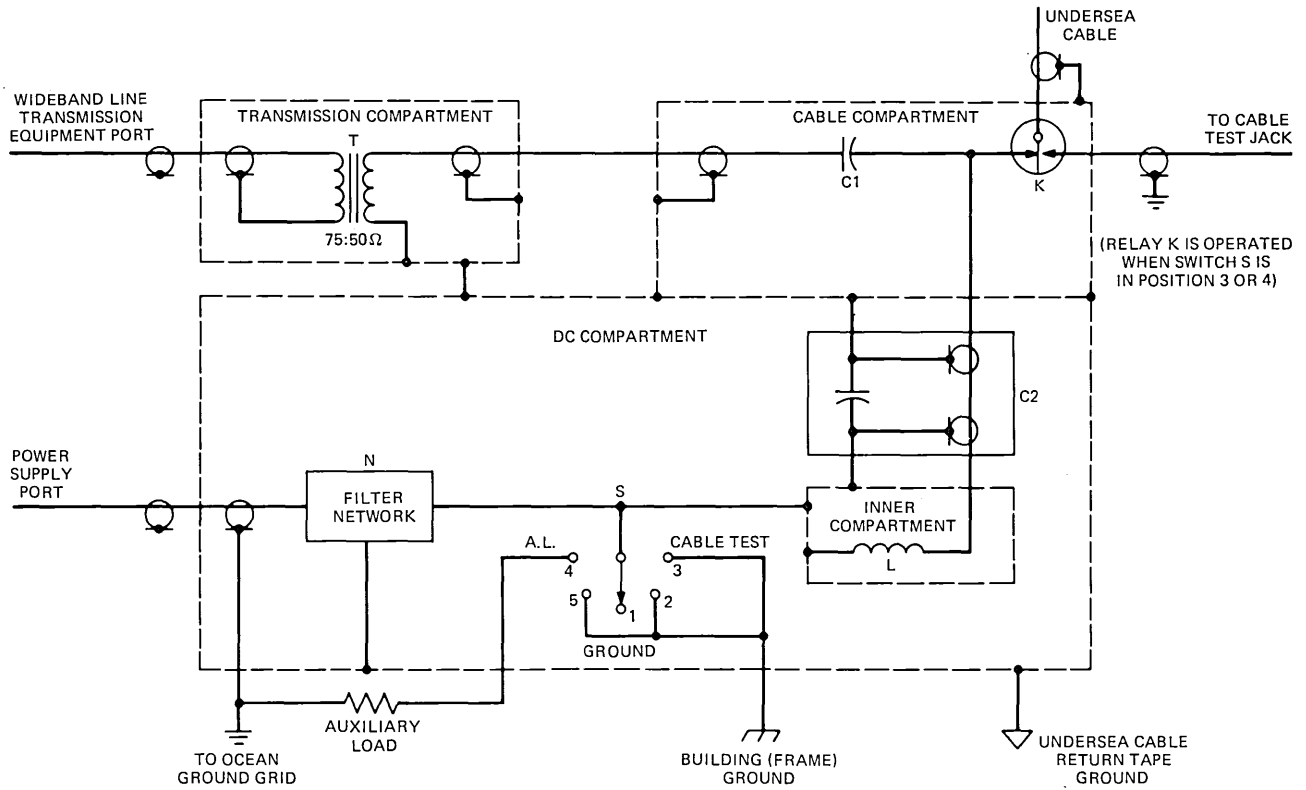


Fig. 8—Simplified circuit of the shore-station power-separation filter.

equivalent series inductance of 53 nH is obtained. Assuming, for illustration, a distributed lead inductance of 3.94 nH/cm (10 nH/inch), the maximum lead length is 13.5 cm (5.31 in.).

To attain the 53-nH requirement, the equivalent series inductance can be reduced by (i) shortening the path length, (ii) reducing the distributed inductance per inch, or (iii) adding shunt compensating capacitance. The path length was minimized by using a small high-voltage vacuum relay (K) to perform the required transmission path switching and by using the small capacitor (type 732A) designed for the SG repeater as the high-voltage blocking capacitor, C1. The distributed inductance of the remaining path was reduced by creating the separate cable compartment for the high-voltage portion of the signal path. The radial dimension of this compartment was made as small as possible (about 5-cm clearance from path to ground plane) consistent with the high-voltage, partial-discharge, activity requirements, thereby reducing the distributed inductance. Shunt compensating capacitance was not added, as this would have required the introduction of additional components into the high-voltage circuits in the cable compartment, increasing the possible sources of impulse noise and reducing reliability.

The actual, achieved path length of open leads through the cable compartment was approximately 20.3 cm (8 in.). The actual achieved return loss was greater than 30 dB over most of the 0.5- to 30-MHz band. Minimum values were 25.3 dB on a laboratory-built exact prototype, and 25.7 dB on the Green Hill PSF.

The principal requirements affecting the design of the high-voltage path are those concerned with high-voltage, partial-discharge activity, which must be kept below some appropriate level to satisfy signal-path impulse-noise objectives and to minimize destructive charge transfer in dielectrics. (The term "partial discharge activity" is preferred over "corona," since it more precisely describes the phenomenon taking place, viz., intermittent partial discharges of the dielectric. Strictly speaking, corona is a continuous discharge accompanied by a glow.) An excellent analysis of high-voltage partial discharge considerations in an SG-type cable system is given by Franke.<sup>14</sup>

Impulse-noise objectives established for SG terminals for the 48-kHz group data bands allow one "pop" (partial discharge pulse) per 15 minutes exceeding a threshold of  $-10$  dBmO. This is equivalent<sup>14</sup> to a peak instantaneous voltage threshold of 100 mV from a 48-kHz bandpass filter placed anywhere in the SG signal band. Since there are a number of possible sources of impulse noise in a terminal other than the PSF, the actual pop rate allocated to the PSF should be significantly less than one each 15 minutes.

Attempting to establish limits to minimize the destructive effects is more difficult. Destructive charge transfer limits for dielectrics are

nebulous and difficult to specify. Franke suggests a maximum value of 10 pC, based on levels permitted in previous undersea cable systems, with a rate corresponding to that of the data transmission interference requirement. For a maximum pulse duration of 50 ns in a 50-ohm system, he calculates a peak voltage threshold of 5 mV.

If the impulse noise and destructive charge transfer requirements are now combined, the resultant partial discharge activity requirement is a threshold of 5 mV, with a rate limitation of under 1 pop per hour.

The creation of a separate cable compartment not only aided in the solution of signal-transmission design problems, but also provided an effective way to isolate the high-voltage and signal paths, and thereby attenuate any noise which might otherwise be introduced via the high-voltage path. High voltage is fed from the dc compartment into the cable compartment via a novel skin-effect, low-pass filter\* consisting of L, C2, and the inner compartment. C2 is a feed-through, ground-separating capacitor (type 729A) constructed like a coaxial cable. The feed-through lead is the center conductor, and the outer conductor is composed of two high-voltage, insulated, concentrically wrapped foils, each of which is connected to a ground cap at opposite ends of the cylindrical structure. At dc, the two ground ends of C2 are isolated, but at higher frequencies, they are effectively connected, and C2 is equivalent to a short piece of coaxial cable. One ground of C2 is connected to the cable compartment, while the other ground is connected to the inner compartment. The high-voltage path from the power supply is connected to the outside surface of the inner compartment. Hence, the inner compartment floats at the cable supply voltage, while for ac signals it is effectively an extension of the cable compartment (undersea-cable-return-tape ground).

The inside surface of the inner compartment is connected to L, which bridges the high voltage onto the signal path via the center conductor of C2. The high-voltage path consequently passes through the wall of the inner compartment, and any noise following this path is attenuated by the skin effect of the 0.0794-cm (0.0313-in.) wall. Using the classical formula for current penetration, it can be shown that, for thickness,  $t$  (cm), and frequency,  $f$  (Hz), at 20°C,

$$\text{Attenuation} = 20 \log_{10} e^{-0.151t\sqrt{f}},$$

which, for  $f = 0.5$  MHz, gives 73.6 dB.

Filter network N provides attenuation for the 20-kHz converter frequency and its harmonics and protects against tones which might be radiated or conducted around the power supply output filters. Together,

---

\* The skin-effect filter concept is from G. H. Deshaies of Bell Laboratories, North Andover, Massachusetts, and was used in the PSFs of the L5 land transmission coaxial system.

N and the skin-effect filter provide a minimum loss of 80 dB from 20 kHz to beyond 60 MHz, as measured from the power supply port to the signal path.

High-voltage performance of the prototype and TAT-6 PSFs was evaluated using a wideband partial discharge detector developed by Franke and Czekaj.<sup>15</sup> With the detector connected to the 50-ohm signal path, the prototype had no pops exceeding 1 mV in 86 hours at +10 kV, and no pops exceeding 2 mV in 56 hours at -10 kV. The Green Hill PSF had no pops exceeding 1.4 mV in 8 hours at +10 kV, and the St. Hilaire PSF had no pops exceeding 1.4 mV in 15 hours at -10 kV. Since normal PSF operating voltages are less than 7.5 kV, these results provide a high degree of confidence that PSF high-voltage performance will not only meet but exceed design objectives.

## VI. SUMMARY

The TAT-6, shore-station, power-feed equipment has been described. A modified version has been developed and installed and is in service on Cable Ship *Long Lines*. The shipboard power-feed equipment can power any long-haul, undersea cable in service at the time of the shipboard installation of the power-feed equipment.

## VII. ACKNOWLEDGMENTS

The multiple-team concept that produced the SB, SD, and SF power-feed equipment was continued in the SG development. Significant contributions have been made by many individuals; directly by those participating as members of the development teams and indirectly by others. It is impractical to acknowledge all of the team members directly involved.

B. H. Hamilton, as leader of the power-supply-circuit-development team, is primarily responsible for both the system concept and specific techniques used in the power conversion, control, monitoring, protection, and switching circuits. From among the several members of this team, E. T. Calkin, W. J. Schatz, and R. E. Schroeder were selected as contributors to this article.

S. Mottel provided leadership for the power-supply-equipment-development team that is represented among the writers by I. Golio. The physical design team was responsible for all aspects of the physical design of the power supply's bays, including the development and implementation of physical design techniques related to EMI suppression, maintainability, component selection, and installation methods, and the generation of manufacturing information.

W. G. Ramsey supervised the activities of D. S. Shull and R. E. Curlee, who were responsible for all aspects of the development of the terminal PSF equipment for both cable installation use and permanent system

operation. Mr. Shull did the general planning and circuit development, and Mr. Curlee did the physical design.

Close cooperation among all three teams contributed to the successful development of the power-feed equipment.

## REFERENCES

1. J. D. Bishop and S. Mottel, "SD System: Cable Power Facility," B.S.T.J., 43, No. 4, Part 1 (July 1964), pp. 1339-1366.
2. E. T. Calkin and I. Golioto, "SF System: Power Conversion," B.S.T.J., 49, No. 5 (May-June 1970), pp. 749-765.
3. J. R. Walters and G. B. Fernie, "Submarine-Cable Earth-Electrode Systems," Post Off. Elec. Eng. J., 57 (July 1964), pp. 105-108.
4. G. A. Axe, "The Effects of the Earth's Magnetism on Submarine Cables," Post Off. Elec. Eng. J., 61, No. 4 (April 1968), p. 41.
5. I. Golioto, "High Voltage Transfer Switch With Cam Controlled Overlap During Transfer," U. S. Patent 4,016,385, applied for October 8, 1975, issued April 5, 1977.
6. E. T. Calkin and B. H. Hamilton, "A Conceptually New Approach for Regulated DC to DC Converters Employing Transistor Switches and Pulsewidth Control," IEEE Trans. Ind. App., 1A-12, No. 4 (July-August 1976), pp. 369-377.
7. E. T. Calkin and B. H. Hamilton, "Circuit Techniques for Improving the Switching Loci of Transistor Switches in Switching Regulators," IEEE Trans. Ind. App., 1A-12, No. 4 (July-August 1976), pp. 364-369.
8. E. T. Calkin, B. H. Hamilton, and F. C. La Porta, "Regulated DC to DC Converter with Regulated Current Source Driving a Non-Regulated Inverter," U. S. Patent 3,737,755, applied for March 1972, issued June 1973.
9. E. T. Calkin, B. H. Hamilton, and F. C. La Porta, "Switching Regulator with Network to Reduce Turnon Power Losses in the Switching Transistor," U. S. Patent 3,745,444, applied for March 1972, issued July 1973.
10. E. T. Calkin, B. H. Hamilton, and F. C. La Porta, "Switching Regulator with High Efficiency Turnoff Loss Reduction Network," U. S. Patent 3,736,495, applied for March 1972, issued May 1973.
11. B. H. Hamilton, F. C. La Porta, and R. E. Schroeder, "DC to DC Converter with Regulation Having Accelerated Soft Start Into Active Control Region of Regulation and Fast Response Overcurrent Limiting Features," U. S. Patent 3,879,647, applied for June 7, 1974, issued April 22, 1975.
12. B. H. Hamilton, "Pulse Modulation and Signal Processing Circuits to Perform Precise Control and Monitoring Functions with High-Voltage Isolation," IEEE Trans. Ind. Appl., 1A-12, No. 4 (July-August 1976), pp. 378-386.
13. M. Brouant, C. Chalhoub, P. Delage, D. N. Harper, H. Soulier, and R. L. Lynch, "SG Undersea Cable System: Terminal Transmission Equipment," B.S.T.J., this issue, pp. 2471-2496.
14. E. A. Franke, "Corona Considerations in Submarine Cable Communications Systems," IEEE Trans. Elect. Insul., EI-9, No. 4 (December 1974), pp. 150-154.
15. E. A. Franke and E. Czekaj, "Wide-Band Partial Discharge Detector," IEEE Trans. Elect. Insul., EI-10, No. 4 (December 1975), pp. 112-116.



## ***SG Undersea Cable System:***

# **Installation and Maintenance of the Undersea System**

By J. E. H. COSIER, A. P. DAVIES, S. W. DAWSON, Jr.,  
R. F. GLEASON, F. E. KIRKLAND, and T. A. MCKENZIE

(Manuscript received May 16, 1978)

*Many changes were made in Cable Ship Long Lines to facilitate installation and maintenance of SG cable and repeaters. This paper describes new equipment provided for the ship and modifications made to existing equipment. Both transmission equipment and cable and repeater handling facilities are discussed.*

### **I. BACKGROUND**

A significant part of the development of a new undersea cable system is involved with the equipment required to install and maintain the system. Much of the basic work concerning cable payout and repeater handling was done as part of the earlier SD Submarine Cable System and the design of Cable Ship *Long Lines*.<sup>1</sup> Even so, for the SG system, many specific changes were necessary. This paper describes the most important ones. The areas or conditions that called for revision or new design can be summarized as follows:

- (i) *Electrical*
  - (a) Test sets
  - (b) Power feeding equipment
  - (c) Transmission equipment
  - (d) Computer facility
  - (e) Repeater monitoring set
- (ii) *Environmental*
  - (a) Repeater temperature control and measurement
  - (b) Cable temperature control and measurement
- (iii) *Physical and Mechanical*
  - (a) Increased cable tensions and cable size

- (b) Large number of repeaters and equalizers
- (c) Burying of cable and repeaters
- (d) Grapnels.

## II. TEST SETS AND PROCEDURES

Installation of a system requires a continuous program of testing beginning when the cable, repeaters, and equalizers are loaded aboard ship and ending with the final splice completing the undersea link. The test equipment, test procedures, and computations are designed to ensure the proper performance of the system, to optimize equalizer settings, and to preserve the acquired data for future use.

### 2.1 *Test set philosophy and design*

New test equipment was designed to facilitate the installation of SG submarine cable systems. The design allows the use of identical test equipment on the ship and at shore terminals. The new installation test equipment designs include the cable laying test set, the repeater monitoring set, the SG high frequency line equipment, the shipboard power-feeding equipment, and a new shipboard computer facility.

#### 2.1.1 *Cable laying test sets*

The cable laying test set (CLTS) was developed for the purpose of making automatic, simultaneous, two-way transmission measurements on SG and SF cable systems during installation and commissioning.<sup>2</sup> As shown in Fig. 1, the cable laying test set has a transmit section and a receive section. The transmit section consists of an oscillator with precision output level control and a digital control unit, while the receive section consists of a selective detector, a digital control unit, and signal monitor unit. Signaling to achieve automatic control between the transmit section and the receive section is accomplished by set command tones. By using a patching arrangement, this signaling scheme allows the transmit and receive sections of the same CLTS to work either directly with each other or with the receive and transmit sections of another CLTS at the other end of a cable system. In the latter case, control is via an order wire channel over the link being installed.

Each section of the CLTS has one manual and five automatic modes of operation. In the manual mode, the transmit and receive digital control units are disabled. The transmit section simply becomes a manually tuned oscillator, and the receive section becomes a manually tuned selective detector with a signal monitoring capability. The signal monitor unit detects the signal power received by the selective detector and provides an audible and visible alarm when the received power level varies by more than  $\pm 1.5$  dB.

The five automatic modes of operation are: SF low band, SF high band,

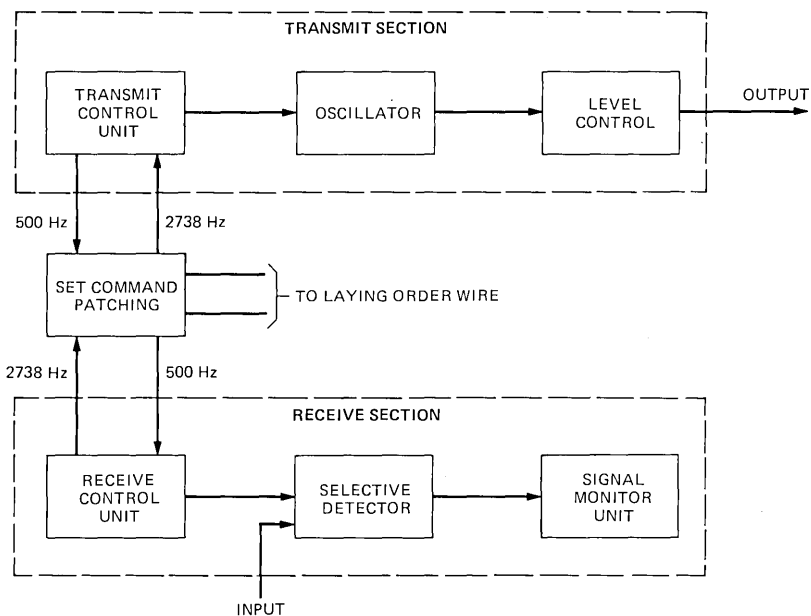


Fig. 1—Cable laying test set.

SG low band, SG high band, and RIPPLE. The RIPPLE mode is the most flexible, and all other modes are special cases of it. In the RIPPLE mode, the transmit and receive operator(s) choose a start frequency, stop frequency, and step frequency interval by setting thumbwheel switches on the front panels of the control units. When the transmit control unit is initialized, it causes the transmit section to begin sending a test tone at the start frequency and also sends a set command tone to the receive section, causing it to measure the received power at the start frequency. When the measurement is complete, the frequency and measured power are recorded via the data translator and teletypewriter (TTY). The receive control unit then sends a set command tone back to the transmit control unit, causing it to step to the next test frequency. To step to the next test frequency, the transmit control unit increments the oscillator frequency in 1-kHz steps at 10,000 steps per second until the next test frequency is reached. The receive control unit increments the measurement frequency in a similar fashion and begins a new cycle. This process continues until the measurement at the stop frequency has been completed and the data have been recorded.

All other automatic modes of operation are similar, except that the start and stop frequencies are fixed, standard values and the step frequency intervals vary in size between the standard frequencies. For these

modes of operation, the start, stop, and step frequency intervals are stored in read-only memory (ROM) in the control units.

The oscillator and selective detector units used in the CLTS are standard Western Electric transmission measuring sets, and thus the basic measurement capability of the CLTS is determined by these units. Both the oscillator and the selective detector are designed to cover the frequency range from 10 kHz to 60 MHz. The level control unit in the transmit section provides an output of  $0.00 \pm 0.02$  dBm (into 75 ohms), which can be attenuated to  $-99.9$  dBm in 0.1-dB increments. The selective detector has a measurement range from 0 to  $-129.9$  dBm. In all automatic modes, measurements can be made over a range from zero to  $-109$  dBm with a readout resolution and repeatability of  $\pm 0.01$  dB.

All the equipment associated with a CLTS, including power supplies and a blower for cooling, is packaged in one bay. Two complete CLTS bays are installed aboard ship, and two additional CLTS bays are installed (on a temporary basis) at the shore terminal from which cable is being laid, thus providing redundancy at both ends of the cable.

### **2.1.2 Power feeding equipment**

New shipboard power feeding equipment was designed for the installation of SG submarine cables.<sup>3</sup>

### **2.1.3 Transmission equipment**

The SG high-frequency line equipment was developed for the installation of SG cable systems. It is permanently installed aboard the Cable Ship *Long Lines* and temporarily installed at cable stations from which cable is laid. This allows the undersea cable system to be installed independent of the installation of the terminal wideband line equipment. The high-frequency line serves as the interface between all the transmission test facilities and the cable system.

The major function of the transmit high-frequency line is to provide level adjustment capability for transmission test tones and the 12-channel laying orderwire signal to obtain acceptable signal-to-noise ratios for each. At the same time, the broadband power transmitted must be limited to a value such that no repeater is overloaded. These functions are achieved for the conditions of transmitting into an inboard- or outboard-end section of cable (whose length can range from essentially zero to a full repeater section) or into the test lead of an ocean block equalizer.<sup>4</sup>

The receive high-frequency line provides three paths of independently adjustable gain for the broadband signal received from the cable system. First, the gain of the transmission test tone path is adjustable to allow for as much gain as possible while limiting the signal level applied to the

receive cable laying test set to less than 0 dBm. Second, the gain of the orderwire path is adjustable to achieve the proper transmission level at the input to the multiplex equipment. Finally, the gain of the supervisory tone path is adjustable so that the power of the supervisory tones at the input to the repeater monitoring set will lie between  $-40$  and  $-100$  dBm. Again, the implementation of the high-frequency line allows all these requirements to be met for receiving at an inboard or outboard cable end section or at an ocean block equalizer test lead.

Two high-frequency line units, regular and spare, are included in each high-frequency line bay. Each unit consists of a directional filter for separating transmit and receive signals, fixed-gain broadband amplifiers, variable attenuators, and hybrid transformers. Regular and spare SG laying orderwire multiplex equipment is also included in each high-frequency line bay. The multiplex units contain the stages of modulation necessary to translate the existing SF laying orderwire spectrum into the SG bands. In addition, the high-frequency line bay contains a patch panel to facilitate the convenient patching of all signals and test equipment used for transmission testing during the installation.

Because of the many different situations that can arise during laying, flexibility of patching the high-frequency line equipment received considerable attention. For example, the use of broadband amplifiers and attenuators throughout the high-frequency line having essentially flat response over the frequency range from 500 kHz to 60 MHz allows the transmit and receive bands to be determined simply by patching the directional filter. The design of the directional filter requires a large band-to-band rejection to preclude leakage from the relatively high-level transmitted signal from overloading the low-level receive section of the high-frequency line. The SG high-frequency line directional filter has an in-band loss of less than 1 dB in each band and a band-to-band rejection of greater than 65 dB.

#### **2.1.4 Computer facility equipment**

The advantages of a shipboard computing facility have been described previously.<sup>5</sup> Figure 2 is a block diagram of the new computing facility aboard Cable Ship *Long Lines*. It consists of a programmable calculator with 15,000-word memory and an internal cassette memory, two additional cassette memory units for program and data storage, a thermal page printer, a plotter, and an optical paper tape reader.

During a cable lay, a detailed record-keeping procedure is employed which consists of entering data and performing computations on a specially prepared set of printed forms. Both the shore terminal and the ship maintain a complete set of all data and computations. The computer software is designed to replace the manual record-keeping procedure

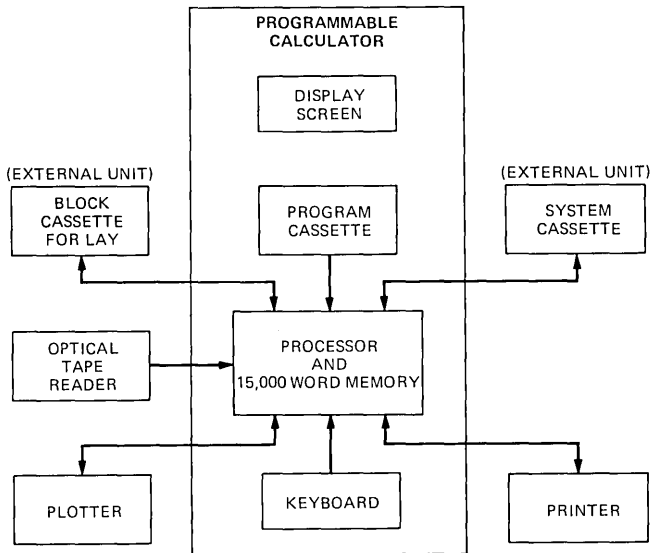


Fig. 2—Shipboard computer facility.

aboard ship. For this reason, it prints out data and computations on pages which replace the forms which would have been filled out manually. Thus, in the event of a computer failure, the manual computations can easily be resumed. In addition, a software package allows operator-controlled manipulation of various data for special calculations during a cable lay.

### 2.1.5 Repeater monitoring set

The repeater monitoring set is designed to be used on the SG system to measure supervisory tones from repeaters as well as to measure the intermodulation performance of repeaters.<sup>4</sup> Unlike the equipment described above, which is used only during installation and commissioning,<sup>6</sup> the repeater monitoring set is a permanent piece of terminal station equipment which is also used during installation. The supervisory tone measurements allow for data acquisition necessary for system administration and for fault localization. Intermodulation tests, which are normally performed on an out-of-service basis, are helpful in localizing a wide variety of faults.

The repeater monitoring set can be operated in a manual mode or in a semi-automatic mode. In the manual mode, input parameters are set on thumbwheel switches by an operator. In the automatic mode, input parameters are entered from mark-sense cards by a card reader. The repeater monitoring set has a visual output of measured data as well as an output suitable for driving a TTY. The set can also be used to measure supervisory tones on the SF system.

For supervisory tone measurements, the repeater monitoring set uses a phase-locked selective detector technique. The measurement bandwidth is 5 Hz, and all the conversion carriers in the selective detector are phase-locked to a highly precise common reference frequency, allowing accurate frequency measurement of the received tones.

The receiver, whose automatic frequency control loop contains a 50-Hz bandwidth IF filter, has an acquisition range of  $\pm 25$  Hz for signals above  $-110$  dBm. Once phase lock is achieved, the frequency and power of the received signal are measured automatically over the range of  $-100$  to  $-40$  dBm. Input bandpass filters, used to prevent overload of the detector by the broadband message signal, can be bypassed, enabling the set to be used as a general-purpose selective detector over the 10-kHz to 60-MHz range.

Because the SG repeaters are highly linear, a special technique was required to obtain accurate intermodulation measurements of individual repeaters on an installed system. This particular measurement is made possible by the common-amplifier repeater configuration and by the different distance and hence different round-trip delay to each repeater. Chirp radar and matched-filter techniques are used to obtain the necessary signal-to-noise ratio under the peak power constraints of the repeaters.

A linear FM (chirp) signal 100 kHz wide with a 10-Hz repetition rate is transmitted together with a single frequency tone. In the low band, an 8.6- to 8.7-MHz chirp and a 12-MHz tone are transmitted. Each repeater produces a second-order intermodulation product whose frequency sweeps from 20.6 to 20.7 MHz and is received in the high band. The return from a given repeater is recovered by demodulating the received signals with a swept carrier identical to the transmitted chirp but translated in frequency by an amount corresponding to the round-trip delay to the given repeater. A single IF signal results (in this case, 20 MHz) which is measured by the 5-Hz bandwidth selective detector. Returns from adjacent repeaters are separated by approximately 100-Hz intervals and are rejected by the detector. The effects of delay distortion on the signal are minimized by choosing the transmit and receive frequencies such that the round-trip delay over the 100-kHz chirp band is constant.

Successful implementation of this method requires precise phase control of two synchronized frequency generators.

## **2.2 Test procedures**

### **2.2.1 Tests during loading**

Repeaters, ocean-block equalizers, and shore-controlled equalizers are individually tested during manufacture and then transported to the dock for loading aboard ship. Following loading and prior to splicing,

resistance checks are made to determine that all repeater housings have a high dc resistance to ground and that all equalizer housings are solidly grounded to the ship's hull. The purpose of these pre-checks is to ensure the validity of the outer-conductor dc resistance tests which are used later to determine cable temperature. The cable, repeaters, and equalizers are then spliced together to form an assembled shipload.

### **2.2.2 Assembled shipload tests**

The assembled shipload is subjected to a series of tests to ensure proper operation. The diagram in Fig. 3 shows the equipment and connections used to perform these tests on a block-by-block basis. Individual block testing is necessary because the differences in temperature and pressure between shipboard and ocean bottom environment can result in large temporary end-to-end misalignment which makes a single measurement of an entire shipload impractical. Block-by-block measurements have some useful benefits. Testing procedures and computations can be mechanized in a generally repetitive manner, and single block tests automatically localize faults to a block.

Each end of the assembled shipload is terminated at a power separation filter. The power separation filters allow high voltage to be applied to the center conductor at one end and dc ground at the other. A broadband connection is also provided for test signals. Transmission tests are performed on each of the blocks (including the partial end blocks) at a selected set of standard frequencies in each band.

For discussion of the actual transmission tests, refer again to Fig. 3. All transmission measurements are made by either the cable laying test sets (CLTSs) or the repeater monitoring set (RMS). For these tests, the CLTSs transmit and receive signals at a standard list of stored frequencies. All the test equipment as well as the orderwire is connected to the assembled cable system through the high-frequency line equipment. The CLTSs are used to measure the transmission response of each block. The measurement starts at the first test frequency and automatically sequences through the standard frequency list. The measured data are automatically recorded by means of the data translator and the teletypewriter in both printed page and punched-paper-tape form. The data translator also causes the TTY to print out heading information which identifies the type of measurement made, the date and time of day, the direction of transmission, the test sets used to make the measurement, the run number, and the block number. The CLTSs are also used to measure all the losses and gains associated with the test configuration (e.g., patch cords and power separation filter). The punched paper tapes allow automatic loading of test data into the shipboard test room computer facility.

Computations are performed using the measurement data described



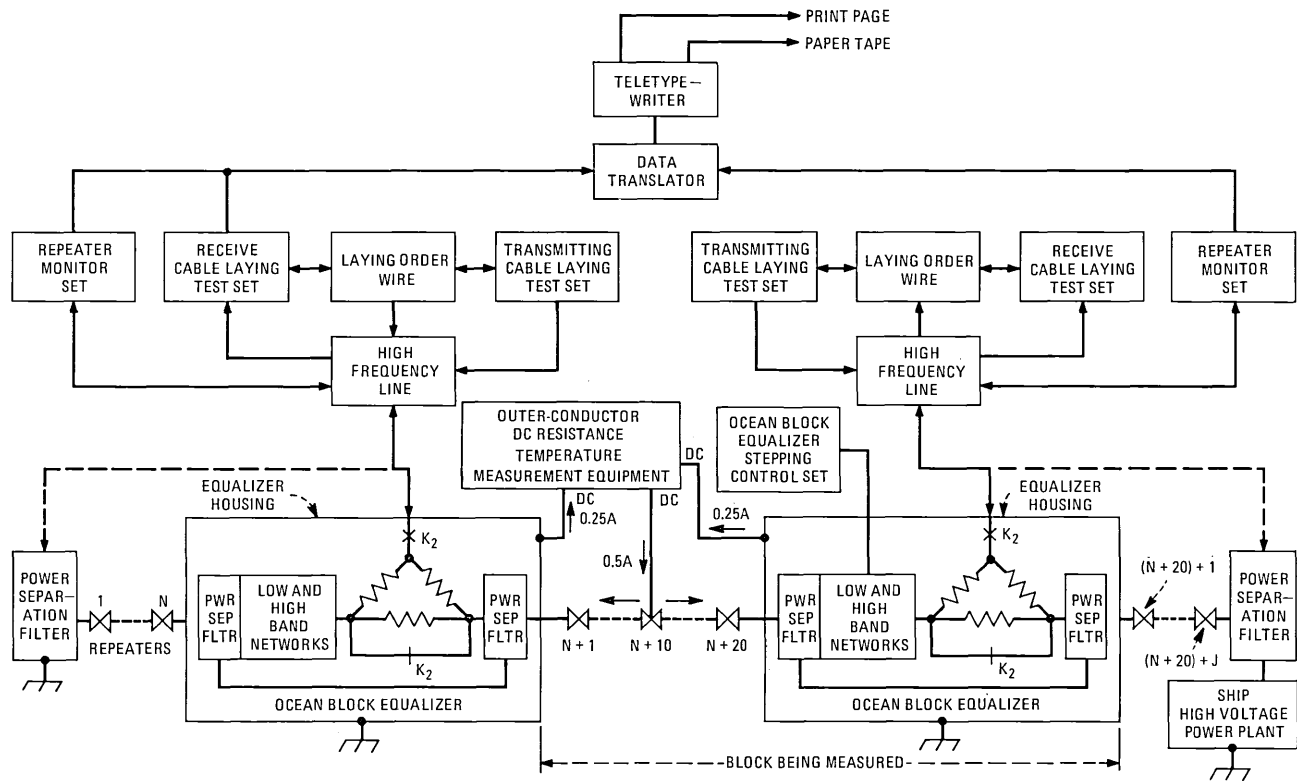


Fig. 3—Assembled shipload transmission test.

above. The primary intent of these calculations is to verify that the assembled shipload is operating properly. To accomplish this, one must be able to predict the expected transmission response. Factory measurements on the actual repeaters, cable sections, and equalizers in each block, which are loaded into the computer memory prior to testing, are used to compute a transmission response to be compared with the shipboard measurements. The computed transmission response must correct for the actual temperature of the repeaters and cable aboard ship, because these are generally not the same as during factory measurements.

### **2.2.3 Tests during laying**

Many of the tests during laying are similar to the assembled shipload tests except that the test path is between ship and shore rather than only within the shipload.

The beginning of a cable lay starts with a cable splice. Before the splice is made, a transmission reconciliation test is made to verify the performance of the previously installed portion of the system. If this reconciliation (comparison with measurements made earlier) is satisfactory, the splice is made. After the splice, another reconciliation transmission test is performed between the shore terminal and the test lead of the most outboard ocean-block equalizer in the shipload. Again, the data are analyzed using the shipboard computer to determine if the measurement is consistent with the previous reconciliation and the assembled shipload measurements.

The primary reasons for transmission tests during laying are to confirm proper operation of the system and to obtain data necessary to choose the optimum ocean-block equalizer settings. Using the test configuration shown in Fig. 4, transmission tests are made at regular intervals. At the end of a standard frequency measurement run, each station has only the measurement data for its receive band. These data are then exchanged via the laying orderwire by using the TTY with a paper tape reader and the data sets. Thus the shore terminal and ship obtain measurement data for both bands.

Between standard frequency runs, while the cable is being payed out, the cable laying test sets are used to send and monitor a single tone in each direction of transmission. The receive cable laying test sets give an automatic alarm when the received power of this tone varies by more than 1.5 dB. Also, the supervisory tone power from each repeater is measured and recorded using the repeater monitoring set, data translator, and TTY. Because adjacent repeaters transmit supervisory tones in opposite directions, the data must be exchanged between the ship and shore terminal. Additional tests performed during laying include (*i*) a transmission test through the next-to-be-laid block to ensure that its

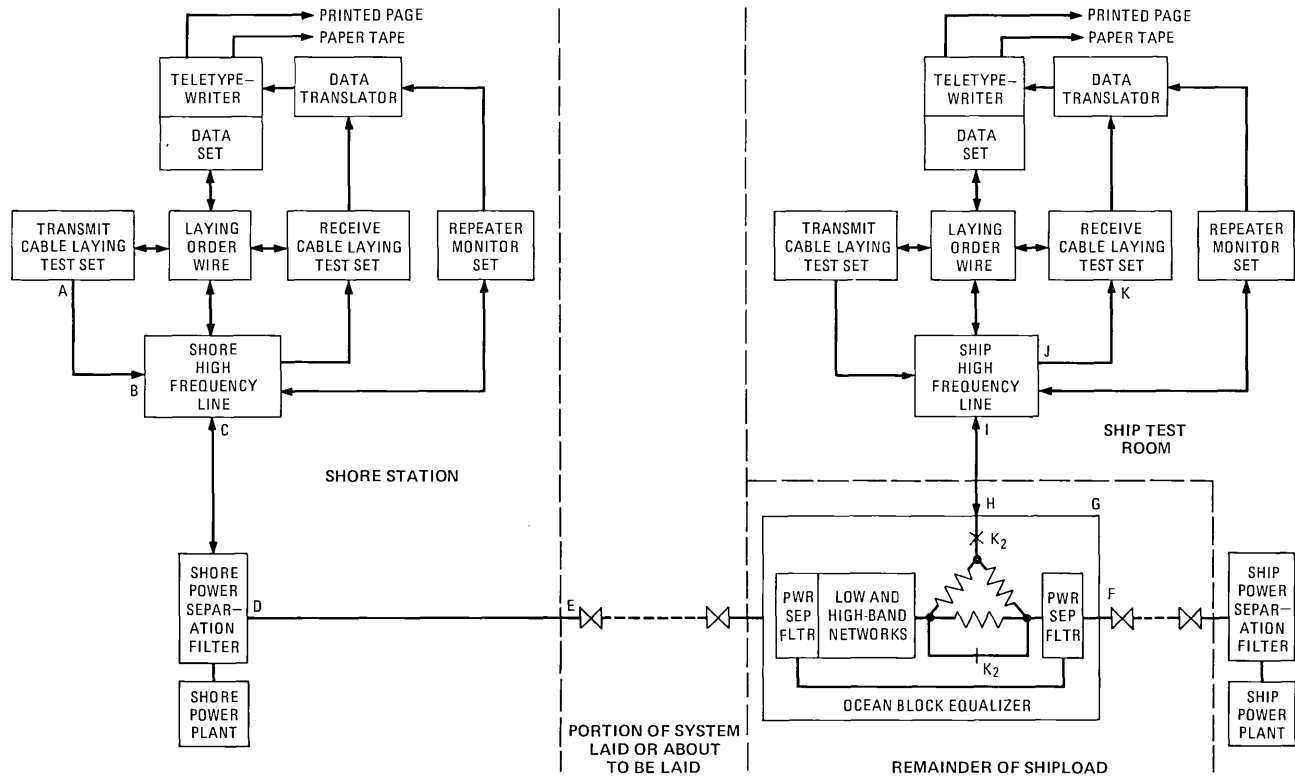


Fig. 4—Transmission tests during laying.

transmission has not changed since the assembled shipload tests, (ii) transmission tests at closely spaced frequency intervals, called ripple runs, and (iii) monitoring the power plant voltage and current.

The process of choosing the optimum equalizer setting typically starts about three hours before the equalizer is scheduled to go overboard. This interval allows time for the equalizer decision to be made and for the test and stepping leads to be sealed by overmolding. First, a transmission objective is computed using the shipboard computer. The transmission objective is the expected test tone power which would be measured at the input to the receive cable laying test set, assuming that the only misalignment in the system is the planned misalignment.\* All the components of this calculation are known either by calculation or by direct measurement with the cable laying test set.

At the time of any standard frequency run, the misalignment of the system consists of the sum of residual misalignment and temporary misalignment. The temporary misalignment is due to the fact that not all the block being laid has stabilized at ocean bottom conditions. Nevertheless, the temporary misalignment must be removed from the measurement data since the equalizer should compensate for only the residual misalignment. This is accomplished as follows. Under steady-state conditions (i.e., constant ship speed, cable payout rate, and shipboard cable and repeater temperature), which are normally closely approximated during laying, temporary misalignment decreases linearly with time (and thus distance) until the equalizer is overboarded. The shipboard computer sorts the standard frequency run data and extrapolates to the expected value corresponding to the time that the equalizer would go overboard. The amount of remaining temporary misalignment due to the cable suspended between the ship and the ocean bottom and due to the thermal inertia of the cable and repeaters is calculated from theoretical considerations and used to correct the extrapolated data.

Direct comparison of the corrected extrapolated data to the transmission objective yields the residual misalignment to be compensated for by the equalizer, which is referred to as block deviation. The computer equalization program then compares the block deviation to the loss shapes available in the equalizer and orders the various setting choices based on a weighted-sum-of-squared-error criterion. The equalizer setting that is selected is typically the one with minimum sum-of-squared-error. The transmission engineers, however, examine the top several choices, taking into account auxiliary information (e.g., anticipated misalignment in the next block), and occasionally choose a different setting.

Once the choice of equalizer setting has been made, four standard

---

\* An example of planned misalignment is gain provided at time of cable installation to precompensate for anticipated increased cable loss with time, i.e., cable aging.

frequency runs are performed. The first two are made immediately before and after the equalizer is switched. A comparison of these two standard frequency runs is made to verify that the correct change in loss has been achieved. Second, the shipboard transmission test lead is moved to the next inboard equalizer, adding the next ocean block to the measurement path. The next two runs are performed before and after the transmission test pad is switched out of the equalizer about to be laid. A comparison of these two standard frequency runs is made to verify that the test pad has, in fact, been switched out. At this point, the equalizer stepping and transmission test leads are sealed, and the equalizer is ready for overboarding. Transmission testing then continues through the next inboard equalizer.

### **III. ENVIRONMENTAL CONSIDERATIONS AND MEASUREMENTS**

#### ***3.1 Repeater temperature control***

In previous undersea cable systems, no special effort was made to control the temperature of repeaters and equalizers on the cable laying ship. For SG, however, reasonably precise control is required.

##### ***3.1.1 Control requirements***

Even though repeaters and equalizers are vacuum-dried during manufacture, some water remains, much of it dissolved in polymeric materials. At high storage temperatures a significant amount of water exists as vapor within the free volume of the repeater. If such a repeater were launched into the ocean, where the bottom temperature is typically 2.5°C, there is a possibility that the water would condense on surfaces within the repeater before it could be reabsorbed by the polymers. Condensed water on and between conducting surfaces can cause repeater failure. A careful experimental investigation showed that condensation would not occur if the ambient storage temperature were less than 32°C for unpowered repeaters and 27°C for powered repeaters. The lower of these two values is controlling, since repeaters are powered when they are laid.

If temperature-controlled repeaters<sup>4</sup> are included in a shipload, it is necessary to know their temperature in order to predict what their transmission characteristics should be. To limit positive misalignment in blocks containing temperature-controlled repeaters, the difference between repeater and cable temperature must be controlled. Because the thermal mass of the cable is much greater than that of the repeaters, it is more efficient to control repeater temperature than cable temperature. Thus it is necessary not only to limit the maximum value of repeater temperature but to be able to set it and maintain it with reasonable precision.

Temperature control is also needed for other repeaters, but the re-

quirements are less stringent because temperature changes produce a much smaller change in transmission. Table I summarizes repeater temperature setability, stability, and measurement accuracy objectives.

### 3.1.2 Temperature-control facilities

To achieve the required setability of repeater temperature, it was decided to use air-conditioning units in each repeater bay and to build tents over each repeater stack. The air-conditioning units are located along the port bulkhead of each repeater bay. The chilled air is piped into a 4-inch-high (102 mm) rectangular telescoping duct located beneath the repeater stack.

When a full load of repeaters is in place, the duct is extended to its full length, spanning the entire stack. As repeaters are payed out during a cable-laying operation, the duct can be shortened ultimately to approximately one-third of its fully extended length. The telescoping feature was provided to keep the incoming air flow concentrated around the remaining repeaters. The return duct for the air flow is on the deck next to the telescoping inlet duct. It contains a series of holes on the top and the side opposite the inlet duct to receive the air. Each hole is fitted with a swivel plate which can be moved to open or close the hole. As repeaters are payed out, the unused holes are sequentially closed.

The repeater stack is covered by an insulating tent with openings on the sides to pass the cable bights. The tent is made in sections so that, as repeaters are payed out, sections can be removed to allow the size of the tent to conform approximately to the size of the stack of remaining repeaters.

Under unusual conditions of very high humidity, condensation can occur on the repeater and equalizer housings in the tent. Drains have been provided to remove this water.

Table I — Shipboard repeater temperature objectives

	Temperature-Controlled Repeaters	Non-Temperature-Controlled Repeaters and Equalizers
Setability	<27°C*	<27°C
Stability in 12 hours	±0.2°C	±2.0°C
Measurement accuracy	±0.2°C	±0.5°C

\* The maximum temperature for the temperature-controlled repeaters is determined in part by the cable temperature. The specific requirement depends on a number of factors. In the worst case, it is sufficient to keep the repeater temperature at or below that of the cable.

### **3.1.3 Repeater temperature measurement**

An automatic temperature measurement and recording system has been installed on Cable Ship *Long Lines*. Twenty-one thermocouples can be placed in each of the three repeater stacks. The thermocouples are attached to the periphery of holes in the end cones of the repeaters using clamps which can be removed readily before the repeater is payed out.

The thermocouple identifying number, the indicated temperature, and the time of measurement are printed out on paper tape. The equipment can be programmed to scan and print data from all of the thermocouples at set intervals, e.g., every eight hours. When calibration and correction procedures are used, the temperature measurement accuracy is about 0.05°C.

### **3.2 Cable temperature control**

With previous cable systems, there was no need to control cable temperature. The temperature was measured with thermocouples at 15 points in each tank, giving adequate information for transmission measurements. For SG, cable temperature stability in each tank has to be maintained.

#### **3.2.1 Control requirements**

As discussed above, temperature setability requirements have been applied to repeaters rather than to cable. Measurements to determine equalizer setting, however, require that the cable temperature remain stable for the measurement period. Specifically, the stability objective is  $\pm 0.2^\circ\text{C}$  over a 12-hour period. Similarly, the measurement accuracy objective is  $\pm 0.2^\circ\text{C}$ .

#### **3.2.2 Temperature-control facilities**

Measurement of cable temperature during installation of the TRANS-PAC-2 SF system showed that the bottom aft portion of the Tank 3 wall was warmer than the rest of the tank. This was traced to the proximity of that area to the ship's main boilers. To improve the uniformity of temperature distribution in the cable, the cable was isolated from the warm area by spacers approximately two inches thick and a sheet of fiberglass to provide a smooth surface adjacent to the cable.

As a further means to provide a uniform cable temperature, the tanks are flooded with water during cable-laying operations. The water level is maintained about two feet below the top of the cable to protect people working in the tank. The water in each tank can be circulated by draining it from drains in the bottom of the tank and pumping it into the top of the tank along the walls. While the tank water temperature does change

slowly in response to sea temperature, the circulating water arrangement provides adequate stability.

### **3.2.3 Cable temperature measurement**

Two means are now provided for measuring cable temperature. The first, similar to that used previously, consists of 12 thermocouples in each tank which are connected to the temperature recording system discussed above for the repeater stacks. The thermocouples are taped to the cable during loading so that they are distributed throughout the tank. Thermocouples have the advantages of simplicity and accuracy but the disadvantage that they provide only point measurements. If the cable temperature is not uniform, it is not possible to determine precisely the average temperature of a cable section or a block from the thermocouple readings.

For transmission measurements, the average temperature of the cable in a block is the most important item of cable temperature data. To provide this information directly, the second cable temperature measurement system was developed. This method consists of measuring the dc resistance of the outer conductor of the cable and inferring from this and factory test data the average temperature.

The repeater and equalizer high-pressure housings are connected in series with the cable outer conductors but contribute negligible resistance. The conductivity of the copper used for the outer conductor of undersea cable is carefully controlled. Since the temperature coefficient of resistivity is directly related to the conductivity,<sup>7</sup> it is thus also carefully controlled. During cable manufacture, the factory determines the dc resistance of the outer conductor of each cable section at 10.0°C. This reference reading and the known temperature coefficient are then sufficient to relate temperature to dc resistance throughout the range of interest. Working the outer conductor during cable handling in the factory and from the factory to the ship increases the resistance by an amount equivalent to approximately 0.25°C temperature change on the average. A correction for this is made in the temperature calculation.

If the ship is stationary, a satisfactory measurement can be made as described above. If the ship is pitching or rolling, however, motion of the coiled cable in the earth's magnetic field induces voltages which can cause errors in the measurement. To overcome this problem, instead of measuring a block directly, the two halves of the block are measured in parallel. In this way, the voltages induced by ship motion in the two halves tend to cancel. As an added precaution, high measuring currents (up to 500 mA) are used to make the voltage drop from measuring current much larger than the motion-induced voltages.

The correlation under carefully controlled conditions between thermocouple and direct current resistance (DCR) measurements has been



quite satisfactory. The high-current DCR method is regarded as the primary cable temperature measurement. The thermocouple results are used for check and backup.

#### IV. CABLE LAYING FACILITIES—C. S. LONG LINES

References 8 to 11 discuss the construction and operation of the Bell System Cable Ship *Long Lines*, first used for installing SD cable systems. This section discusses the extensive changes made to the ship to permit handling of SG cable and repeaters.

##### 4.1 Reasons for modifications

Cable used in the SG system is larger, heavier, and stronger than the cable used in previous systems. Table II compares the size, strength, and weight of SG armorless cable and SF armorless cable. The larger diameter of SG cable limits a single shipload to approximately 770 nautical miles (1429 km). With 5.1-nmi (9.46 km) repeater spacing, one equalizer for each 30 repeaters and one-half mile of cable between the equalizer and each adjacent repeater, there is an average of 4.8 nmi of cable for each repeater and equalizer. Thus, it is necessary to stow approximately 160 repeater plus equalizer “bodies” on the ship.

##### 4.2 Linear cable engine

The greater weight and resultant greater laying loads for SG cable required extensive modifications to the linear cable engine. In its original configuration, it had one drive power unit (electric motor and hydraulic pump combination), one main brake, and one hydraulic motor each for payout and pickup operation.

###### 4.2.1 New drive motor and drive power unit

To increase the laying tension capability at 8 knots payout speed from 8000 to 16,000 pounds (3629 to 7257 kg), a new hydraulic motor was added and connected, through a gear box, to the upper forward sprocket shaft. The new motor operates only in the payout (hold-back) mode. A second drive power unit was then added to provide sufficient high pressure oil flow to drive both the old and the new motors simulta-

Table II — Comparison of physical properties of SF and SG armorless cable

	SG	SF
Outer diameter (inches/mm)	2.07/52.6	1.75/44.5
Strength (pounds/kg)	37,000/16,783	16,000/7257
Weight per nautical mile, in sea water (pounds/kg)	3,500/1588	2,000/907
Expected laying tension in 3 miles of water (pounds/kg)	10,500/4763	6,000/2722

neously. Isolation and cross-connection features are provided so that the engine can be run with both motors and both power units or, for lower laying loads, in the original one-motor configuration with either power unit. The engine cannot be operated with the new motor only since the old motor cannot readily be disconnected.

#### **4.2.2 Track modification**

The shear-limiting feature of the linear cable engine<sup>10</sup> was modified for the SG laying loads. Since the extensional elastic properties of the cable, as well as the weight in water, are determined primarily by the steel center strand as in previous cable designs, the maximum required shear limiter travel remained unchanged at one-half inch. This allowed the modification to be made without major redesign of the roller carriages. The higher loads were accommodated by using higher modulus springs in the roller carriage assemblies and by preloading the springs to approximately twice the load used previously.

New gripper blocks were designed for the larger diameter of SG cable. These blocks will handle SF and SG cable satisfactorily, but not SD cable.

#### **4.2.3 New brake**

Increased braking capability is required for the higher SG strength and loads. To provide this, a new hydraulically operated, spring-release brake unit was added on the upper forward sprocket shaft. This provides enough capacity so that, in an emergency, the cable will part before the brakes slip.

#### **4.2.4 Tension displays**

The original aft tension displays used a linear scale from 0 to 16,000 pounds (0 to 7257 kg). The system was changed to provide a quasi-logarithmic\* scale from 0 to 50,000 pounds (0 to 22,680 kg). The scaling gives 0- to 10,000-pound (0 to 4536 kg) indication on the lower half of a 330-degree display, allowing greater resolution in the most commonly used range.

The forward tension displays were similarly changed. The dual 0- to 16,000- and 0- to 100,000-pound (0 to 45,360 kg) linear displays were replaced by 0- to 100,000-pound quasi-logarithmic displays with 0 to 20,000 pounds (0 to 9072 kg) on the lower half.

---

\* The pointer motion is proportional to  $\log(1 + bT)$ , with  $T$  the tension and  $b$  a scaling factor.

### **4.3 Repeater stowage**

In each of bays two and three, repeaters and equalizers are stacked in a rectangular array 16 wide by 4 high, allowing storage of 64 bodies. This is adequate for the 300 nautical miles (557 km) of cable which can be held in each of tanks 2 and 3. Tank 1 can hold 170 nautical miles (315 km). To accommodate this, the repeater stack in bay one is nine repeaters wide by four high. Thus a total of 164 repeaters and equalizers can be carried. For an SF shipload, 116 repeaters and equalizers are required.

### **4.4 Cable stowage**

Figure 5 shows the stowage configuration for cable and repeaters typical of tanks 2 or 3. The arrangement for tank 1 is similar except for the different repeater stack orientation.

The cable is coiled in the tanks in the same way it has been for previous systems. The ends of the cable sections which feed from the tank up to the repeater stack on deck are called up-and-down runners, the up-runner being the end payed out ahead of a repeater, the down-runner the end payed out after the repeater. To prevent crossovers and kinking of the cable, these runners are neatly dressed into slots which lie on the forward wall of the cable tank. They are held in the slots with thick rubber flaps which deform to let the cable come out of the slot during payout.

Because of the larger diameter of SG cable, the slots had to be modified. In tank 1, there are now six up- and six down-runner slots, each deep enough to hold seven runners. This is sufficient to accommodate 41 repeaters, two runners being reserved to lead to the test room or to other cable tanks. In tanks 2 and 3, there are ten up- and ten down-runner slots, each seven runners deep, so 69 repeaters can be accommodated in each of these tanks.

### **4.5 Grapnels**

The SG system uses larger and stronger cables, and closer repeater spacing than earlier systems. These changes led to a need for improved grapnels for repair operations in both shallow and deep water. Three areas of development were undertaken: (i) the design of conventional grapnels with increased strength, with dimensions changed for SG cable, (ii) the design of a powered cut-and-hold grapnel for deep-sea use, and (iii) the design of a simple detrenching grapnel for recovering buried cable.

#### **4.5.1 Conventional grapnels**

Stronger versions of three standard grapnels, the Gifford, the Rennie, and the Flatfish, have been designed and manufactured. These grapnels are illustrated in Figs. 6 and 7.

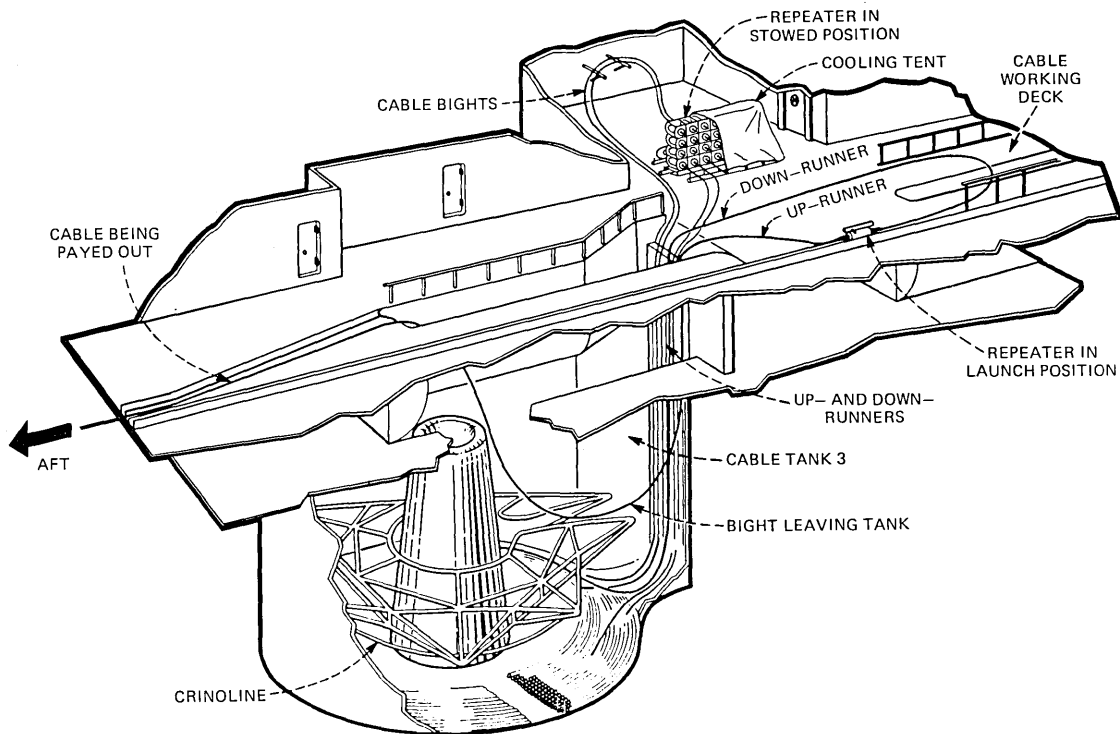


Fig. 5—SG cable and repeater stowage on C. S. Long Lines.

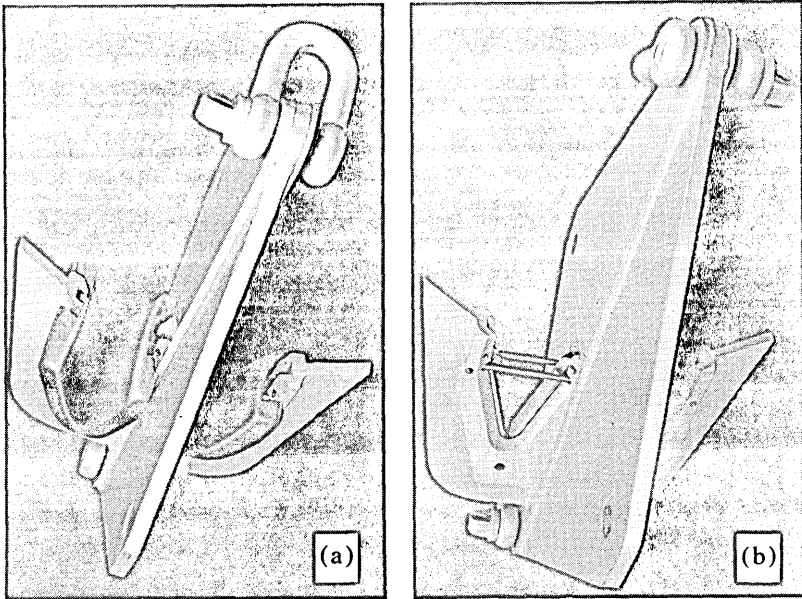


Fig. 6—Flatfish grapnel for SG cable: (a) fitted with “gloves”; (b) fitted with breakaway bars.

The Flatfish grapnel, Fig. 6, has been designed to cut or to hold all types of SG cable. If the grapnel is required for recovering cable, “gloves” are fitted over the blades at their base. For use in the cutting mode, two types of cutting blades have been produced, curved blades for armorless cable and conventional straight blades in a V-formation for armored cable. In addition, the grapnel can be fitted with bars located either side of the open end of the blades. As the cable tension increases, the bars suddenly break, and the cable impacts against the cutting blade, thus increasing the cutting action.

The Rennie grapnel, Fig. 7a, is conventional except for the use of replaceable prongs. The Gifford, Fig. 7b, is also conventional in design except for the inner surface of the “hook”; this has a V-formation, which reduces cable slip through the grapnel.

The new designs were tension-tested to 67,000 pounds (30,390 kg) and proved to be suitable by use during the TAT-6 laying operation.

#### **4.5.2 Cut-and-hold grapnel**

When carrying out a deep-sea repair, the cable must be cut before the ends can be brought to the surface. To prevent damage to the repeaters, they should not be dragged along the sea bed during this operation. The cut-and-hold grapnel is designed to cut the cable and also to hold onto

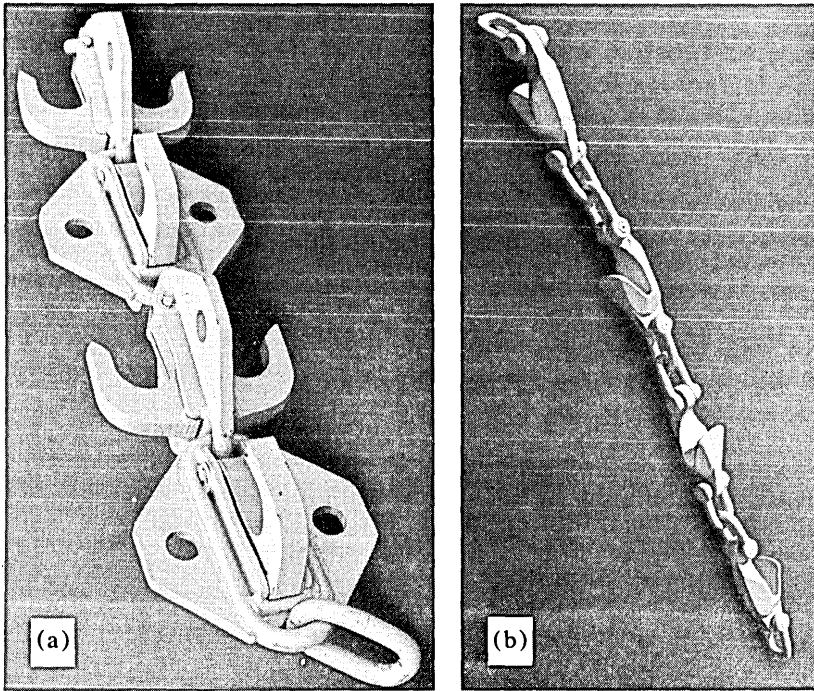


Fig. 7—Rennie and Gifford grapnels.

one end without applying a large tension which would displace the cable from its route.

The grapnel is powered by stored compressed nitrogen, and is hydraulically actuated. When the cable is engaged, a valve is operated which switches oil at 5,000 psi to a large ram with a six-start thread on the periphery of the cylinder. The ramrod is fixed, so the cylinder advances and, as it passes through a fixed nut, it rotates. Protruding horns are fixed to the cylinder and, when one of the horns catches the cable, a bight (loop) is belayed (wound) around the cylinder. At the end of the ram stroke, a second valve is operated which drives two guillotines whose blades can be positioned so that a predetermined side of the cable can be cut away, no matter which side is up when the grapnel lands on the sea bed, while the other cable end is left belayed around the cylinder. Thus one grapnel run cuts the cable and recovers one end.

A sonar surveillance system is built into the grapnel. The rate of transmitted pulses indicates the progress of the operation. The grapnel is suitable for operation to depths of 5000 fathoms.

#### **4.5.3 Detrenching grapnel**

An anchor-shaped detrenching grapnel was developed for the recovery

of those sections buried by the cable plow. A prototype grapnel designed for a 36-inch (0.914 m) penetration in a granular sea-bed was successfully tried at sea in June 1976. Towing forces, although manageable, were high, and therefore a reduced penetration of 26 inches (0.660 m) has been chosen for the production grapnels. These should require towing forces of no more than 18,000 pounds (8165 kg).

## V. CABLE PLOW

A new Bell System cable plow, designated Sea Plow IV,<sup>12,13</sup> was used to bury cable on both ends of TAT-6. The new plow is capable of burying cable and repeaters to a depth of 24 inches and of working in water depths up to 500 fathoms.

## VI. CONCLUSION

This paper summarizes the electrical and mechanical designs and design modifications which were needed to lay, measure, and maintain an SG undersea cable link. The new automated laying test sets and shipboard computer facility were powerful and versatile tools which lifted the pressure of routine chores from test room personnel. The repeater monitoring set proved to be a highly useful and sensitive source of performance information on the undersea system. Modifications of the cable and repeater stowage and handling arrangements served well in the TAT-6 installation. The modified linear cable engine handled the large diameter SG cable smoothly.

The success of these numerous designs, involving several technical disciplines, is due to the expertise, dedication, and teamwork of many contributors, on both sides of the Atlantic. The authors humbly acknowledge their vital contributions.

## REFERENCES

1. SD Submarine Cable System, B.S.T.J., 43, No. 4 (July 1964).
2. D. N. Harper, B. O. Larson, and M. Laurette, "SG Undersea Cable System: Commissioning: Final System Alignment and Evaluation," B.S.T.J., this issue, pp. 2547-2564.
3. E. T. Calkin, I. Golioto, W. J. Schatz, R. E. Schroeder, and D. S. Shull, "SG Undersea Cable System: Undersea System Power," B.S.T.J., this issue, pp. 2497-2522.
4. C. D. Anderson, W. E. Hower, J. J. Kassig, V. M. Krygowski, R. L. Lynch, G. A. Reinold, and P. A. Yeisley, "SG Undersea Cable System: Repeater and Equalizer Design and Manufacture," B.S.T.J., this issue, pp. 2355-2403.
5. W. B. Hirt and D. O. Oldfather, "Transmission Tests, Computations and Equalization During Installation," B.S.T.J., 49, No. 5 (May-June 1970), pp. 783-798.
6. W. G. Ramsey, Jr., W. B. Hirt, P. P. Theophall, and G. A. Ferguson, "Tuning to Concert Pitch—Installation Techniques," National Telecommunications Conference, 1976, Conference Record.
7. *Copper Wire Tables*, National Bureau of Standards Handbook 100, February 21, 1966.
8. R. D. Ehrbar, "A Cable Laying Facility," B.S.T.J., 43, No. 4, Part 1 (July 1964), pp. 1367-1372.
9. O. D. Grismore, "Cable and Repeater Handling System," B.S.T.J., 43, No. 4, Part 1 (July 1964), pp. 1373-1394.

10. R. W. Gretter, "Cable Payout System," *B.S.T.J.*, 43, No. 4, Part 1 (July 1964), pp. 1395-1434.
11. J. H. Butler, C. J. Altenburg, R. J. McSweeney and L. E. Sutton, "Design and Powering of Cable Ship Long Lines," *B.S.T.J.*, 43, No. 4, Part 1 (July 1964), pp. 1435-1459.
12. G. S. Cobb, D. L. Garren, and T. H. Rose, "Sea Plow IV: Digging-in the Newest Transatlantic Cable," *Bell Laboratories Record*, 54, No. 8 (September 1976), pp. 220-224.
13. D. L. Garren, "Two Feet Under Is Ten Times Safer—New Techniques for Plowing Cables and Repeaters," National Telecommunications Conference, 1976, Conference Record.



## ***SG Undersea Cable System:***

# **Commissioning: Final System Alignment and Evaluation**

By D. N. HARPER, B. O. LARSON, and M. LAURETTE

(Manuscript received October 7, 1977)

*A comprehensive line-up and test program called commissioning was developed for the SG Undersea Cable System. The program provides instructions for measurement, alignment, and evaluation of various performance parameters of the system. Equalization, optimization of signal-to-noise ratio, and system alignment are the primary objectives of commissioning. Measurement of performance parameters such as differential gain and phase, phase jitter, and impulse noise count distribution with threshold level are included in the test program. This paper describes the commissioning process, interspersing both a general description of procedures and selected test results from the TAT-6 link.*

## **I. INTRODUCTION**

Commissioning, a British Post Office term, is the test and adjustment program (or process) performed on a newly installed undersea cable link before it is placed in service. The cable system is measured and aligned, and its performance is optimized. This process starts during installation and continues until the terminal-to-terminal link is ready to be released for service. The bulk of the effort takes place after cable laying<sup>1</sup> is finished; that is, after the final splice, and can take several weeks to complete. This paper describes the commissioning process for the SG system. General descriptions of the test program and illustrative data from the TAT-6 link are provided. Fault localization reference data, although part of commissioning, are not discussed.

Successful completion of commissioning means that the cable and

terminal transmission equipment (supergroup-to-supergroup) are equalized, signal-to-noise ratio is optimized over the transmission bands, and the terminal equipment is adjusted so that service may begin. Accurate commissioning test data are vitally important because these data are used also to:

- (i) Determine link operating performance.
- (ii) Compare actual with computed performance.
- (iii) Provide initial data so that future link performance may be evaluated.
- (iv) Obtain reference data for maintenance purposes.

Incidentally, the SG system differs from the SF and SD systems<sup>2,3</sup> in that the undersea link transmission can be adjusted from the terminal, by means of shore-controlled equalizers.<sup>4</sup> Five sectors, each approximately 650 nautical miles (nmi) long, were created in the TAT-6 link by using four shore-controlled equalizers. Undersea link transmission is separately adjustable for four of the five sectors using these equalizers (discussed in Section IV); terminal adjustments affect the entire link.

## II. THE TRANSMISSION LINK

The system is designed to provide at least 4000 three-kHz channels (from supergroup to supergroup) over ocean distances of up to 4000 nmi. Associated with the undersea single-cable link are two-wire to four-wire terminals located at opposite ends of the link<sup>5</sup> (see Fig. 1). The two terminals are defined "A" and "B" terminals, respectively. At line (cable) frequency, the A terminal transmits in the low band or A-to-B direction, 0.8 to 13.9 MHz, and receives in the high band or B-to-A direction, 16.5 to 30.0 MHz; the B terminal is complementary. A 31.62-MHz conversion frequency is used to translate the high-band baseband, 1.6 to 15.1 MHz, to line frequency at the B terminal and re-establish the baseband at the A terminal. The low-band baseband and line frequencies are identical. These frequency ranges individually and collectively are termed wideband.

Each terminal is composed of separate transmit and receive sections that are used to provide the four-wire supergroup connection to the domestic network external to the terminal. Towards the undersea link, transmit and receive signal paths are combined in a directional filter furnishing the two-wire match with that link. To achieve reliability, major parts of the terminal are duplicated; this feature increased the amount of data-taking and record-keeping needed for commissioning.

For commissioning, the terminal-to-terminal link can be thought of as being made up of three nested links as shown in Fig. 1:

- (i) Wideband-to-wideband link (wideband link).\*
- (ii) Hypergroup-to-hypergroup link (hypergroup link).†

---

\* The undersea link is part of the wideband link.

† A hypergroup is an ordered frequency-contiguous set of supergroups (see Ref. 5).

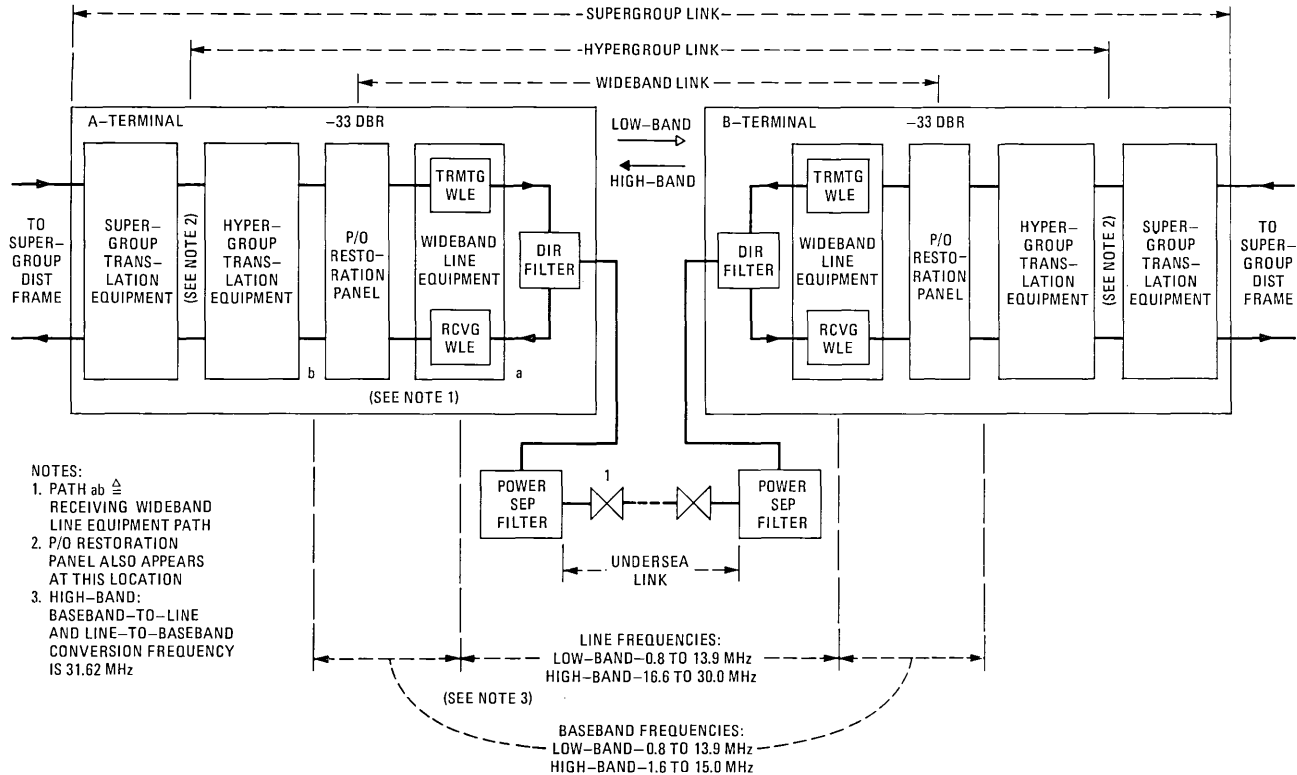


Fig. 1—SG undersea cable system.

(iii) Supergroup-to-supergroup link (supergroup link).

Following any necessary adjustments in the undersea link using the shore-controlled equalizers, measurements and adjustments proceed from the wideband to hypergroup to supergroup links.

The wideband/hypergroup interface is the restoration panel.\* This interface is a  $-33$  dBr<sup>†</sup> nominal flat-level point, for both transmit and receive. Transmission measurements between restoration panels in the two terminals define the misalignment of the wideband link which is due primarily to the long undersea section.

### III. COMMISSIONING TEST PROGRAM

Development of the commissioning test program is a process that requires data and other information from virtually all areas of cable system development such as repeaters and equalizers,<sup>4</sup> terminals,<sup>5</sup> cable,<sup>6</sup> and power separation filter.<sup>7</sup> Use of specialized test equipment developed for the SG system, such as the cable laying test set, the data translator, and the repeater monitoring set, is integrated into the test program<sup>1</sup> as is the use of a modern table-top computer system.

The commissioning test program is divided into four categories of tests. The four groups of tests are carried out sequentially, each succeeding category building more or less upon the results of its predecessors:

- (i) Undersea link tests—between cable laying operations.
- (ii) Shore preparation tests—prior to final splice.
- (iii) Line-up tests—after final splice.
- (iv) Reference and special tests—follows link alignment.

#### 3.1 Objectives

Even though the four groups of commissioning tests are done sequentially, it is more illuminating to consider the line-up tests, (iii), as being central to commissioning. Most preceding tests, (i) and (ii), are preparatory to line-up. Most subsequent tests, (iv), are designed to provide information that can be used to maintain the lined-up link status or confirm the engineering design of the system. Equalization, optimization of the signal-to-noise ratio (s/n) over each baseband, and terminal adjustments (including pilots) are the major objectives of the line-up procedures.

Transmission data from the line-up tests, however, cannot be referenced in level unless various transmission path gains (or losses) of the terminal, the power separation filter, and the shore section<sup>‡</sup> are measured

---

\* The restoration panel provides a manual patching arrangement used to accomplish alternative traffic routing in the event of an undersea transmission failure.

<sup>†</sup> dBr is equivalent to dB TLP (TLP is transmission level point).

<sup>‡</sup> The shore section is the cable between the terminal and the repeater closest to the terminal.

or computed beforehand. For example, the transmission gain of path *ab*, Fig. 1, is measured.

Prior to the shore preparation tests, undersea system tests are made to determine (or estimate) performance parameters such as warm-up time and cable aging.\* Figure 2 shows the TAT-6 warm-up characteristic at high-band supervisory tone frequencies (approximately 27.7 MHz) after power turn-up. Most of the gain change occurs over the two continental shelves and takes place within about 10 hours. The change is due largely to internal warm-up of temperature-controlled repeaters.<sup>4</sup> Obviously, it is important that equalization be based on nonchanging data taken after this 10-hour warm-up period.

After the line-up tests are completed, reference and special tests are performed. The objective of the reference tests is to obtain for future comparison initial supervisory tone, pilot, and transmission measurements (made at discrete frequencies between supergroups). Identical measurements can be made in the future without service interruption, thereby providing an excellent way to monitor changes in undersea link transmission.

The objective of the special tests is to obtain by direct measurement such engineering parameters as change in system gain with line current, differential gain and phase, phase jitter, and impulse noise count distribution, to name a few. Figure 3 shows the measured TAT-6 high-band

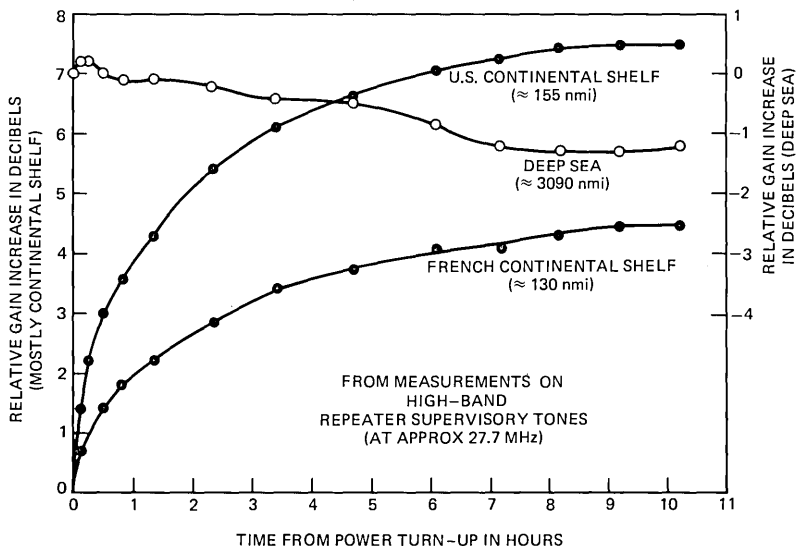


Fig. 2—TAT-6 high-band warm-up characteristic following power turn-up from cold start.

\* Warm-up time is the relatively short-term interval required to reach transmission stabilization following power turn-up from a cold start. Cable aging is the long-term cable transmission change with time (Ref. 8).

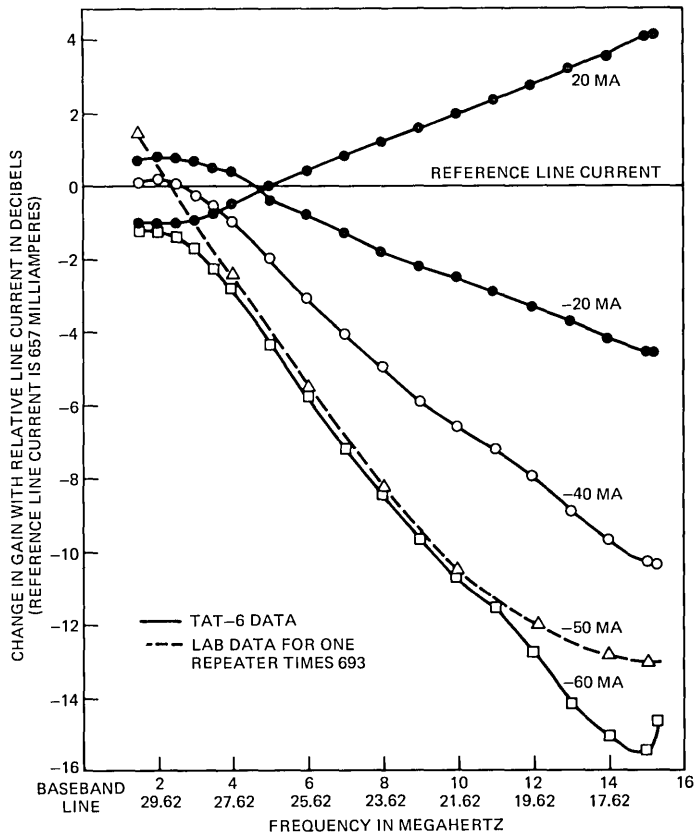


Fig. 3—TAT-6 high-band change in gain with line current.

change in gain as line current is stepped from the nominal 657 milliamperes. Measured gain-change data correlated well with laboratory data on a single repeater scaled by 693 (the number of repeaters in TAT-6). In the event of a shunt fault in the undersea link, there is always the possibility that changes in line current, along with other adjustments, could be used to modify undersea misalignment so that some service could continue until repair was possible. The other engineering parameters listed above are discussed in Section VI.

### 3.2 Methodology

The lengthy commissioning test program must be grounded in well-defined procedures no more complicated than absolutely necessary, making use of:

- (i) Standard data forms.
- (ii) Standard definitions.
- (iii) Standard list of test frequencies.

Considerable effort was put into developing individual, but standardized, data forms for the various commissioning tests. The forms, in general, represent a method of entering data, and intermediate and final results as a function of frequency. Short equations are provided on the forms, as necessary, to describe how the measured data should be handled to compute an intermediate or final result. These equations can be used as a computer program instruction for keyboard entry into the table-top computer system mentioned previously. A general-purpose program called UTILITY was written to implement this capability. In summary, the computer system served several purposes. It provided:

- (i) Speed of data manipulation and computation.
- (ii) Data storage.
- (iii) Plotting.
- (iv) Analysis of on-site tests not specifically listed in the test program.
- (v) Backup, since the computer can be used to compute results based on data from either station.
- (vi) Supergroup equalizer design (Section 4.4).

Finally, attention was paid to historical and practical ways of defining submarine cable link transmission subpaths to optimize the testing process. Commissioning test frequencies covering the wideband portion of the SG system were chosen to be compatible with the use of the cable laying test set.<sup>1</sup> Defined transmission subpaths and the testing frequencies were integrated into the standardized test forms.

## **IV. EQUALIZATION**

### **4.1 The equalization process**

During installation of the undersea link, residual misalignment is substantially compensated for at the end of laying each ocean block using the associated ocean-block equalizer (OBE).<sup>4</sup> A buildup of misalignment unequalizable in the OBEs invariably occurs, accumulating along the length of the undersea link. This end-to-end residual misalignment is compensated for (to the extent possible) in two ways:

- (i) By adjustment of undersea link levels on a sector basis using the shore-controlled equalizers.
- (ii) By terminal equalization adjustments.

### **4.2 Undersea link adjustment**

Four shore-controlled equalizers (SCE),\* which divided the undersea link into five sectors, were deployed to compensate for transmission changes due to cable aging<sup>8</sup> over the life of TAT-6 (see Section I). How-

---

\* The shore-controlled equalizers are controllable from the Green Hill Station, with SCE 1 being closest to that station.

ever, sufficient aging (added loss) had occurred over the five-month installation interval to justify a reoptimization of SCE settings following the final splice.

The average transmission level\* of each of the four sectors beyond SCE 1 was adjusted to the extent possible to the average level of Sector 1. Since only broadband equalizer shapes are available in the SCEs, the selected settings are a compromise. In the low band only SCE 1 needed readjustment; in the high band, SCE 1, SCE 2, and SCE 3 were reset. Figures 4a and 4b show undersea link levels versus distance at two typical frequencies, 19 and 26 MHz, before and after SCE adjustment.

### 4.3 Terminal equalization—wideband

#### 4.3.1 The plan

The terminal wideband equalization plan is illustrated in Fig. 5. Equalizer networks are discussed in more detail in Ref. 5. For the ideal situation (no equalization required), *line buildout (LBO) networks* are used to build out shore section loss to 3/4 of a cable section (3.83 nmi<sup>†</sup>) to conform to SG system design. In addition, the transmit combination of *shore section, LBO networks, pre-emphasis network, and path equalizer network* is designed to shape the flat-level signal coming from the inland network to a computed characteristic which provides optimum s/n in the undersea link. The receive part of the terminal at the other end of the undersea link is complementary, restoring the shaped signal to a flat level for transmission to the inland network.

In the real world, however, remaining misalignment, principally in the undersea link, will require terminal equalization. Additional transmit terminal signal shaping will also be needed to optimize s/n in the undersea link, since most levels end up being nonideal. Terminal equalization is carried out in three phases:

- (i) Wideband equalization, transmit end only (before optimization of wideband s/n).
- (ii) Wideband equalization, receive end only (after optimization of wideband s/n).
- (iii) Supergroup equalization, where required.

Transmit-end equalization (before s/n optimization) is accomplished using *residual equalizer networks, adjustable corrector networks, and adjustable bump equalizer networks*. Normally, most of the transmit-

---

\* The average level of an undersea sector is the average of the level averages of individual blocks in that sector. (The undersea link levels were determined on a broadband basis during cable laying. Subsequently, level can only be measured at supervisory tone frequencies, essentially one frequency in each band. This latter level information is interpolated to other frequencies by fitting an equation of the form  $a\sqrt{f} + bf$  to the data.)

† The shore section is between 1/4 and 3/4 of the nominal repeater spacing (5.1 nmi of 1.7-inch cable).



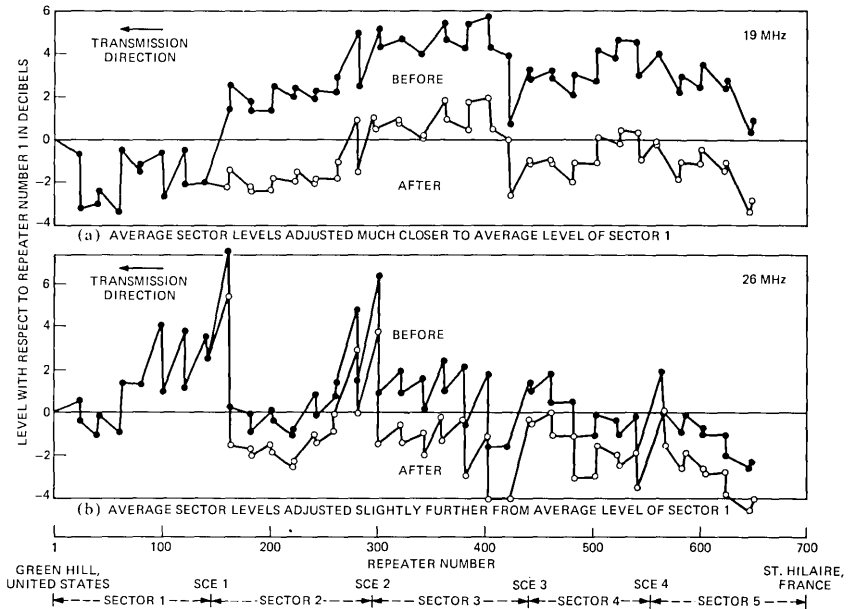


Fig. 4—TAT-6 lengthwise level distribution at 19 and 26 MHz before and after SCE adjustment.

end misalignment (and receive-end misalignment also) is equalized with the residual equalizer networks.

The residual equalizer networks are of the bridged-T type, custom-designed during commissioning using a previously written computer program. For TAT-6, a data link from Green Hill to the Bell Laboratories computer at Holmdel was utilized. Residual networks are built from a stock of high-quality components at the terminal sites and tested there for circuit integrity and transmission performance before being installed in the terminal.

Adjustable corrector equalizer networks are wideband networks of four types, each front-panel-adjustable around a nominal setting:

- (i) Attenuator.
- (ii) Square-root-of-frequency.
- (iii) Slope.
- (iv) Curvature.

Following s/n optimization (details are discussed in Section V), the remaining misalignment (including level changes introduced by s/n optimization) is equalized in the receive part of the terminal. Networks identical to those mentioned above are used to implement receive-end equalization. Figures 6a and 6b show that the remaining misalignment in the low and high bands, respectively, after terminal equalization is

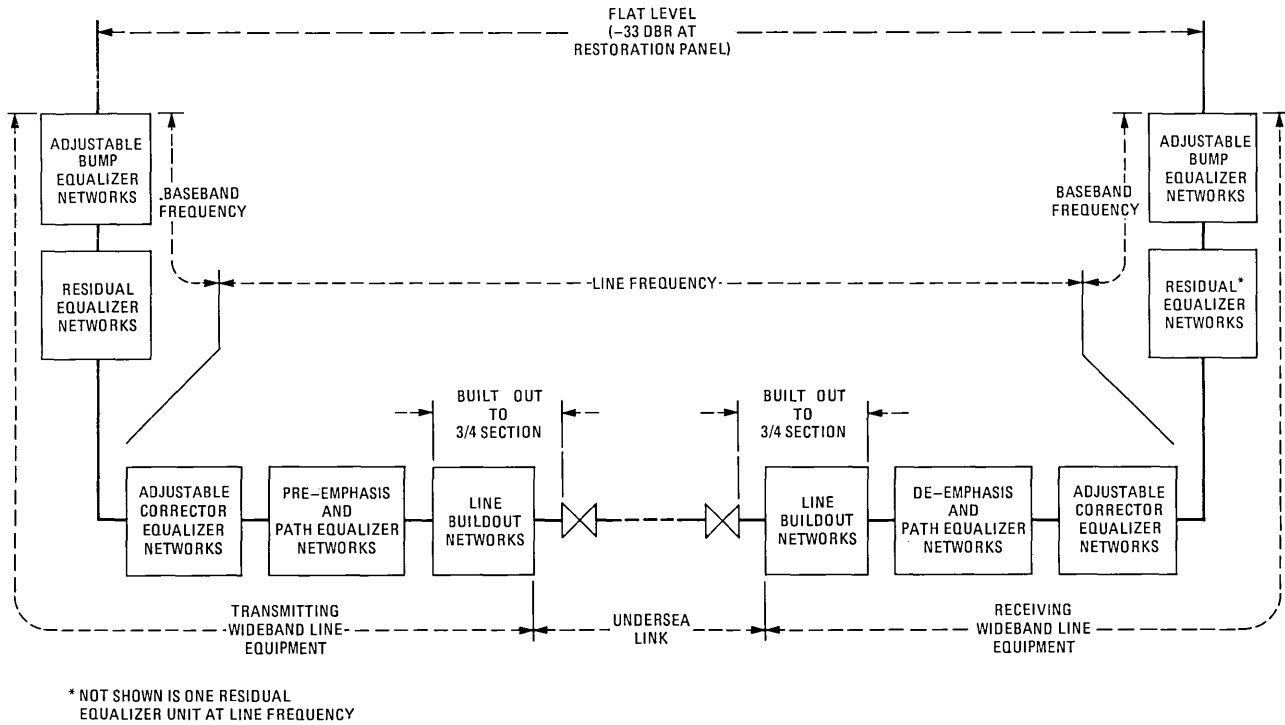


Fig. 5—Terminal wideband equalization plan.

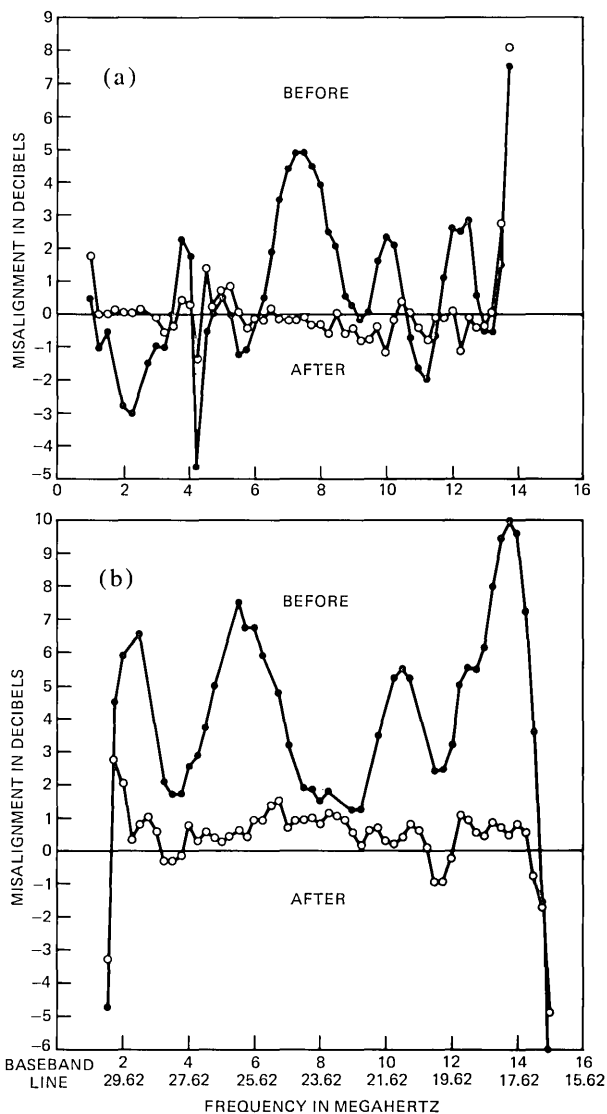


Fig. 6—TAT-6 misalignment before and after terminal equalization. (a) Low band. (b) High band.

for the most part within  $\pm 1$  dB, except near the band edges. Band-edge misalignment is more conveniently equalized at the supergroup level (discussed in Section 4.4).

#### 4.3.2 Transmit-end equalization

Normally, one-half of the wideband undersea misalignment is equa-

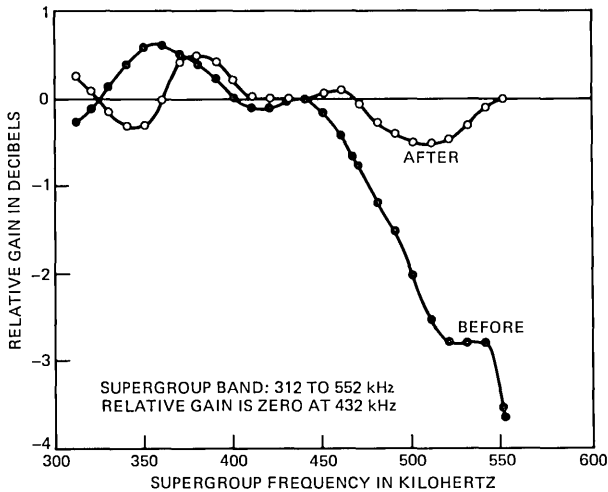


Fig. 7—TAT-6 low-band hypergroup 1, supergroup 4 response before and after supergroup equalization.

lized at the transmit end of the link. Assuming uniform misalignment with distance, this division of equalization should minimize the noise penalty due to misalignment. On TAT-6, however, misalignment is not uniform with distance. Because wideband average level versus frequency had been computed in preparation for the SCE adjustment procedure, it seemed more appropriate to decide the extent of transmit-end equalization by comparing the following three parameters:

- (i) Average level.
- (ii) End-to-end misalignment.
- (iii) Estimated obtainable equalization from residual equalizers.

The final transmit-end equalization decision is obviously a compromise based on computations and experience. This equalization decision is too detailed to be discussed here.

#### 4.4 Terminal equalization—supergroup

Supergroups are equalized individually only if the magnitude of the differences in transmission between the center of the band, 432 kHz, and the rest of the band, 312 to 552 kHz, exceeds 1.5 dB.<sup>9</sup> Supergroup equalization, where required, is carried out after final wideband equalization.

Supergroup equalization is accomplished in the *receive supergroup equalization unit*. For the fifty-some supergroups in each band of TAT-6, at most four band-edge supergroups in each band required equalization, plus two in-band supergroups in the low band. Figure 7 shows how the relative low-band misalignment in hypergroup 1, supergroup 4 (812 to

1052 kHz at line frequency) was equalized at supergroup frequency. An approximate +0.6 to -3.6 dB misalignment range was equalized to within  $\pm 0.5$  dB.

## V. OPTIMIZATION OF WIDEBAND SIGNAL-TO-NOISE RATIO

Optimization of the wideband s/n in the SG system is accomplished by changing one or more of the adjustable corrector or bump equalizer networks in the transmit terminal. This changing reshapes the broadband undersea transmission levels (additional signal shaping). The adjustment process is semi-empirical in that it determines, mostly by trial and error, whether or not a particular equalizer adjustment improves or degrades performance. The test signal load is broadband Gaussian white noise. (Test signal power is varied step-wise to define the maximum s/n at the frequency of test.) The process is actually one of obtaining undersea link levels versus wideband frequency for which the difference between the test signal noise load and the power sum of thermal noise and intermodulation distortion in narrowband test slots (the noise power ratio [NPR] in decibels) is a maximum.

For the TAT-6 link, NPR is measured in several narrow-band test slots in the low and high bands using a white noise test set. The wideband noise load, which is inserted at the transmit -33 dBr flat-level point on the restoration panel, is adjusted to be equivalent to a load of 4000 channels with an average channel power of -13 dBm0. A relatively narrow bandstop filter (part of the test set) is introduced to clear a slot in the transmitted noise load. The noise power which appears at the receive terminal restoration panel is measured at this slot frequency in an even narrower band (using test set filtering), both without and with the bandstop filter. The ratio of these two measurements is the NPR.

The final NPR data from the TAT-6 commissioning is given in Table I, including the equivalent 3-kHz channel noise in dBrnC0. Because of an unforeseen problem which resulted in higher-than-expected third-order intermodulation products, the desired NPR was not attained in

Table I — TAT-6 optimized noise power ratio and equivalent 3-kHz channel noise power

Low Band			High Band		
Freq (MHz)	Noise Pwr Ratio (dB)	3-kHz Ch Noise Pwr (dBrnC0)	Freq (MHz)	Noise Pwr Ratio (dB)	3-kHz Ch Noise Pwr (dBrnC0)
1.248	42.8	31.7	18.142	37.6	36.9
2.438	42.8	31.7	21.494	36.0	38.5
5.340	44.0	30.5	22.948	36.0	38.5
8.672	41.0	33.5	26.280	30.1	44.4
10.126	41.7	32.8	26.970	29.5	45.0
13.478	39.8	34.7	29.182	28.6	45.9

Table II — TAT-6 differential gain in undersea link

Low Band					High Band				
Freq (MHz)	Differential Gain in dB dB Above Design Load				Freq (MHz)	Differential Gain in dB dB Above Design Load			
	2	4	6	8		2	4	6	8
1.248	-0.1	-0.2	-0.3	-0.4	18.142	-0.1	-0.2	-0.3	-0.5
2.438	-0.05	-0.2	-0.15	-0.2	20.046	-0.1	-0.3	-0.4	-0.6
3.886	-0.05	-0.15	-0.3	-0.45	21.494	-0.1	-0.2	-0.5	-0.8
5.340	-0.1	-0.2	-0.4	-0.65	22.948	-0.1	-0.3	-0.5	-0.7
8.672	-0.2	-0.4	-0.8	-1.2	26.280	-0.1	-0.4	-0.7	-1.1
10.126	-0.25	-0.65	-1.15	-1.9	26.970	-0.2	-0.5	-0.9	-1.3
11.574	-0.1	-0.2	-0.4	-0.8	29.182	-0.1	-0.3	-0.5	-0.8
13.478	0.0	0.1	0.1	0.1					

Design load is 23 dBm0 per band.

the upper part of the high band.<sup>4,8</sup> In the low band, the attained NPR performance ranged from 3.8 to 8.0 dB better than the objective.

## VI. SELECTED PERFORMANCE DATA—TAT-6

### 6.1 Differential gain—undersea link

Table II gives the differential gain of the undersea link as a function of relative signal load. For this test, a  $-20$  dBm0 tone was inserted in a cleared slot in a broadband white noise test signal load. This test load was varied from 26 dBm0 (the design load) to 8 dB higher, with the difference between the received power of the  $-20$  dBm0 tone at test loading and at design load being differential gain. The data show compression at all frequencies except near the top of the low band, where there is 0.1 dB of expansion. Maximum compression occurs near 10 MHz in the low band and 27 MHz in the high band. Below design load, it was determined that expansion (with respect to design load) was negligible.

### 6.2 Differential phase—undersea link

Figure 8 shows the differential phase of the undersea link in the high band as a function of signal load relative to high-band design load. A novel method making use of the repeater monitoring set (RMS) was used to measure differential phase. (The RMS is described in Ref. 1.) First, using standard techniques, a composite test signal was sent from the transmit end of the link:

- (i) High band noise load amplitude modulated at 5 Hz to a depth of approximately 90 percent.
- (ii) A tone of  $-20$  dBm0 inserted in a cleared slot of the white noise load (the tone was not modulated).

The peak power (crest of modulation) of the modulated load is set at the desired test loading in the high band; the minimum power (valley of modulation) is approximately equivalent to no load. Second, at the re-

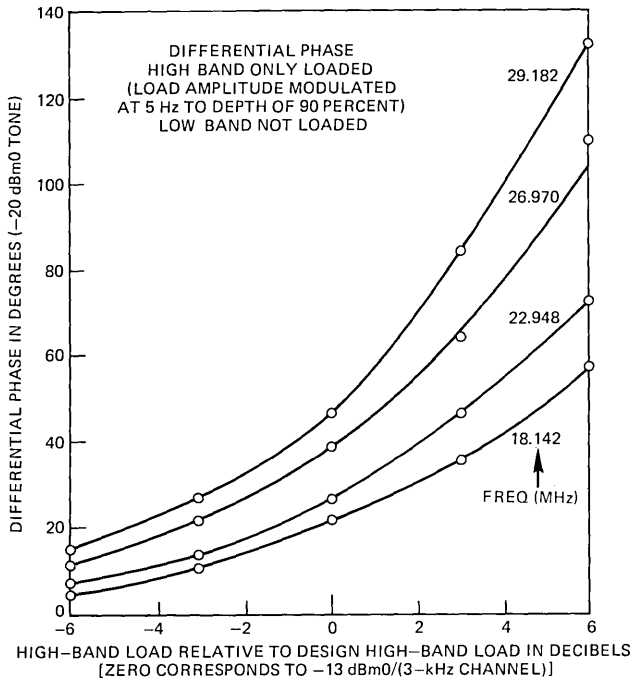


Fig. 8—TAT-6 high-band differential phase in undersea link.

ceive end of the link the composite signal is connected to the RMS. The transmit noise load is then reduced to essentially zero using an attenuator, and the RMS is phase-locked to the tone. Following this operation, the 50-Hz-wide, 100-kHz phase-locked loop of the RMS is opened. The transmit noise load is then reapplied.

The relative positions of the RMS reference 100-kHz signal and the phase-locked-loop 100-kHz error signal are monitored on an oscilloscope. Each of these signals is a square wave, and any movement of the error signal is easily calibrated in degrees. The difference between the position of the error signal at test loading power (crest of modulation) and no load (valley of modulation) is the differential phase of the undersea link. Drifting in the opened phase-locked loop is minimal, as can be observed on the oscilloscope by comparing the 100-kHz reference signal with the error signal at no load.

Maximum differential phase occurs at the top end of the high band, being 47 degrees at high-band design load and 133 degrees at 6 dB above this design load. The 133-degree figure has some relevance because undersea link highband levels will be increased from commissioning levels when the effect of third-order intermodulation products is reduced by terminal cancellation arrangements.<sup>4,8</sup>

Table III — TAT-6 measured phase jitter

Low Band			High Band		
Approximate Line Freq in MHz	Hyper- group— Supergroup	Phase Jitter in Degrees Peak-to-Peak	Approximate Line Freq in MHz	Hyper- group— Supergroup	Phase Jitter in Degrees Peak-to-Peak
1.0	1-4	0.8	16.9	6-11	1.2
4.2	2-13	0.8	19.8	5-12	1.2
7.5	3-9	0.9	22.2	4-12	1.2
10.2	4-9	1.1	24.9	3-13	1.4
13.5	5-5	1.1	26.7	2-10	2.4
			29.4	1-9	3.1

Measurements made in channel 1, group 1 of listed supergroup.

### 6.3 Phase jitter

Table III gives the measured phase jitter of the TAT-6 link. Phase jitter was measured in channel 1 of group 1 in a sufficient number of supergroups to characterize the low and high bands. Phase jitter is 0.8 degree peak-to-peak at the bottom of the low band and increases with frequency across the low- and high-band spectrum to approximately 3.1 degrees peak-to-peak.\*

### 6.4 Impulse noise

Impulse noise power peaks exceeding approximately 12, 14, 16, and 18 dB above average (continuous) noise power were counted over 15-minute intervals for several supergroups to sample the low and high bands. Measurements were made at the channel level and supergroup level using different test instruments. The impulse noise count data were reduced to the fraction of time that signal peaks exceed peak amplitude threshold. Figure 9 shows these data for the low band at channel level.

Essentially, Fig. 9 confirms that the number of impulse counts measured at different peak amplitude thresholds follows a Gaussian distribution typical of thermal noise. The important observation from Fig. 9 is that, as long as the reduced data curves parallel that of the thermal noise, the source of the impulses is indistinguishable from system noise and not due to non-Gaussian processes such as corona. The fact that the curves do not lie on the thermal noise curve is caused by several factors, the largest being (iii), which fortunately causes only a horizontal offset:

- (i) Error in measurement.
- (ii) Calibration of test instrument.

\* The phase jitter data are believed to be pessimistic because the measurements were influenced by channel noise, particularly at the higher line frequencies.



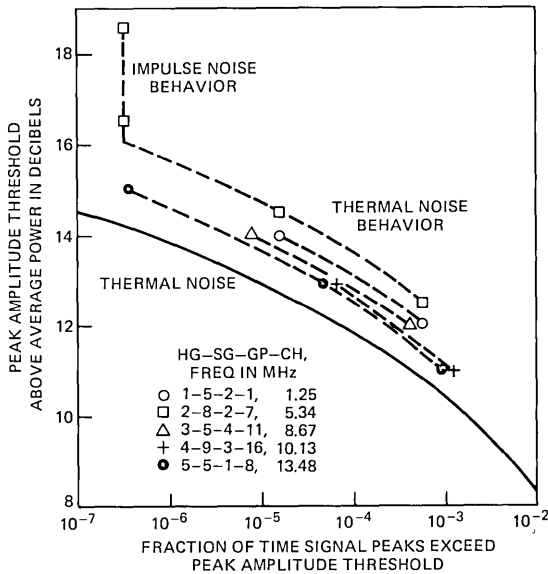


Fig. 9—TAT-6 low-band distribution of impulse noise count data.

(iii) Estimate of available number of time slots for which impulses could be counted.

The one indication of an impulse, a count exceeding two different threshold levels, may have been due to inadvertent terminal switching (probably caused by a carrier supply phase problem evident during the time that this test was made).

## VII. COMPILED OF COMMISSIONING DATA

Commissioning data are compiled in three areas, basically:

- (i) Data books.
- (ii) Punched paper tape.
- (iii) Magnetic cassette tape.

The more important data from both stations are compiled at each station; therefore, duplication of data records is achieved. A separate data book is maintained for each of the four categories of tests mentioned in Section III. Each of the data books is sectionalized so that data from specific tests may be easily entered or retrieved.

The commissioning tests are generally run in sequence as directed in the test instructions, each succeeding test relying more or less upon the results of one or more previous tests. As the tests proceed day after day, the books are completed section by section, forming a permanent record of measured and computed data. Supplementing this record are selected

TTY punched tapes of measured data and magnetic cassette tapes. The printed page output from the computer system printer and graphs from the plotter are also entered into the data books where required. The punched tapes and magnetic cassette tapes are especially useful for comparison of data from identical tests separated in time, since these tapes provide an easy way to enter data into the computer.

Regarding residual equalizer design information, a complete record is kept in a separate book at each station:

- (i) Identifying nomenclature.
- (ii) Schematic (with element values).
- (iii) Design and measured transmission.
- (iv) Notes.

In addition to its record function, this book is used for maintenance purposes

### VIII. ACKNOWLEDGMENTS

The authors wish to acknowledge the contributions made by other members of the British Post Office, the Centre National d'Etudes des Télécommunications of France, and Bell Laboratories in carrying out the extensive commissioning test program. Particularly, we want to acknowledge the work of Messrs. P. P. Theophall and W. B. Hirt in adapting many parts of the test program to computer operation.

### REFERENCES

1. J. E. H. Cosier, A. P. Davies, S. W. Dawson, Jr., R. F. Gleason, F. E. Kirkland, and T. A. McKenzie, "SG Undersea Cable System: Installation and Maintenance of Undersea System," *B.S.T.J.*, this issue, pp. 2523-2545.
2. "SF Submarine Cable System," *B.S.T.J.*, 49, No. 5 (May-June 1970), pp. 601-798.
3. "SD Submarine Cable System," *B.S.T.J.*, 43, No. 4, Part 1 (July 1964), pp. 1145-1479.
4. C. D. Anderson, W. E. Hower, J. J. Kassig, V. M. Krygowski, R. L. Lynch, G. A. Reinold, and P. A. Yeisley, "SG Undersea Cable System: Repeater and Equalizer Design and Manufacture," *B.S.T.J.*, this issue, pp. 2355-2402.
5. M. Brouant, C. Chalhoub, P. Delage, D. N. Harper, R. L. Lynch, and H. Soulier, "SG Undersea Cable System: Terminal Transmission Equipment," *B.S.T.J.*, this issue, pp. 2471-2496.
6. G. E. Morse, S. Ayers, R. F. Gleason, and J. R. Stauffer, "SG Undersea Cable System: Cable and Coupling Design," *B.S.T.J.*, this issue, pp. 2435-2469.
7. E. T. Calkin, I. Golioto, W. J. Schatz, R. F. Schroeder, and D. S. Shull, "SG Undersea Cable System: Undersea System Power," *B.S.T.J.*, this issue, pp. 2497-2522.
8. S. T. Brewer, R. L. Easton, H. Soulier, and S. A. Taylor, "SG Undersea Cable System: Requirements and Performance," *B.S.T.J.*, this issue, pp. 2319-2354.
9. Recommendation M46, "Bringing Internation Group, Supergroup, etc., Links Into Service," Vol. IV.1 of CCRTT Green Book.

## Contributors to This Issue

**Cleo D. Anderson**, B.S.E.E., 1960, University of Idaho; M.E.E., 1962, New York University, Bell Laboratories, 1960—Mr. Anderson was involved in systems analysis of the SD and SF undersea cable systems. He then supervised a high-frequency radio group designing facilities for handling overseas and high-seas traffic. Returning to undersea cable work, he was responsible for circuit design of repeaters and the repeater monitoring set for the SG system. Currently, he supervises a group responsible for analyses of undersea cable systems. Member, IEEE, Sigma Tau, Phi Kappa Phi, Eta Kappa Nu.

**Sheila Ayers**, Birkbeck College, London University; British Post Office, Research Department, 1943—. Ms. Ayers has investigated non-linear resistors, piezoelectricity, ferroelectricity, magnetostriction, electro-optics, and low-loss dielectrics. Since 1973, she has been head of a group investigating materials problems in submarine cables and measurement techniques associated with these investigations.

**S. Theodore Brewer**, B.S. (E.E.), 1937, M.S. (E), 1938, Purdue University, Bell Laboratories, 1937—. In his early assignments, Mr. Brewer contributed to the development of broadband coaxial systems and video feedback amplifiers. Later, he explored network control for electronically-controlled switching systems. More recently he was responsible for system and undersea electronics design of the SF Undersea Cable System. Currently, he heads a department which was responsible for system and undersea electronics design for the SG Undersea Cable System. Exploratory work under his direction includes an undersea system of 16,000 channels' capacity. He holds patents on control and feedback systems, switching networks, and repeater circuits. Member, IEEE, Eta Kappa Nu, Tau Beta Pi, Sigma Xi.

**Michael Brouant**, graduate, Ecole Nationale Supérieure de l'Aéronautique, Paris, 1962; CIT-Alcatel, 1964—. At CIT-Alcatel, Mr. Brouant worked on the design of analog line equipment. Since 1968, he has directed the Undersea Terminal Design Section which has carried out detailed design of terminals for the French S1, S5, and S25 systems, as well as the 60-MHz land system. He also was responsible for detailed design of terminals for the SG undersea cable system. In 1975, he took charge of the lightwave transmission section which is developing applications of optical fibers to telecommunications.

**Edwin T. Calkin**, B.S. (Eng.), 1961, the Cooper Union School of Engineering; M.S.E.E., 1963, New York University; Bell Laboratories, 1961—. From 1964 to 1975, Mr. Calkin was principally engaged in circuit development for power converters that energize land and undersea cables. Since 1975, he has been responsible for circuits in low- and medium-power converters used in a variety of Bell System applications. Member, IEEE, AES, and Tau Beta Pi.

**Christian Chalhoub**, graduate, Ecole Supérieure d'Electricité, Paris, 1941. Mr. Chalhoub started his career in the Société d'Etudes pour Liaisons Téléphoniques where he first worked on measurement technology and later on equipment for studio broadcasting. He worked briefly for a firm concerned with medical electronics and then, in 1945, joined CNET (Centre National d'Etudes des Télécommunications), where he was responsible for the laboratory studying high-frequency terminal transmission equipment for carrier systems. In 1956 he joined CIT (Compagnie Industrielle des Télécommunications), a subsidiary of CGE (Compagnie Générale d'Electricité), where he managed the department designing line systems for both land and undersea use. He is currently Deputy Director in charge of Product Policy in the Transmission Division of CIT. Member, SEE (Société des Electriciens, des Electroniciens et des Radioélectriciens).

**J. E. H. Cosier** has been with the British Post Office Research Department for 41 years, the last 32 on undersea repeater systems. His work has covered the field of housings, high pressure seals, undersea cable jointing methods, terminations and taut wire equipment. He is a co-inventor and patentee of the British design of the linear cable engine, and of the cut-and-hold grapnel. Since 1972, he has been Head of the Mechanical Design and Shipboard Laying Equipment Section of the Research Department.

**A. Peter Davies**, British Post Office. Mr. Davies started as a telecommunications apprentice on automatic switching in a London telephone district in 1936. He shifted to cable transmission early in World War II, seeing Army service on the undersea cables laid to serve the European front. Later, he was involved with the development of the U.K. coaxial cable network begun about 1948, transferring to undersea cables in 1962, where he has remained ever since. His interests include the practical application of submerged repeater technology in the marine environment. He is presently Head of the BPO section responsible for undersea plant development, installation, and maintenance.

**S. W. Dawson, Jr.**, B.E.E., 1968, University of Virginia; M.S.E.E., 1970, Duke University; Bell Laboratories, 1968—. Mr. Dawson worked on specialized test equipment design for military undersea cable systems before his work on the SG system installation test equipment. He is currently engaged in military hardware systems design. Member, Tau Beta Pit, Eta Kappa Nu.

**Paul Delage**, graduate, Ecole d'Electricité Industrielle, Paris, 1942. Mr. Delage entered the Société d'Etudes pour Liaisons Téléphoniques et Télégraphiques à Longue Distance in 1942, where he worked on measurement, installation, and splicing of long-distance cables. Following this, he worked in the Alcatel Laboratories, which later became CIT-Alcatel, developing multi-channel analog transmission equipment. This work extended from channel banks to equipment for the 60-MHz coaxial system. He is now Deputy Head of the Analog and Digital Multiplex Laboratories.

**Robert L. Easton**, B.S. (M.E.), 1953, M.S. (M.E.), 1954, California Institute of Technology; Bell Laboratories, 1954—. Mr. Easton was responsible for system aspects of the earlier SD and SF Submarine Cable Systems. In the development of the SG system, he was responsible for economic studies, signal analysis, and equalization. Currently, he heads a group concerned with undersea system planning and studies associated with a new time-assignment speech interpolation system. Member, Tau Beta Pi.

**Robert D. Ehrbar**, B.S.E.E., 1937, Johns Hopkins University; Bell Laboratories, 1937—. When he joined Bell Laboratories, Mr. Ehrbar worked on cable carrier systems. During World War II, he helped develop various airborne radar systems and after the war worked on the development of a high-capacity coaxial cable system. In 1955 he became Head, Submarine Cable Systems Department and in 1964 Head, Exchange Transmission Department. In December 1968, he was appointed Director, Exchange Transmission Laboratory and in April 1971, Director, Undersea Cable Laboratory. Member, IEEE.

**Arthur E. Ford**, British Post Office Research Laboratories, 1938—. Early in his career Mr. Ford was engaged in precision HF techniques, and in the evolution of sweep-frequency scanning and white noise measurement. He left the Research Laboratories in 1962, and joined the Telecommunications Headquarters Division, planning and laying those world-wide undersea cable systems in which the BPO had an interest. He currently heads this division. He was honored by her Majesty Queen

Elizabeth II with the award of Order of the British Empire in 1976 for his services to undersea cables.

**W. M. Fox**, B.S., 1951, Muhlenberg College; M.S., 1953, St. Lawrence University; The Franklin Institute Laboratories, 1953–1957; Bell Laboratories, 1957—. Mr. Fox has been engaged in transistor development, including devices for the SF and SG undersea systems. Currently, he is working on the development of linear high-frequency power transistors and on low-power, low-noise transistors.

**Guy Gerbier**, graduate, Ecole Polytechnique of Paris, 1954; Ecole Nationale Supérieure des Télécommunications of Paris, 1957. Upon completing his studies, Mr. Gerbier joined CNET (Centre National d'Etudes des Télécommunications), where he worked on the qualification of components for electronic switching and electronic automatic controls. Next, he headed the Department of Research in Postal Mechanization and later assumed responsibility for the CNET Division of Postal Mechanization. In 1969, he joined the Transmission Lines and Equipment Division of CNET as Deputy Director, and later became Division Director. In this responsibility, he worked on cables and their final realization, long-distance transmission systems, and local networks. Currently, as General Engineer he is responsible for the ground communications network of the French Navy. Member, SEE (Société des Electriciens, des Electroniciens et des Radioélectriciens).

**R. F. Gleason**, B.S., Engineering Science, 1961, Case Institute; M.S., Engineering Mechanics, 1963, N.Y.U.; Ph.D., 1967, Stanford University. Bell Laboratories, 1961—. At Bell Laboratories, Mr. Gleason has worked on undersea cable system physical design. He has been responsible for stress and vibration analysis of repeaters and equalizers and for design of high pressure feed-through terminals for undersea use. He presently supervises a group with responsibilities including cable and cable termination design, and development of cable handling equipment and methods.

**Igor Golioto**, M.E. 1961, Stevens Institute of Technology; M.S.M.E., 1963, New York University; Bell Laboratories, 1961–1977. Mr. Golioto was a member of the Power Systems Physical Design Department until his death in April 1977. He was responsible for the physical design of power converters for carrier and microwave systems, for No. 1 ESS, and for the SF, SG, and military undersea cables.

**Douglas N. Harper.** Mr. Harper joined the British Post Office in 1946. Since 1961, he has been involved in determining intercontinental transmission standards for both cable and satellite facilities and has been responsible for overall planning and preparation of specifications for a number of major submarine cable system projects. These include U.K.-Portugal, MAT 1 and several U.K.-European cables. During the procurement of MAT 1 he was a consultant to Italcable for the detailed planning, installation, and commissioning of the system. More recently, Mr. Harper has been involved in the SG cable system development, particularly in the terminal transmission equipment area, and in commissioning the TAT-6 system. Currently he is Head of the Trans-Atlantic Systems Planning Group, with specific responsibilities as the BPO Co-ordinator for the TAT-7 project.

**W. E. Hower, B.S.(E.E.),** Newark College of Engineering; M.S. (Management Science), Stevens Institute of Technology; Western Electric, 1961—. Mr. Hower began in Western Electric with assignments in industrial engineering and test set development. He was promoted to Department Chief in 1969 and in December of that year assumed responsibility for undersea cable repeater assembly and test engineering. He is currently responsible for customer-premise power engineering in Kearny.

**J. J. Kassig, B.S.E.E.,** 1952, Massachusetts Institute of Technology; M.S.E.E., 1955, Rutgers University; Bell Laboratories, 1955—. Mr. Kassig has worked on the design of repeaters for the SD, SF, and SG undersea systems. He has also been involved in the areas of semiconductor device characterization, in network optimization techniques using digital computers, and in the application of signal flow graphs to the design of feedback amplifiers. He is currently exploring design of a high-speed regenerator for an undersea optical fiber system.

**F. E. Kirkland, B.S.E.E.,** 1957, Auburn University; Western Electric, 1957-1962; Bell Laboratories, 1962-1976; American Telephone and Telegraph Company, Long Lines Department, 1976—. Mr. Kirkland's early work at Western Electric involved preparation of technical publications. Subsequently, he was engaged in design and development of Naval surface weapons direction equipment, first with Western Electric, then at Bell Laboratories. In 1973, he began design work on new generation undersea cable laying test equipment which was being developed for the SF and SG systems. He participated extensively in the installation

of the HAW-3/TRANSPAC-2 links, and the TAT-6 project. At American Telephone and Telegraph Company, Long Lines, Overseas, he is currently involved with various transmission measurement systems.

**Victor M. Krygowski**, B.S.M.E., 1942, N.J. Institute of Technology, M.S. (Engineering Management), 1951, Stevens Institute of Technology; Western Electric, 1946—. Mr. Krygowski's areas of responsibility have covered engineering, shop, inspection and testing, quality control, data processing, production service, and plant maintenance. Among the items worked on were PBXs, key equipment, and apparatus and piece parts. He was promoted to Department Chief in Manufacturing Engineering in 1955 and to Assistant Manager in 1959. From 1972 to 1975, Mr. Krygowski was Engineering Assistant Manager in the undersea cable repeater shops in Clark, N.J., where he was responsible for manufacturing and planning for the SDC, SF, and SG undersea repeaters and equalizers. He is presently Assistant Manager, Industrial Engineering and Wage Practices at the Kearny Works.

**Bror O. Larson**, B.S.E.E., 1958, Pennsylvania State University; M.S.E.E., 1960, New York University; Bell Laboratories, 1958—. Mr. Larson participated in the Telstar satellite development, with responsibility for the command tracker and command transmitter systems. Subsequently, he was involved in the development of single-sideband radio transmitters for the high-seas and point-to-point services maintained by the Long Lines Department of AT&T. He prepared the detailed test specifications and procedures for the installation and the final system alignment and evaluation of the SG Undersea Cable System, and participated in the commissioning of TAT-6. Currently, he is a member of the Undersea Cable Laboratory. Member, IEEE, Eta Kappa Nu, Phi Kappa Phi, Tau Beta Pi.

**Michel Laurette**, graduate, Ecole Polytechnique de Paris and Ecole Nationale Supérieure des Télécommunications; Centre National D'Etudes Des Télécommunications (CNET), 1967—. Mr. Laurette has participated in the development of French analog transmission systems, including a 60-MHz terrestrial facility and a 25-MHz undersea system. He participated in the SG system project, primarily with regard to the terminal equipment and final system alignment and evaluation of the TAT-6 link. Currently, as Transmission Engineer, he heads the Line and Transmission Equipment Engineering Department at CNET. Mr. Laurette is a member of CCITT, where he is the French representative for Study Commission XV.

**Robert L. Lynch**, A.S., Kansas City (Missouri) Junior College; B.S.E.E., 1957, Kansas University; M.E.E., 1959, New York University; Bell Laboratories, 1957—. Mr. Lynch's early work included development of cable machinery for the Bell System Cable Ship *Long Lines* and design



of transmission equipment for the shore terminals of the SD and SF undersea cable systems. His first supervisory responsibilities concerned the physical design of the SF system terminal transmission equipment and of the TASI-B system. Subsequently, he was assigned responsibility for the complete SF transmission terminal. More recently, his group has been responsible for a number of facets of SG undersea cable system design including undersea equalization and the testing procedures used during cable laying and commissioning. He provided liaison with the British and French Post Offices on these matters, and, in particular, with CIT-Alcatel during development of the SG terminal transmission equipment. He participated extensively in the installation of the TAT-6 link.

**T. A. McKenzie**, B.S.E.E., 1955, University of Tennessee; Bell Laboratories, 1955–1978. Initially, Mr. McKenzie worked on military undersea cable systems. In the SG development, he was responsible for the design of specialized test equipment. He retired from Bell Laboratories in 1978. Member, Phi Eta Sigma, Eta Kappa Nu, Tau Beta Pi, Phi Kappa Phi.

**Geoffrey E. Morse**, C. Eng.; British Post Office, Research Department, 1944—. Initially, Mr. Morse was concerned with the design of the British 0.99-in. and 1.47-in. lightweight cables. Since 1956, he has been engaged in undersea cable development. At commencement of the SG project, he became head of the cable group. Member, I.E.R.E.

**Paul R. Munk**, B.S.E.E., 1951, Purdue University; M.S.E.E., 1952, Purdue University; Bell Laboratories, 1952—. At Bell Laboratories, Mr. Munk designed inductors and transformers for a number of Bell System and military applications, including the Telstar satellite and undersea cable systems. He is currently developing computer software for the Mechanized Loop Testing System. Member, Eta Kappa Nu, Sigma Xi.

**G. A. Reinold**, B.S.M.E., 1962, Union College; M.S.M.E., 1964, New York University; Bell Laboratories, 1962—. Mr. Reinold was first involved in the development of undersea cable installation and repair techniques. He later worked on methods for installing cables underground with minimal soil disturbance. He then participated in ocean cable design for the military. In 1969, he became supervisor of the undersea apparatus mechanical design group, where he was responsible for the physical design of the SG repeater. He is currently responsible for the physical design of future undersea cable repeaters and for the cable location system on the SCARAB submersible.

**Eugene F. Sartori**, B.S., 1942, Massachusetts Institute of Technology; M.S., 1961, Stevens Institute of Technology; Bell Laboratories, 1942—. Mr. Sartori was initially concerned with the design of magnetic apparatus for both military and Bell System applications. He was responsible for high-reliability transformer design for the Telstar satellite and for undersea cable systems. He is presently involved in terminal equipment studies and subscriber loop maintenance.

**William J. Schatz**, B.S. (E.E.), 1965, New Jersey Institute of Technology; Bell Laboratories, 1958—. Since 1965, Mr. Schatz has been involved in circuit development in the Electronic Power Systems Laboratory.

**Robert E. Schroeder**, B.S.E.E., 1975, New Jersey Institute of Technology; Bell Laboratories, 1967—. Mr. Schroeder has been responsible for circuit development of dc-dc converters and regulators used in the T2 carrier system, the power converters for the SG undersea cable system, and recent exploratory work on high-power dc-dc converter plants.

**Daniel S. Shull**, B.S.E.E., 1951, University of South Carolina; M.S.E.E., 1960, Carnegie Institute of Technology; Ph.D., 1965, Carnegie Institute of Technology; Bell Laboratories, 1964—. Mr. Shull joined Bell Laboratories with the Power Apparatus Department in Winston-Salem, N.C., where he was involved in the development and design of magnetic devices and power equipment for defense applications. Upon his transfer to the SG Installation Equipment Group in 1971, he assumed responsibility for the development and design of SG-terminal-PSF equipment for both cable installation use and permanent system operation. Since 1974, he has been assigned to the Local Electronic Switching Systems Development Laboratory. He is a senior member of the IEEE, and has served on the Administrative Committee of the IEEE Magnetics Society, and is a past chairman of the technical program committee of the IEEE International Magnetics Conference. Member, Tau Beta Pi, Phi Beta Kappa.

**Henri Soulier**, graduate, Ecole Polytechnique, Paris, 1958; Ecole Nationale Supérieure des Télécommunications, Paris, 1961. Mr. Soulier began his career at CNET (Centre National d'Etudes des Télécommunications) working on semiconductors. Since joining the Transmission Department of CNET in 1964, his activities have concerned analog transmission: multiplex equipment and particularly system design for coaxial cable facilities, both land and undersea. He was responsible for

planning and specifying the terminal transmission equipment of the SG system. Appointed Chief Engineer in August 1972, he is now Deputy Director of the Cable and Microwave Radio Transmission Division. Member, SEE (Société des Electriciens, des Electroniciens et des Radioélectriciens).

**J. R. Stauffer**, B.S.E.E., 1962, Purdue University; M.S.E.E., 1964, New York University; Bell Laboratories, 1962—. Mr. Stauffer worked on various aspects of the SF undersea cable repeater, and subsequently supervised a group that developed trunk electronics for military systems. Working with the British Post Office, his group assisted in characterizing the transmission properties of cable use in the SG undersea system. Recently, Mr. Stauffer has been investigating the possibility of applying fiber optics to undersea cable systems. Member, Tau Beta Pi, Eta Kappa Nu.

**S. A. Taylor**, B.S.C. (Tech.), 1950, Manchester University, England; British Post Office, Research Department, 1950—. Initially, Mr. Taylor worked on the development of wideband feedback amplifiers and the electrical design of submarine repeaters. He is currently head of the Submarine and Inland Cable Systems Division of the Research Department. Member, IEE.

**P. A. Yeisley, Jr.**, B.S. (Physics), 1952, Lafayette College; Bell Laboratories, 1952—. Mr. Yeisley first worked on the development of the L3 coaxial cable system. Since 1954, he has worked on the physical design of the SB, SD, SF, and SG undersea cable systems.

**W. H. Yocom**, B.A. (Physics), 1940, Oberlin College; S.B. (Electrical Engineering), 1942, Massachusetts Institute of Technology; M.S. (Electrical Engineering), Stevens Institute of Technology; Bell Laboratories, 1942–1956, 1964—. Mr. Yocom had assignments in physical design of radar and test equipment, then studied electron dynamics and did research on traveling wave tubes and optical delay lines. Later he supervised a group developing tantalum thin-film hybrid circuits, and now supervises a group that coordinates the application and design of discrete passive electronic components. Senior Member, IEEE, Sigma Xi.







**THE BELL SYSTEM TECHNICAL JOURNAL** is abstracted or indexed by *Abstract Journal in Earthquake Engineering, Applied Mechanics Review, Applied Science & Technology Index, Chemical Abstracts, Computer Abstracts, Computer & Control Abstracts, Current Contents/Engineering, Technology & Applied Sciences, Current Contents/Physical & Chemical Sciences, Current Index to Statistics, Current Papers in Electrical & Electronic Engineering, Current Papers on Computers & Control, Electrical & Electronic Abstracts, Electronics & Communications Abstracts Journal, The Engineering Index, International Aerospace Abstracts, Journal of Current Laser Abstracts, Language and Language Behavior Abstracts, Mathematical Reviews, Metals Abstracts, Science Abstracts, Science Citation Index, and Solid State Abstracts Journal*. Reproductions of the Journal by years are available in microform from University Microfilms, 300 N. Zeeb Road, Ann Arbor, Michigan 48106.



**Bell System**